THE UNIVERSITY of EDINBURGH

Title	Characterization of lung and systemic immune response throughout the disease process of severe acute pancreatitis
Author	Yip, Vincent Sui Kwong.
Qualification	PhD
Year	2012

Digitisation notes:

- Page number 124 skipped in original document

Characterization of Lung and Systemic Immune Response throughout the Disease Process of Severe Acute Pancreatitis

Vincent Sui Kwong YIP

Doctor of Medicine (MD)

The University of Edinburgh

2012

Declaration of Works:

I affirm that:

The thesis has been composed by myself.

- The work forming the thesis is my own.
- The work forming the basis for the thesis was undertaken solely in South-East Scotland.
- The thesis has not been submitted for any other degree, diploma or professional qualification.

Vincent S K YIP

Declaration of Major Technical Problems

In line with the philosophy to "reduce, refine and replace" in animal experimentation, a decision was taken at the start of the project to use an isogenic strain of animals, and Fischer 344 rats were chosen for the use. Rats were obtained from a commercial breeder. Unfortunately, towards the end of the research period another group within the University of Edinburgh discovered that the "isogenic" Fischer rats had been contaminated by another strain of rat. The commercial breeders therefore culled the colony before our final experiments, leading to an earlier termination of our experiments as the source of equivalent animals for our studies was no longer available.

In addition to the premature loss of the supply of experimental animals, a -70^{0}C freezer in which experimental samples were stored broke down leading to the loss of samples for a series of experiments.

The loss of samples and the inability to complete all the animal studies means that some aspects of the proposed experiments are under-powered. This is especially so in the cytokine section in chapter 7. All results need to be interpreted with caution.

Acknowledgements

I would like to thank the following individuals:

Professor Jim A Ross for his supervision and guidance throughout my period of research. This is especially for his supervision in the laboratory aspects of this research.

Mr Jim J Powell for his supervision and guidance throughout my period of research. Also for his original idea for this research project.

Professor O J Garden for allowing me to carry out this research project within the Department of Surgery, the University of Edinburgh. Most thankfully, for his financial support during the last year of my research period.

Mr Ian F Ansell for his dedicated laboratory technical assistance, without which this research would not be possible to be completed; Also, special thanks for his contribution to review this thesis.

Mr C Bellamy for his histopathological advice.

Ms K Sangster and Mr J Black for their expert technical support.

Mr J Henderson for his assistance in the animal technical support.

Dr A J Colborne of Abbivale Editorial Services for proof-reading this thesis.

In addition, I would like to send my deepest gratitude to my parents for their continuing spiritual and financial support throughout the ups and downs of my research.

Finally, I would like to thank Janet Kung for her kind spiritual support throughout my research and the write-up of this thesis. The sequential misfortunes during my research have made her suffer with me through my disappointments. Janet has made Edinburgh a very special and memorable place in my heart during my research years.

List of Abbreviations

ABTS	2, 2'-azinobis 3-ethylbenzothiazoline-6-sulphonic acid
ALI	acute lung injury
AM	alveolar macrophage
ARDS	acute (adult) respiratory distress syndrome
BAL	broncho-alveolar lavage
BHT	butylated hydroxy toluene
CCK	cholecystokinin
CNPG	2-chloro-*p*-nitrophenyl-α-D-maltotrioside
COX	cyclo-oxygenase
DAB	3,3-diaminobenzidine
DMEM	Dulbecco's Modified Eagle Medium
ELISA	enzyme linked immunosorbent assay
ERCP	endoscopic retrograde cholangiopancreatography
FAEE	fatty acid ethanol ester
FACS	Fluorescence-activated cell sorting
FCS	Flow cytometry standard

FITC	fluorescein isothiocyanate
G-CSF	granulocyte colony-stimulating factor
GM-CSF	granulocyte–macrophage colony-stimulating factor
HO	haemoxygenase
HRP	horseradish peroxidase
IκB	Inhibitor of nuclear factor κB
ICAM	intercellular adhesion molecule
IF	interferon
IL	interleukin
MIP	macrophage inflammatory protein
NF-κB	Nuclear transcription factor -κB
PAF	platelet activating factor
PBS	phosphate-buffered saline
PDTC	pyrrolidine dithiocarbamate
ROS	reactive oxygen species
RPMI	Roswell Park Memorial Institute medium
SDS	sodium dodecyl sulphate
SIRS	systemic inflammatory response syndrome

SPINK1	Serine peptidase inhibitor, Kazal type 1
TAP	trypsinogen activation peptide
TEAC	Trolox equivalent antioxidant capacity
TGF	transforming growth factor
THB	tissue homogenizing buffer
TNF	tumour necrosis factor
VCAM	vascular cell adhesion molecule

ABSTRACT

Acute pancreatitis is an acute inflammatory process of the pancreas, with variable involvement of other local and remote organs. There are similarities in terms of clinical presentations and manifestations between acute pancreatitis and sepsis. Recent theories from sepsis studies suggested that there is a pro-inflammatory response at the beginning and a subsequent anti-inflammatory response at a later stage of the disease. It has been proposed that it is the uncontrolled pro-inflammatory response which leads to multi-organ dysfunction; whereas the later anti-inflammatory response contributes to an immuno-compromised state, and therefore increases the likelihood for nosocomial infection. The main aim of this project is therefore to characterise the dynamics of the pro- and anti-inflammatory responses during an episode of severe acute pancreatitis, using both lung and peripheral blood as the surrogate markers for remote organ and systemic immune responses respectively during the disease process.

Arginine- and caerulein- induced acute pancreatitis rodent models were used to investigate the immune responses. Although there was a trend of more severe acute pancreatitis in the arginine model than the caerulein model, there was no statistical difference in the histological scorings of both acute pancreatitis models.

The present studies therefore suggest that:

There was a trend of increased alveolar macrophage phagocytic capacity halfway through the disease process. However, the alveolar macrophage phagocytosis was only significantly elevated when the rodents had completely recovered from the episode of severe acute pancreatitis;

The overall phagocytic capacities of both monocytes and granulocytes were significantly dampened halfway through the disease process. Granulocytes contributed to the majority of this dampening effect. At the same studied time-point, further analysis on the survival of granulocytes revealed a reduction of apoptosis/necrosis of granulocytes. These observations would therefore suggest a malfunction of bacterial clearance by granulocytes, despite their increased survival. The reason for this malfunction is uncertain. In a similar manner to the alveolar macrophages, monocyte phagocytosis was significantly upregulated in rodents with pancreatitis towards the resolution of the acute pancreatitis episode.

Using lipopolysaccharides (LPS) to simulate septic events at different stages of acute pancreatitis in this rodent model, there was a net reduction in granulocyte and monocyte apoptosis halfway through the disease process, but not at any other time-points during an episode of severe acute pancreatitis. This phenomenon suggested that sepsis exerts its most profound effects on leukocyte survival halfway through the recovery from acute

pancreatitis, and that this coincided with the reduction in the ability to perform bacterial clearance.

In addition, the immune response in the liver, as another remote organ target, during acute pancreatitis was investigated. It was discovered that HO-1 (an anti-oxidant and heat shock protein) was induced within the liver parenchyma at the beginning of the disease process. Its reduction throughout the acute inflammatory process was associated with an increase in oxidation within the liver parenchyma.

The results are discussed in the light of current knowledge on the pathophysiology of acute pancreatitis.

Contents

LIST OF FIGURES

LIST OF TABLES

1 INTRODUCTION

1.1 DEFINITION OF ACUTE PANCREATITIS

Acute pancreatitis is defined as an acute inflammatory process of the pancreas, with variable involvement of other regional tissues or remote organ systems. Various classifications for the severity of acute pancreatitis have been proposed. Some of these classifications were based on pancreatic morphology, which was not practical clinically due to the limited availability of tissue samples for diagnosis. Because of the practicality and diversity of the classification of acute pancreatitis, the first clinically based classification was established after the international symposium in Atlanta, USA in 1992. This classification was further revisited and revised in 1998.

Severe form of the disease is defined as acute pancreatitis with the association of organ failure and/or local complications such as necrosis, abscess or pseudocyst formation (1). This definition is not perfect because it categorizes both local and systemic complications as severe forms of the disease process. Based on clinical observations, not every patient suffering from pancreatic necrosis or the formation of a pseudocyst will have multiple organ failure, which is a major contributor to the mortality. Nevertheless, this is still the best available published and accepted definition for acute pancreatitis in use with international consent.

The majority of patients suffer from a mild form of the disease. However, a proportion of acute pancreatitis patients progresses to the severe form of the illness, and may require intensive-care support. The mode of managing this disease is mainly supportive management of its complications. Few direct therapeutic measures have been found to be successful in altering outcomes (2). Despite the recent advancement of supportive therapeutic management in the intensive care unit, acute pancreatitis still carries a significant mortality of approximately 10–17% in its severe form (3, 4). It is therefore vital to identify patients with the potential to develop severe acute pancreatitis, which will determine outcomes of the disease.

1.2 DEMOGRAPHICS OF ACUTE PANCREATITIS

The incidence rate of acute pancreatitis varies from country to country (3-5) (Table 1-1). In a study based on the Scottish Mortality Record, the incidence of acute pancreatitis in Scotland increased from 25.8 to 41.8 per 100,000 between 1985 and 1995 (3). A study in the Netherlands using their nationwide automated database (National Information System on Hospital care) recorded an increase of 3.5 per 100,000 over the same 10-year period (6). In England, Goldacre et al and Tinto et al both revealed a rise in the general trend of the incidence of acute pancreatitis (7-9). Goldacre et al noted that the largest increase in incidence during the period of study was among young women (11% per annum) (9). Although there are variations in terms of the absolute figure of the incidence in Western countries, the overall trend is an increase in the incidence of acute pancreatitis over the last two decades (3, 6-8, 10, 11).

Epidemiological studies also revealed gender differences in the incidence of the disease (3, 6-8, 10-13). These studies revealed more frequent prevalence of acute pancreatitis in males compared to the female group. However, an epidemiological study from Denmark revealed a considerable rise in the incidence of female acute pancreatitis after 1997 (11). Although women had not surpassed men in terms of the absolute incidence rate, this trend of increase in acute pancreatitis among females was also reported in England over the last decade (9).

The cause of acute pancreatitis in men tends to be alcohol-related, whilst gallstones predominate in women as a precipitating factor (9). In addition, the age when acute pancreatitis occurs in men is younger than in women. Roberts *et al* recently investigated the relationship between acute pancreatitis and socio-economic factors in England (9). They discovered an increase in binge-drinking alcohol consumption among women of a younger age group (<35 years old), which they postulated as possibly the main cause for the surge of acute pancreatitis in women.

Table 1-1 Summaries of the incidence rate, gender distribution , and the mortality rate of acute pancreatitis in Western countries

COUNTRY	AUTHORS	INCIDENCE	GENDER TRENDS	MORTALITY	NOTES
England	Goldacre et al [43] (1963–1998)	4.6/100,000 (1960s) 10.2/100,000 (1990s)	Incidence increased in both sexes (p>0.05) Incidence increased in the younger age group	30-day mortality: 30 times of normal population No improvement in mortality rate across studied period	No comment on individual incidence in relation to alcohol or gallstones
England	Tinto et al [44] (1989–2000)	Relaive incidence increased by 43%	Male incidence greater than female	No improvement in mortality In-hospital case fatality rate declined significantly in both sexes	Increased trend of alcohol consumption in female especially in younger age group
Scotland	McKay et al [45] (1985–95)	25.8/100,000 (1985) 41.8/100,000 (1995) Incidence rise in age group >40yr old	Male incidence greater than female	Reduction in mortality from 9.1% (1984) to 6.6% (1994) 60% of death in age >40yr old No improvement in-hospital mortality	45% caused by gallstones; 35% secondary to alcohol consumption
Malmo, Sweden	Appelros et al [46] (1985–94); Lindkvist et al [47] (1985–99)	♂: approx. 30/100,000 ♀: approx. 20/100,000 Relative increase of 3.9% acute pancreatitis per year	Male incidence greater than female	Annual mortality: 1.3/100,000	Gallstones : alcohol aetiology = 1:1 Alcoholic pancreatitis doubled the risk of recurrence

Norway	Gislason et al [29] (10-yr period)	30.6/100,000	Male : Female incidence ratio: approx. 2:1	Severe acute pancreatitis accounted for 20% of admission Overall mortality = 3%	Gallstone aetiology (48.5%) > alcohol aetiology More recurrence in alcohol- induced AP
Denmark	Floyd et al [48] (1981–2000)	Increase of incidence in both sexes	Before 1997: Male incidence greater than female After 1997: Female incidence greater than male	30-day mortality: 7.5% 65.5% of death happened within 14 days	
Netherlands	Eland et al [49] (1985–95)	12.4/100,000 (1985) 15.9/100,000 (1995) Incidence rise in elderly age group	Male incidence greater than female	10% case fatality between 1985 and 1995 Mortality rise >85yr old	
Boston, USA	Mutinga et al [50] (1982–95)			Mortality: 2.1% Ratio of mortality of <14 days and >14 days is 1:1	No comparison of trend in early vs. late mortality

1.3 AETIOLOGY OF ACUTE PANCREATITIS

Numerous causes are known to trigger an episode of acute pancreatitis (Table 1.2). Alcohol and gallstones are the most common causes of acute pancreatitis (approximately 70–80%) (4, 12, 13). When Gullo et al reviewed the aetiology of acute pancreatitis of five European countries (Germany, Hungary, France, Greece and Italy), there was marked variation in the predominant cause of acute pancreatitis between gallstones and alcohol. For instance, alcohol accounted for only 6% of cases of acute pancreatitis in Greece, whereas it contributed 60.7% in Hungary. In France, only 24.6% of acute pancreatitis was caused by cholelithiasis, as compared to 71.4% in Greece (4). In the United Kingdom, gallstone disease is the most common cause for acute pancreatitis, representing 40–60% of the total incidence (14-16).

Table 1-2 Causes of acute pancreatitis

Common causes	Uncommon Causes
Gallstones	Trauma/iatrogenic: ERCP Sphincterotomy Biliary manometry
Alcohol	Pancreatic duct obstruction: Neoplasia
	Drugs: Azathioprine Steroid
	Metabolic: Hypercalcaemia Hyperlipidaemia Hypothermia
	Infections: Mumps Coxsackie B HIV
	Autoimmune: Polyarteritis nodosa Systemic lupus erythematosus
	Vascular: Ischaemia Cardiopulmonary bypass
	Congenital: Hereditary pancreatitis Cystic fibrosis
	Idiopathic

1.4 PATHOPHYSIOLOGY OF ACUTE PANCREATITIS

The pancreas has both exocrine and endocrine functions. The endocrine function is contributed by the islet cells of the pancreas, and is not believed to play a significant role in the pathophysiology of acute pancreatitis (17). The endocrine function of the pancreas will therefore not be discussed in this thesis. The function of the exocrine pancreas consists of the synthesis and secretion of digestive enzymes (proteases) to catalyse the food contents in the intestine. Many of these enzymes are synthesized by pancreatic acinar cells as pro-enzymes (zymogens), which are inactive within the cells. The activation of these zymogens requires cleavage of their pro-peptide.

Trypsinogen is one of the many zymogens synthesized in the acinar cells of the pancreas. Reaching the small intestine, trypsinogen will be cleaved by enterokinase at the intestinal brush-border to become trypsin. Trypsin is the most important of all pancreatic proteases, because once activated it is capable of catalysing further zymogens into their active forms. This cascade mechanism ensures that zymogens are in their inactive form during synthesis, transport and storage within the acinar cell. However, because of the complexity of the whole process, there are potential pitfalls in the early activation of trypsinogen to trypsin within the pancreatic acinar cells, leading to auto-digestion of the pancreas. This phenomenon of auto-digestion contributes to one of the theories for the early events in acute pancreatitis.

The pathophysiology of acute pancreatitis is complex and not fully understood. In broad terms, the whole acute pancreatitis process can be divided into three phases – the initiation, propagation, and resolution phases. Most research and studies to date have investigated the first two phases of acute pancreatitis. These three phases will be discussed in more detail in this chapter.

1.4.1 Initiation Phase of Acute Pancreatitis

This initiation phase of acute pancreatitis consists of the triggering mechanism for the pancreatic inflammatory process and the immediate cellular and molecular cascading effects after the initial trigger. The initiation process of acute pancreatitis is not as well studied in human subjects as compared to the propagation phase of the disease, which is discussed in section 1.1.1. One of the main reasons is that tissue sampling from the retroperitoneal pancreas is not required to establish the clinical diagnosis of acute pancreatitis and to initiate clinical management. By the time a patient presents to hospital, the disease has already progressed beyond the initiation phase, making the study of this initial mechanism difficult. The understanding of the initiation phase of acute pancreatitis is therefore mostly derived from studies on experimental animal models of acute pancreatitis or via tissue culture techniques.

1.4.1.1 **Triggers of acute pancreatitis**

Since alcohol and gallstone diseases are the most common aetiologies of acute pancreatitis in clinical practice, most studies focused on the pathogenic mechanisms of these two disease processes. These studies have provided valuable knowledge regarding how these two aetiologies trigger the inflammatory process of the pancreas.

Another group that has provided invaluable insights into the intracellular mechanisms during the triggering process of the disease is patients with hereditary acute pancreatitis. Using genetic knockout models based on the knowledge from hereditary acute pancreatitis has further extended the understanding of the initiation process. This will be discussed further in section 1.4.1.2.

Alcohol-induced acute pancreatitis

Alcohol ingestion by itself does not always induce acute pancreatitis. Using a continuous intra-gastric infusion model of ethanol for several weeks, only ethanol-induced liver injury was demonstrated among the rodents, but no acute pancreatitis was induced during the process (18). This observation also correlates with patients in clinical practice: some alcohol-abused patients develop acute pancreatitis, whereas others do not. When Pandol et al exposed rodents to long-term continuous ethanol ingestion, they demonstrated an increased susceptibility of acute pancreatitis with a smaller dose of cholecystokinin octapeptide (19). *In vivo* and *in vitro* experimental models have also

suggested increased vulnerability for insult in pancreatic acinar cells after exposure to ethanol (20). These results confirmed that ethanol sensitizes the pancreas, and therefore increases its susceptibility to acute pancreatitis (21, 22).

The majority of alcohol consumed is oxidized in the liver by alcohol dehydrogenase to acetaldehyde, which is then converted to acetate via acetaldehyde dehydrogenase. The other, alternative metabolic pathway for the metabolism of alcohol is the non-oxidative route using fatty acid ethyl ester synthase, with fatty acid ethanol esters (FAEEs) as the end metabolites. Gukovskaya et al suggested that the long-term exposure of ethanol activates different transcription factors (NF-κB and Activator Protein-1), depending on the domination of either oxidative or non-oxidative pathway within the pancreas (23). Because of a significantly smaller oxidative capability for alcohol within the pancreas as compared with the liver, most of the ethanol is metabolized through this non-oxidative pathway within the pancreas (24). It is generally believed that the formation of FAEEs within the pancreatic acinar cells increases cytosolic calcium concentration, leading to mitochondrial injury and subsequent acinar cell damage (23-30). This will play a role in ethanol toxicity in the pancreas.

Pandol et al further confirmed a significant alteration of the pancreatic gene expression after long-term exposure of ethanol (31). Pandol et al discovered a significant upregulation of the mRNA of Activating transcription factor 3, HSP 27 and 70 (heat

shock proteins), and meso-trypsinogen, and downregulation of the mRNA of pancreatitis-associated proteins (PAPs), folate carrier, and metallothionein. Among all these mRNA upregulations within the pancreas, the authors advocated that the upregulation of meso-trypsinogen, a minor form of trypsinogen, is potentially significant because of the rapid hydrolysis ability causing irreversible degradation of serine peptidase inhibitor, Kazal type 1 (SPINK1), which is a major endogenous trypsin inhibitor. Recent studies have shown that an overexpression of SPINK1 in transgenic animals is able to protect against the development of severe acute pancreatitis (32). SPINK1 mutations are also linked with chronic pancreatitis (33). Therefore, ethanol-induced high levels of mesotrypsin could reduce the levels of functional SPINK1 and thereby exacerbate the acinar cell damage during acute pancreatitis.

Apart from the increase of FAEEs with ethanol consumption in animal models, ethanol has also been shown to increase the activation of NF-κB within the acinar cells through protein kinase C (34). Activation of NF-κB, a transcription factor, contributes to an important effect on the pro-inflammatory immune function through the regulation of interleukin (IL)-6, MCP1 and ICAM (35-37), and blocking some signalling pathways of apoptosis via reduction of caspase expression (38). Expression and activity of cathepsin B were also found to be upregulated after ethanol exposure (see section 1.4.1.2) (38). The combination of these effects from alcohol leads to pancreatic cell injury, more so in the form of necrosis than apoptosis.

Due to these multiple plausible effects of alcohol on the pancreas, it is now believed that alcohol consumption itself is not enough to induce acute pancreatitis; rather it hypersensitizes the pancreas for the susceptibility to insults. Most of these studies were performed using rodent pancreatitis models; it is therefore uncertain whether this theory is transferrable to humans.

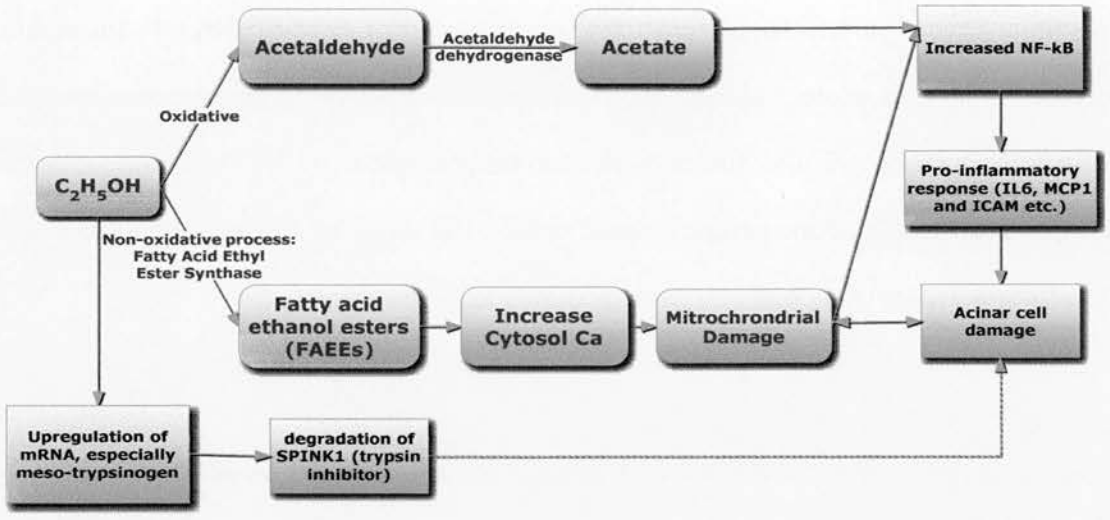

Figure 1-1 illustrates the metabolic pathways and effects of the consumption of ethanol in the pancreas

Biliary pancreatitis

The exact mechanism of how gallstone disease triggers acute pancreatitis remains debatable. Opie proposed over a century ago that a gallstone at the ampulla of Vater causes reflux of bile to the pancreas through the common channel between the common bile duct and pancreatic duct, leading to acute pancreatitis (39). This "double channel"

theory formed the basis of the belief in gallstone pancreatitis for a long time, and was supported by the reproducible acute pancreatitis rodent models using direct injection of bile salts into the pancreatic duct (40). However, this theory was challenged when necrotizing pancreatitis was induced in an opossum model by separate ligation of the pancreatic duct and common bile duct (41). In another pancreatitis model using combined duct ligation and replacement of bile-pancreatic juice via the duodenum to reduce the neurohormonal pancreatic stimulation, there was histological evidence of reduction of pancreatic inflammatory changes (42-46). This led to another theory that it is the combination of *ductal obstruction* with the activation of trypsin and then subsequent *hyperstimulation* of the pancreas via a neurohormonal pathway which exacerbates the severity of acute pancreatitis (47). It is unclear which of these theories is best suited to explain the human clinical scenario. Nevertheless, both models achieved acute inflammation to pancreatic acinar cells, causing acute pancreatitis.

1.4.1.2 **Early cellular events of acute pancreatitis**

Irrespective of the aetiologies causing acute pancreatitis, there is a consensus that a final "common" pathway of changes exists within the pancreatic acinar cells during the disease process (48). After the initial triggers of acute pancreatitis, as discussed in section 1.4.1.1, multiple events occur within the acinar cells prior to the cascading inflammatory response, leading to the propagation phase of acute pancreatitis. In broad terms, these are mainly intracellular calcium signalling, co-localization of enzyme and the activation of NF-κB. All these signalling pathways have a common endpoint, which

is to activate the zymogen, causing autodigestion within the acinar cells. It is also during the propagation phase of the disease, where clinical symptoms and signs manifestate.

Calcium signalling in pancreatic acinar cells

Calcium is an important intracellular messenger within the pancreatic acinar cells. The cytosolic calcium concentration [Ca^{2+}] is lower than the extracellular compartment. This concentration gradient is maintained by the active-transport process through magnesium-dependent calcium-ATPase at the plasma membrane, which pumps Ca^{2+} out of the cytosol (49). Endoplasmic reticulum, which is situated close to the nuclear envelope, is responsible for the intracellular storage of calcium.

During the normal physiological response to pancreatic secretagogues, such as acetylcholine and cholecystokinin (CCK), the secretagogues attaches to the receptor of the acinar cell surface. This molecule–receptor interaction will couple to the G-protein leading to the intracellular signalling by second messengers (50). One of these second messengers is inositol 1,4,5-triphosphate (IP_3), derived from the cleavage of membrane bound phosphatidylinositol 4,5-bisphosphate by phospholipase C-β. The interaction of the IP_3 and its receptors causes the release of Ca^{2+} from endoplasmic reticulum to the cytosol, with the reduction of Ca^{2+} re-uptake at the same time (51, 52). The combination of these two mechanisms increases the calcium concentration within pancreatic acinar

cells. The location of Ca^{2+}-releasing channel at the endoplasmic reticulum is closely associated with the zymogen granules at the secretory pole of the acinar cell (53).

During a physiological response to the secretagogues described above, Ca^{2+} is released repeatedly, in a cyclical manner. Because of the close association of the Ca^{2+}-releasing channel and the secretory pole of the acinar cell, this oscillatory release is associated with the secretion of zymogen granules into the lumen (53, 54). There is also a prolongation of this oscillatory cycle as well as an elevation of the intracellular baseline Ca^{2+} level demonstrated in the CCK hyperstimulatory pancreatitis model (55). The combined effect leads to mitochondrial dysfunction, disruption of cytoskeleton and gene expression (56, 57). This dysregulation of Ca^{2+} control and the continuous mitochondrial depolarization will ultimately lead to apoptosis and the subsequent secondary acinar cell necrosis (58).

Cytosolic calcium was also found to be required during the activation process of the zymogens after the co-localization, which will be discussed in the next section (59). In fact, cytosolic calcium concentration was elevated during the early phase of acute pancreatitis, leading to disturbances of mitochondrial membrane depolarization and subsequent production of ATP. This is similar to the calcium dysregulation described above. To provide further experimental evidence that calcium regulation within the acinar cell was vital to the zymogen activation, the addition of calcium chelator to

pancreatic acinar cells *in vitro* prevented zymogen activation (55, 60, 61). However, it is important to highlight that the increase of cytoplasmic calcium concentration by itself does not lead to the activation of zymogens; Rather, calcium signalling plays a vital role as a co-factor in the activation of zymogens.

Enzyme co-localization

Because of the exocrine function of the pancreas, namely its production and storage of all these precursors of digestive enzymes (zymogens), it is logical to hypothesize that the premature activation of these zymogens within the acinar cell is responsible for the initiation of acute pancreatitis. Due to the fact that the activation of other zymogens relies on the presence of trypsin, the activation of trypsinogen to trypsin was suggested to be the prime suspect for the trigger of acinar cell injuries. There is evidence that intra-acinar activation of zymogens is actually a key event in the pathophysiology of acute pancreatitis, and that the activation of the zymogens is always within the acinar cell to trigger acute pancreatitis (62-66).

One of the theories regarding the activation of trypsinogen is the "co-localization" theory, which is based on the hypothesis that zymogens co-localize with lysosomal enzymes for their activation. Using subcellular fractionation and immunolocalization techniques of a caerulein-induced model, cathepsin B – one of the lysosomal hydrolases within the lysosomal vacuoles – was detected to be in close association with zymogen

granules (63, 67). This phenomenon was detected prior to the morphological and biochemical evidence of acinar cell injury during acute pancreatitis (63). This co-localization process has therefore been advocated as one of the key elements in the activation of the zymogens, and not simply an event subsequent to the pathological process of acute pancreatitis.

During the activation process of trypsinogen to the formation of trypsin, trypsinogen activation peptide (TAP) is formed as a by-product. In addition to the lysosomo-zymogen co-localization process mentioned above, TAP was found to co-exist with cathepsin B within the same subcellular compartment (63, 68, 69). This suggested that not only did zymogen granules and lysosomal vacuoles co-localize during acute pancreatitis, trypsinogen was activated during the process too. To provide further evidence that cathepsin B was required for the activation of trypsinogen, Acker et al demonstrated that trypsin was activated within acinar cell and the severity of acute pancreatitis was reduced when cathepsin B activity was inhibited prior to the induction of acute pancreatitis (70). A similar phenomenon also occurred when acute pancreatitis was induced in cathepsin B knockout mice (71). The findings that pancreas-derived digestive zymogens become co-localized with lysosomal hydrolysis in acinar cell cytoplasmic vacuoles, and that lysosomal hydrolases, such as cathepsin B, activate trypsinogen formed the basis of the "Co-localisation Hypothesis".

Nuclear Factor κB

Once the intra-acinar zymogens have been activated and subsequently led to mitochondrial injury through the above process, NF-κB plays an important role in further cascading the inflammatory process.

NF-κB is a transcriptional factor, which normally locates within the cytoplasm. In its inactive state, it is accompanied by IκB to form a stable complex. IκB is an inhibitor and its prime function is to mask the nucleus localization sequence of NF-κB. The formation of this complex prevents the translocation of NF-κB to the nucleus to act as a transcription factor. To allow transcription of DNA by NF-κB, the inhibitory protein needs to be removed from the complex by either dissociation or degradation. Whether it is the dissociation process or the degradation process that unmasks the nuclei localization sequence of NF-κB depends on the type of acinar-cell stress response. For cytokines, growth factors, mitogens and hormonal response, IκB becomes phosphorylated by IκB kinase to allow degradation of IκB; whereas for the stress response, such as hypoxia, reactive oxygen species or other physical insult to the acinar cell, IκB is phosphorylated by an unknown kinase to allow dissociation of the inhibitory protein. With the disappearance of IκB from the complex, translocation of NFκB to the nucleus would then be feasible to allow gene transcription.

The activation of NF-κB was discovered within the acinar cells of several rodent acute pancreatitis models during the early phase of disease (35, 72, 73). In caerulein acute pancreatitis, the activation of NF-κB has been demonstrated to follow a biphasic pattern – the first activation occurs 30 minutes post-induction, and the second activation occurs after 3 hours post-induction and lasted for up to 6 hours (35). The activation of NF-κB upregulates protein production involved in various inflammatory processes. In taurocholate biopancreatic ductal injection model, NF-κB is found to be translocated to the nuclei and subsequently upregulates P-selectin, ICAM-1 and adhesion molecules in acinar and endothelial cells. The upregulation of these proteins increases the adherence of neutrophils to the injured site, and the migration of neutrophils through endothelial cell lining. The responses of neutrophils will be discussed in detail later in section 1.4.3.1.

Because NF-κB has such a profound effect on the immune function, especially on the pro-inflammatory response, it was uncertain whether the activation or inhibition of NF-κB is beneficial to patients with severe acute pancreatitis. The general consensus from different animal studies suggested that reduction of the severity of acute pancreatitis was associated with the inhibition of NF-κB (74-77). However, Steinle et al had demonstrated that *in vivo* inhibition of NF-κB by PDTC was associated with adverse outcome in caerulein-induced acute pancreatitis (78). Most of these studies used anti-oxidants that inhibit the signalling pathway of cyclo-oxygenase 2 (COX-2). The main problem was therefore the specificity in targeting the inhibition of NF-κB alone in these

studies. To address the specific role of NF-κB in acute pancreatitis, Altavilla et al induced acute pancreatitis in NF-κB knockout mice, and compared the cytokine expression and oxidative responses with the wild-type mice (74). They demonstrated a significant reduction in pancreatic NF-κB DNA-binding activity, tumour necrosis factor (TNF)-α expression and oxidative stress within the knockout group as compared to the wild-type controls.

Over the last few years, the role of NF-κB in acute pancreatitis has been intensely investigated in rodent models. There is more evidence pointing towards a beneficial effect with blockade of NF-κB in experimental models, via a reduction of pro-inflammatory responses during acute pancreatitis. However, its role in human pancreatitis is yet to be determined.

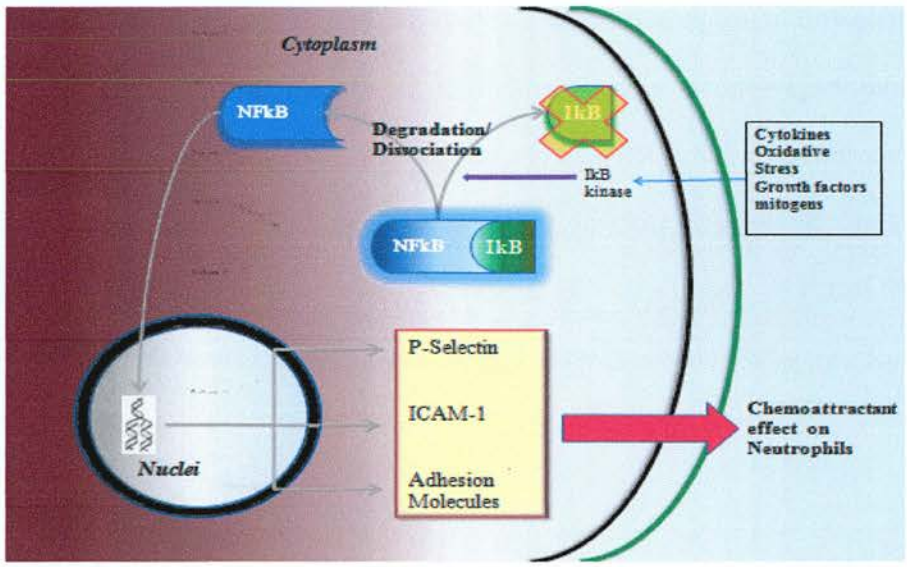

Figure 1-2 summaries the cell signalling process of NFκB by external stimuli, such as cytokine and reactive oxygen species, to induce chemoattractant effect on neutrophils

1.4.2 Propagation Phase of Acute Pancreatitis

Once individual acinar cell injury is triggered, an acute inflammatory response can evolve causing local pancreatic acute inflammation, which can subsequently initiate further remote organ damage. This injury mechanism signifies an important part of the whole disease process: the propagation phase of acute pancreatitis. It is during this phase that the clinical manifestation of the disease occurs. Both local pancreatic inflammatory involvement and distant multi-organ dysfunction can co-exist during this phase of acute pancreatitis. It is the latter that normally dictates poor clinical outcomes (5, 79).

1.4.2.1 **SIRS/sepsis and acute pancreatitis**

Systemic inflammatory response syndrome (SIRS) is usually part of the clinical presentation of acute pancreatitis. SIRS was a term derived at the American College of Chest Physicians and Society of Critical Care Medicine (ACCP/SCCM) consensus conference in 1992 (80, 81). The aim of this terminology is to provide a clear and well-defined definition of sepsis, which was loosely applied before the consensus.

SIRS can be triggered by various sources (see Figure 1-3). Clinically, a patient is suffering from SIRS when two or more of the following conditions are fulfilled: temperature $>38^0$C or $<36^0$C; heart rate >90 beats/min; respiratory rate >20 breaths/min or $PaCO_2$ <4.3kPa; white cell counts >12,000 cells/mm^3, <4000 cells/mm^3 (80). Sepsis is defined as SIRS with an identifiable focus of infection caused by bacteria, virus, fungus or parasite; whereas severe SIRS/sepsis is defined as organ dysfunction, hypoperfusion or hypotension in addition to SIRS/sepsis. When hypotension (systolic blood pressure <90mmHg or reduction of >40mmHg from baseline) occurs despite adequate fluid resuscitation during SIRS or sepsis, the terminology of "SIRS shock" or septic shock is used.

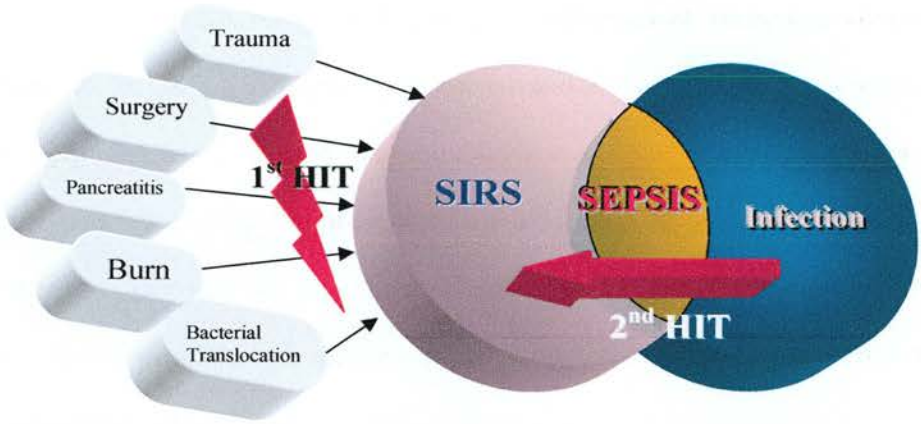

Figure 1-3 The concept of SIRS as a common response to many initiating factors. The interrelationship between SIRS, sepsis and infection is shown here. [Diagram reproduced from J Pharmacol Sci 101, 189 – 198 (2006)]. Permission obtained from Professor Hattori

Early epidemiologic studies demonstrated that infection with systemic SIRS was the common pathway for the development of acute respiratory distress syndrome (ARDS) and eventual multiple organ failure. It is now believed that an initial traumatic insult creates severe SIRS independent of infection (one-hit model). Alternatively, a less severe traumatic insult can create an inflammatory environment (i.e., primes the host) such that a later, otherwise innocuous, secondary inflammatory insult precipitates severe SIRS (second hit) (82). This biphasic mode of inflammatory response was also observed in severe acute pancreatitis in clinical practice (3, 83). About 50% of mortality occurs within the first week of severe attack. These early deaths were found to be due to multi-organ dysfunctions (MODs), whereas the later deaths were commonly secondary to infective necrotic pancreatic tissues and/or other nosocomial infection (84).

Initial research in severe acute pancreatitis suggested that it was the excessive pro-inflammatory response which initiated and sustained multiple organ failure at the early phase (85). Recently there has been growing evidence that an anti-inflammatory state exists during the disease process (86). Clinical studies revealed that the level of serum IL-10, an anti-inflammatory cytokine, correlates well with the severity of acute pancreatitis (87-89). Some authors have therefore proposed that it is an imbalance between the pro- and anti-inflammatory state during acute pancreatitis that determines outcome (90). This theory correlates well with the clinical scenario where the net pro-inflammatory response at the early stage of the disease contributes to multiple organ failure (first hit); and the subsequent overwhelmed anti-inflammatory response leads to nosocomial infection (second hit) in severe acute pancreatitis.

1.4.2.2 **Role of acinar cells in leukocyte attraction**

To understand the disease progression from acinar cell injuries to SIRS response, it is essential to look into the events beyond the activation of trypsinogen within the acinar cells, and discuss the links between the acinar cell injuries and SIRS.

Gukovskaya et al demonstrated that NF-κB was activated within acinar cells during the early event of acute pancreatitis (37). They further established that acinar cells express TNF-α, providing the first evidence that non-leukocyte can produce pro-inflammatory cytokines within the pancreas. This evidence of pro-inflammatory cytokine production

by the pancreatic acinar cells provided an important piece of jigsaw regarding how the subsequent inflammatory process can propagate within and beyond the pancreas. TNF-α secreted by the acinar cells recruits inflammatory cells by upregulating selectins, ICAM-1 and VCAM-1 (91). The upregulation of these proteins is vital in the recruitment of inflammatory cells to the pancreas. The recruitment of leukocytes involves: 1) leukocyte-rolling by selectins; 2) firm adhesion of leukocytes to endothelium by ICAM-1 and VCAM-1; and then 3) subsequent diapedesis. It is generally believed that it is the activation of leukocytes that subsequently leads to the chain-reaction of inflammatory responses.

ICAM-1 and VCAM-1 are both cellular adhesion molecules, which are upregulated during an inflammatory process (92, 93). These molecules interact with the surface receptors, such as CD11/CD18, to allow and enhance the adhesion of activated leukocytes e.g. neutrophils. The upregulation of ICAM-1 of acinar cells has been shown to increase the adherence of neutrophils to the inflamed pancreas. This phenomenon was demonstrated in both *in vivo* and *in vitro* experimental acute pancreatitis models (36). Zaninovic et al has shown that this increased neutrophil adherence to the pancreas is neutralized when ICAM-1 antibody was applied in both acinar cell culture and experimental rodent pancreatitis model (36). When acute pancreatitis was induced in ICAM-1 knockout mice, a milder degree of acute pancreatitis and associated lung injury were observed within the knockout group as compared to the wild type (94). A similar protective effect was also noted when neutrophils were depleted prior to the induction of

acute pancreatitis. However, there was no extra protective effect in combined ICAM-1 knockout and neutrophil-depletion. These findings suggested that ICAM-1 exerts its pro-inflammatory acute pancreatic response possibly via the involvement of neutrophil migration and activation. In clinical observation, the plasma level of ICAM-1 was also found to be elevated in patients with severe acute pancreatitis compared to those with a mild form of the disease (95).

Interestingly, Ramudo et al demonstrated that not only was TNF-α secreted by acinar cell, an anti-inflammatory cytokine, IL-10, was also secreted by acinar cells during acute pancreatitis in a bile-duct ligated model (96). However, how this anti-inflammatory response has any further influence on the subsequent acute inflammatory process is uncertain.

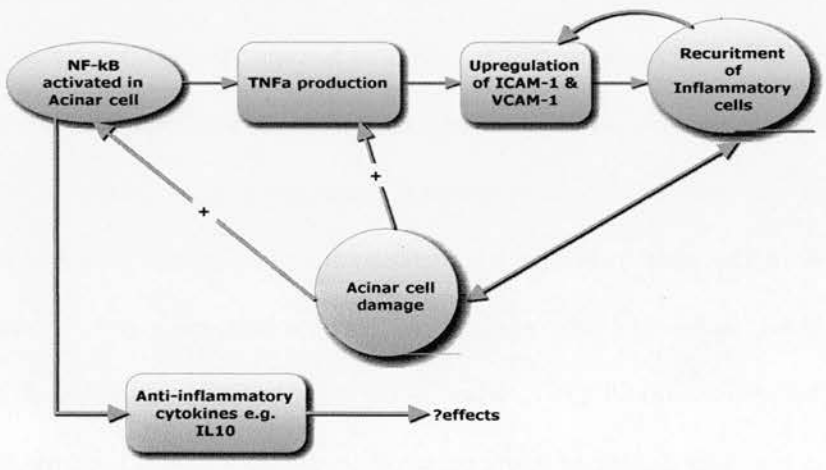

Figure 1-4 summaries the potential role of acinar cells in leukocyte attraction during acute inflammatory processes

1.4.2.3 **Granulocyte and monocyte infiltration**

Neutrophil involvement is a key element in the acute inflammatory process. Its accumulation within the pancreas is a common feature during the early phase of acute pancreatitis (97). It has been shown in animal models that neutrophils appear within the pancreas as early as 3 hours from the induction of the disease. The production of free oxygen radicals, myeloperoxidase and other proteases by the activated neutrophils leads to increased toxicity and subsequently pancreatic tissue damage (98). When neutrophils were depleted by anti-neutrophil serum injection prior to induction of acute pancreatitis, there was a significant reduction in the neutrophil infiltration as well as severity of disease as shown by its histological scoring and biochemical analysis (99, 100). A similar protective effect was demonstrated when oxygen-radical scavenger superoxide dismutase or anti-ICAM antibody was given to rodents prior to the induction of acute pancreatitis (101, 102). Not only did Poch et al notice a reduction in oxidative stress, they also demonstrated a reduction of neutrophil infiltration to the pancreas during the disease process (101). These studies highlighted the important role of neutrophils and their generation of free radicals in the contribution of pancreatic injuries during the disease process.

The infiltration of monocytes/macrophages follows along with the influx of neutrophils to the pancreas during acute pancreatitis (103). This infiltration of monocytes/macrophages has been strongly linked to the increase of pro-inflammatory

cytokine secretion within an inflamed pancreatic tissue, especially IL-1, IL-6 and TNF-α (104). These pro-inflammatory cytokines contribute significantly to the "primary" hit of the SIRS response, which was discussed in section 1.4.2.1.

1.4.2.4 **Pro-inflammatory mediators**

Tumour Necrosis Factor Alpha (TNF-α)

The excessive production of TNF-α has been classically viewed as the trigger for the excessive inflammatory response at the beginning of SIRS/sepsis and severe acute pancreatitis. Once the injury of the acinar cells is triggered by the early intracellular events, TNF-α is secreted by acinar cells (37). These in turn attract the accumulation and activation of neutrophils and monocytes from the circulation to the inflammatory areas. The locally secreted TNF-α further signals monocytes/macrophages, which activate transcriptional factor NFκB, to upregulate the production of TNF-α, IL-1 and IL-6 (see Figure 1-2). Within a short period, there is a sudden surge of pro-inflammatory cytokines locally. In fact, TNF-α has been detected within the pancreas and serum in less than an hour after the induction of acute pancreatitis in an animal model (104). This surge of TNF-α has been suggested to play a role in the development of the clinical manifestation of shock during severe SIRS, possibly via the synthesis of nitric oxide as the vasodilator (105). The other function of TNF-α is to enhance the expression of adhesional molecules on cell surfaces. The two adhesional molecules are intercellular adhesion molecule-1 (ICAM-1) and vascular cell adhesion molecule-1 (VCAM-1).

These in turn increase integrin adhesiveness and promote extravasation of leukocytes to remote organs, which can then do damage to remote organs. (This will be discussed further in Section 1.4.3.3.)

Interleukin-6

IL-6 is another pro-inflammatory cytokine, which can be produced by almost all inflammatory cell types following an appropriate stimulus (106). Monocytes/macrophages contribute a significant amount to IL-6 production during acute pancreatitis (107). This again is likely due to the activation of transcriptional factor NFκB. There is evidence suggesting that serum IL-6 correlates to the haemodynamic instability in experimental acute pancreatitis (108). Because serum IL-6 level demonstrates a close correlation with the severity of acute pancreatitis in humans, it has been suggested that the measurement of IL-6 is an accurate biochemical marker to predict the likelihood for patients to develop severe acute pancreatitis within 24 hours of the onset of disease (109, 110). The production of IL-6 triggers the synthesis of acute phase proteins by the liver, such as C-reactive protein (CRP) and fibrinogens. The measurement of CRP has been validated as an invaluable tool to establish the severity of acute pancreatitis 48 hours after hospital admission in clinical practice (111).

Despite the above evidence, the exact role of IL-6 in severe SIRS/sepsis remains unknown. The first line of evidence suggesting that IL-6 is involved in the pathogenesis

of the severity of acute pancreatitis was revealed by Suzuki et al, when IL-6 transgenic mice were used (112). They showed that over-expression of IL-6 was associated with an increased susceptibility to severe acute pancreatitis, whereas a protective effect was noted with the administration of monoclonal anti-IL6 antibody (112, 113).

Chemokines

Chemokines are a family of small (8 – 10kD) secreted cytokines that function as a chemoattractant, and are involved in leukocyte trafficking, recruiting and recirculation. They can be constitutionally expressed or induced. The secreted groups are homeostatic chemokines and are involved with basal leukocyte trafficking and the organization of lymphoid tissue. Examples included Stromal cell-derived factor (SDF)-1 and macrophage-derived chemokine (MDC). The other more common group are the induced chemokines, which are upregulated in response to various inflammatory stimuli, including all the inflammatory mediators discussed in this section. They can be further subcategorised into two major groups based on the orientation of the first two cysteine residues – C-C chemokines and C-x-C chemokines. C-C chemokines are believed to act mainly on the monocytes, whereas the C-x-C chemokines are believed to act on the neutrophils.

Interleukin-8 (IL-8) is a type of C-x-C chemokine and is a potent neutrophil chemoattractant (114, 115). The level of IL-8 had been shown to be associated with the

severity of acute pancreatitis. An increased level coincided with an upregulated plasma neutrophil elastase concentration (116). When anti-IL8 antibody was infused 30 minutes prior induction of acute pancreatitis, the severity of lung injury was reduced (117). A similar pulmonary protective effect was also identified when the gene of MIP-1α/ RANTES receptor, CCR1, was knocked out in a mouse caerulein model (118). Little protection against local pancreatic damage was revealed in this study. The plasma level of IL8 has also been shown to be closely related to the response of IL-6 and the clinical severity of acute pancreatitis in a human study (119). There is clearly a role for chemokines in the pathogenesis of acute pancreatitis. This is probably more so in the association with the pancreatitis-associated lung injury, which is discussed in section 1.4.3.

Other mediators

Apart from those mediators described above, platelet activating factor (PAF) was another non-cytokine mediator which has been extensively investigated. PAF is a lipid mediator that binds to the surface receptors of platelets, leukocytes and enothelial cells. It has been recognized as an important inflammatory mediator for SIRS/sepsis since its discovery in the 1970s (120). Its association with acute pancreatitis was revealed in studies using animal pancreatitis models (121-123). Initial research in these animal pancreatitis models suggested a histological improvement in pancreatic inflammation and an overall reduction of systemic inflammation after the inhibition of PAF (124-126).

A clinical trial was carried out in the hope that the antagonizing of PAF would provide clinical improvement and an overall survival benefit in human acute pancreatitis. However, the initial success of lexipafant (PAF antagonist) in animal models of acute pancreatitis and the Phase II clinical trial (127, 128) could not be reproduced in the Phase III human trial (129). This phase III trial has two treatment arms – the lexipafant and the placebo groups. The study hypothesized that lexipafant could have dampened the development of multi-organ dysfunctions in severe acute pancreatitis. However, this primary hypothesis was invalidated due to the unexpected high number of patients with sepsis at the entry of the study (Lexipanfant vs. Placebo group: 13/138 vs. 14/148; p=0.02). Although there was a significant reduction in interleukin-8 among the patients of the lexipafant group, lexipafant did not alter the development of new organ failure throughout the study.

These were disappointing findings. Nevertheless, it highlighted the complex physiological response of acute pancreatitis in human beings. PAF therefore represents one of the many responsible mediators during the whole inflammatory response. It is almost certain that other important, but yet unknown, mediators are contributing to this complicated scenario when PAF is antagonized during acute pancreatitis.

1.4.2.5 **Anti-inflammatory response**

Due to the belief of an excessive pro-inflammatory response during SIRS/ sepsis before the 90s, two double-blinded human trials using monoclonal antibodies targeted directly against the pro-inflammatory mediators were studied in the context of sepsis (130, 131). No successful improvement in mortality was reported in any of these attempts. In terms of severe acute pancreatitis, it was generally believed that the mortality in acute pancreatitis was due to the excessive pro-inflammatory response before the 1990s. The role of "compensatory anti-inflammatory response syndrome" (CARS) was then suggested by Bone et al in the mid-to-late 1990s, when more investigation was attempted to study the dynamic balance between pro- and anti- inflammatory responses in SIRS and acute pancreatitis (132).

Many anti-inflammatory mediators, such as IL-4, -10, -11, -13, complement 5a (C5a), transforming growth factor (TGF)-β, colony-stimulating factor (CSF), surface receptors to TNF, and IL-1 receptor antagonist have been studied widely. Of these, IL-10 and C5a are the most commonly investigated anti-inflammatory mediators in acute pancreatitis. Because of this, only IL-10 and C5a are discussed in the following sections.

Interleukin-10

IL-10 is produced and released by both monocytes and T-helper cells. It was originally known as cytokine synthesis inhibiting factor (CSIF). It primarily acts as an anti-

inflammatory agent, which modulates the expression of pro-inflammatory cytokines (133). The production of IL-10 stimulates the production of IL-1 receptor antagonist and the release of soluble TNF receptor. The combined effects neutralize the pro-inflammatory effects of IL-1, TNF-α, IL-8 and MCP-1 (134). Using a bile-pancreatic duct ligated pancreatitis model, Ramudo et al discovered the failure of IL-10 production in injured acinar cells at 3 hours post-induction as compared to the control group. When the acinar cells were treated with *N*-acetylecysteine to reduce oxidative damage during pancreatic inflammation, acinar cells were shown to regain the ability for IL-10 production (96). Similarly, when IL-10 was measured within 24 hours after the onset of acute pancreatitis in human studies, the serum level was found to be significantly higher in the mild acute pancreatitis group in comparison to the severe group (86). The production of an anti-inflammatory response at an early onset of acute pancreatitis might therefore correlate with outcome.

In addition to local anti-inflammatory effect, IL-10 has been shown to inhibit the production of pro-inflammatory mediators by alveolar macrophages in patients with ARDS (135). A clinical study using broncho-alveolar lavage fluid from patients with ARDS also demonstrated a reduction of IL-10 level (136). These studies confirmed the role of IL-10 in the local and remote anti-inflammatory response during severe SIRS.

Complement 5a (C5a)

C5a is part of the complement system, which is an innate immune system 'complementing' the ability of antibodies and phagocytes to tackle pathogens. C5a is a cleaved fragment of complement factor C5, and is also a powerful anaphylatoxin. It is an effective chemoattractant for leukocytes, especially neutrophils. It is therefore believed to play a role of pro-inflammatory mediator. Studies of severe sepsis using a caecal-ligation and puncture (CLP) model revealed a significant increase in survival of the treatment group after blockade of either C5a or the C5a receptor (137, 138). However, a similar response was not observed in acute pancreatitis. The severity of acute pancreatitis was greater in mice lacking the C5a receptor genes than the wild type (139). In addition, pancreatitis-associated lung injury was significantly worse among the knockout group. Apart from the traditional concept that C5a has a pro-inflammatory effect, Bhatia et al suggested that C5a could potentially exert on both anti-inflammatory response as well as pro-inflammatory response during acute pancreatitis. Further research has also led to the discoveries that C5a responses differ in various cell types under different circumstances. For instance, IL-6 mRNA expression was significantly suppressed after the exposure to C5a in the HUVEC cell line (140); C5a suppresses lipopolysaccharide-induced TNF-α production in neutrophils, whereas an increase in TNF-α production was found to have a synergistic effect in monocytes or macrophages (141, 142). The final verdict for C5a in relation to its "pro-" and "anti-" inflammatory responses during acute pancreatitis is still unclear.

1.4.3 Remote Organ Injury and Immune Response

Once intracellular processes within the acinar cells are triggered leading to acute pancreatitis, the inflammatory changes will manifest clinically as systemic inflammatory response syndrome (SIRS), as described above, with or without the involvement of other remote organs. Among all remote organ injuries, acute pulmonary injury is the most frequent and potentially the most serious complication of severe acute pancreatitis (143). The lungs have been indicated as the primary organ system responsible for the mortality in acute pancreatitis, and a potential surrogate marker for remote organ injuries during acute pancreatitis (144). It is therefore important to discuss remote organ insults during acute pancreatitis in the context of acute lung injury (ALI) or acute respiratory distress syndrome (ARDS).

The degree of pulmonary complications of acute pancreatitis varies from hypoxaemia, pleural effusion and atelectasis to severe pulmonary insults in the form of ALI or ARDS. ARDS can occur in 15–20% of patients who are diagnosed with acute pancreatitis (145). When pulmonary infiltrates and severe hypoxaemia occur with severe acute pancreatitis, it has been shown that mortality rate can reach above 50% (146).

1.4.3.1 **Pathophysiology of ALI or ARDS in acute pancreatitis**

The exact mechanism leading to ARDS in acute pancreatitis is not well understood. Studies have suggested that the development of ARDS is multi-factorial, with the

involvement of multiple mediators, some of which were discussed in sections 1.4.2.4 and 1.4.2.5 above. The factors that have been suggested in leading to ALI are pancreatic enzymes, infiltration and interaction between leukocyte, pneumocytes and alveolar macrophages and inflammatory mediators.

Alveolar–capillary membrane

In clinical practice, pulmonary oedema is identified on plain chest film in approximately 10% of acute pancreatitis patients. Within hours to days, progressive hypoxaemia develops in one-third of patients with pulmonary oedema (147). De Troyer et al, looking at the pulmonary diffusing capacity for carbon monoxide, discovered a significant reduction in the acute pancreatitis group (78% of the predicted value) (148). When lung vascular permeability was studied in acute pancreatitis within 48 hours after hospital admission, the mortality group had a significant increase in vascular permeability compared with the survival group (149). These findings correlate well with the histopathological findings of intra-alveolar oedema, distal airway contraction, endothelial cellular damage, and leukocyte sequestration within the lung parenchyma during experimental acute pancreatitis (150). These data suggested that inflammation at the alveolar-capillary level plays a role in the development of ALI during acute pancreatitis. However, the key question remains regarding how does inflammation from the pancreas lead to an acute inflammatory response in the lung at the alveolar-capillary level?

Neutrophil infiltration into pulmonary tissue, its activation and effect

Protein signalling or cell-to-cell interaction is a logical theory to explain the propagation of inflammation to a remote organ. One of the key factors in cell-to-cell interaction is the involvement of neutrophils during acute pancreatitis, both locally and remotely. Using an intra-ductal taurocholate pancreatitis model with and without portocaval shunting, Closa et al demonstrated that there was an increased production of TNF-α, NO and MIP-2 (chemokine) by alveolar macrophages using *ex vivo* culture in the non-shunting group, suggesting an activation of alveolar macrophages (151). Supernatants of these macrophages exhibited a chemotactic activity for neutrophils when instilled into the lungs of untreated animals. All these effects were abolished when portocaval shunting was carried out before induction of pancreatitis. Not only did Closa et al confirm that the activation of alveolar macrophages played an important role in the neutrophil's chemotactic attraction to the lung alveoli, they also suggested that the liver played a vital role in the activation of the alveolar macrophages. This role of liver in acute pancreatitis will be discussed further in section 1.5. Apart from TNF-α mentioned above, macrophage inflammatory protein-2 (MIP-2) and interleukin-8 (IL-8), another chemokine, have been shown to be upregulated within the lung parenchyma during surgical trauma or in patients with ARDS (152, 153). All these cytokines and chemokines act as potent chemoattractants between neutrophils and alveoli, causing the microscopic changes of leukocyte sequestration.

The other important immuno-modulator which has been shown to enhance the recruitment of neutrophils in the lung is ICAM-1 (CD54). Because of the augmentation of the pro-inflammatory response during acute pancreatitis, large amounts of inflammatory mediators were released into the systemic circulation, and subsequently distributed within the lung parenchyma. Frossard et al have shown that ICAM-1 was significantly upregulated within the lung parenchyma during acute pancreatitis (94). As mentioned in section 1.4.2.2 regarding the relationship of the upregulation of ICAM-1 and neutrophil recruitment among pancreatic acinar cells, significant reduction in lung injury and the severity of acute pancreatitis was observed when either neutrophils were depleted or ICAM-1 knockout mice were used for the induction of acute pancreatitis (94, 154). However, the combined effect of both neutrophil depletion and ICAM-1 deficiency did not have synergistic effect in the degree of local or remote organ inflammation during acute pancreatitis. This suggests that other mechanisms apart from neutrophil infiltration play a role in the severity of the disease process.

ICAM-1 (CD54) expression on the surface of endothelial lining interacts with macrophage-1 antigen (MAC-1) on the neutrophil surface. MAC-1 is a complement receptor consisting of 2 integrins, CD11b and CD18. This forms an important first step in the sequential events involving leukocyte migration during acute inflammation. A similar upregulation of MAC-1 on neutrophils was illustrated in *in vivo* experiment by incubating normal neutrophils with serum or ascitic fluid from acute pancreatic rodents. With the activation of neutrophil–ligand interaction with ICAM-1, conformational

changes of the actin cytoskeleton of neutrophils further enhanced the entrapment of neutrophils within the alveolar-endothelial capillary bed leading to pulmonary congestion (155), which is an early histological sign of lung injury.

As TNF-α is one of the first cytokines upregulated during acute pancreatitis (section 1.4.2.4), this circulating cytokine stimulates alveolar macrophages to produce more pro-inflammatory cytokines, as described earlier, via a p38 mitogen-activated protein (MAP)-kinase activated pathway (156). The production of local TNF-α will increase the phosphorylation of IκB to allow translocation of transcriptional factor NFκB to nuclei for binding to the promoter gene of ICAM-1. This positive feedback loop will augment the production of ICAM-1, and enhance further recruitment and entrapment of neutrophils to this remote site.

With the accumulation of activated neutrophils through the mechanisms discussed above, a perfect environment for the release of reactive oxygen species (ROS) and proteolytic enzymes, such as elastase, is provided. The release of the ROS damages the underlying lung parenchymal tissue. Not only does the release of ROS and enzymes cause damage to the pulmonary tissue, large amounts of blood coagulation-promoting substances are released by pulmonary epithelial and endothelial cells (157). All these responses promote an increase in pulmonary vascular resistance and permeability as well as pulmonary oedema, and finally cause full-blown symptoms and signs of ALI (158).

1.4.3.2 **Role of alveolar macrophages in bacterial clearance in SIRS / Acute Pancreatitis**

Being a resident macrophage, the alveolar macrophage is situated at the air–tissue interface within the alveoli. The alveolar macrophage strategically behaves very differently from other resident macrophages in that it encounters the micro-organisms directly from the outside world and functions as an important first-line innate immune defence mechanism against these micro-organisms. As a macrophage, one of the key features for this defence mechanism is its phagocytic capacity. Apart from phagocytosis, the alveolar macrophage also plays a vital part in immuno-regulatory functions upon appropriate stimulation. It exerts these functions mainly by the secretion of biologically active products, such as the cytokines, interleukins and complements described earlier. Its functions as an immuno-modulator have been extensively investigated in various models of lung disease (159).

Most of the evidence regarding the immune function of alveolar macrophages came from those studies of severe sepsis using a rodent model, namely caecal ligation and puncture (CLP). In an earlier study of bacterial clearance by alveolar macrophages in severe pneumonia, Broug-Holub et al discovered that alveolar macrophage phagocytosis was defective in Klebsiella pneumonia (160). Similar reduction of alveolar macrophage phagocytic capacity was demonstrated in studies using the CLP sepsis model (161, 162). Steinhauser et al further proposed that it was the anti-inflammatory cytokine, IL-10, which was responsible for the reduction of bacterial clearance by the alveolar macrophages (161). They induced Pseudomonas pneumonia 24 hours post-induction of

sepsis using the CLP sepsis model. To test their hypothesis, an anti-IL-10 serum was administered via the intra-tracheal route to the CLP group prior to the induction of Pseudomonas pneumonia. They discovered that the bacterial clearance ability was partly reversed after IL-10 was neutralized. These findings were corroborated by Reddy et al using the same sepsis model (163). Not only did Reddy et al suggest that IL-10 played a part in the defect of bacterial clearance by alveolar macrophages, they also revealed a significant reduction of pro-inflammatory cytokine secretion by the alveolar macrophages during sepsis in *ex vivo* experiments (163). Based on this *ex vivo* finding, the group hypothesized that pro-inflammatory cytokine secretion by alveolar macrophages was impaired *in vivo* during sepsis. However, a recent *in vivo* study by Traeger et al, using a similar sepsis model, suggested a different result (162): there was no significant difference in cytokine concentration within the lung parenchyma with or without depletion of alveolar macrophages during sepsis. This experiment concluded that the cytokine production within the lung parenchyma is independent of the presence of alveolar macrophages. This is therefore a direct contradiction to the *ex vivo* findings of Reddy et al. Given the influx of leukocytes in the lung parenchyma during sepsis, it is logical to extrapolate that the overall net production of pro-inflammatory cytokines by the overall leukocyte infiltration might have balanced-out the reduction of cytokine production by the alveolar macrophages alone (164). Unfortunately, Traeger et al did not specifically measure the cytokine secretion by the infiltrating leukocytes in their studies. Using a haemorrhagic transgenic mouse model, deficient in macrophage colony-stimulating factor-1, Lomas-Neira et al supported the fact that the net pro-inflammatory cytokine production was independent of the presence of alveolar macrophages (165).

Although no difference in terms of pro-inflammatory cytokine production was demonstrated with or without alveolar macrophage depletion, Traeger et al highlighted the role of alveolar macrophages for bacterial clearance within the lung parenchyma (162). They demonstrated a higher bacterial load within the lung parenchyma in the group where alveolar macrophages were depleted prior to the induction of sepsis. The total numbers of alveolar macrophages are therefore important to the eradication of inhaled pathogens. Another research group has also identified a significant increase in the apoptosis of alveolar macrophage during sepsis (166). The combination of the reduction of pro-inflammatory cytokines within the lung parenchyma and the reduction of alveolar macrophages through apoptosis might further explain the deficiency of its total bacterial clearance during SIRS.

With some of the basic similarities between SIRS/sepsis and severe acute pancreatitis, it is not unreasonable to extrapolate the findings discussed above from sepsis to severe acute pancreatitis. During this extrapolation of experimental findings, it is important to bear in mind that the current understanding of the function of alveolar macrophages in severe acute pancreatitis is limited and more investigations are needed to allow a full exploration of the role of alveolar macrophages during the disease process.

1.4.3.3 **Role of peripheral blood phagocytes in SIRS / acute pancreatitis**

The peripheral blood leukocyte plays an important role in bacterial clearance during bacteraemia. As mentioned in section 1.4.2.1, the first-hit and second-hit theory was recognized in observational clinical studies during severe SIRS/sepsis/acute pancreatitis – early multiple organ dysfunction and late nosocomial infection. Both human and animal studies demonstrated a decrease of peripheral blood neutrophil phagocytosis during severe sepsis (167). This late nosocomial infection could therefore be secondary to the deficiency of bacterial clearance during these acute events.

Holzer et al compared the phagocytic function of human peripheral blood neutrophils and the intra-peritoneal neutrophils in patients with peritonitis and those after elective abdominal surgery (168). They discovered a significant reduction of bacterial phagocytosis by the peripheral blood neutrophils at day 3 in the septic group. Similar findings were found by Simms et al using a swine CLP sepsis model (167). Simms et al compared the neutrophil biological function of the CLP septic group with those of sham laparotomy group. They discovered a significantly reduced neutrophil phagocytic capacity in the treated group versus the untreated group. However, there was a difference in approach between these two studies. The obvious difference was the subject of interests: Simms et al were based on an animal model, whereas Holzer et al measured the function in human subjects. Simms et al emphasized more on the investigation of neutrophil phagocytic capacity after the source of sepsis had been

eradicated, whereas Holzer et al measured the phagocytic capacity when there was ongoing sepsis.

Similar research was also studied in human acute pancreatitis by Liras et al (169), who compared peripheral leukocyte phagocytosis in patients with mild or severe acute pancreatitis. The study did not include any normal subjects as controls. A direct comparison of the biochemical and physiological findings of patients with acute pancreatitis and normal human subjects was therefore not feasible. Nevertheless, they discovered a significant reduction of neutrophil and monocyte phagocytosis among the severe acute pancreatitis (versus the mild pancreatic) group before day 3 from the onset of the disease; the leukocyte phagocytosis ability was comparable in the two studied groups by day 5.

Thus far, there is evidence from both human and animal studies that peripheral leukocyte phagocytosis is compromised at the early stage of SIRS/sepsis/acute pancreatitis. However, it is unknown regarding how leukocyte phagocytosis behaviour would alter during the whole disease process. It is thus uncertain whether leukocyte apoptosis would have any association with its corresponding phagocytosis behaviour.

1.4.3.4 **Opsonin receptor expression and leukocyte phagocytosis during acute pancreatitis**

Opsonization of pathogens by either complements or immunoglobulin facilitates ingestion of bacteria by phagocytes. Interaction between these immuno-complexes with phagocytes activates the circulating leukocytes, e.g. neutrophils. Surface opsonin receptors, such as CD11b/CD18, CD32 and CD16, play vital roles in the recruitment and activation of phagocytes. However, excessive activation of neutrophils or complements leads to remote organ failures via the neutrophil–endothelial cell adhesion cascade (170).

CD11b, a complement receptor 3, is involved in iC3b binding, phagocytosis and reactive oxygen production (171). Its neutrophil–epithelial binding ability provides a vital role in neutrophil transmigration (172). Neutrophil expression of CD11b is upregulated during acute pancreatitis (173-175), and is associated with an increased influx of neutrophils within the lung parenchyma during acute pancreatitis (176, 177). This activation of CD11b could therefore be one of the mechanisms resulting in remote lung injury, as discussed in section 1.4.3.1.

To further illustrate that neutrophil activation is important to the severity of acute pancreatitis, Hac et al demonstrated an attenuation of pancreatic inflammatory process when CD11b was selectively blocked by a monoclonal antibody (178, 179).

Interestingly, CD11b expression of peritoneal neutrophils was found to be downregulated in the severe versus mild acute pancreatitis, despite an upregulation of its expression in peripheral blood neutrophils among the severe group (180). Authors further speculated that these "underactive" peritoneal neutrophils around the inflamed pancreas might contribute to local infectious complications, whereas the activation of peripheral neutrophils via CD11b might contribute to remote organ injuries. The role of CD11b is certainly important but remains largely unclear. In addition to investigating CD11b, Hatano et al also looked at the expression of CD32 and CD16 in peripheral blood neutrophils (180). Having previously been shown to play a role in activating phagocytosis and bacterial clearance, CD16 and CD32, which are immunoglobulin G Fc receptors II and III respectively, have been found to have a similar response as CD11b during acute pancreatitis (181, 182). However, their upregulation response is less marked than that of CD11b.

With the activation of peripheral leukocytes during acute pancreatitis, it is unclear whether this activation has any positive impact on improving peripheral leukocyte phagocytic capacity. Research on this topic is limited. However, most findings suggest a defective leukocyte phagocytosis, despite an upregulation of opsonin surface receptors during either sepsis or acute pancreatitis (168, 169).

1.4.3.5 **Peripheral leukocyte apoptosis/necrosis during SIRS / acute pancreatitis**

Apoptosis, a programmed cell death, is an essential homeostatic process in which cells are removed in a controlled manner to minimize damage to the surrounding environment. This process is triggered via either an intrinsic or extrinsic pathway. Detailed discussion of these pathways is beyond the scope of this chapter. Briefly, the intrinsic pathway is activated by mitochondrial injury and is mediated by caspase 9 (183-185); whereas the extrinsic pathway is activated via surface receptors to inducing-factors (e.g. TNF-α, Fas, etc.) and is mediated by caspase 8 (183-185). Both caspase 8 and 9 will ultimately activate caspase 3, by which the execution phase of apoptosis is undertaken (i.e. a step at which there would be no return for the apoptotic process).

Throughout the last decade, there has been a substantial increase of research on apoptosis. It is becoming clear that apoptosis plays vital roles in inflammatory processes. Some of the roles of apoptosis in the inflammatory process are discussed in section 1.4.4. Lymphoid and, to a slightly lesser extent, myeloid immune cell types have been the focus of apoptotic study during sepsis, mainly because their apoptotic processes are easier to detect than non-lymphoid or non-immune tissues (186). Again, most of this work was done utilising septic animal models, rather than specifically looking at acute pancreatitis. Since the report by Nishikawa et al that pancreatitis-associated ascitic fluid induces apoptosis in other cell types, there has been increasing interest in studying acinar-cell apoptosis in relation to the severity of acute pancreatitis (187-189).

Nearly all studies of peripheral blood leukocyte apoptosis during acute pancreatitis revealed a delayed neutrophil or lymphocyte apoptosis during the disease process. As neutrophil involvement has been shown to directly correspond to the severity of the acute pancreatitis (99, 179, 190-194), the delay in leukocyte apoptosis has been suggested to be the cause of the increased neutrophil involvement.

Lymphocyte apoptosis in SIRS / acute pancreatitis

The first evidence that lymphocytes played a role in acute pancreatitis was back in the 1980s, when T-cell lymphocytes were found in significantly reduced numbers during acute pancreatitis (195, 196). There is increasing evidence suggesting that sepsis is associated with a reduction in the total lymphocyte counts, possibly through apoptosis. One of the important evidence came from Hotchkiss et al (197, 198), who discovered that mortality increased significantly when sepsis secondary to caecal ligation and perforation was induced in lymphocyte-deficient mice (198). At the same time, they also demonstrated that the increase in survival is associated with a reduction of lymphocyte apoptosis mediated either by over-expression of Bcl-2 (antiapoptotic mitochrondrial protein) in transgenic model or by downstream caspase inhibition (197). The absolute lymphocyte count was also found to be reduced in subjects with severe acute pancreatitis as compared to those with mild disease or normal subjects in both humans and animal models. Takeyama et al demonstrated that this reduction was due to lymphocyte apoptosis (199). Another, similar study by Salomone et al also suggested that there is

lymphocyte apoptosis throughout acute pancreatitis. However, lymphocyte apoptosis was significantly dampened among the severe group versus the mild/control groups (200). This is in contradiction to the results obtained by Takeyama et al and similar studies in sepsis models.

Lymphocyte apoptosis is not only confined to peripheral blood during sepsis. Splenic lymphocyte apoptosis was identified in septic mice, which was shown to be associated with mortality (201, 202). A similar phenomenon of splenic lymphocyte apoptosis did not occur in a rodent pancreatitis model (203). However, functional alterations of splenocytes were demonstrated by the same research group (204). Ueda et al demonstrated a significant reduction of cytokine secretion (IL-2, interferon-γ, and IL-10) by splenocytes in severe acute pancreatitis. They further speculated that this alteration of splenocyte function could contribute to the subsequent septic complications of acute pancreatitis.

Interferon-γ (IFN-γ) is a cytokine that is critical for innate and adaptive immunity against viral and intracellular bacterial infections and for tumour control. IFN-γ is predominatedly produced by CD4 and CD8 cytotoxic T-helper cells. The importance of this cytokine in the immune response is secondary to its immunostimulatory and immunomodulatory effects. IFN-γ exerts these effects through its potent macrophage activation, and the induction of T-helper type 1 (Th1) response. Using a CLP sepsis

model, Hotchkiss et al adoptively transfer either apoptotic (irradiated) or necrotic (freeze thaw) splenocyte to C57BL6/J mice. They demonstrated a survival benefit when there was a transfer of necrotic splenocyte versus apoptotic splenocyte. This benefit was reversed when IFN-γ was blocked in a transgenic model or by anti-IFN-γ antibody (205). This suggested that the survival benefit could be due to the effect of IFN-γ. Identifying this role of IFN-γ is particularly interesting because of its potential role as a therapeutic target.

Overall, there is a plausible role of lymphocyte apoptosis in association with a more severe form of acute pancreatitis. Similarities of lymphocyte apoptosis have also been demonstrated between SIRS/sepsis and acute pancreatitis. Despite the demonstration of a trend that there is a survival benefit to those with acute pancreatitis to be gained by reversing lymphocyte apoptosis, research regarding how lymphocyte apoptosis might alter outcome remains scarce.

Neutrophil apoptosis in SIRS / acute pancreatitis

Neutrophils possess potent oxidative and proteolytic potential, which is usually the first line of defence against invading pathogens. With it contributing significantly to remote organ dysfunctions (section 1.4.3.3), it is crucial to understand the mechanisms through which neutrophil activation can be reduced to alter its damaging effect, but to retain its beneficial quality.

In contrast to the biochemical response of lymphoid cells, spontaneous neutrophil apoptosis was delayed during SIRS/sepsis (206, 207). Fialkow et al proposed using the delay of neutrophil apoptosis as a biological marker for the severity of the sepsis (208). The exact mechanism of neutrophil apoptosis in sepsis is complex and not completely understood. It was thought to be due to the interaction of various pro-inflammatory mediators such as TNF-α, IFN-γ, granulocyte colony-stimulating factor (G-CSF), granulocyte-macrophage colony-stimulating factor (GM-CSF) and IL-2 (209-213). In normal circumstances, these mediators were known to induce apoptosis instead of delaying the process (214). Interestingly, when GM-CSF and IL-10 were antagonized by their corresponding monoclonal antibodies, the initial delay of neutrophil apoptosis secondary to SIRS response was restored (215, 216). Cox et al, using peripheral blood neutrophils with broncho-epithelial cell-derived conditioned media, also demonstrated similar findings (211). Fanning et al further discovered that neutralization of GM-CSF and IL-10 in plasma of patients with SIRS was associated with a reduction of reactive oxygen species production (216). To complicate matters, van den Berg et al demonstrated that this delay in neutrophil apoptosis by TNF-α is concentration-dependent (217). They discovered that neutrophils underwent apoptosis when TNF-α concentration was high enough to produce a respiratory burst.

A similar finding of delaying neutrophil apoptosis has also been noted within 24 hours from the onset of acute pancreatitis (218, 219). O'Neill et al revealed a resistance in FAS

antibody-induced neutrophil apoptosis during the disease process (218). A decrease of pro-caspase 3 within the cytoplasm during acute pancreatitis was also reported, suggesting a possible increased conversion of pro-caspase 3 to activated-caspase 3. Since the activation of caspase 3 represents an inevitable process for apoptosis, the increased conversion of pro-caspase 3 should lead to an increase of neutrophil apoptosis. This logical extrapolation contradicts the findings of reduction in neutrophil apoptosis in the study. Unfortunately, the authors did not quantify the activated caspase 3 within the neutrophil cytoplasm in their study. Further studies would therefore be required to determine the significance of reduced pro-caspase 3 in apoptosis-resistant neutrophils.

More recently, Chen et al discovered that melatonin, a potent anti-inflammatory agent, could reduce the activation of neutrophils via CD18, as well as partially restore the characteristic of spontaneous neutrophil apoptosis during both moderate and severe acute pancreatitis (219). Although there was some restoration of spontaneous neutrophil apoptosis, melatonin did not reverse the delay of neutrophil apoptosis in the pancreatic groups to the level of normal controls. Whatever the mechanism may be that melatonin exerts on neutrophils, melatonin would not be solely responsible for the delay of neutrophil apoptosis during acute pancreatitis.

All investigations of neutrophil apoptosis focused on the early stage of acute pancreatitis. Limited knowledge is available in the literature regarding the dynamic

mechanism of neutrophil apoptosis subsequent to the initial pancreatic insults. The understanding of how neutrophils behave in the middle or late stages of the disease process could provide useful information regarding how acute pancreatitis resolves.

1.4.4 Resolution Phase of Acute Pancreatitis

Acute pancreatitis is an acute inflammatory process. Resolution of acute pancreatitis is an important phase of the disease. As mentioned in previous sections, most of the therapeutic intents and investigations of acute pancreatitis had been aiming at counteracting the acute response during the initiation and propagation phase of the disease (sections 1.4.1 and 1.1.1). In comparison, there has been little investigation in this resolution phase of the disease process.

Over the last decades, significant progress has been made in the understanding of how acute inflammation resolves. One of the key factors for this evolution is through the increasing knowledge of apoptosis, which has been touched on in section 1.4.3.5. There is now evidence of pancreatic acinar-cell apoptosis during acute pancreatitis. Further studies looking at the severity of acute pancreatitis have suggested that the severe form of the disease process is associated with necrosis, whereas the mild form is associated with apoptotic cell death (220, 221). With these observations, there have been some changes in the research direction of acute pancreatitis to investigate the apoptosis of the acinar cells during the inflammatory process. However, the investigation of leukocyte/phagocyte apoptosis during acute pancreatitis remains limited.

Phagocytes, such as neutrophils, monocytes and macrophages, have been shown to be heavily involved during acute inflammation. One of their main roles is to eliminate

intruders and cell debris. However, the by-product of all their involvements is excessive pro-inflammatory response, as explained in previous sections. To safely remove all these "professional" phagocytes once they have served their purpose of eliminating intruders, researchers have identified a tight regulatory process between neutrophils, monocytes and macrophages towards the end of an acute inflammation in order to exert a "brake" on the inflammatory process. In broad terms, this "braking" process involves a) limiting the recruitment of neutrophils; b) further signalling to dampen the activation of neutrophils; c) a neutrophil self-elimination process through apoptosis; and finally d) the clearance of neutrophil apoptotic bodies through macrophage phagocytosis to restore haemostasis. These processes are complex. It is therefore beyond the scope of this thesis to discuss all the stages involved in the resolution of acute inflammation. Neutrophil apoptosis in acute pancreatitis / sepsis has also been discussed in section 1.4.3.5.

1.4.4.1 **Macrophage restoration of homeostasis**

Once a neutrophil undergoes apoptosis, it will express "eat me" signals at the cell surface to allow phagocyte recognition. One of these cell surface signals is phosphatidylserine, which is one of the best-studied markers of apoptosis (222). In addition to the clearance of microbial intruders, macrophages play a vital role in the uptake of apoptotic neutrophils. Macrophages will in turn secrete mediators to suppress local inflammatory responses. Macrophage phagocytosis of apoptotic neutrophils has been shown to increase the production of anti-inflammatory mediators, such as TGF-β,

but inhibit the production of pro-inflammatory cytokines (such as TNF-α, IL-1β, GM-CSF etc.) (223, 224).

Although the clearance of apoptotic neutrophils by macrophages allows a localized suppression of the pro-inflammatory response and therefore protects the surrounding healthy tissues, these secreted anti-inflammatory mediators can potentially dampen the anti-microbial mechanisms. Recent studies by Medeiros et al demonstrated an impairment of alveolar macrophage bacterial phagocytosis after instillation of apoptotic cells into the lung parenchyma (225). This phenomenon suggests that the timing of the initiation of the repair process can potentially dictate the likelihood of bacterial infection during resolution of acute inflammation, and therefore the outcome.

In summary, the recruitment and clearance of neutrophils plays a central role in both triggering and resolution of acute inflammation in general. The interactions among phagocytes and the subsequent phagocytosis of apoptotic cells by phagocytes creating an anti-inflammatory condition are crucial for the success of the resolution of acute inflammation. It is therefore important to understand the timing of the phagocytosis of apoptotic bodies that will allow a successful resolution of acute inflammation, but not to create an anti-inflammatory environment for microbial infection. Further, it is important to demonstrate that the above phagocytic response also occurs during an episode of acute pancreatitis.

1.5 The Liver and Acute Pancreatitis

1.5.1 Role of the Liver during Acute Pancreatitis

When it comes to dealing with the remote organ dysfunction during severe acute pancreatitis, most investigators focus on the acute pulmonary response as the surrogate marker. Given the hepatic Kupffer cells host the major source of inflammatory cytokines in the liver (226, 227), and that all the blood supply from the gastrointestinal tract passes through the hepato-portal system before returning to the systemic circulation, it would be logical to postulate the theory that the liver functions as a source organ to augment the pro-inflammatory response, and therefore contribute to the remote organ dysfunction during an episode of acute pancreatitis (151, 228-230).

This theory was supported by Closa et al when they demonstrated a reduction in lung injury within a hepato-cava shunting group compared to a control group in an intra-ductal sodium taurocholate infusion pancreatitis model (151). This role of the liver in remote organ injury was further illustrated when Kupffer cell function was blocked by gadolinium chloride during acute pancreatitis (230, 231). When Gloor et al sampled serum from the portal and hepatic veins and the systemic circulation; they discovered a significant elevation of serum concentration of pro-inflammatory cytokines in the hepatic vein as well as the systemic circulation in the acute pancreatitis group after gadolinium chloride treatment. These findings suggested that the liver has a role in altering the pro-inflammatory response during acute pancreatitis.

To further establish whether the Kupffer cell was the only prime suspect in provoking the pro-inflammatory response during acute pancreatitis, Pastor et al hypothesized that the combination of neutrophil depletion and blockade of Kupffer cell activity would reduce the remote organ injury (100). They compared the local and remote organ inflammatory responses between the neutrophil-depleted group, the Kupffer cell inactivation/gadolinium group, and the combined neutrophil-depleted/gadolinium group. Although there was reduction of systemic IL-6 and IL-10 in the gadolinium group, lung permeability and cytokine concentration were not significantly reduced compared with the neutrophil-depleted group. They confirmed that activated neutrophils aggravate organ injury in acute pancreatitis, whereas it was less obvious after the inactivation of Kupffer cells.

1.5.2 HAEMOXYGENASE-1 AND ACUTE PANCREATITIS

In addition to inflammatory cytokine production, oxidative molecules, such as reactive oxygen species (ROS), are produced by inflammatory cells during acute pancreatitis. They react with the adjacent structures or cells causing damage at various levels. There is evidence that ROS play a role in various inflammatory disease processes, including acute pancreatitis (76, 232). The majority of these studies have investigated the oxidative stress response within 24 hours from the induction of acute pancreatitis. The nature of the oxidative stress response during later phases remains largely unknown.

In order to counterbalance the oxidative damage from ROS, anti-oxidants are produced and consumed by the surrounding tissues. Haemoxygenase (HO) is one of the most highly conserved molecules across all forms of life. It is an anti-oxidant as well as one of the heat shock proteins, HSP-32. There are three different isoforms of haemoxygenase. HO-1 is an inducible isoform, whereas HO-2 is constitutively synthesized; and HO-3 is only recently discovered.

The main role of HO is to degrade haem proteins. Apart from playing important physiological functions such as oxygen transport, mitochondrial respiration and signalling transduction (233), haem also exerts cytotoxic activity via the formation of ROS and lipid peroxidation (234-236). HO degrades haem to form an equal molar quantity of carbon monoxide (CO), iron and biliverdin, which is subsequently reduced to bilirubin via biliverdin reductase.

HO-1 is located within the cytoplasm, and is inducible by more diverse stimuli than any other enzyme described to date (237). Most of the inducers for the upregulation of HO-1 lead to oxidative stress. Among all three isoforms, HO-1 has been the most characterized. Its role as an anti-oxidant during the inflammatory process has been extensively studied. Its function to exert a cytoprotective effect is undisputable, especially in solid organ transplantation (238-241) and cardiovascular research (242). In

the ischaemic/reperfusion pancreatitis model, there was significant reduction of microcirculation within the pancreas compared with the control group. By the use of cobalt protoporphyrin to induce HO-1 prior to induction of ischaemia/reperfusion, the functional capillary density of the pancreas was found to be comparable to the control; whereas this protective effect was diminished when tin protoporphyrin, an HO-1 inhibitor, was used in conjunction with cobalt protoporphyrin (243). This suggested that there is a protective role of HO-1 within the pancreas parenchyma during acute pancreatitis.

However, the role of this molecule during acute pancreatitis has not been extensively studied. Given that HO-1 has been demonstrated to play a significant role in cellular protection against metabolic insults, it is therefore not unreasonable to investigate the role of this molecule in acute pancreatitis (244-246). Although there is a close link between the function of the liver and severe acute pancreatitis, the role of HO-1 regulation and its association with ROS production in the liver during the disease process are unclear.

2 AIMS AND HYPOTHESES

Most studies of acute pancreatitis to date have focused on the initial systemic and remote inflammatory responses. Little is known about what happens during the resolution phase of the disease. To study this resolution phase of acute pancreatitis, the first aim was to establish a robust rodent pancreatitis model, which could provide adequate severity to study the severe state of the disease, but not too severe as to cause mortality, so that the resolution of acute pancreatitis could also be investigated.

Recent theories from sepsis studies suggested that there is a pro-inflammatory response at the beginning and a subsequent anti-inflammatory response at a later stage. It has been proposed that it is the uncontrolled pro-inflammatory response which leads to multi-organ dysfunction; whereas the later anti-inflammatory response contributes to an immuno-compromised state, and therefore increases the likelihood for nosocomial infection. Although there are similarities between severe acute pancreatitis and sepsis in observational studies, it is not clear regarding the balance of the "pro-" and "anti-" inflammatory responses during severe acute pancreatitis. One of the aims was therefore to investigate how these pro- and anti-inflammatory responses alter throughout an episode of acute pancreatitis.

As the lung is an end-organ frequently involved during severe acute pancreatitis, the investigation of the alveolar macrophages and lung immune response is therefore a

logical and reasonable surrogate marker for the remote organ inflammatory response throughout the disease process. The bacterial engulfment by phagocytes, cytokine production and inflammatory cell apoptosis or necrosis were used to investigate the dynamics of the pro- and anti-inflammatory responses throughout an episode of acute pancreatitis.

Provided that there is a pro-inflammatory response at the early stage and anti-inflammatory response at the later stage, it was therefore hypothesized that:

- Peripheral leukocytes survive longer and increase efficiency in bacterial engulfment at the early stage of the disease secondary to a pro-inflammatory state; and peripheral leukocytes undergo increased apoptosis/necrosis, and have a reduction in bacterial clearance secondary to an anti-inflammatory state at the later stage of acute pancreatitis;
- There is active alveolar macrophage phagocytosis at the early stage of acute pancreatitis, whereas phagocytosis is dampened at the later stage of the disease process;
- Given that the above hypotheses are correct, lung and systemic immune function correspond in a similar manner to each other during the whole episode of acute pancreatitis.

3 RODENT EXPERIMENTAL ACUTE PANCREATITIS MODELS

3.1 INTRODUCTION

The complexity of the biological systems underpinning the immune system, along with the heterogeneity of patients with acute pancreatitis, makes the elucidation of the pathophysiological mechanisms difficult. It is also difficult to fully investigate the pathophysiological process of acute pancreatitis in human subjects. Research using an appropriate rodent model is essential to further enhance the knowledge of the pathogenetic mechanisms in acute pancreatitis.

Two models of inducing acute pancreatitis, secretagogue- induced and arginine- induced acute pancreatitis, were used in this thesis. The characteritistic of the two models were briefly outlined in the following sections below.

- *Secretagogue-induced acute pancreatitis model*

Physiological concentrations of secretagogue trigger normal secretion from the pancreas. Using excessive exogenous secretagogue, the theory was that secretagogue stimulates high levels of digestive enzymes, resulting in acute pancreatitis. Caerulein is the most commonly used cholecystokinin analogue to induce acute pancreatitis. Not only did studies reveal comparable histological findings between caerulein-induced acute

pancreatitis in rodents and humans (247), acute pancreatitis was also shown to be induced effectively by caerulein in many animals including mice, rats, rabbits (123, 248) and dogs (249). The most common way for caerulein to be used as an induction agent is via serial intra-peritoneal injections. This relatively rapid, mildly invasive method with its high repeatability and applicability makes caerulein one of the most frequently used acute pancreatitis models in rodents.

Acute pancreatitis-associated lung injury in both mice and rats has frequently been reported to occur in the caerulein model (174, 250-254). This model is therefore a good model to use in the study of acute pancreatitis-associated lung injury.

- *Arginine-induced acute pancreatitis model*

The arginine-induced acute pancreatitis model was first introduced at the beginning of the 1990s. It has not been widely used in pancreatitis research compared to the caerulein model, and therefore arginine-induced acute pancreatitis is not as well characterized as caerulein-induced acute pancreatitis. The arginine-induced model is a relatively less invasive acute pancreatitis model compared to other models described in the literature thus far. It relies on a single intra-peritoneal injection of arginine to induce acute necrotizing pancreatitis. Intra-peritoneal injection of arginine has been shown to induce acute necrotizing pancreatitis in rats (255-262), rabbits (263) and mice (264). The exact

mechanism by which arginine induces acute pancreatitis remains unknown. Kishino et al proposed that arginine inhibited protein synthesis leading to acute pancreatitis (265).

In addition to its minimally invasive induction property, the severity of acute pancreatitis induced depends roughly on the dose of arginine injection and time of exposure. A mild degree of acute pancreatitis can be induced by a low-dose arginine injection (approx. 250mg/100g) (266), whereas necrotizing acute pancreatitis can be induced with a single high-dose arginine injection (400–500mg/100g) (255, 267). For the severe acute pancreatitis group, pulmonary injury had been reported to occur in this model (102, 259, 268).

Although both local and systemic changes similar to those in human acute pancreatitis are seen in this model, the clinical relevance of arginine-induced acute pancreatitis is not clear. Because of these uncertainties, this model was not chosen as the sole model to investigate the immune response in acute pancreatitis.

3.2 ETHICAL DECLARATION

This animal work covering the induction of acute pancreatitis has been reviewed by a local ethical committee and granted a Project Licence by Home Office United Kingdom (PPL 60/3228). The author of this thesis has completed the Personal Licensing Course for Animal Handling with the award of a Personal Licence Certificate (PIL 60/9568) to perform the experiments below. The maximum licensed dose for arginine intra-peritoneal injection is 500mg/100g for each individual rodent; whereas that for the caerulein injection is six consecutive hourly injections of 50μg/kg of caerulein.

3.3 PREPARATION OF L-ARGININE AND CAERULEIN

L-arginine (A5006, Sigma-Aldrich) was dissolved in 0.9% sterile normal saline to a final 20% concentration and was buffered to pH 7.35 using 5N hydrochloric acid. The solution was sterilized by 0.22μl syringe filter (Corning, UK) prior to injection. The L-arginine solution was freshly prepared immediately prior to the induction of acute pancreatitis.

1mg caerulein (C9026, Sigma-Aldrich, UK) was dissolved in 200ml 0.9% sterile saline to a final concentration of 5μg/ml. The solution was filtered for sterilization as above. 5ml aliquots of the mixture were stored at -20^{0}C until use.

3.4 STRAINS OF RODENTS

Wild-type rodents have mostly been used for the induction of acute pancreatitis in previously published literature (65, 269-272). In order to minimize the variation of immune responses secondary to wild-type genetic components, isogenic strains of rodents were chosen for the study. Provided that there is a successful development of both arginine- and caerulein- induced acute pancreatitis models in our research centre, mouse model will facilitate further development or investigation with the use of transgenic models. Both mice and rats rodents were therefore used simultaneously at the beginning of this dose ranging experiment.

For the rat model, the commercially available Fischer strain (Harlan, UK) was chosen for the induction of acute pancreatitis by both of the inducing agents. For the mouse model, Balb/C and C57 strains (BRF, Edinburgh Animal Welfare Unit, Edinburgh) were used throughout the dose-ranging experiments.

3.5 SPECIMEN HARVESTING

All animals were euthanized by intra-peritoneal injection of an overdose of phenobarbitone. Midline sternotomy and laparotomy was performed to gain access to the heart and abdominal organs. A 23G needle (BD Medical, UK) on a 10-ml Syringe (for rats) / 2-ml syringe (for mice) was used for cardiac puncture to exsanguinate the rodents. The whole blood was immediately transferred to a lithium (Li)-heparin blood

container and centrifuged for 10 minutes at 1,500rpm to separate the plasma and blood cells. Plasma was frozen at -70^0C until analysis.

The tail of the pancreas was identified at the hilum of the spleen. The whole pancreas was dissected free at the superior and inferior border towards the duodenum. The pancreas was transected longitudinally into two halves. One half of the pancreas was fixed in 4% formaldehyde for 24 hours prior to paraffin processing, and the other half was snap-frozen in liquid nitrogen, and was then stored at -70^0C till analysis.

The thyroid gland was dissected in the midline to expose the trachea. The trachea was mobilized from the oesophagus. A small transverse incision was made at the anterior trachea. A 14G (Brown) cannula was inserted via the opening and was secured by 4/0 silk suture. 4% formaldehyde was instilled to the lung until all areas of the lung were fully expanded. The trachea was ligated. The lungs were dissected free from the mediastum and surrounding tissues and immersed in 4% formaldehyde for a minimum of 24 hours prior to paraffin processing.

3.6 Tissue Processing and Preparation

Pancreas and lung tissues were embedded in paraffin wax. Tissues were dehydrated by sequential dehydration with 30%, 50%, 70%, 80%, 90%, and 100% ethanol for 2 hours

each. The tissues were cleared in xylene for 2 hours. The blocks were then immersed in xylene/paraffin solution at approximately 56–58^{0}C for 2 hours before the final immersion in paraffin. Tissues were embedded in paraffin blocks and sectioned at 4μm for light microscopy.

Haemotoxylin and eosin (H&E) staining of tissues

Tissue sections (4μm) were mounted on histological slides (BDH; Cat. No. 406/0286/00). Sections were deparaffinized in xylene, and sequentially rehydrated in 100%, 95%, 80% and deionised H_2O for 3 minutes each. Each slide was immersed in haematoxylin for 5 minutes, before being immersed in tap water for another 5 minutes. Each slide was then dipped in 1% acid-alcohol for a few times, prior to being rinsed in tap water and deionised H_2O for 1 minute each. Eosin was then used to stain the cytoplasm for another 30 seconds. A dehydration process followed eosin staining with 80%, 95%, 100% ethanol and then xylene (2 x 5 minutes) before sections were mounted in DPX mounting agent (BDH Poole, Dorset).

Plasma amylase analysis

Plasma was thawed from –70^{0}C and analysed by automated biochemical analyser (Roche/Hitachi 912). This method relies on the hydrolysis of 2-choloro-*p*-nitrophenyl-α-D-maltotrioside (CNPG3) by α-amylase to 2-chloro-4-nitrophenol, which is monitored

spectrophotometrically at 405nm. The other hydrolysis products include 2-chloro-4-nitrophenyl-α-D-maltoside (CNPG2), maltotriose and glucose. The rate of formation of 2-chloro-4-nitrophenol is proportional to the α-amylase activity within the plasma.

The principle procedure for the analyzer is as below. Briefly, 1ml of α-amylase reagent (Synermed, UK) was pipetted into the appropriate number of cuvettes for samples and for one blank. The cuvettes were transferred to a spectrophotometer and were equilibrated to 37 ± 1^0C. 25µl of plasma and control sample were pipetted into the cuvettes and were mixed; whereas 25µl of normal saline was pipetted into the blank cuvette. Absorbance at 405nm was recorded for each of the blank, plasma and control samples after 60 seconds and then again after 120 seconds. The differences in the absorbance values between 60 and 120 seconds were calculated to obtain the ΔA/nm value for each of the blank, control and samples. α-Amylase activity/concentration was then calculated.

3.7 Dose-Ranging Experiments For Arginine And Caerulein Acute Pancreatitis Models

For dose-ranging experiments, an arbitrary time-point of 48 hours post-injection was chosen, because most inflammatory changes of the pancreas would have occurred by that time point (255). Intra-peritoneal injection with 0.9% normal saline was used as

control. The total amount of normal saline used for injection in the control group was the same volume as the corresponding dose used in the treated groups based on the body weight of the rodent. To maintain a stable temperature throughout, all cages were placed on top of thermal blankets with thermostatic control. Subcutaneous injection of buprenorphine and normal saline were used for analgesic control and fluid replacement, whenever required. A total of 6 rodents were used per dose-ranging experiment – 2 for each treated group (Arginine or Caerulein) and 2 for each control group.

3.7.1 L-Arginine Induced Acute Pancreatitis – Dose-Ranging Experiments

3.7.1.1 **125mg/100g of buffered L-arginine**

125mg/100g of buffered L-arginine was injected via the intra-peritoneal route to both mice and rats. No deterioration of clinical signs was observed in either treated or control rodents at this dose for 48 hours following injection. There was no microscopic evidence suggesting any pancreatic injury at this arginine dose for either mice or rats at 48 hours following induction.

- *Remarks*

During the initial experiment, 20% *non-buffered* L-arginine solution was used for intra-peritoneal injection. Signs of back hunching, piloerection, increased corneal secretion, reduced interaction and peripheral shutdown developed within 4 hours post-injection.

All control and treated groups were euthanized according to Schedule 1 protocol. Pancreas, small intestines with mesenteries, lung, spleen and liver were all retrieved and fixed in 10% formaldehyde for histopathological diagnosis. The histopathology report revealed necrotic small bowel around the injection site, with no other inflammatory changes in other organs, including the pancreas. The cause of this adverse clinical response was secondary to chemical peritonitis and bowel necrosis. All L-arginine solutions were therefore buffered to pH 7.35–7.45 prior to injection after this initial experiment.

3.7.1.2 **300mg/100g of buffered L-arginine**

Buffered L-arginine at a dose of 300mg/100g was used on rats for this set of experiments. All L-arginine treated rodents were clinically unwell for a few hours immediately post-injection. They revealed signs of back hunching, piloerection, peripheral shutdown, and reduction in interaction during handling. All rodents survived up until the 48 hours time-point. At this arginine dose, there were histological changes in the rat pancreas, which were suggestive of severe acute pancreatitis. When compared to the normal pancreas, there was increased monocyte infiltration 48 hours after induction, oedema causing separation between pancreatic lobules, and necrosis of acinar cells (Figure 3-1). Mice were not used at this dose range.

3.7.1.3 **400mg/100g of L-arginine intra-peritoneal injection**

To establish the maximum dose of buffered L-arginine to induce the maximum severity of acute pancreatitis, but without leading to mortality, the dose of 400mg/100g of L-arginine was used in both rats and mice.

Treated rats deteriorated rapidly after injection and showed clinical signs as described in section 3.7.1.2. Instead of recovering from the initial insult as in the experiment described in section 3.7.1.2, there was one death within 24 hours from the initial injection. The planned experimental time-point at 48 hours was therefore abandoned. Schedule 1 procedure was performed on all treated rats and controls at 36 hours.

Macroscopic fat necrosis was noted within the peritoneal cavity, associated with retroperitoneal haemorrhage surrounding the pancreas. There was extensive acinar cell necrosis in pancreas histology, suggestive of severe acute pancreatitis. Alveolar congestion was also noted in pulmonary histology sections from the rat model. This suggested a possibility of an early acute lung injury. In contrast to the rat model, only a very mild degree of pancreatic inflammation was evident on examining mouse pancreatic histology. (See Figure 3-2.)

3.7.1.4 **350mg/100g rat of L-arginine for intra-peritoneal injection**

To allow fine adjustment of the maximum dose of L-arginine, 350mg/100g of L-arginine was used for the induction of the rat model. All treated rats were severely distressed thirty-six hours post-injection. The clinical severity was above the severity that was allowed within the project licence. All rats were euthanized by terminal anaesthesia at 36 hours. Pancreas H&E sections demonstrated acute inflammatory changes with acinar cell necrosis. No evidence of acute lung injury was seen in lung H&E sections. (See Figure 3-3.)

3.7.1.5 **500mg/100g of L-arginine intra-peritoneal injection for the mouse acute pancreatitis model**

500mg/100g of buffered 20% L-arginine dose was used on two different strains of mice – Balb/C and C57. Because of the unsuccessful induction of acute pancreatitis in mice using the previous arginine dose, this experiment was repeated on two separate occasions. The first experiment suggested acute inflammatory changes within the pancreas in the Balb/C strain. However, the repeated experiment on the Balb/C strain did not reveal the same degree of acute inflammation in the pancreas. No acute inflammatory changes within the pancreas were identified in the C57 strain on either occasion. (See Figure 3-4.)

a.

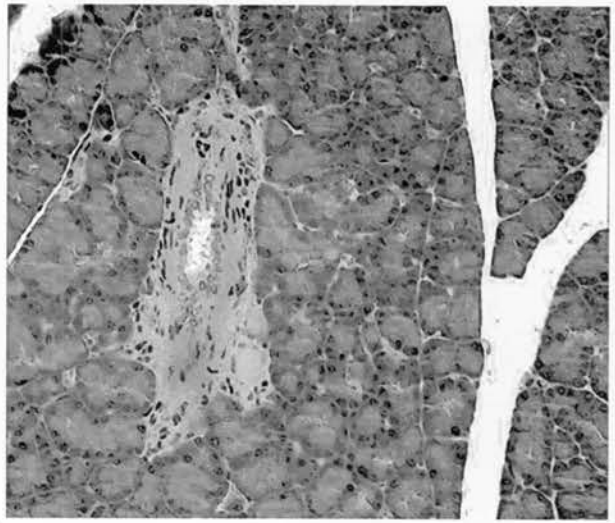

b.

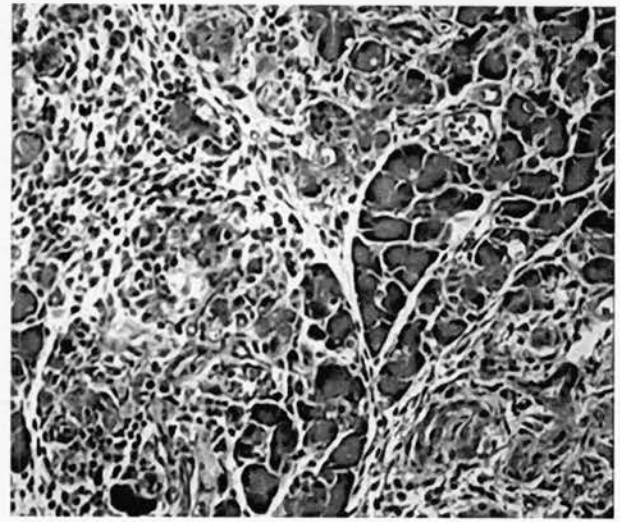

c.

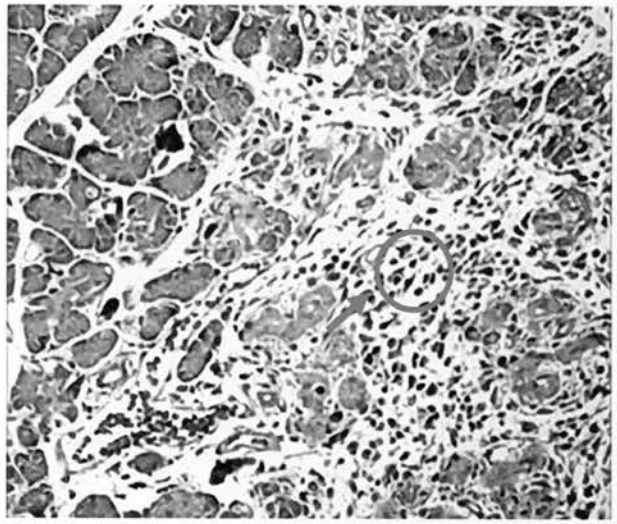

Figure 3-1(a) illustrates the H&E staining (x20 magnification) of a normal pancreas. (b) & (c) represent the H&E staining of the pancreatic section 48 hours after the ip injection of 300mg/100g arginine. There was evidence of infiltration of leukocytes (see arrows & circle). This was confirmed by immunostaining in Figure 3-9.

a.

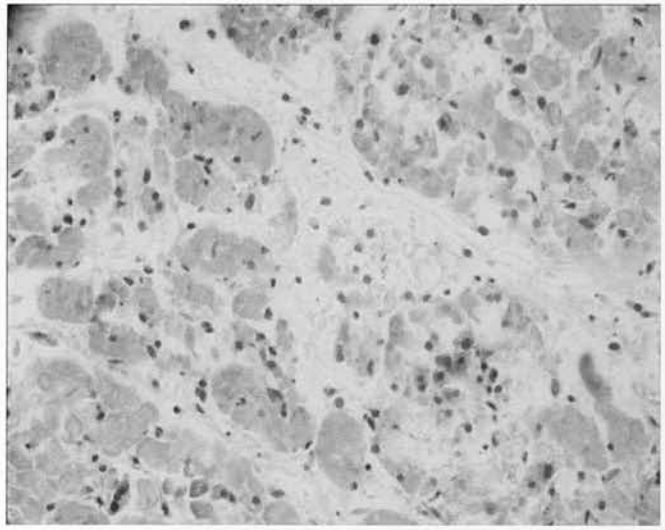

b.

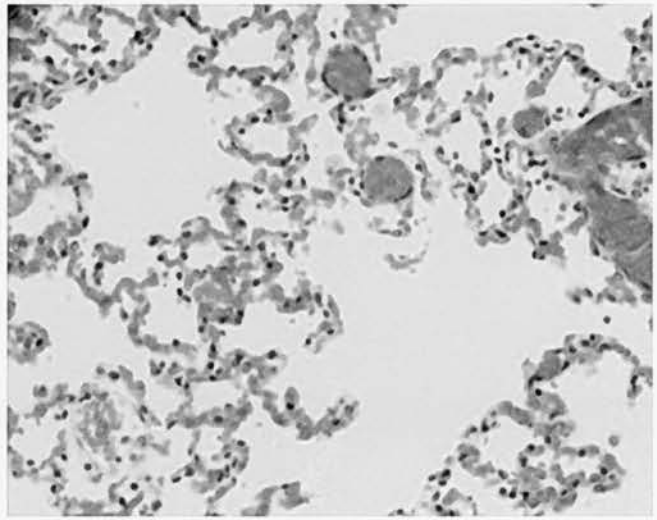

c.

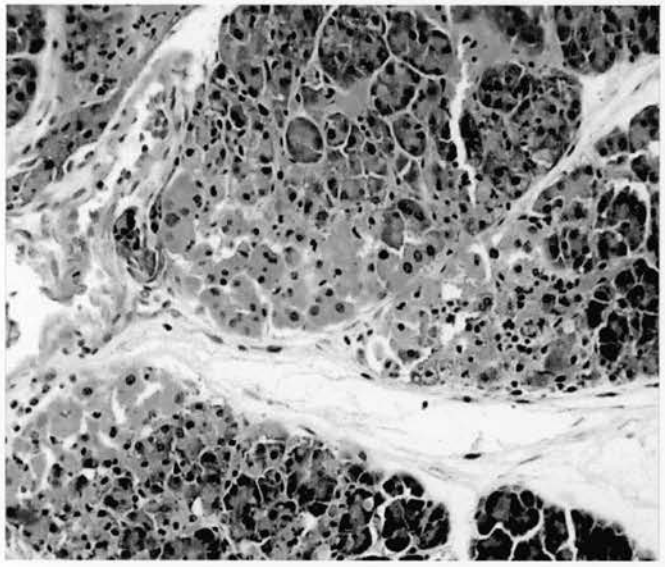

Figure 3-2 (a) illustrates the H&E staining (x20 magnification) of pancreas tissue 36 hours post 400mg/100g L-arginine ip injection. There was evidence of acinar cell necrosis. Pulmonary congestion was witnessed in the lung H&E section (b). Compared to the rat arginine model at 400mg/100g, there were significantly less acinar cell injuries in the mouse model (Balb/C) as illustrated in (c).

a. 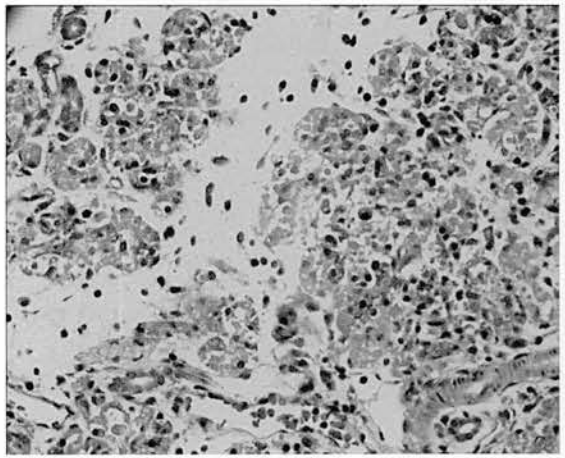

b. 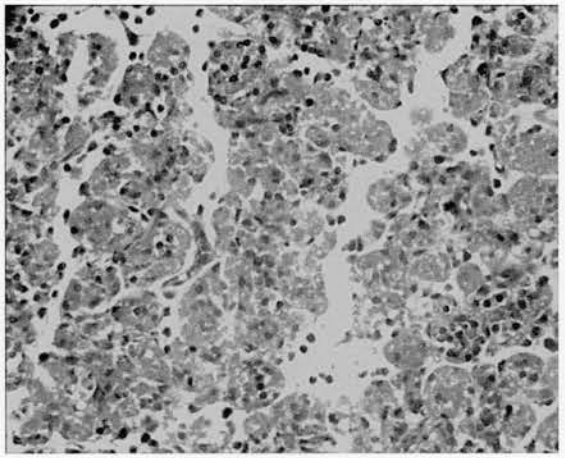

c. 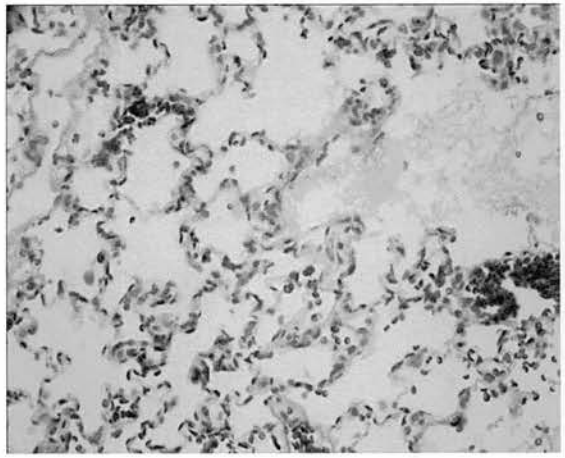

d. 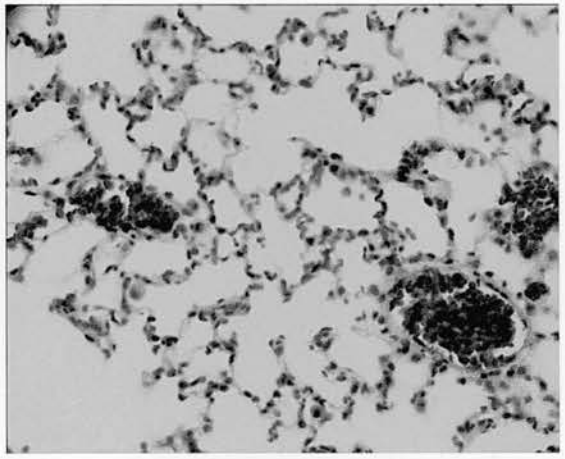

Figure 3-3 (a) & (b) illustrate the H&E staining (x20 magnification) of pancreas sections at an arginine dose of 350mg/100g in Fischer rats. There was evidence of acinar cell necrosis on the H&E sections. At the same arginine dose, there was no histological evidence suggesting any pulmonary injuries [(c) & (d)].

a.

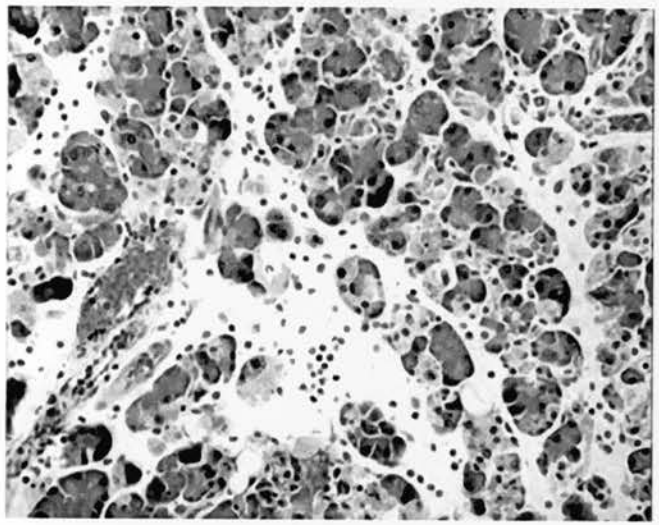

b.

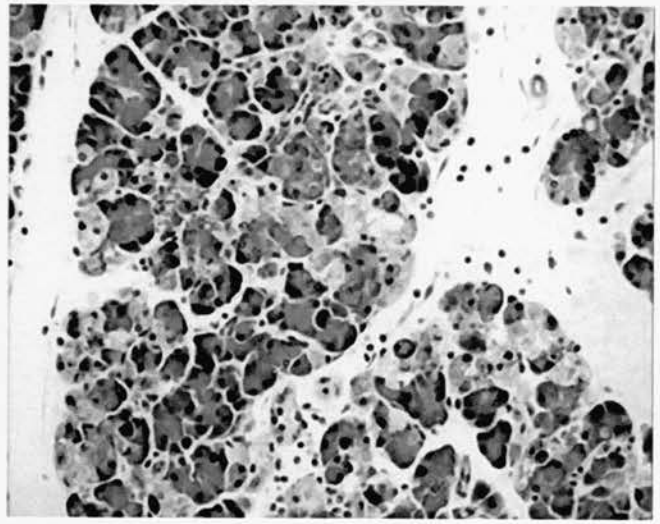

c.

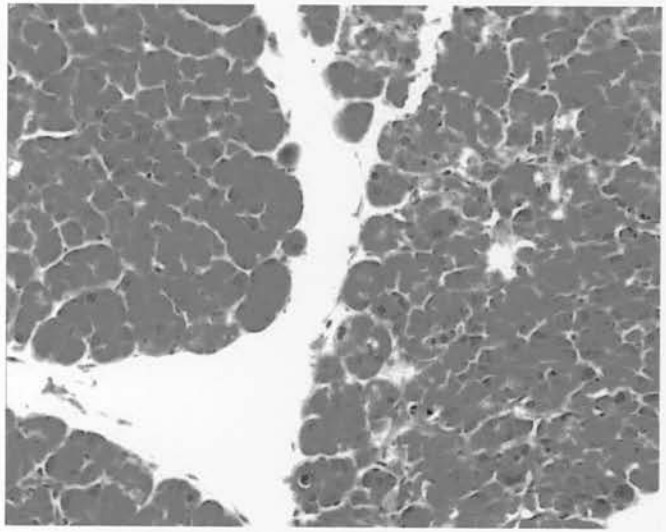

Figure 3-4. (a) & (b) illustrate the H&E (x 20 magnifications) stained pancreas sections of Balb/C strain 48h after arginine injection with a dose of 500mg/100g. Pancreatic acinar cellular injuries were minimal on repeated experiments (c).

3.7.2 CAERULEIN-INDUCED ACUTE PANCREATITIS

3.7.2.1 **50μg/kg x3 consecutive intra-peritoneal caerulein injections**

Three consecutive hourly intra-peritoneal injections were performed in this set of preliminary experiments. As with the previous protocol, 2 rodents (either rats or mice) were used for each treatment group, and all groups of rodents were euthanized at 48 hours following the initial caerulein injection. The same strains of rodents were used as in the L-arginine induction experiments.

Rodents demonstrated signs of distress after the initial two intra-peritoneal injections of caerulein. The signs were similar to those described in section 3.7.1.2. All of the treated rodents recovered rapidly by the last injection. None of the rodents demonstrated any histological evidence of acute inflammation of the pancreas at this caerulein dose.

3.7.2.2 **50μg/kg x6 hourly caerulein intra-peritoneal injections**

50μg/kg of caerulein was injected intra-peritoneally for six consecutive hours, and was tested in both the rats and the mouse models. Apart from the dose variation, all other experimental conditions were the same as previously described. There was microscopic evidence of inflammatory leukocyte infiltration and loss of acinar cells within the rat pancreas 48 hours post-injection (Figure 3-5).

Although there was acute pancreatic inflammation in the Balb/C mouse model at this dose, the degree of acute inflammation was mild when compared to the rat pancreatitis model (Figure 3-5). These inflammatory changes did not occur in the C57 mouse model.

a. 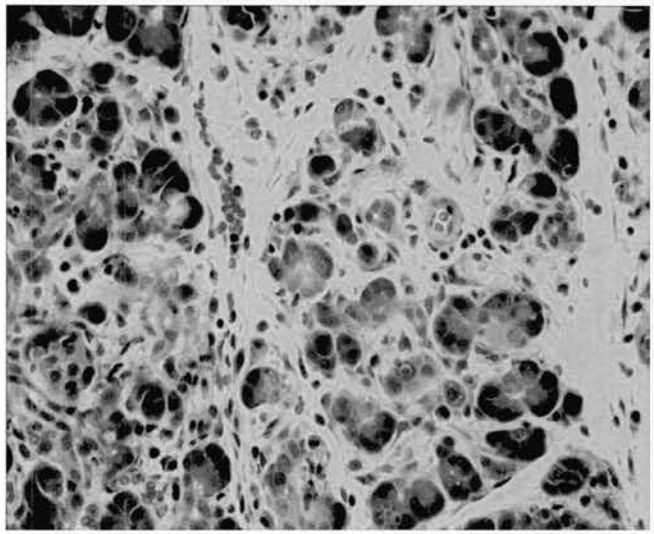

b. 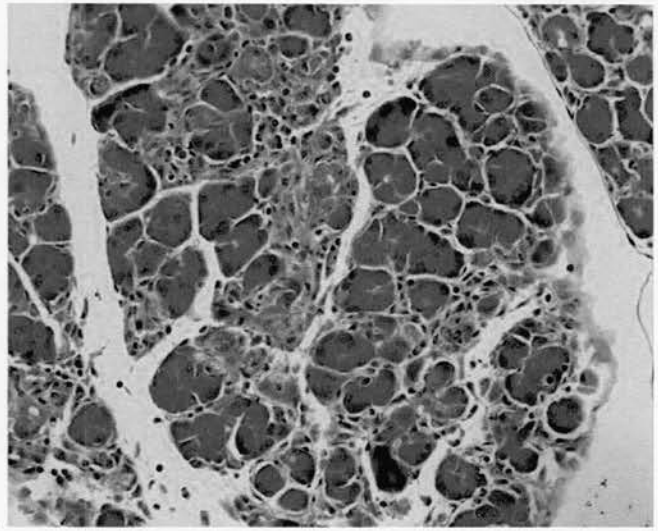

c. 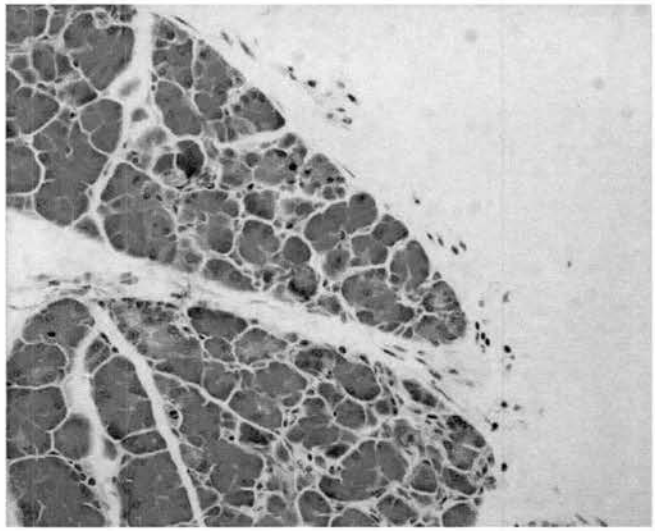

Figure 3-5 (a) illustrates the H&E staining (x20 magnification) of the rat pancreas 48 hours after 6 hourly ip injection of 50mcg/kg caerulein. (b) & (c) illustrate the H&E staining (x20 magnification) of the mouse (Balb/C strain) pancreas at the same caerulein dose as the rat model 48 hours after 6 hourly ip injections.

3.7.3 Resolution Of Acute Pancreatitis Model

According to Tani et al, the arginine model of acute pancreatitis resolves by day 14 following induction (255). For the purpose of our study, it was essential to ensure that acute pancreatitis of both the arginine and caerulein pancreatitis models could completely resolve within a set time-point.

Using the dose of 300mg/100g L-arginine and 50μg/kg x6 hourly caerulein injections, acute pancreatitis was induced as before. Due to difficulties in establishing the mouse acute pancreatitis within the licensed dose, only Fischer rats were used for the induction of acute pancreatitis. All treated rodents were euthanized at day 14. Resolution of acute pancreatitis was determined and confirmed, based on histology (Figure 3-7).

3.7.4 Statistical analysis

For both dose- ranging experiment and the full experimental time-points study, all three treatment groups (arginine, caerulein and control) were analysed by non-parametric Kruskal- Wallis ANOVA at each time point. P-value <0.05 is considered as statistically significance. SigmaPlot v11 (SyStat, USA) was used as the statistical package to perform the statistical analysis.

3.7.5 RESULTS OF DOSE-RANGING EXPERIMENT

3.7.5.1 **Amylase result of dose-ranging experiment**

During the dose-ranging experiment, only the plasma amylase level of the arginine and caerulein pancreatitis models at day 2 was analysed. The plasma amylase of the caerulein group at day 14 was not analysed because the result on day 2 for the caerulein group was not significantly elevated compared with the control (Figure 3-6). There was significant elevation of plasma amylase in the arginine group versus control on day 2 ($H(2)=8.19$, $p=0.005$). However, no statistical significance was achieved for the caerulein group versus the control at the same time-point.

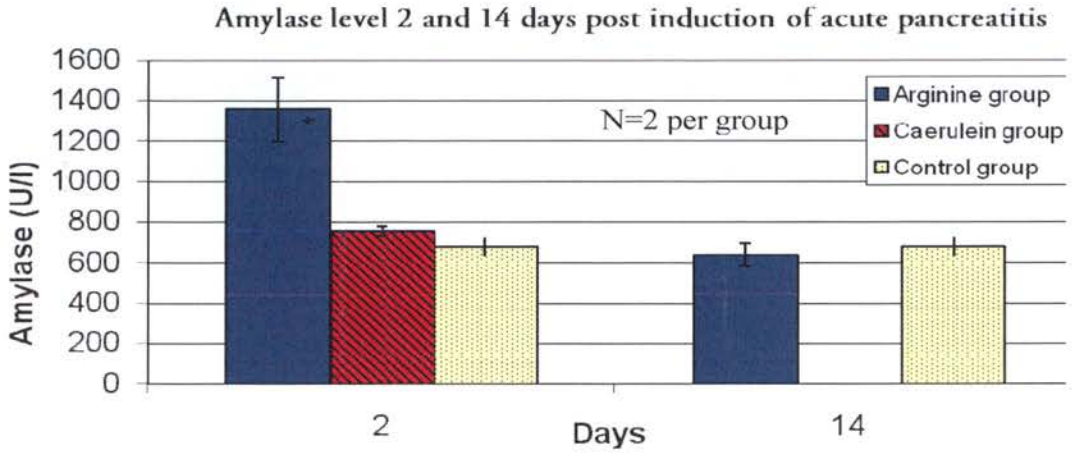

Figure 3-6 demonstrates the amylase results of both arginine (300mg/100g) and caerulein (50µg/kg x6 doses) induced acute pancreatitis at day 2 and day 14 as compared to the control during the dose-ranging experiments. Only the amylase result of the arginine group but not the caerulein group at day 14 is illustrated in this figure.

a.

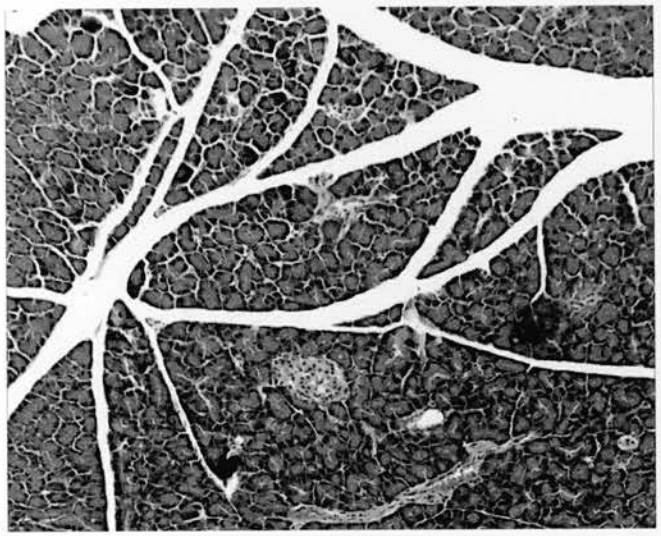

b.

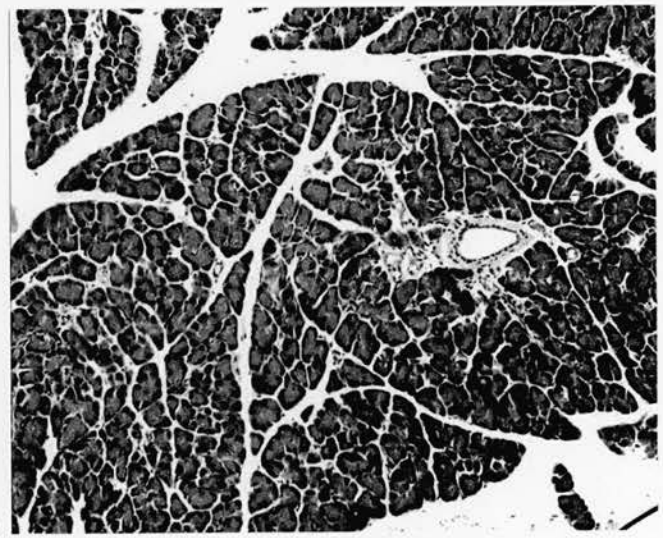

c.

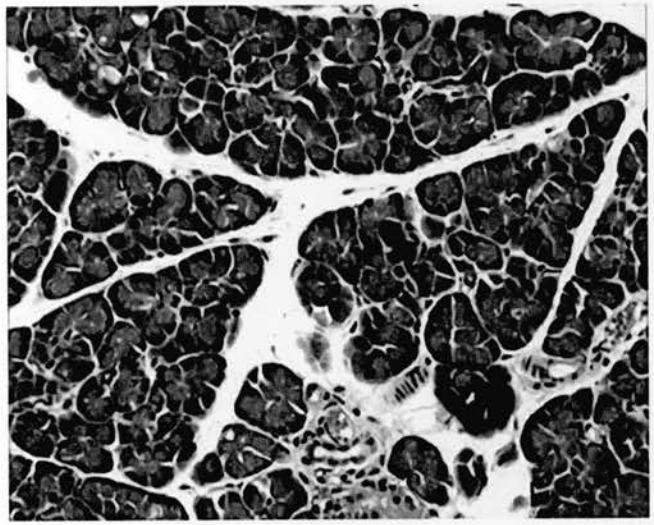

Figure 3-7 These pictures are H&E staining of the pancreas harvested on day 14 following the induction of acute pancreatitis. (a) illustrates H&E staining of the control (x20 magnification); whereas (b) & (c) are H&E staining of the pancreatic section of arginine (x20 magnification) and caerulein (x40 magnification) models at day 14 from the initial injections respectively.

3.7.6 IMMUNOHISTOCHEMISTRY OF PANCREAS DURING ACUTE PANCREATITIS

To further characterize the pattern of leukocyte infiltration and acinar cell injuries, immunohistochemical staining was performed on rat pancreas sections of acute pancreatitis models at 48 hours. Antibodies against cytokeratin-8, ED1 (MCA341PE, Serotec, UK), and cleaved caspase-3 (Catalogue No. 9661, Cell Signalling, UK) were used to stain for pancreatic acinar cells, monocyte/macrophages, and apoptotic cells, respectively.

Single immunostaining of pancreas section

4μm thickness of pancreas paraffin sections were exposed to an anti-CK8, anti-ED1, and anti-activated caspase-3, after paraffin removal, antigen retrieval and inhibiting endogenous peroxidase with 3% hydrogen peroxide. All primary antibodies were incubated for 1 hour at room temperature. The endogenous pancreas biotin was blocked with Avidin/Biotin kit (VectorLab, SP-2001). The sections were incubated with biotinylated secondary antibodies and streptavidin–biotin–horseradish peroxidase (HRP) complex (Dako, UK) for 30 minutes each. Phosphate-bufered saline (PBS) was used to wash the antibodies for 5 minutes in between steps. 3,3-diaminobenzidine (DAB) was then added for visualization. The sections were counterstained with haematoxylin. Hyperimmune mouse or rabbit serum was substituted for primary antibody as a negative control.

Table 3-1 Primary antibodies used

Primary antibody	Source	Isotype	Antigen retrieval method	Dilution
ED-1 (MCA341PE, Serotec, UK)	Mouse	IgG1	MW	1:300
CK-8 (in-house antibody)	Mouse	IgG1	MW	neat
Cleaved caspase-3 (Cat No. 9661, cell signalling)	Rabbit	IgG	MW	1:300

Secondary antibody	Source	Isotype	
Anti-mouse- biotinylated (Dako, UK)	Rabbit	Polyclonal	1:100
Anti-rabbit biotinylated (Dako, UK)	Goat	Polyclonal	1:100

NOTE: Abbreviation: MW, microwave irradiation for 3x 5 minutes in Vector Retrieval agents.

Dual-immunostaining of pancreas section

Dual-immunostaining of ED-1 and cleaved caspase-3, CK-8 and cleaved caspase-3 were performed as previously described (273). Antigen–Antibody reactions were visualized by alkaline phosphatase technique (APAAP), mouse DAKO REAL detection system for either CK-8 or ED-1 (K5000, Dako, UK) and 3, 3'-diaminobenzidine for anti-cleaved Caspase-3 (Dako, UK).

3.7.6.1 **Results of immunostaining**

Reduction of the acinar cells during acute pancreatitis

By 48 hours after the induction of acute pancreatitis, there was a significant reduction of the number of CK8-positive staining cells when compared to control rodents. This suggested a reduction in the total number of acinar cells in the acute pancreatitis model. When dual staining of CK8 and cleaved Caspase-3 was performed, there was co-staining of both antigens within the same cell, signifying that acinar cells underwent apoptosis during the disease process. (See Figure 3-8.)

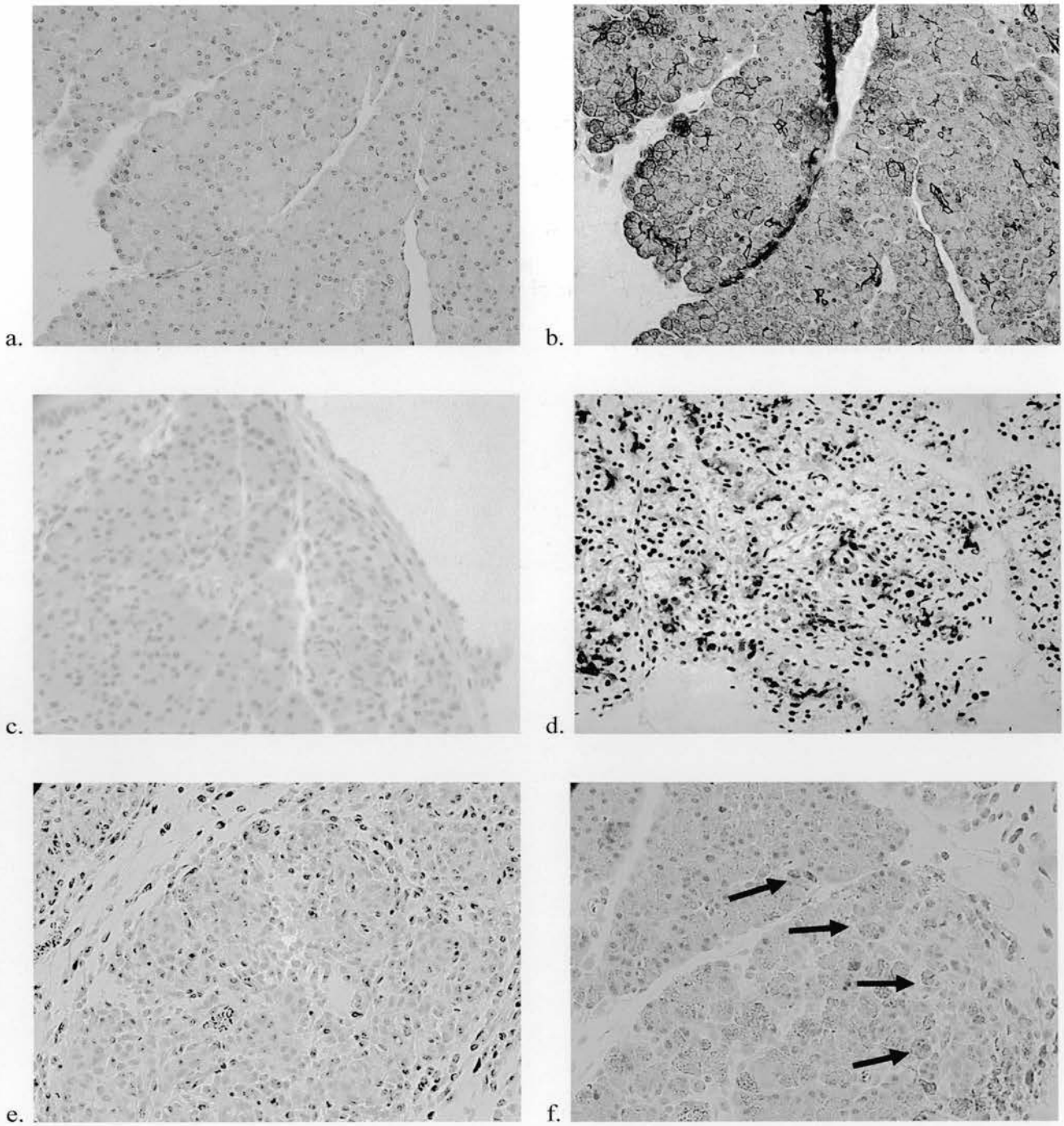

Figure 3-8 (a), (c) & (e) are the negative controls of (b), (d) & (f) respectively. (c), (d), (e) & (f) are from the same pancreatic rodent. (a) & (b) are pancreas sections of the control group (x20 magnification); whereas (c) & (d) are pancreas sections at 48 hours after the induction of arginine acute pancreatitis. (b) & (d) were stained with anti-CK8 alone. There was significant reduction of acinar cells during acute pancreatitis. (e) & (f) are sections (x20 magnification) stained with negative control and both anti-CK8 (red) & anti-cleaved caspase-3 (brown) antibodies. There is co-localization of both immunostainings [arrows at (f)], suggesting acinar cell apoptosis during acute pancreatitis.

Increased macrophage infiltration during acute pancreatitis

Whilst there was significant reduction in acinar cells, there was an increase in the infiltration of leukocytes by 48 hours during acute pancreatitis. The majority of this leukocyte infiltration was contributed by macrophage infiltration as evidenced by ED1-positive staining and the mononuclear morphology of the cells. When dual staining of ED1 and cleaved caspase-3 was performed, there was positive staining of both antigens. Limited co-localization of both antigens was detected within the same cells. However, due to the close similarities between the brown and red colours, and the fact that both antigens located within the same intracellular compartment, it was difficult to differentiate them based on chromogenic colour discrimination by light microscopy. (See Figure 3-9)

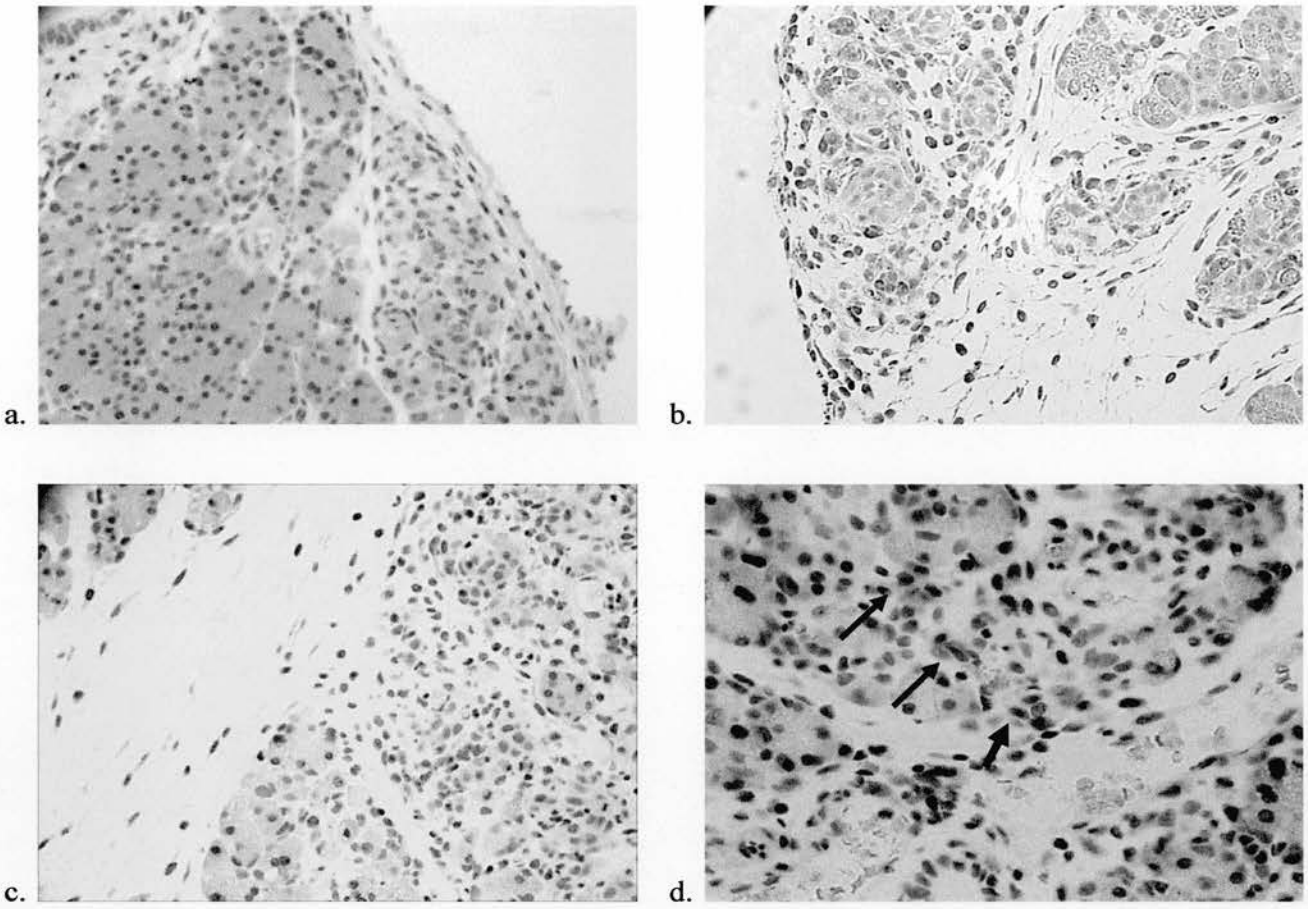

Figure 3-9 (a) & (c) are negative controls of (b) & (d) respectively. (b) Illustrates immunostaining of ED1 (x20 magnification) using fast red as the substrate. (d) illustrates the dual immunostaining of ED1 (fast red) and cleaved Caspase-3 (DAB). Because of the close similarity of colours between the substrate fast red and DAB, it is difficult to differentiate the type of immuno-positive cells. Blue arrow in (d) suggests a cleaved caspase-3 positive cell, whereas the red arrows suggest ED-1- positive cells.

3.7.7 Summary of Dose-Ranging Experiments

A consistent degree of severe acute pancreatic inflammation was induced in Fischer rats using both L-arginine and caerulein at the 48 hours time-point. Although there was acute inflammatory changes within the pancreatic parenchyma of Balb/C mice, the degree of pancreatic inflammation was inconsistent and too mild for the purposes of the study following both arginine and caerulein induction methods. No acute inflammatory changes have been witnessed within the pancreas using C57 mice. Based on these findings, further work on the mouse acute pancreatitis model was abandoned.

An L-arginine dose of 350mg/100g or 400mg/100g induced acute pancreatitis in Fischer rats with severity above that regulated by the Project Licence. These doses resulted in subsequent mortality of the Fischer rats. Study of the resolution of acute pancreatitis was therefore not feasible using doses above 300mg/100g L-arginine. A 300mg/100g L-arginine dose was therefore selected as the dose for the induction in the L-arginine rat pancreatitis model for this thesis. For the caerulein model, 50μg/kg of caerulein with 6 hourly intra-peritoneal injections was chosen to be the most appropriate dose. At this dosage, there was evidence that acute pancreatitis did resolve after 14 days from the initial induction in the models. These models allowed further characterization of the immune response during the resolution phase of acute pancreatitis as described in section 3.8.

3.8 Experimental Time-Points to Study Resolution of Acute Pancreatitis

To study various immune responses throughout the whole episode of acute pancreatitis, days 1, 3, 7, 10 and 14 were selected as the experimental time-points. Three treatment groups were used at each time-point, namely control, arginine and caerulein groups as shown in Figure 3-10.

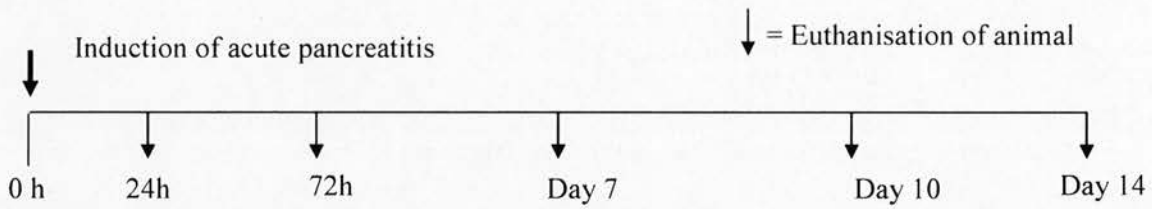

Figure 3-10. Experimental timeline: This figure illustrates the time-point for euthanization and tissue harvesting after the induction of severe acute pancreatitis by both arginine and caerulein in Fischer rats.

For each time-point above, lung, liver, pancreas and blood were harvested from each rodent as before. To characterize the severity of acute pancreatitis at each time-point, plasma amylase was measured at the early time-points and pancreas H&E sections were scored by an independent pathologist. A histological score of the severity of pancreatic injury was the summative score based on the degree of oedema [0(mild) to 3(severe)], pancreatic necrosis [0(mild) to 4(severe)] and leukocyte infiltration [0(mild) to 3(severe)]. The maximum histological score was 10.

3.8.1 POWER CALCULATION FOR THE TOTAL NUMBER OF RODENTS

It was difficult to determine at the outset the exact number of animal subjects that were required. To estimate the total number of animals needed in order to achieve statistical power, the Mead Resources Equation was the most appropriate in this setting (274). The Meads Resources Equation states that $\mathbf{E = N - B - T}$, where **E** is the error degree of freedom (df) and should be between 10 and 20; N is the total df, B is the blocks df, and T is the treatments df. To achieve an adequate statistical power using a block experimental design (i.e. $10<\mathbf{E}<20$), 3 separate blocks of experiments and 3 treatment groups with 2 samples per group were used. This is illustrated in Figure 3-11 below. This provided a total N per time-point = (3x3x2) – 1 = 17, B = 3–1= 2, and T = 3–1 = 2. The error degree of freedom of **E** is 13. Based on the Mead Resources Equation above, this suggested an adequate estimated statistical power for the study. With 5 time-points in total, the total number of rats required is therefore 90.

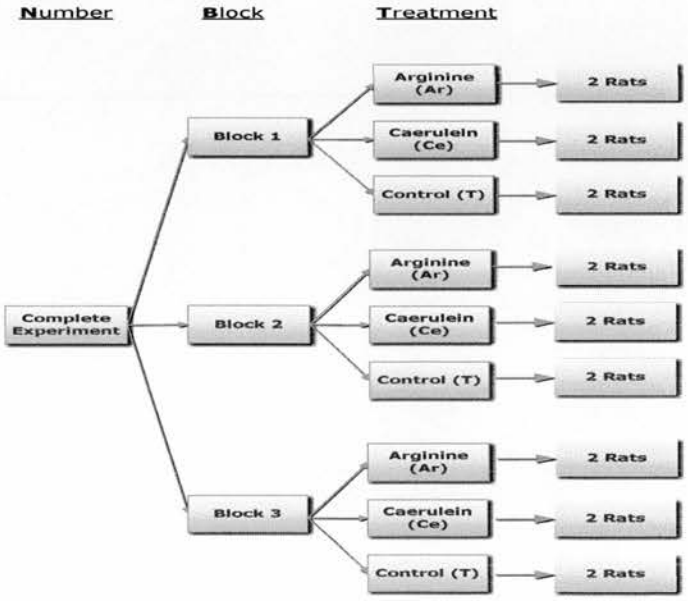

Figure 3-11 Schematic approach illustrates the design of the whole experiment.

3.9 RESULTS

3.9.1 AMYLASE RESULTS ON DAYS 1 AND 3 DURING THE ACUTE PANCREATITIS RESOLUTION MODEL

During the resolution model of acute pancreatitis, plasma amylase on days 1 and 3 was analysed as described above. 6 rodents per treatment group were analysed. There was significant increase of plasma amylase on day 1 in both acute pancreatitis groups versus the control ($H(2)=13.05$, $p = 0.001$) (Figure 3-12). However, there was no statistical difference of amylase results on day 3 between the pancreatitis groups and the control ($H(2)=3.01$, $p=0.22$). Plasma amylase was therefore not evaluated at other time points beyond day 3.

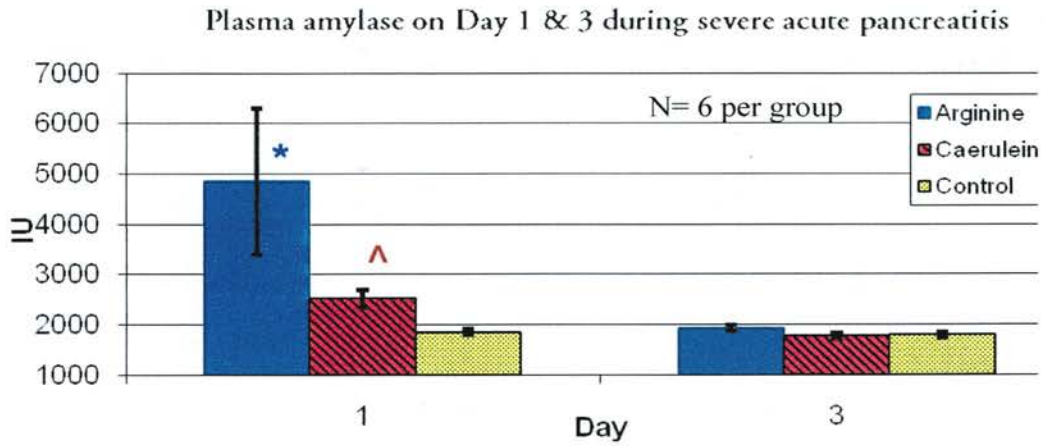

Figure 3-12 Plasma amylase results on days 1 & 3 of severe acute pancreatitis model. Symbols * & ^ illustrate significant elevation of plasma amylase as comparing to control using Kruskal–Wallis One Way Analysis of Variance on Ranks statistical analysis.

Plasma amylase results on day 1 & 3 of severe acute pancreatitis.

	Arginine		Caerulein		Control		
Day	Mean	S.E.	Mean	S.E.	Mean	S.E.	*p*-value
1	4848.33	1452.54	2522.17	170.89	1860.17	62.88	0.001
3	1930.17	62.78	1771.83	58.22	1798.17	58.34	0.22

Table 3-2 illustrates the amylase level (IU) of all three treatment groups at day 1 and 3

3.9.2 HISTOLOGY AND HISTOLOGICAL SCORING OF ACUTE PANCREATITIS

Diagrams below illustrated the H&E staining of pancreatic sections of all 3 treatment groups at different experimental time-points (Figure 3-13 & Figure 3-14). Figure 3-13 illustrates the histological changes within the pancreas of the arginine model. There were increasing gaps between the acinar cells and between the lobules of the pancreas. The lobular architecture of the pancreas was distorted. The normal pancreatic architecture was destroyed further at days 3 and 7, and was replaced by atrophic acinar cells and inflammatory leukocytes. The pancreas started to regenerate from day 7 onwards after the initial induction. Similar histological changes were observed in the pancreas of the caerulein model (Figure 3-14). By day 10, the loss of acinar lobules was more evident within the arginine group as compared to the caerulein group, suggesting a lesser degree of pancreatic inflammation or faster acinar cell regeneration in the caerulein model. This was further quantified by the histological scoring of the H&E pancreatic sections (Figure 3-15).

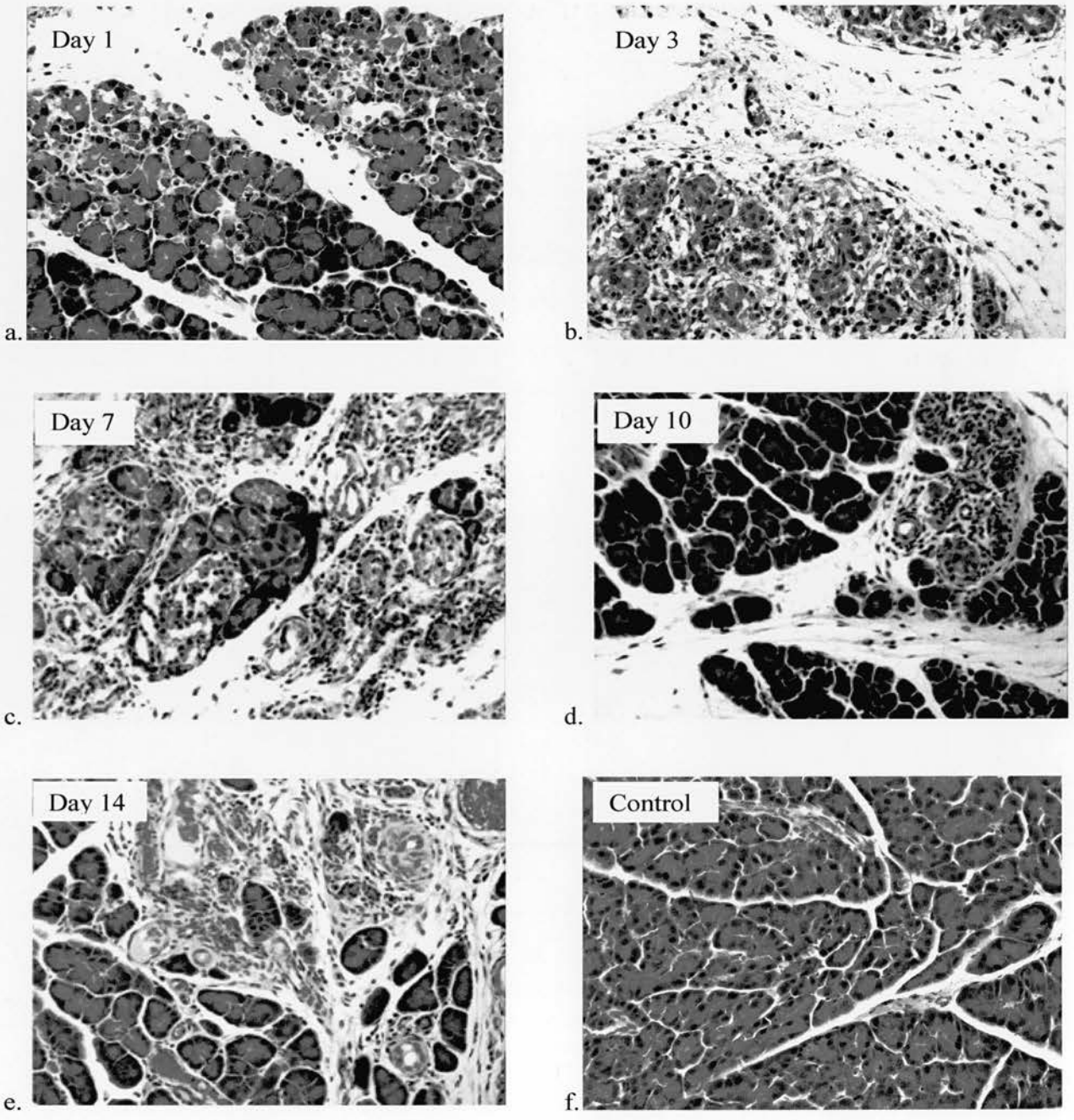

Figure 3-13 (a-e) illustrates the H&E staining of pancreatic sections (x20 magnifications) of the arginine model at days 1, 3, 7, 10 and 14, with the control pictured at the bottom right hand corner (f).

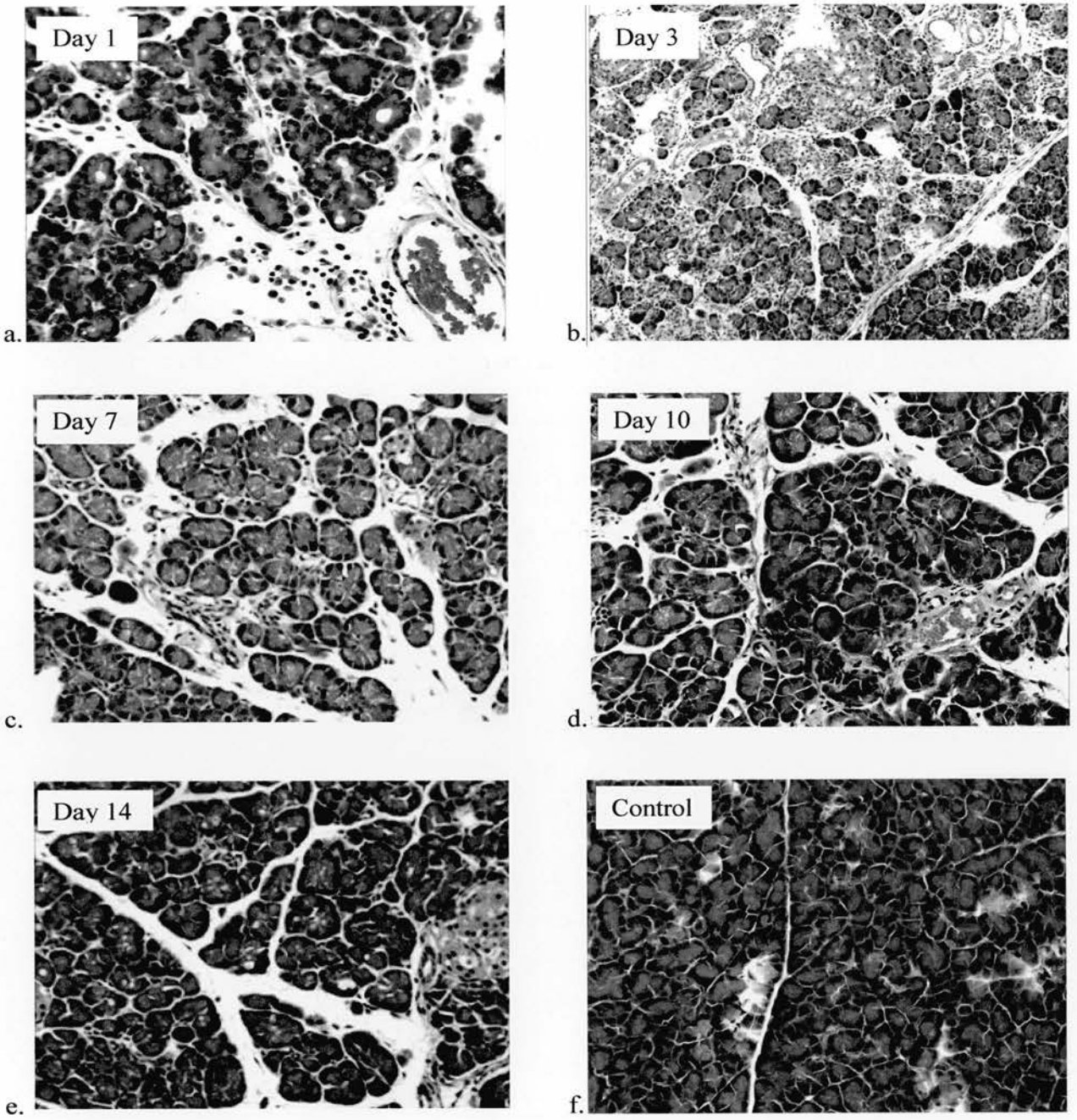

Figure 3-14 (a-e) illustrates the H&E staining of the pancreatic sections (x20 magnifications) of the caerulein acute pancreatitis model at days 1, 3, 7, 10 & 14. (f) is the control.

The combined histological scorings for all 3 treatment groups are illustrated in Figure 3-15. Significant increase in histological score was observed on day 1 in both arginine- and caerulein-induced acute pancreatitis as compared to the control group [$H(2)=34.68$, $p<0.001$]. The degree of acute pancreatic inflammation peaked on day 1 for the caerulein model, and subsided gradually with time, whereas the severity of acute pancreatitis peaked on day 3 for the arginine model. Histological scoring for the arginine model was consistently higher than the caerulein model until day 10, by which time-point the scores were comparable for either group. There was no statistical difference between the histology scores of the arginine group and the caerulein group in any of the experimental time-points. Both arginine and caerulein groups were significantly higher than the controls until day 10, when there were no differences compared to the controls beyond that time point.

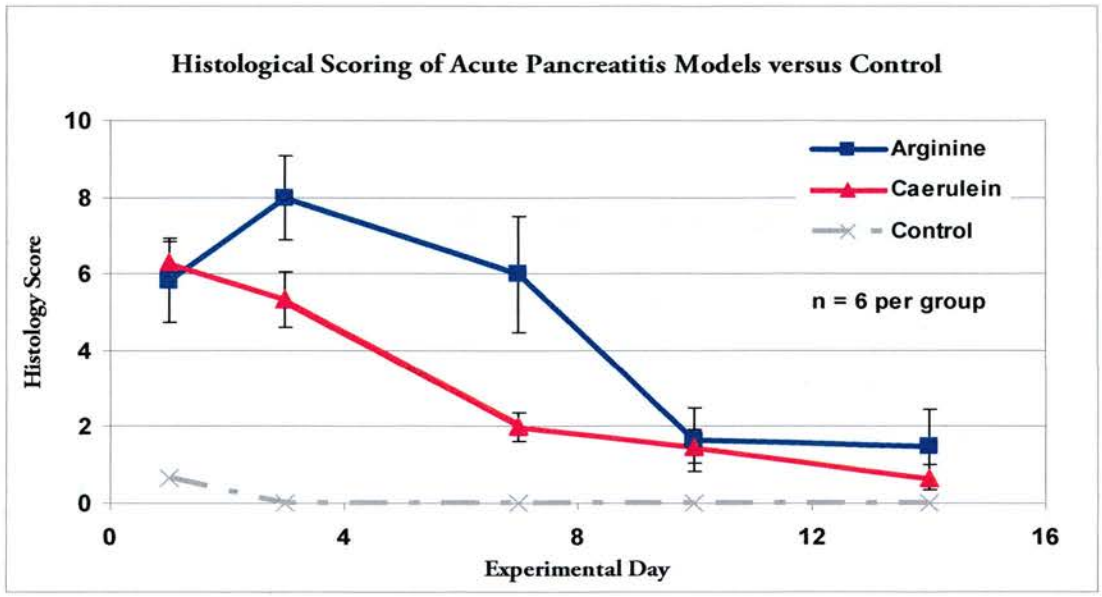

Figure 3-15. This graph represents the combined histological scoring of the 3 treatment groups (arginine and caerulein pancreatitis groups, and control group).

	Histology Score of Pancreas (n=6 per group)		
Day	Arginine Median score	Caerulein Median score	Control Median score
1	6	6	1
3	8	5	0
7	6	2	0
10	2	2	0
14	2	1	0

Table 3-3 Histology score of all three treatment groups of acute pancreatitis

3.10 DISCUSSION

Based on the dose-ranging experiments described in section 3.7.5, it was discovered that L-arginine solution required buffering to pH 7.4–7.5 prior to initial injections of the rodents. Disregarding the dose of L-arginine, non-buffered L-arginine solution will lead to mortality secondary to chemical peritonitis rather than acute pancreatitis. The dose of L-arginine injection is proportional to the severity of acute pancreatitis. Mortalities or significant morbidities occurred with doses above 300mg/100g of L-arginine. The study of the resolution of acute pancreatitis would therefore not be possible above that dose. It was decided therefore that 300mg/100g L-arginine was to be the dose for all the subsequent experiments in the arginine model. Six consecutive intra-peritoneal injections of caerulein dose 50μg/mg achieved a desirable level of severity of acute pancreatitis. Acute pancreatitis induced by both methods resolved by day 14.

Using immunohistochemical staining, we identified that the majority of the infiltrating leukocytes were, in fact, monocyte-derived macrophages (see Figure 3-9), whereas the loss of pancreas architecture was due to the disappearance of pancreatic acinar cells (see Figure 3-8). These findings were similar to the findings by Meyerholz et al who investigated the morphological changes of the pancreas from 1 hour to 48 hours post-induction using a duct-ligated pancreatitis model (275). They also attempted to qualify and quantify the apoptotic changes within the pancreas during the disease process. Surprisingly, there was an increase in apoptosis among the sham pancreatic group at 48 hours versus that at 0 hour. They did not detect any significant changes in apoptosis

within the pancreas during acute pancreatitis. This finding was unexpected since most studies suggested that acinar cell apoptosis is associated with a milder form of acute pancreatitis, whereas necrosis is more frequently observed in a more severe form of the disease (113, 276-278).

All these studies quantified the degree of apoptosis with single immunostaining of a pancreatic section or immunoblotting of homogenized pancreatic tissue. Using dual-immunostaining in our study provided information regarding what cell type underwent apoptosis. As demonstrated in Figure 3-8, there is evidence suggesting that the acinar cell undergoes apoptosis during acute pancreatitis. This could explain the reduction of acinar cells seen in Figure 3-13 and Figure 3-14 at the early stage of the disease. Our immunohistochemistry results also suggested apoptosis in monocyte-derived macrophages. However, this result has to be interpreted with caution. An uptake of apoptotic cells by surrounding macrophages will allow a positive dual-staining of both activated cleaved caspase-3 for the apoptotic bodies and ED-1 for macrophages.

Cleaved caspase-3 is localized within the cytoplasm, which is also where cytokeratin-8 and ED-1 antigens locate. In addition, cleaved caspase-3 is much less abundant than the other antigens within the cytoplasm. This caused potential overlapping of colours between the two types of chromogen: new Fuchsin and DAB. Among all the methodologies that are available for apoptotic staining, the TUNNEL assay is one of the

most frequently used (279). The assay relies on the presence of nicks in the DNA, which can be identified by terminal deoxynucleotidyl transferase, an enzyme that will catalyze the addition of dUTPs that are secondarily labelled with a marker. However, this method allows cross-staining of necrotic cells and, therefore, is not entirely specific to apoptosis (280).

Serum or plasma amylase measurement is a biochemical method used for the detection of pancreatic inflammation in both clinical and laboratory settings. However, it had been demonstrated in animal models and humans that the amylase level does not correlate well with the severity of acute pancreatitis (281). Although there was no significant increase in amylase in the caerulein-treated versus the control groups at 48 hours during the dose-ranging experiment, there was a significant elevation of its level at 24 hours from the induction in the 14-day time-point experiment (section 3.9.1). The elevation of plasma amylase illustrated an initial pancreatic injury. However, severity is best determined by histological findings.

The histological scoring system used in this study is similar to the one previously as described by Schmidt et al (282). Schmidt et al scored pancreatic inflammation based on the degree of oedema, inflammation, cellular necrosis and haemorrhage. Each category was assigned a score from 0 to 3 depending on the severity, 3 being the most severe in each category. In our models, there was no evidence of a haemorrhagic event

surrounding the pancreas in either model. This category was subsequently removed in our modified scoring system. Because of the variation of the degree of necrosis, an extra scoring point of 4 was assigned if there was a diffuse cellular necrosis within the pancreatic parenchyma at the studied time-point. As noted in Figure 3-15, there were differences in terms of the trend of histological scorings between the arginine and the caerulein pancreatic models. Histological severity peaked between days 1 and 3 for the arginine pancreatitis model, whereas it peaked at day 1 for the caerulein pancreatitis model. These findings of histological severity are similar to that suggested by Hegyi et al in the arginine model (283). Although there was a trend suggesting that arginine-induced acute pancreatitis manifested in a more severe manner than did the caerulein-induced group, no statistical differences were achieved in the histological scorings between the two treated groups using ANOVA.

Based on histological scoring shown in Figure 3-15, there is evidence that these two models achieved consistent severity of acute pancreatitis, which subsequently resolved by day 14. All rodents in either model survived throughout the induction of acute pancreatitis. These models would therefore be suitable for further investigation for the lung and systemic immunological responses during the resolution phase of acute pancreatitis.

4 ALVEOLAR MACROPHAGE PHAGOCYTOSIS DURING ACUTE PANCREATITIS

4.1 INTRODUCTION

The primary objective of the work described in this chapter was to develop an appropriate technique to investigate the phagocytosis of alveolar macrophages at each time-point (see Figure 3-10) during severe acute pancreatitis. This chapter details the development of an assay for phagocytosis in alveolar macrophages.

Two main macrophage phagocytosis techniques have been described in the literature. They are mainly divided into microscopic (light and fluorescent) (284, 285) and flow cytometric (286, 287) techniques. Because multiple live assays were required at each experimental time-point, a fast and reliable quantitative technique for alveolar macrophage phagocytosis was essential for this study.

4.2 ALVEOLAR MACROPHAGE HARVESTING

Alveolar macrophages (AMs) were harvested by broncho-alveolar lavage (BAL) as previously described (102, 266, 288, 289). Briefly, midline sternotomy was performed with the exposure of the trachea after terminal anaesthesia. A 14G cannula was inserted via the trachea, through which normal saline (Baxter Healthcare, UK) was instilled until the lung was fully expanded without leakage (approximately 5–7ml). A minimum of

100ml of normal saline from the lung of each rat was collected after BAL. All BAL fluid was centrifuged at 1,500rpm for 10 minutes. Only the first aliquot of BAL fluid supernatant was collected separately, and stored at -70^0C for cytokine analysis. The pellet of harvested cells from the BAL was washed twice with phosphate-buffered saline (PBS). Harvested cells were reconstituted with culture medium (RPMI 1640, 21875-034, Gibco Invitrogen, UK), streptomycin/penicillin to a concentration of 1×10^6 cells/ml.

4.3 Confirmation of Alveolar Macrophages

250µl (2.5×10^5 cells) of the above cellular suspension was added to each well of an 8-well chambered slide (177402, Lab-Tek, UK). The suspension was cultured at 37^0C with 5% humidified CO_2 for 2 hours to allow all cells to adhere to the bottom of the well.

Adhered cells were washed twice with PBS. The PBS was gently pipetted out of each well, which was then allowed to air-dry for 20 minutes. 100% methanol at -20^0C was added for 10 minutes to each well to fix adhered cells. Methanol was removed from each well, which was washed with PBS for 3x 5 minutes. Adhered cells were permeabilized by adding 0.1% Triton X-100 for 20 minutes. After washing with PBS, 5% rabbit serum (X0902, Dako, UK) was added to each well for 30 minutes as blocking agent. Each well was exposed to 1:300 ED1 mouse anti-rat monoclonal antibody (MCA341PE, Serotec, UK) for 1 hour. No primary antibody was added for the control well. Each well was washed with PBS in between additions of antibodies. The slides were incubated

sequentially with a biotinylated rabbit anti-mouse polyclonal antibody (Dako, UK), streptavidin–biotin–horseradish peroxidase (HRP) complex (Dako, UK) and 3,3-diaminobenzidine (DAB) for the visualization of staining. Finally, the chamber slide was counterstained with haematoxylin (Figure 4-1).

a. 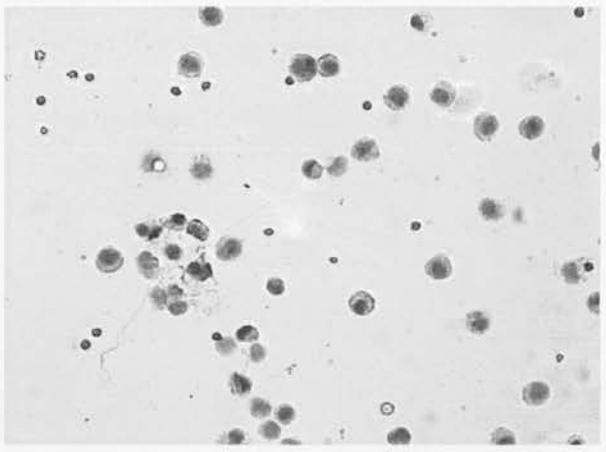 b. 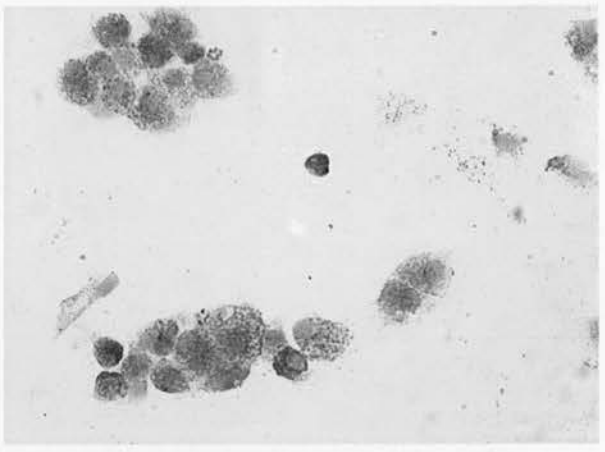

Figure 4-1 illustrates immunohistochemistry of alveolar macrophage using anti-ED1 antibody. (a) is the negative control, whereas (b) demonstrates positive staining of ED1 using DAB as the chromogen for visualization.

4.4 ALVEOLAR MACROPHAGE PHAGOCYTOSIS ASSAY

For the purpose of establishing the technical aspects of the assay, Sprague Dawley rats were used instead of Fischer rats due to the fact that they were abundant in our in-house Animal Unit. AMs were harvested as section 4.2. The assay was developed in two phases. The first phase was to establish evidence of phagocytosis using light and fluorescent microscopy; the subsequent stage was to set up the flow cytometric phagocytosis technique for robust quantification.

4.4.1 PHASE ONE: LIGHT MICROSCOPY

4.4.1.1 **Phagocytosis using fluorescent beads**

AMs were harvested and plated out in 8-well chamber slides as in section 4.3. In each experiment, two chamber slides were used – one for the experimental conditions at 37^0C and the other slide as a negative control at 4^0C. Cells were washed twice with PBS after 2 hours of incubation at 37^0C. A mixture containing 100µl of Dulbecco's Modified Eagle Medium (DMEM) (11880-028, Gibco Invitrogen, UK) without phenol red and 1µl of microspheres (Cat. No. 15702, Frostbite Yellow Green Carboxylate microspheres, Polysciences) was added to each well. They were co-cultured at 37^0C for 60 minutes. 5µl of cytochalasin D (C8273, Sigma-Aldrich, UK) was added to the chamber slide of the negative controls, which were then incubated at 4^0C. Supernatant was removed from each well after 1-hour incubation. Each well was then washed once with ice-cold PBS. Slides were allowed to air-dry. AMs were fixed by -20^0C methanol as above. The Dif-Quik staining method was used to counterstain both nuclei and cytoplasm (1 minute each in both Dif-Quik Solutions 1 & 2) (290). The slides were air-dried overnight. Slides were mounted in xylene on the following day. Fluorescent and light microscopy (Leica fluorescent microscope DM IL) were used to capture experimental images. The fluorescent and light microscopic images were superimposed on each other using Adobe Photoshop software (Adobe Corporate Software).

- Results

Figure 4-2 illustrates the internalization of the fluorescent beads by AMs in the superimposed light and fluorescent microscopic picture. The fluorescent beads were quenched by xylene solution during the mounting step at the end. (291, 292).

a. 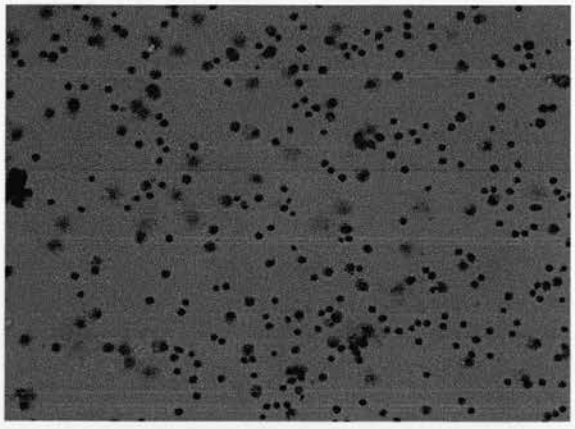 b. 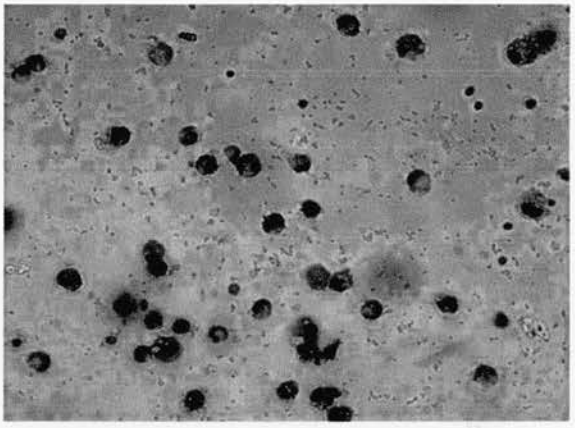

Figure 4-2 (a) is the negative control of the assay, at which the alveolar macrophages were incubated at 4^{0}C for 60 minutes. (b) illustrates alveolar macrophage phagocytosis after 1 hour of incubation at 37^{0}C with fluorescent microsphere (Fluorescent green). Alveolar macrophages were counterstained by Diff-Quik solutions. Non-internalized fluorescent beads were quenched after Xylene mounting (orange arrow).

4.4.1.2 **FITC-labelled *E. coli* (Molecular Probes) fluorescent microscopic phagocytosis assay**

Preparation of FITC-labelled E. coli

$3x10^8$ per mg of FITC-labelled *Escherichia coli* (E-13231, Molecular Probes, Invitrogen, UK) were opsonised prior to use. FITC–*E. coli* was reconstituted and mixed well with 500µl of PBS. 500µl of PBS was used to reconstitute the opsonising agent (E-2870, Molecular Probes, Invitrogen, UK). *E. coli* and opsonising agent were mixed at a ratio of 1:1, and incubated together at 37^0C for 1 hour. The mixed suspension was washed 3 times with PBS. It was centrifuged at 800–1500 x g for 15 minutes in between washings. This reconstituted suspension was stored at 4^0C with sodium azide to a final concentration of 2mM. The suspension was washed 3 times with PBS as above immediately prior to use.

AMs were prepared as per section 4.3. 10µl of FITC–*E. coli* (approx. 1 x 10^6 bacteria/µl) was added to each 300µl DMEM culture medium. Bacteria were added to each well containing adhered AMs. The bacteria in suspension were spun down at 250 x g for 1 minute. The mixture was then incubated for 60–90 minutes (depending on the set of experiment) at 37^0C. The control experiment was performed under the same condition above, but at 4^0C. Microscopic pictures were taken in-between steps. 100µl of 0.8mg/ml

crystal violet (Cat No.C6158, Sigma-Aldrich, UK) was used as the quenching solution at the end of the incubation.

- *Results*

Figure 4-3 (a) illustrates the mixture of AMs and FITC-labeled *E. coli* after 90 minutes of incubation at 37^0C, before the addition of crystal violet. Figure 4-3 (b) illustrates the exact same image as Figure 4-3 (a), but after the addition of crystal violet quenching solution to the cultured slide. Both the adhered and non-phagocytosed FITC-labeled *E. coli* lost their fluorescence after the addition of crystal violet.

a. 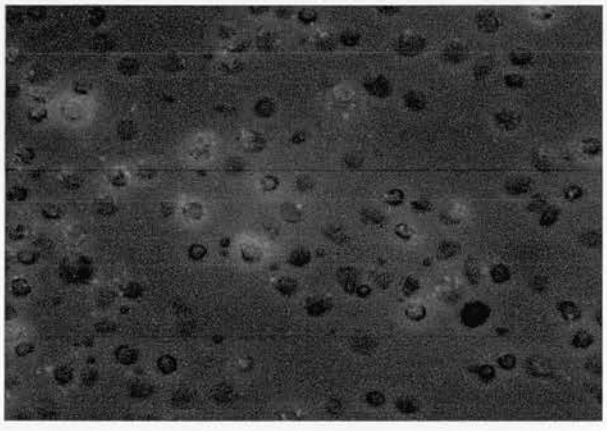 b. 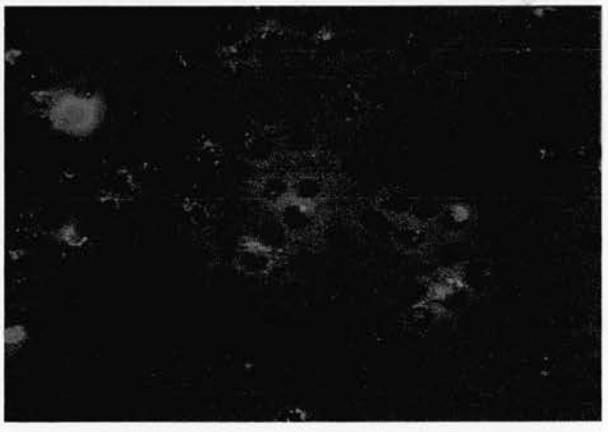

Figure 4-3 (a) illustrates alveolar macrophage phagocytosis of FITC- labelled E.coli after incubation for 90 minutes before addition of crystal violet for quenching. (b) was taken immediately after the addition of crystal violet.

4.4.2 PHASE TWO: PHAGOCYTOSIS ASSAY USING FLOW CYTOMETRY

4.4.2.1 **Alveolar macrophage phagocytosis assay using Frostbite Yellow Green fluorescent microspheres**

The same culture conditions as in section 4.4.1.1 were applied to the flow cytometric phagocytosis assay. 1ml of 1 x 10^6 AMs was plated into each well of a 12-well plate (CLS3512, Corning Costar cell culture plate, Sigma). Two, 12-well plates were used – one was for the control with incubation at 4^0C, and the other was for the incubation at 37^0C. AMs were allowed to adhere to the bottom of the well after incubation for 2 hours. Non-adherent cells were washed away with PBS. 1µl of Frostbite microspheres were added per 600µl of DMEM without the presence of phenol red or any other additives. The plate was centrifuged for 1 minute at 250rpm. 20, 30 and 60 minutes incubation time were used.

AMs were detached from the bottom of the plates by mechanical means. The suspension of all detached cells was transferred to an LP3 5-ml tube (Falcon Flow cytometry tube) and was fixed by the lysing solution from a Phagotest kit (Orpegen Pharma, Germany) for 20 minutes at room temperature. Propidium iodide was added to each tube after being washed twice with PBS. The suspension was analysed by Coulter Epics XL flow cytometer (Beckman-Coulter, UK).

4.4.2.2 **Alveolar macrophage phagocytosis assay using FITC-labelled *E. coli* (Molecular Probes)**

Fluorescein (494/518)-labelled *E. coli* BioParticles (E-2861, Molecular Probes, Invitrogen, UK) were used and prepared as section 4.4.1.2. The fluorescent microscopic technique is generally regarded as the "gold standard" in phagocytosis quantification. To compare and validate the flow cytometric technique, both flow cytometric and fluorescent microscopic phagocytosis assays were performed in parallel to each other.

Microscopic and flow cytometric experiments were performed in the same manner as described in previous sections. An arbitrary ratio of 30:1 bacterium (3×10^7 *E. coli*) to alveolar macrophage was used for each assay. *E. coli* were suspended in DMEM without phenol red. 600µl of the bacteria/medium mixed suspension was added to each well of the 12-well plate, whereas 150µl per well was used for the 8-well chamber slide. For each set of experiments (both flow cytometric and fluorescent microscopic techniques) a negative control was included as before with the addition of cytochalasin D at a final concentration of 5µl, and incubated at 4^0C. The bacteria were spun down to the bottom of the well by centrifugation at 250rpm for 1 minute as above.

Determination of concentration of quenching agents

One of the most important elements in the phagocytosis assay is to ensure that the quenching solution used allows adequate quenching of adhered particles, but is not

strong enough to either penetrate or quench the internalized particles. While maintaining the same culture conditions, various concentrations of trypan blue (Cat. No. T8154, Sigma-Aldrich, UK) and crystal violet (Cat No. C6158, Sigma-Aldrich, UK) at 0.1%, 0.25%, 0.33%, 0.5%, 0.67% 1% and 2% were tested for flow cytometry analysis. These experiments aimed to determine the optimal concentration for each of the quenching compounds. A fixed incubation period of 90 minutes was used for the experiment to determine the concentration of the quenching agent.

AMs were prepared as described above. They were harvested from each well by mechanical means after 90 minutes of incubation at both 4^0C and 37^0C. The harvested AMs/*E. coli* suspension was then split into 7 LP3 tubes. All LP3 tubes were immersed in ice until analysis. 400µl of various concentrations of the selected quenching solutions was added to each LP3 tube immediately prior to flow cytometric analysis. The percentage of phagocytosis based on the flow cytometric technique was plotted against concentration of the two selected quenching agents (Figure 4-5).

Determination of the optimal incubation period for AM phagocytosis

Having decided the optimal concentration of each potential quenching agent, the optimal incubation period for both alveolar AMs and *E. coli* was then determined. Based on the literature, the incubation period for *in vitro* or *ex vivo* phagocytosis assay of phagocytes and bacteria ranged from 60 minutes to 180 minutes (286, 293, 294). 60, 90, and 120

minutes were selected as the studied time-points. Assays incubated at 4^0C were used as controls (see previous section). Experiments were undertaken in duplicate each time and were performed at least three times on separate occasions.

Apart from the variation of the incubation period, the experiments were performed as stated in the previous section. Fluorescent microscopic experiments were performed in parallel to the flow cytometry experiment under exactly the same culture conditions. Immediately prior to flow cytometry analysis, 400µl of either trypan blue or crystal violet at previously determined concentration was added to each sample.

To further determine whether there are any differences in delayed measurement of phagocytosis after the addition of the two quenching agents, phagocytosis was measured immediately and 30 minutes after the addition of either quenching agent.

Quantification and analysis

For the quantification of fluorescent microscopy, five random pictures at x20 magnification were taken from each well of the 8-well chamber slide. For each image, the number of AMs and AMs containing phagocytosed bacteria in each picture were counted separately within each field. A total minimum of 100 AMs was counted for each

experiment. The percentage of AM phagocytosis = (the sum of AMs with phagocytosed bacteria) / (total number of AMs of the 5 images) x 100%.

For the quantification of AM phagocytosis by the flow cytometric technique, AMs were gated based on the forward/side scatter graph (see Figure 4-4). The percentage of AM phagocytosis at a specific time-point was calculated by the Overton cumulative histogram subtraction algorithm (295), using the corresponding assay cultured at 4^0C as a baseline comparison. All flow cytometry data were analysed by a flow cytometry software (FCS Express V3, De Novo Software Ltd, USA).

The percentage of AM phagocytosis measured using trypan blue as the quenching agent by flow cytometry was compared with that of crystal violet. The findings of flow cytometry in either trypan blue or crystal violet groups were also compared with their corresponding manual counting groups at each of the studied time-points. The student t-test was used if the data fulfilled parametric distribution. Otherwise, Mann–Whitney Rank Sum test was used. $p<0.05$ was considered as statistically significant. SigmaStat v3.5 (Systat Software Inc., USA) was the chosen statistical analysis package.

4.4.3 Results of Alveolar Macrophage Flow Cytometric Phagocytosis Assay

4.4.3.1 **Results of Frostbite microsphere phagocytosis assay (flow cytometry)**

Figure 4-4 illustrates the results of the Frostbite microsphere flow cytometric phagocytosis assay. Increasing the incubation time enhances the engulfment of the microspheres by the AMs. Comparing with the corresponding controls, the percentage of phagocytosis was 46% after 30 minutes culture versus 36% after 20 minutes culture. However, a large amount of the AMs in the control group (black lines in Figure 4-4 c & d) recorded positive fluorescence. Given that there was no background fluorescence after xylene mounting in Figure 4-2, the increased fluorescence of the control group was therefore due to adhesion of the fluorescent microspheres to the surface of AMs rather than internalization. The fluorescence of Frostbite microspheres was too bright for quenching by either trypan blue or crystal violet solution. This assay using Frostbite microspheres as the phagocytic target for the phagocytes was therefore not sensitive enough to distinguish those adherent microspheres from phagocytosed microspheres for accurate phagocytosis quantification by flow cytometry. Further use of the Frostbite microsphere methodology was not suitable for the purpose.

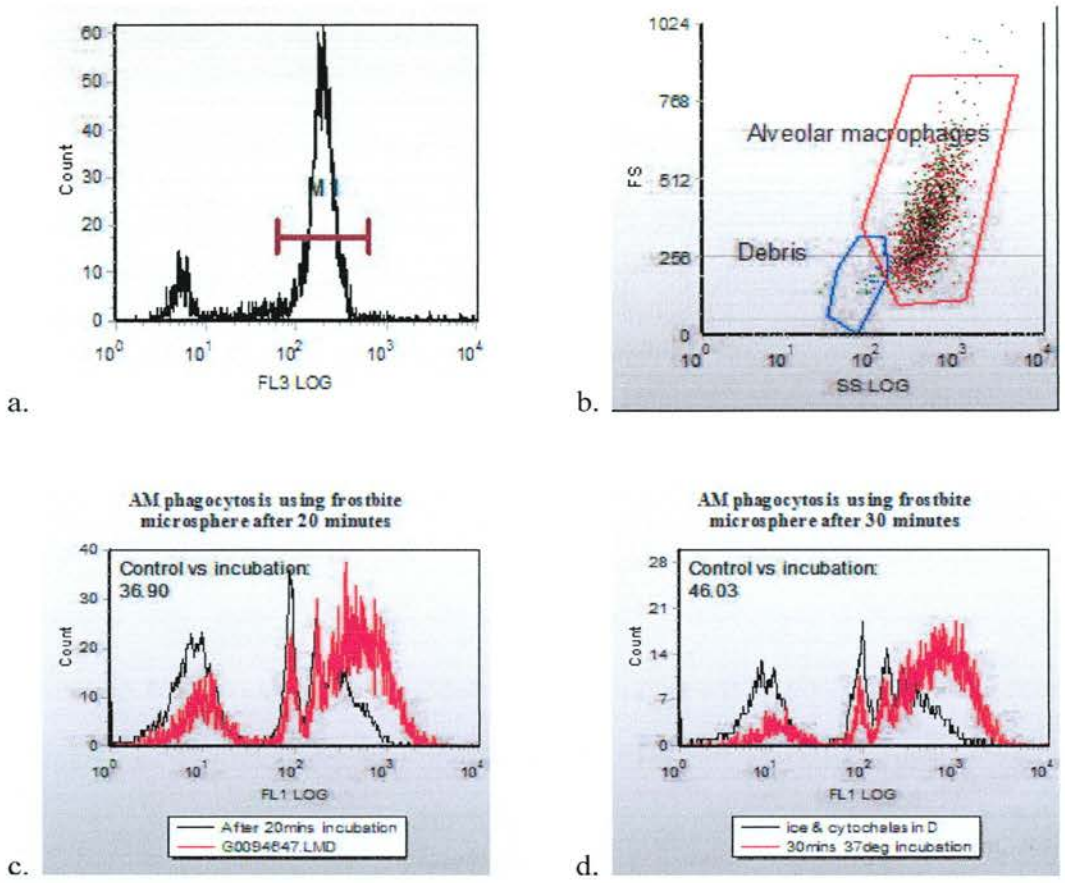

Figure 4-4 (a) demonstrates the histogram of the total alveolar macrophage/ *E. coli* suspension after each experimental time-point. With the addition of lysing solution of the Phagotest kit, the cell membrane was permeablized and allowed positive nuclei staining by propodium iodide (PI). These cells are represented within gate M1. All subsequent analyses based on gate M1 would therefore eliminate all non-nucleated cells and organisms. (b) is the forward/side scatterogram of all cells within gate M1. The Red gate indicates alveolar macrophages, whereas the blue gate indicates debris. (c) & (d) are histograms of alveolar macrophage phagocytosis based on the red gate in (b) after 20 and 30 minutes of incubation

4.4.3.2 Results of experiments to determine the type of quenching solution and alveolar macrophage–bacteria incubation period

As illustrated in Figure 4-5, 0.67mg/ml of trypan blue and 0.5mg/ml of crystal violet achieved an adequate quenching ability on the flow cytometer, and did not lead to complete quenching of the fluorescence. These concentrations were used throughout the rest of the phagocytic experiments.

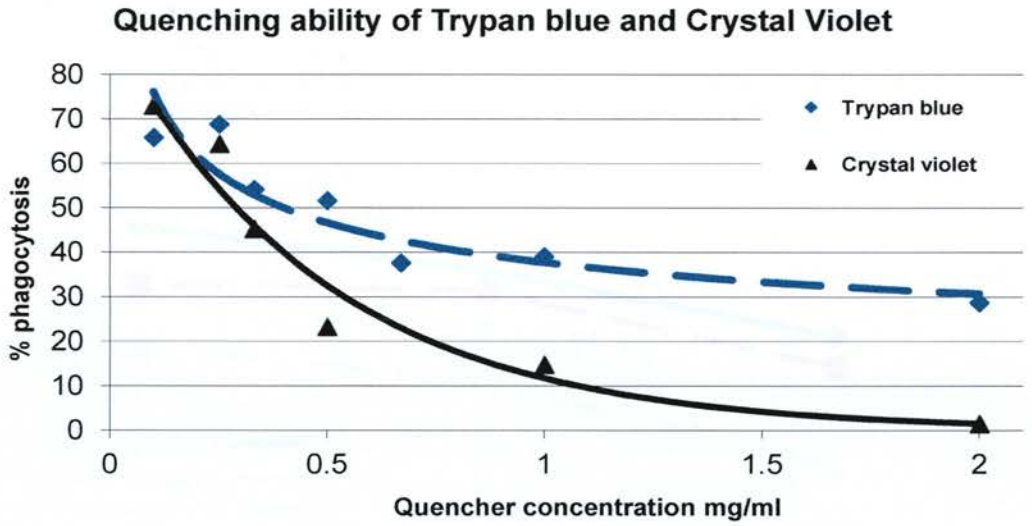

Figure 4-5 This diagram illustrates the percentage of measured alveolar macrophage phagocytosis immediately after the addition of either trypan blue or crystal violet at different concentrations. Solid and dashed lines are the trendlines of trypan blue and crystal violet quenching.

Table 4-1 illustrates the absolute percentage of alveolar macrophage phagocytosis as plotted in Figure 4-6

Time-points (mins)	TB (%)		TB (delayed) %		CV %		CV (delayed) %	
	Mean	S.E.	Mean	S.E.	Mean	S.E.	Mean	S.E.
60	34.90	0.44	32.25	0.44	23.78	1.74	18.04	0.94
90	40.52	4.69	38.80	3.58	30.82	5.19	25.90	4.24
120	44.30	2.29	39.37	2.48	34.23	1.24	30.00	0.38

There were statistical differences in the percentage of AM phagocytosis detected by flow cytometry between trypan blue and crystal violet groups at the 60-minute ($p=0.002$, Mann-Whitney test) and the 120-minute ($p=0.002$, Mann-Whitney) time-points. With a 30-minute delayed measure, there was a general trend of an overall reduction in the percentage of AM phagocytosis measured. There was a statistical difference between the immediate and delayed AM phagocytosis measurement within the trypan blue groups at the 60-minute time-point ($p=0.03$, Mann-Whitney test); whereas there were statistical differences at both the 60-minute ($p=0.009$, Mann-Whitney test) and the 120-minute ($p=0.041$, Mann-Whitney test) time-points of the crystal violet groups.

Flow cytometry versus manual counting at 60, 90 and 120 minutes time-points

Figure 4-7 illustrates the combined findings of AM phagocytosis percentage measured by both flow cytometry and manual counting techniques. There was no statistical difference in the percentage of AM phagocytosis using the manual counting technique between the trypan blue and crystal violet groups at all studied time-points. When the measured percentage of AM phagocytosis was compared between flow cytometric and

manual counting techniques among either trypan blue or crystal violet groups, no statistical differences was achieved at any of the studied time-points.

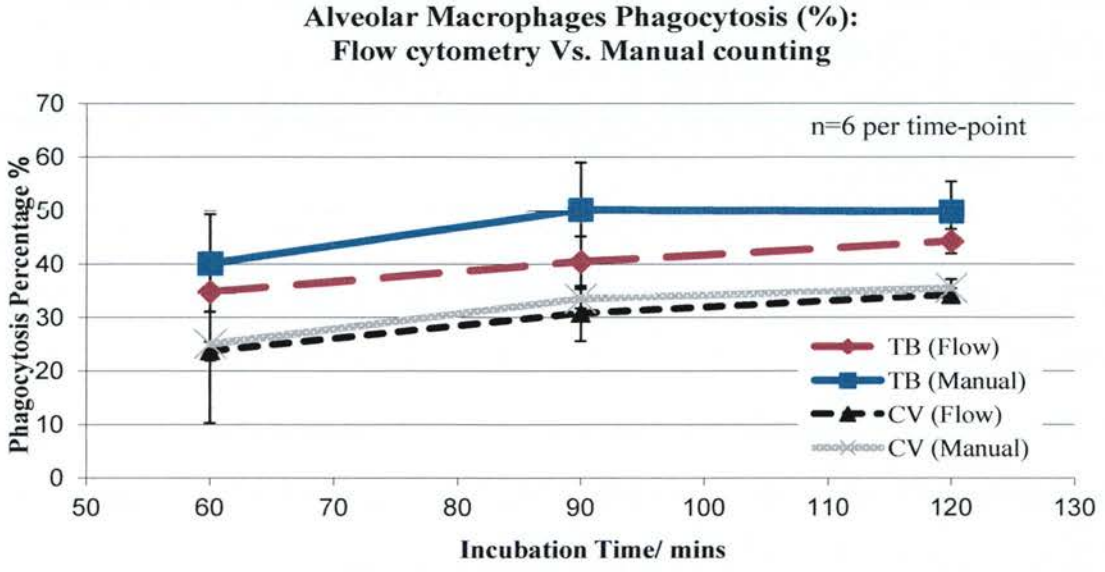

Figure 4-7. This graph illustrates the percentage of alveolar macrophage phagocytosis measured by flow cytometry as compared to manual counting at the 60, 90 and 120 minutes time-points using either trypan blue (TB) or crystal violet (CV) as the quenching agent.

Table 4-2 illustrates the absolute percentage of alveolar macrophage phagocytosis as plotted in Figure 4-7.

Time-points (mins)	TB (flow) %		TB (Manual) %		CV (flow) %		CV (Manual) %	
	Mean	S.E.	Mean	S.E.	Mean	S.E.	Mean	S.E.
60	34.90	0.44	40.22	9.11	23.78	1.74	25.08	14.76
90	40.52	4.69	50.23	8.79	30.82	5.19	33.57	1.79
120	44.30	2.29	49.90	5.61	34.23	1.24	35.54	1.61

4.4.4 SUMMARY FOR SECTION 4.4

Based on the findings of the above experiments, 0.67% of trypan blue was selected as the quenching agent for the AM phagocytosis assay in the two acute pancreatitis models. 90 minutes of incubation was also chosen for the AM phagocytosis assay in the subsequent pancreatitis model.

4.5 Alveolar Macrophage Phagocytosis Throughout Severe Acute Pancreatitis

Having established and validated the alveolar macrophage phagocytosis assay in pervious sections, this section aims to discuss the methodologies and findings of AM phagocytosis throughout the whole disease process of severe acute pancreatitis.

AMs were harvested and prepared as in section 4.2 above. As described in the previous chapter, 6 rats per treatment group (arginine, caerulein and control) were used at each experimental time-point. The experimental time-points were days 1, 3, 7 10 and 14. The AM specimen from each rat was performed in duplicate, and with an internal control cultured at 4^0C.

AMs were allowed to adhere to the bottom of the well after 2 hours of incubation at 37^0C. Each well was washed twice using ice-cold PBS, before the addition of 600µl of DMEM/*E. coli* (30:1) mixture. The AM/*E. coli* mixture was spun down at 250rpm for 1 minute at 4^0C. The AM/*E. coli* suspension was then co-cultured for 90 minutes at either 37^0C or 4^0C (internal control group). All adhered cells were harvested by mechanical means at the end of the incubation period. They were immediately transferred to pre-marked 5-ml LP3 tubes and immersed under ice till analysis. 400µl of 0.67% trypan blue was added to the each tube immediately prior to flow cytometric analysis.

4.5.1 Quantification and Analysis of Alveolar Macrophage Phagocytosis

As stated in the previous chapter at section 3.8.1, there were 3 blocks of acute pancreatitis induction experiments. For each block of acute pancreatitis induction experiment, 2 control, 2 arginine-treated and 2 caerulein-treated rats were used. To minimize the variation between the experimental conditions for different sets of experiments, the relative percentage of AM phagocytosis was used for analysis: Relative percentage = [the absolute percentage of the AM phagocytosis of an individual rodent of either of 2 treatment groups (arginine & caerulein) for each set of experiments] / [absolute percentage of AM phagocytosis of the corresponding control group]. The relative AM phagocytic capacities of all three blocks of experiments were then combined together. Only the relative phagocytosis activity was reported and analysed for the final result.

Non-parametric Kruskal-Wallis One Way Analysis of Variance on Ranks was used for the analysis of each time-point. SigmaStat (Systat, US) was used as the statistical package.

4.5.2 Results for Alveolar Macrophage Phagocytosis Throughout Acute Pancreatitis

Figure 4-8 demonstrates the changes of the relative AM phagocytosis of the two treatment groups (arginine and caerulein groups) and the control group from day 1 to day 14. Both arginine and caerulein pancreatic groups followed similar trends to each other throughout the resolution of the disease, apart from day 1 when there was an apparent increase in AM phagocytic capacity of the arginine group. Although there was a trend of increase in AM phagocytosis by day 7, there was no statistical difference to support an increase in AM phagocytic capacity during severe acute pancreatitis in our models. There was significant upregulation of the AM phagocytic capacity at day 14 in both arginine and caerulein treatment groups as comparing to the control group [$H(2)=6.14$, $p<0.05$].

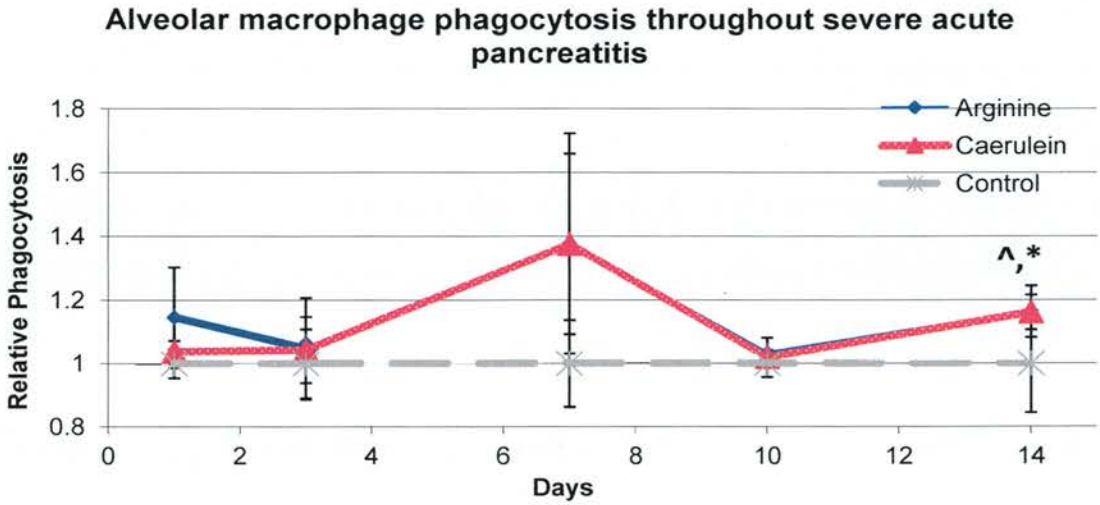

Figure 4-8 This graph represents the changes of the relative alveolar macrophage phagocytosis of the two induced acute pancreatitis groups (arginine and caerulein) and the control group throughout an episode of severe acute pancreatitis. The trend of alveolar macrophage phagocytosis of the arginine pancreatitis group follows closely with the caerulein group. Alveolar macrophage phagocytosis of both pancreatitis groups was significantly increased at day 14. '^,*' denotes statistical significant of arginine- and caerulein groups versus control respectively.

Table 4-3 illustrates the relative value of alveolar macrophage phagocytosis of three treatment groups during acute pancreatitis. '*' represents statistically significant value.

	Relative value for AM phagocytosis						*p*-value *
	Arginine		Caerulein		Control		
Day	Mean	S.E.	Mean	S.E.	Mean	S.E.	
1	1.14	0.16	1.04	0.03	1.00	0.04	0.82
3	1.05	0.16	1.04	0.10	1.00	0.04	0.94
7	1.38	0.35	1.38	0.28	1.00	0.04	0.39
10	1.03	0.05	1.02	0.06	1.00	0.04	0.91
14	1.16	0.08	1.16	0.06	1.00	0.04	0.046*

4.6 DISCUSSION

The experiments described in section 4.4 have demonstrated that flow cytometry is a reliable and effective technique to measure phagocytosis as compared with fluorescent microscopic manual counting, which is generally regarded as the "gold standard". All subsequent analysis of the phagocytosis assay was performed by flow cytometry.

The choice of the phagocytic particle for phagocytes is important for the quantification of the phagocytosis assay. Not only did we have to ensure that the particles could be internalized by the studied phagocytes, it was also important to be able to distinguish and quantify the internalized particles by the phagocytes from the adherent particles. Failing this principle will over-estimate the phagocytic capacity of the phagocyte of interest, which is the alveolar macrophage (AM) in our case.

There is a general trend of increase in the percentage of phagocytosis with the increase in the incubation period. However, for AMs, this increase seems to plateau after 90 minutes of incubation with *E. coli*. Different quenching agents produce different "absolute" phagocytic capacity of a phagocyte. Our experiments, using either trypan blue or crystal violet as the quenching agent for the AM phagocytosis assay, produced a significant variation of results, when it was measured by flow cytometry. There were also measureable differences in the manual counting results using either trypan blue or crystal violet as the quenching agents. These experiments suggest that the measured

values of phagocytosis capacity depend on the type of quenching agents. Provided that the same quenching agent was used, flow cytometry should closely represent the results of manual counting

Disregarding the "absolute value" of phagocytic capacity measured in either trypan blue or crystal violet groups, there was an overall increase in the trend of phagocytosis with the length of incubation time. Although there was no significant statistical differences between the measured phagocytosis within either the trypan blue or crystal violet groups, when there were delays between the timing of the addiction of quenching agent and timing for analysis, there appeared to be a reduction of measured phagocytosis within the crystal violet group during a delayed measurement. This could be explained by the fact that trypan blue is excluded from cells with an intact cell membrane, whereas crystal violet can penetrate through an intact cell membrane. Crystal violet will therefore quench the internalized fluorescent particles. The staining of the AM cytoplasm with crystal violet is witnessed immediately after the addition of the quenching solution. Based on this observation, trypan blue is the more reliable quenching agent of the two for phagocytosis assay, as crystal violet could potentially under-estimate the amount of phagocytosed particles. Nevertheless, both agents have been widely used throughout the literature as acceptable quenching agents for phagocytosis assay (291).

4.6.1 Alveolar Macrophage Phagocytosis During Acute Pancreatitis

The patterns of AM phagocytosis between the two acute pancreatitis models were similar throughout the episode of the disease. The only time-point that achieved significant AM phagocytosis in both acute pancreatitis models versus the control was day 14. There was a general trend of increasing AM phagocytosis by day 7 in both acute pancreatitis models.

These findings differ from those of AM phagocytosis in a rodent septic model. Studies using the caecal puncture and ligation sepsis model suggested a compromised bacterial clearance by the AMs (161, 162), suggesting a status of immunosuppression during sepsis. This immunosuppressive state was confirmed when the administration of anti-IL-10 sera partially reversed the defective AM phagocytosis ability (163). The exact reason for this discrepancy is uncertain. Although there are similarities of lung injury between acute pancreatitis and severe sepsis, the pathophysiology of the AMs could be different in acute pancreatitis. The other possible explanation is that the severity of the inflammatory response of the sepsis models described in the literature was much more severe than the response of the acute pancreatitis models used in this thesis. The immunological response by the AMs could therefore be different. However, one of the elements that need to be emphasized is that the studied time-points for the AM phagocytosis in these sepsis models were all within 24 hours from the induction of sepsis. This is different from the time-points that were studied in this thesis. Direct comparison of the AM phagocytosis in these studies is therefore difficult.

5 PERIPHERAL BLOOD PHAGOCYTOSIS DURING SEVERE ACUTE PANCREATITIS

5.1 INTRODUCTION

As part of the innate defence mechanism, one of the properties of granulocytes and monocytes in the bloodstream is the clearance of bacteria causing systemic infection. There is evidence from human studies that leukocyte phagocytic function is impaired at the early stage of acute pancreatitis (169). However, how phagocytosis changes towards the recovery phase of severe acute pancreatitis function is unknown.

This chapter aims to investigate how peripheral blood phagocytosis alters throughout the whole disease process, until the complete resolution of the disease. This can allow direct comparison of systemic bacterial clearance with that of alveolar macrophages within the lung parenchyma, which was described in Chapter 4.

5.2 PERIPHERAL BLOOD PHAGOTEST PHAGOCYTOSIS ASSAY

The Phagotest kit (Orpegen Pharma, Germany) was used for the peripheral blood phagocytosis assay. The principle for Phagotest is the same as the phagocytosis assay described in section 4.4.2.2. The kit contained: 2ml of stabilized and opsonised FITC-labelled *E. coli* suspension (1 x 10^9 bacteria/ml); 10ml of quenching solution for suppressing fluorescence of the bacteria attached to the outside of the cell; 20ml of

DNA-staining solution for cytometric discrimination of bacteria during leukocyte analysis; 20ml of lysing solution (10 x stock solution for storage, 1:10 dilution with double-distilled water for lysing erythrocytes and simultaneous fixing of leukocytes); one bottle of Instamed-Salts as a washing solution (reconstituted in 1000ml aqua bidest, provides 1000ml ready-to-use washing solution).

Whole blood was collected in a heparinised blood tube as previously described. After removing the plasma from the whole blood for biochemical analysis, a 100µl aliquot of the remaining cellular suspension was transferred into a LP3 tube, which was then incubated in an ice bath prior to the addition of opsonised *E. coli* bacteria. 10µl of FITC-labelled opsonised *E. coli* was then added to each LP3 tube containing the whole blood sample on ice.

The treated LP3 blood/bacteria mixture was then incubated at 37^0C for exactly 2 minutes on a roller. All the treated LP3 tubes were immediately immersed back in ice following the 37^0C incubation. The rest of the process was performed at 4^0C until the lysing step. All solutions were prepared at 4^0C throughout the experiment. 100µl of quenching solution was added to all LP3 tubes, prior to the addition of 2ml of ice-cold washing solution. All LP3 tubes were centrifuged at 1,500rpm for 5 minutes. This washing step was repeated twice. Each sample was incubated for 20 minutes at room temperature with 2ml of pre-warmed (room temperature) lysing solution. The sample was washed, prior to

the addition of 100µl of DNA-staining solution. All samples were analysed by flow cytometery within 60 minutes.

5.2.1 Flow Cytometric Analysis

During data acquisition, bacteria were excluded by using fluorescence triggering in the FL3 channel (see gate M1 in Figure 5-1a). Peripheral blood leukocytes were plotted using forward/side scatter derived from the gate M1 (see Figure 5-1b). Granulocytes, monocytes and lymphocytes were identified by their forward/side scatter distribution. The percentage of phagocytosis of each individual cell type was calculated based on the difference between the histogram of the corresponding cell type at 37^0C and 4^0C, using the Overton subtraction method (295) (see Figure 5-1 c & d for granulocytes and for monocyte phagocytosis).

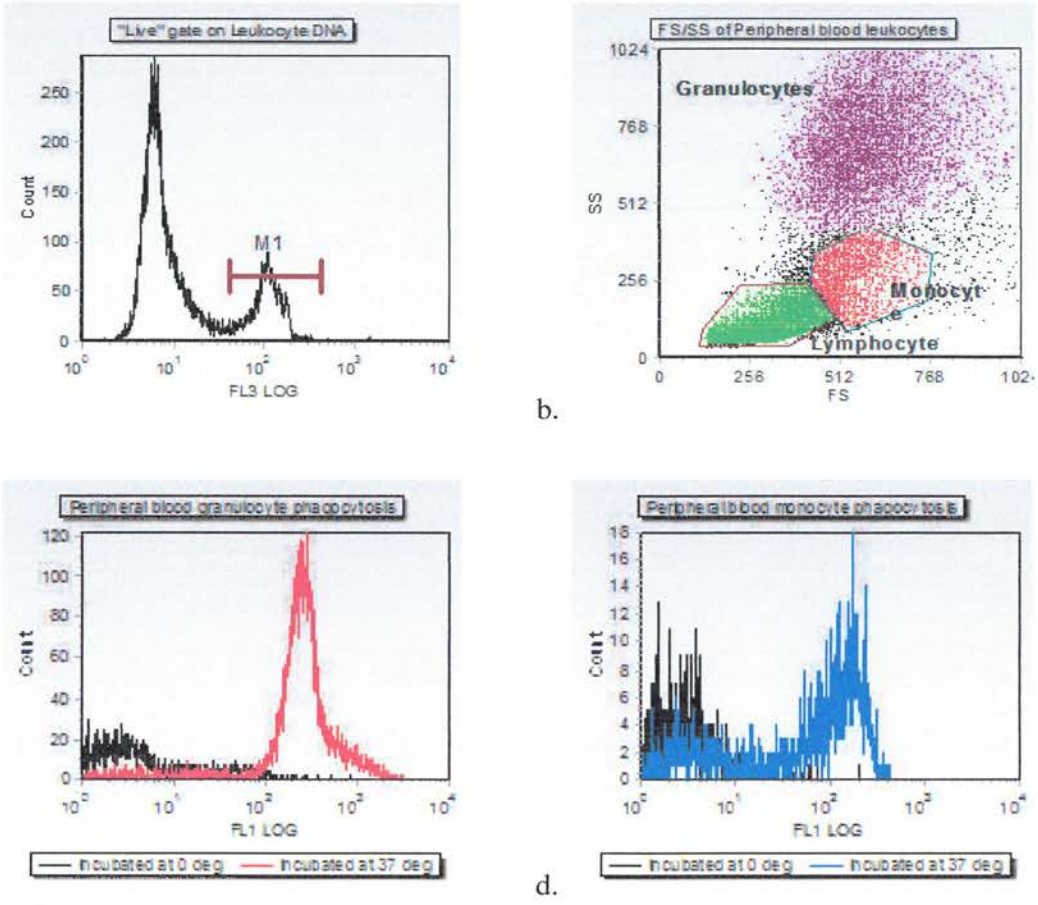

Figure 5-1 (a) After the addition of the lysing solution and the DNA staining solution, gate M1 represents all leukocytes with nuclei. (b) is the forward/side scatter based on gate M1. Granulocytes were gated in purple, monocytes were gated in red, and lymphocytes in green. (c) illustrates *E. coli.* phagocytosis by granulocytes after 2 minutes of 37^0C incubation. The black line is the control (incubation at 4^0C), and the red line is the treatment group at 37^0C. (d) illustrates the monocyte phagocytosis [red coloured gate in (b)]. Blue line represents the treatment group at 37^0C versus the control (black line).

5.3 PERIPHERAL LEUKOCYTE PHAGOCYTOSIS THROUGHOUT THE RESOLUTION OF SEVERE ACUTE PANCREATITIS

The peripheral blood from each sample at each acute pancreatitis time-point above was analysed for its phagoctyic ability. Duplicate experiments were performed for each subject. An internal control, as in the alveolar macrophage (AM) phagocytosis experiment in Chapter 4, was incubated in ice for the whole time. The methodologies of the assay and the flow cytometric analysis were the same as in section 5.2.1.

5.3.1 QUANTIFICATION AND STATISTICAL ANALYSIS OF PERIPHERAL BLOOD PHAGOCYTOSIS IN ACUTE PANCREATITIS

The percentages of overall leukocyte, granulocyte and monocyte phagocytosis were calculated based on the difference between the measurement at 37^0C and 4^0C. To eliminate the variation between blocks of experiments, a relative phagocytic value was used similar to that described in section 4.5.1 for AMs. The relative blood leukocyte phagocytosis of the acute pancreatitis groups was measured with reference to the control group. The relative phagocytic values of all control subjects at all time-points were combined together for statistical analysis below. Non-parametric Kruskall-Wallis One Way Analysis of Variance on Ranks was the statistical test of choice. Dunn's method was used as the post-hoc test against the control. SigmaStat v3.1 (Systats Software, USA) was used as the statistical package for data analysis.

5.3.2 Results of Peripheral Blood Phagocytosis During Acute Pancreatitis

Figure 5-2, Figure 5-3 and Figure 5-4 illustrate the relative phagocytic capacity of total leukocytes, monocytes and granulocytes of all 3 treatment groups (arginine, caerulein and control). Peripheral blood leukocytes in both acute pancreatitis models demonstrated similar phagocytic responses during severe acute pancreatitis, apart from day 1 post-induction. There was a trend towards an increase in overall leukocyte phagocytic capacity on day 1 in the arginine model when compared to the control. At day 7, there was a significant decrease in caerulein leukocyte phagocytosis compared to control [$H(2)= 7.74$, $p=0.02$]. This downward trend in phagocytosis slowly recovered in the following 7 days of the disease process. By day 14, the overall leukocyte phagocytic capacity of the caerulein acute pancreatitis model was above the control group [$H(2)= 7.81$, $p= 0.02$].

When granulocyte and monocyte phaogcytosis were analysed separately, there was a significant reduction in granulocyte phagocytosis in both acute pancreatitis models versus control at day 7 [$H(2)= 13.83$, $p<0.01$]. Although similar statistical significance was not achieved at day 7 for monocyte phagocytosis, there was a downward trend of monocyte phagocytosis in both acute pancreatitis models. By day 10 in the arginine group [$H(2)= 6.56$, $p<0.04$] and day 14 in the caerulein group [$H(2)=11.12$, $p<0.01$], monocyte phagocytosis was found to be significantly upregulated.

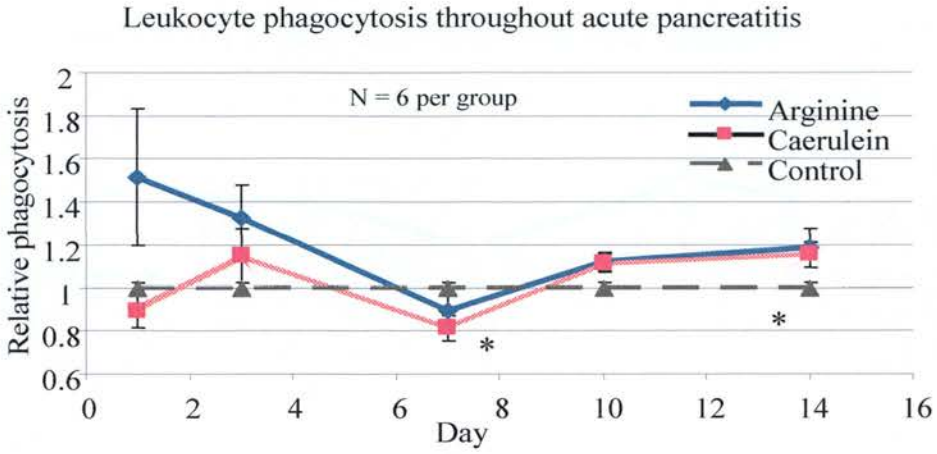

Figure 5-2 This graph illustrates the overall leukocyte phagocytosis throughout an episode of acute pancreatitis. On day 7, there was a significant reduction in the overall phagocytosis in the caerulein group versus the control; whereas by day 14, there was significant increase in the overall leukocyte phagocytosis in both arginine- and caerulein-induced models compared with the control. * denote statistical significance of caerulein versus control group.

Day	Relative value of total leukocyte phagocytosis						p-value
	Arginine		Caerulein		Control		
	mean	SE	Mean	SE	Mean	SE	
1	1.51	0.32	0.89	0.08	1.00	0.02	0.03
3	1.32	0.15	1.15	0.12	1.00	0.02	0.03
7	0.89	0.11	0.81	0.06	1.00	0.02	0.02
10	1.12	0.05	1.12	0.04	1.00	0.02	0.02
14	1.18	0.09	1.15	0.06	1.00	0.02	0.02

Table 5-1 illustrates the relative value of total leukocyte phagocytosis of the three treatment groups of acute pancreatitis at all the studied time-points. Although p-values at all studied time-points were <0.05, the Dunn's method of comparison between the two pancreatitis models and control only revealed significant results at day 7 and day 14.

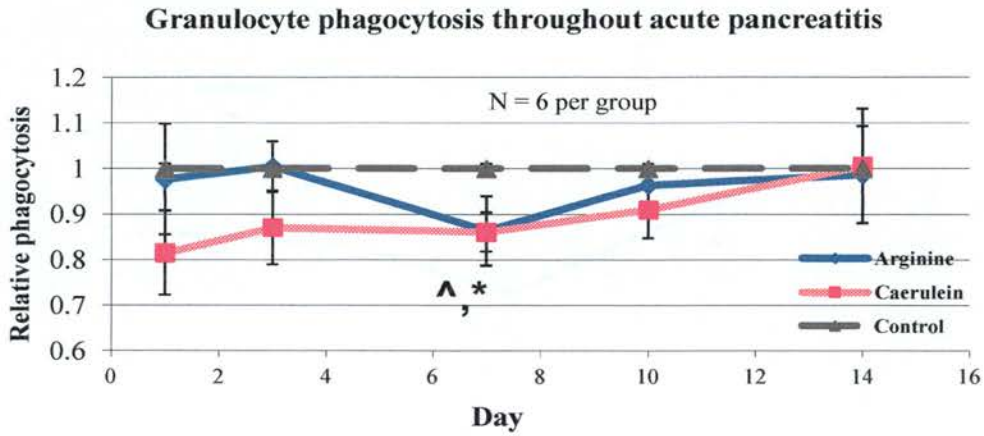

Figure 5-3. This graph illustrates the granulocyte phagocytosis during an episode of acute pancreatitis. This graph illustrates a significant suppression of granulocyte phagocytosis at day 7 in both pancreatitis groups versus the control. *,^ denote statistical significance between caerulein and arginine versus control groups respectively.

Day	Relative value of granulocyte phagocytosis						p-value
	Arginine		Caerulein		Control		
	Mean	SE	Mean	SE	Mean	SE	
1	0.98	0.12	0.82	0.09	1.00	0.01	0.05
3	1.00	0.06	0.87	0.08	1.00	0.01	0.30
7	0.86	0.08	0.86	0.04	1.00	0.01	0.001
10	0.96	0.04	0.91	0.06	1.00	0.01	0.22
14	0.99	0.11	1.01	0.12	1.00	0.01	0.39

Table 5-2 illustrates the relative value of granulocyte phagocytosis of the three treatment groups of acute pancreatitis at all studied time-points

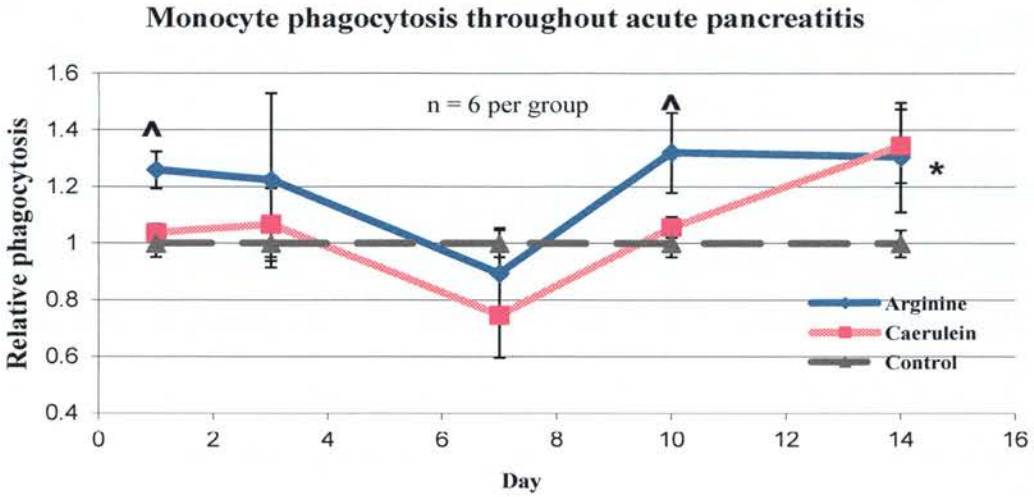

Figure 5-4. This graph illustrates the monocyte phagocytosis throughout an episode of acute pancreatitis. There were significant increases in monocyte phagocytosis on day 1 and 10 in the arginine model versus the control; whereas monocyte phagocytosis was significantly increased only at day14 in the caerulein model. *,^ denote statistical significance between caerulein and arginine versus control groups respectively.

Day	Relative value of monocyte phagocytosis						p-value
	Arginine		Caerulein		Control		
	Mean	SE	mean	SE	Mean	SE	
1	1.26	0.07	1.04	0.03	1.00	0.05	0.01
3	1.22	0.31	1.07	0.13	1.00	0.05	0.77
7	0.89	0.16	0.75	0.15	1.00	0.05	0.21
10	1.32	0.14	1.06	0.04	1.00	0.05	0.04
14	1.30	0.19	1.34	0.13	1.00	0.05	0.005

Table 5-3 illustrates the relative value of monocyte phagocytosis of each of the treatment group of acute pancreatitis at all the studied time-points

5.4 DISCUSSION

The findings of this section resemblance some elements of bacterial clearance during the early onset of acute pancreatitis in humans. Liras et al demonstrated a reduction of leukocyte phagocytosis in the severe versus mild forms of acute pancreatitis at the early onset of the disease (169). Our rodent experiment has confirmed that there was a reduction of bacterial clearance in peripheral blood leukocytes at the early stage of acute pancreatitis. Based on the findings of the peripheral blood phagocytosis, day 7 appeared to be a defining time-point of the immunological responses between an acute and recovery phase of the disease process.

As illustrated above, leukocyte phagocytosis follows a similar pattern in both acute pancreatitis models. The main difference between the two models is at the initial time-point. The exact reason for this increase in leukocyte phagocytosis in the arginine model on day 1 is unknown. Given that there was no significant difference in histological scoring of the pancreas between the two models, the early difference could be explained by the differences in the inducing agents. This argument is supported by Moffat et al (296). Moffat et al studied *Staphylococcus. auerus* phagocytosis by human blood neutrophils with various concentration of L-arginine as substrate *in vitro*. They concluded that there was an increase in neutrophil phagocytosis with L-arginine supplementation. However, this effect was dose dependent. They further suggested that

the possible mechanism is via the nitric oxide synthase pathway. Although the blood concentration of L-arginine in the arginine pancreatitis model was not determined in this thesis, this theory provided a feasible explanation of the variation of immunological response between the two models at the early stage of the disease.

By day 7 after induction, granulocytes of both models showed a significant reduction in bacterial clearance. Although a similar trend was also observed in monocyte phagocytosis, it did not achieve statistical significance in either model. Since most of the bacterial clearance within the bloodstream is contributed by granulocytes and monocytes, it is therefore likely that combination of the reduction in granulocyte and monocyte phagocytosis resulted in a significant reduction for the overall phagocytosis in the caerulein pancreatitis model, and the downward trend of leukocyte phagocytosis in the arginine group. These findings could potentially explain the increased likelihood of nosocomial infection during an episode of acute pancreatitis, which is observed in clinical studies (3, 83).

Towards the complete recovery of severe acute pancreatitis after day 7, there was an increase in the overall phagocytic capacity in both acute pancreatitis models versus the control. Granulocyte phagocytosis almost reverted to normal after day 7. Given that there was no significant increase in granulocyte phagocytic capacity in either pancreatitis model at the recovery phase, the overall increase in the leukocyte

phagocytosis in the recovery phase could only be explained by the gradual increase in the monocyte phagocytic capacity.

Most studies of acute pancreatitis or sepsis have focused on the innate immunity during the acute event (297, 298). Few studies have examined the immunological behaviour, including phagocytosis, of the leukocyte during the recovery phase of the acute pancreatitis. It is interesting to identify a deficiency in neutrophil phagocytosis throughout an episode of acute pancreatitis, and most markedly, halfway through the disease process. This deficiency in bacterial clearance could possibly explain the increased likelihood of nosocomial infections at a later stage of the disease in clinical observational studies. At the same time, an upregulation of monocyte phagocytosis was also noted towards the recovery of acute pancreatitis. This response is similar to that of the AMs towards the end of recovery. However, it is uncertain what the factors are contributing to the upregulation of monocyte phagocytic capacity. In order to investigate the response of neutrophil phagocytosis observed in this chapter, it is useful to correlate these findings with the survival, apoptosis and necrosis of neutrophils at the same experimental time-point, in Chapter 6.

6 PERIPHERAL BLOOD LEUKOCYTE APOPTOSIS AND NECROSIS DURING ACUTE PANCREATITIS

6.1 INTRODUCTION

Leukocyte apoptosis plays a vital role in the resolution of inflammation (299). O'Neil et al and others have demonstrated that there is a role for neutrophil and lymphocyte apoptosis at the beginning of acute pancreatitis (200, 218). However, it is unclear how these inflammatory cells behave during the process of recovery in acute pancreatitis.

The objective of this chapter is to characterize the survival, apoptosis and necrosis of leukocyte lineages (mainly granulocytes and lymphocytes) throughout the resolution of acute pancreatitis. The relationship between the survival/death of leukocytes and the event of sepsis was explored using an *ex vivo* whole blood culture model (section 6.2.3). With these findings, it was hoped to establish a correlation between leukocyte survival and the corresponding phagocytic capacity during acute pancreatitis.

6.2 PERIPHERAL BLOOD LEUKOCYTE APOPTOTIC ASSAYS

Whole blood was harvested from experimental rodents as described in the Chapter 5.2. Red blood cells were lysed using Pharmlyse solution (Cat. No. 555899, BD Pharmingen, UK). Briefly, Pharmlyse solution was diluted to the recommended concentration (x1) using distilled water. 50µl of whole blood was added to each LP3 tube. 2ml of diluted

Pharmlyse solution (at room temperature) was added to the LP3 tube. The mixture was gently vortexed immediately after adding the lysing solution. The suspension, which was protected from light, was left at room temperature for 15 minutes. It was then centrifuged at 1,500rpm for 5 minutes. The supernatant was carefully aspirated without disturbing the cell pellet. The cell pellet was then washed twice with phosphate-buffered saline (PBS). The cells were used for subsequent apoptotic assays.

Each of the methods to detect and measure apoptosis has its advantages and limitations. Because the cellular mechanisms that result in apoptosis are complex, most published methods cannot by themselves detect apoptosis unambiguously. It was because of this fact that both Annexin V and YOPRO dye were chosen as the apoptotic markers for flow cytometry (279, 300).

Annexin V binds to phosphatidylserine, which flips from the inside of the cell membrane to the outer surface of the cell membrane during apoptosis, whereas YOPRO-1 passes through the weakened plasma membrane during apoptosis, which allows accurate and effective detection of apoptosis.

6.2.1 Annexin V/PI Apoptotic Assay

Annexin V/PI (propodium iodide) kit (BMS306FICE, Bender Med System, UK) was used for this study. After the leukocyte pellet had been washed twice with PBS, it was

re-suspended in 195µl binding buffer (x1 concentration) (containing Ca^{2+}). 5µl of Annexin V was added to the suspension. The whole suspension was then incubated for 15 minutes at room temperature in the dark. The suspension was washed once with PBS. At the end of the assay, 190µl of binding buffer was added prior to analysis. The whole suspension was left in ice till flow cytometry analysis. Each specimen was prepared and analysed in duplicate.

6.2.2 YOPRO/7-AAD Apoptotic Assay

YOPRO from the Vybrant apoptosis assay kit #4 (V-13243, Invitrogen, UK) was used for the assay. 7-Amino actinomycin D (7-AAD) has been shown to be a useful marker to quantify apoptosis by itself (301). To increase the sensitivity and differentiation of detecting apoptosis, 7-AAD was selected for use alongside YOPRO as one of the apoptotic assays.

7-AAD (1mg, A1310, Invitrogen, UK) was prepared by dissolving first in 50µl of methanol and then diluted to 1ml with PBS. The leukocyte pellet was resuspended in 1ml of RPMI culture medium with 10% fetal calf serum. 1µl of YOPRO and 20µl of 7-AAD were added to the suspension. The suspension was incubated on ice in the dark for 30 minutes. The assay was then analysed immediately after the incubation. Each specimen was prepared and analysed in duplicate.

6.2.3 Peripheral Blood Leukocyte Apoptosis After Lipopolysaccharide Stimulation

Experiments above aim to provide insights into how peripheral blood leukocytes survive or die during an episode of severe acute pancreatitis. To simulate the impact of bacterial infection on the survival of peripheral blood leukocytes during acute pancreatitis, lipopolysaccharide (LPS), a bacterial endotoxin which is a major constituent of the outer membrane of Gram-negative bacteria, was used for *in vitro* experiments to mimic bacteraemia/septicaemia at different time-points throughout an episode of acute pancreatitis (302).

500µl of whole blood was resuspended in 4.5ml of RPMI culture medium with penicillin/streptomycin and glutamine. The suspended blood was split into two sets: in one set, 1.25µg of LPS (L7895, Sigma-Aldrich, UK) was added to one 2.5ml of diluted whole blood, whereas no additive was added to the other set. Each set of whole blood was cultured in duplicate in a 12-well plate at 37^0C for 18 hours.

After 18 hours of incubation, specimens were transferred to labelled Eppendorff tubes, and were centrifuged for 5 minutes at 2500rpm. Supernatants were removed and stored at -70^0C till analysis. 25µl of the remaining leukocyte pellet in each tube was transferred to an LP3 tube. Again, duplicates were performed for each subject. The Annexin V/PI

assay was used as the only apoptotic marker for this set of experiments. The assay was performed in the same manner as in section 6.2.1.

6.2.4 Flow Cytometry Gate-Setting, Quantification and Statistical Analysis

All assays were analysed by Coulter Epics XL flow cytometer. The raw data was analysed by FCS Express v3 (De Novo Software, Los Angeles, USA). The apoptosis of lymphocytes, monocytes, granulocytes and total leukocytes was analysed. Subsets of leukocytes were identified based on their forward/side scatter distribution (Figure 6-1 & Figure 6-2). For each individual cell type, the FL3 gate (PI or 7-AAD) was plotted against the FITC or FL1 gate (Annexin V or YOPRO). For the graph of FL3 against FL1 axes, three subpopulations could be discriminated: (1) annexin-V or YOPRO-FITC-*negative* / PI or 7-AAD-*negative* cells (this group represents viable cells); (2) annexin-V or YOPRO-FITC-*positive* / PI or 7-AAD-*negative* cells (this group represents apoptotic cells); and (3) annexin-V or YOPRO-*positive* / PI or 7-AAD-*positive* cells (this group represents late apoptotic/necrotic cells).

The percentages of apoptosis and necrosis for each leukocyte subpopulation of different treatment groups were recorded. As illustrated in chapters 4 and 1, the relative value of apoptosis/necrosis to the control group was used for analysis in order to minimize the variations between blocks of experiments. The measured absolute value for

survival/death of leukocytes of each subject is equivalent to the average of the duplicate. This relative value is derived from the division of the absolute value of the treated group by that of the control group of the corresponding block of experiment.

Relative values of leukocyte subpopulations of all three sets of experiments were analysed by non-parametric Kruskal-Wallis ANOVA. Dunn's comparison method was applied for in-between groups analysis against the control group. All statistical analysis was performed using SigmaStat software (Systat Software Inc., USA).

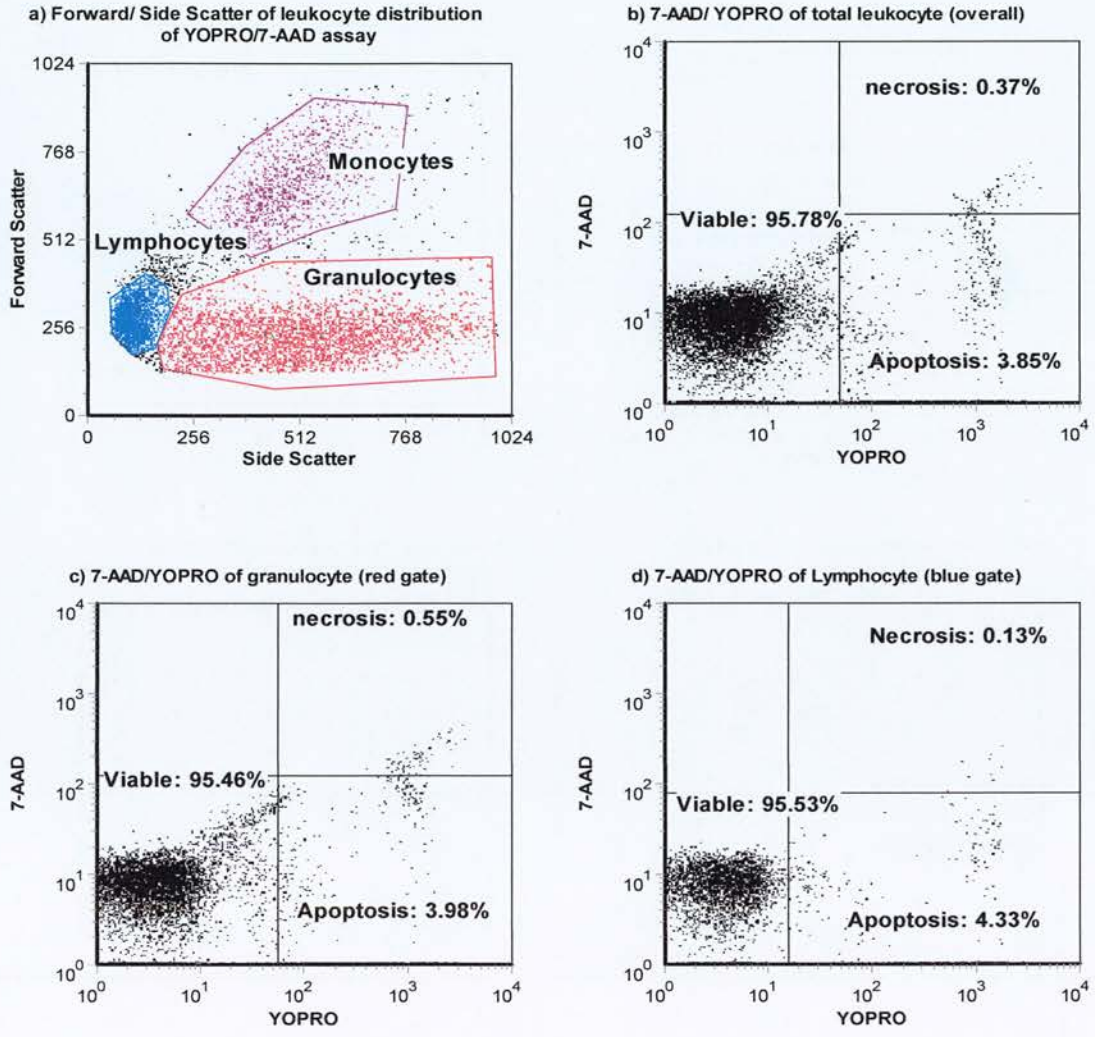

Figure 6-1(a) illustrates the forward/side scatter distribution of the overall blood leukocyte of YOPRO/7-AAD assay after lysing the red blood cells. Granulocytes were gated as red, lymphocytes as blue and monocytes as purple. (b) is the 7-AAD/YOPRO histogram distribution of the combination of granulocytes, monocytes and lymphocytes. The bottom left-hand quadrant represents viable cells; the bottom right-hand quadrant represents apoptotic cells, and the top right-hand corner represents necrotic cells. (c) is the 7-AAD/YOPRO histogram distribution of granulocytes (red gate) , and (d) is the histogram distribution of lympocytes (blue gate).

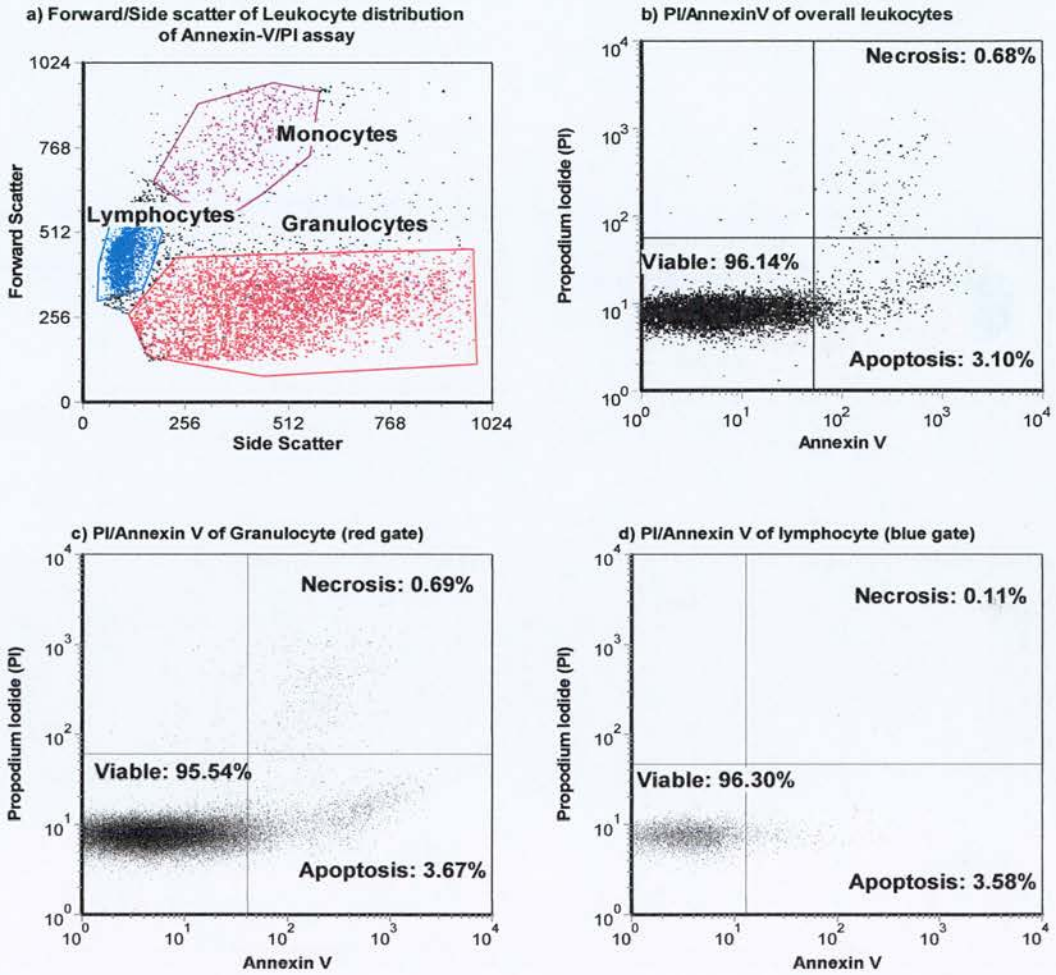

Figure 6-2 illustrates similar diagrams as in Figure 6-1, but the Annexin V/PI assay was used. (a) represents the forward/side scatter of leukocyte distribution using Annexin V/PI assay after lysing the red blood cells. (b) is the PI/ Annexin V histogram distribution of the combination of granulocytes, monocytes and lymphocytes. (c) is the PI/ Annexin V histogram distribution of granulocytes (red gate), and (d) is the histogram distribution of lympocytes (blue gate).

6.3 RESULTS

6.3.1 OVERALL LEUKOCYTE APOPTOSIS AND NECROSIS DURING ACUTE PANCREATITIS

Figure 6-3 illustrates the quantification of apoptosis and necrosis of the overall leukocytes during severe acute pancreatitis in all three treatment groups. There is no statistical difference in leukocyte necrosis between the two pancreatitis groups (arginine and caerulein) and the control group at any of the studied time-points, when the necrosis was measured by both YOPRO/7-AAD and Annexin V/PI.

There was a close resemblance of the trend of leukocyte apoptosis in the caerulein group when apoptosis was measured by either Annexin V/PI or YOPRO/7-AAD methods. There was significant reduction in leukocyte apoptosis of the caerulein group on day 3 [YOPRO assay: $H(2)=9.05$, $p=0.01$; Annexin V assay: $H(2)= 7.30$, $p<0.03$], and day 14 [YOPRO assay: $H(2)=8.98$, $p=0.01$] when compared with the control.

For the arginine pancreatic group, leukocyte apoptosis followed a similar trend when measured by both the YOPRO/7-AAD and the Annexin-V/PI assay at all time-points, except from day 1. The YOPRO assay detected a significant reduction of leukocyte apoptosis in the arginine group on day 1 when compared with the control [$H(2)=8.23$, $p<0.02$]; whereas the Annexin V assay revealed a significant increase in leukocyte

apoptosis at the same time-point[H(2)=12.97,p<0.01]No statistical significance was achieved for the rest of the time-points.

6.3.2 Granulocyte Apoptosis and Necrosis During Acute Pancreatitis

Figure 6-4 illustrates the graphs of granulocyte apoptosis and necrosis throughout acute pancreatitis when measured by Annexin V/PI and YOPRO/7-AAD assays. The analyses for the granulocyte apoptosis and necrosis are similar to those reported in section 6.3.1. The analyses were based on the gated granulocytes (blue gate) population shown in Figure 6-1 and Figure 6-2. Both Annexin V/PI and YOPRO/7-AAD assays revealed similar results for granulocyte necrosis and apoptosis, especially among the caerulein pancreatitis group. Although there was a trend of increasing apoptosis and necrosis from day 7 onwards, there was no statistical difference in granulocyte apoptosis and necrosis between the arginine pancreatitis group and the control group at any studied time-point.

For the caerulein group, there was a significant reduction in granulocyte necrosis using both the Annexin V/PI [H(2)=10.10, p<0.01] and the YOPRO/7-AAD [H(2)=8.79, p<0.02] assays at day 3. Using YOPRO/7-AAD analysis, there was significant increase in granulocyte necrosis at day 1 [H(2)=10.96, p<0.01] and a significant reduction of granulocyte apoptosis at day 3 [H(2)=10.24, p<0.01] in the caerulein group versus the control group. Although these changes did not achieve statistical significance when analysed using the Annexin V assay, similar trends were also observed at those time-

points. In addition, the pattern of granulocyte apoptosis and necrosis closely resemble each other in both of the acute pancreatitis models at all studied time-points.

6.3.3 Lymphocyte Apoptosis and Necrosis During Acute Pancreatitis

The trends of lymphocyte necrosis and apoptosis measured by either Annexin V/PI or YOPRO/7-AAD assays were different (see Figure 6-5). The only time-point that was similar between the two assays was the measurement of lymphocyte necrosis in the arginine model at day 3. Both assays revealed significant increase in lymphocyte necrosis within the arginine group at day 3 when compared to the control group [YOPRO assay: $H(2)=11.11$, $p<0.001$; Annexin V assay: $H(2)=7.78$, $p=0.02$]. Using the Annexin V/PI assay, the degree of lymphocyte necrosis in the caerulein group was significantly increased as compared to the control [$H(2)=7.89$, $p<0.02$] at day 10. Although statistical significance was not achieved in either pancreatitis group at day 10 when the YOPRO/7-AAD assay was used, there was a trend in increase in lymphocyte necrosis of the caerulein group.

The trend of lymphocyte apoptosis in both acute pancreatitis groups measured by the YOPRO/7-AAD assay was again dissimilar to that of the annexinV/PI assay. Lymphocyte apoptosis measured by the Annexin V/PI assay was significantly increased on day 1 in both acute pancreatitis models [$H(2)=10.13$, $p<0.01$]; whereas there was significant reduction in the caerulein group using YOPRO/7-AAD assay [$H(2)=7.45$,

p=0.02]. There was also a significant increase in lymphocyte apoptosis measured by YOPRO/7-AAD in the caerulein group versus the control at day 10 [H(2)=11.52, p<0.01]. No statistical significance was achieved at day 10 in either pancreatitis group when lymphocyte apoptosis was measured by the Annexin V/PI assay.

6.3.4 Overall Leukocyte apoptosis and necrosis with or without Lipopolysaccharide Stimulation

Figure 6-6 illustrates the total leukocyte necrosis and apoptosis after 18 hours of co-culture with or without lipopolysaccharide (LPS) in our acute pancreatitis models. Significant reduction of leukocyte necrosis was found in the caerulein model at day 3 without LPS stimulation [H(2)=9.06, p<0.02]. Although no statistical significance was achieved, leukocyte necrosis of the caerulein model with LPS co-culture demonstrated a similar trend to that without LPS stimulation.

The results for leukocyte apoptosis were different between the two models with and without LPS co-culture. At day 14, there was significant reduction in leukocyte apoptosis of the caerulein model without LPS [H(2)=11.36, p<0.01) co-culture compared to the control. There was a trend of reduction in leukocyte apoptosis of the caerulein model after LPS co-culture at the same time-point, but there was no statistical significance.

Although there was no significant reduction or increase in leukocyte apoptosis by day 7, there was a trend of increased leukocyte apoptosis after 18 hours co-culture without LPS stimulation in the arginine model, suggesting an increase in survival of the leukocytes. When LPS was co-cultured with the whole blood of both pancreatitis models at the same time point, this increasing trend of leukocyte apoptosis disappeared.

6.3.5 Granulocyte Apoptosis and Necrosis With Or Without Lipopolysaccharide Stimulation During Acute Pancreatitis

Figure 6-7 represents granulocyte necrosis and apoptosis in all three treatment groups after 18 hours of culture with or without LPS stimulation. Granulocyte necrosis was significantly reduced at day 3 in the caerulein group when compared to the control group in experiments with [$H(2)=7.42$, $p=0.02$] or without [$H(2)=6.05$, $p<0.05$] LPS stimulation. No significant differences of granulocyte necrosis between the two acute pancreatic groups and the control group were identified at other time-points.

By day 7, there was a significant reduction of granulocyte apoptosis in the caerulein group with LPS co-culture [$H(2)=9.87$, $p<0.01$]. Although no statistical significance in granulocyte apoptosis of the arginine group was achieved at day 7, a similar trend to the caerulein model suggested a reduction of granulocyte apoptosis after LPS stimulation. At day 14, granulocyte apoptosis in the caerulein group in both co-culture assays was again found to be significantly reduced, when compared to the control [with LPS:

H(2)=6.67, p=0.04; without LPS: H(2)=6.57, p=0.04]. This pattern of granulocyte survival/death is similar overall to that of the leukocyte experiment described in the previous section. It is therefore reasonable to speculate that the majority of the overall leukocyte apoptosis discussed in section 6.3.4 could have been mainly contributed by the injuries of granulocytes during the acute pancreatitis.

6.3.6 Lymphocyte Apoptosis and Necrosis With and Without Lipopolysaccharide

Figure 6-8 illustrates lymphocyte apoptosis and necrosis with and without LPS co-culture throughout severe acute pancreatitis, as per the previous section. There were significant reductions in lymphocyte necrosis at day 3 in the caerulein model versus the control, both with [H(2)=9.15, p=0.01] and without [H(2)=12.01, p<0.01] LPS. At the same time-point, significant reduction of lymphocyte necrosis of the arginine model was also noted in the assay without LPS co-culture. At day 10, there was a significant increase in lymphocyte necrosis in the arginine-induced pancreatitis group without the addition of LPS [H(2)=12.48, p<0.01]. This increase in lymphocyte necrosis was dampened by the addition of LPS.

No significant differences of lymphocyte apoptosis between the pancreatitis groups and the control were noted at all time-points in the experiment with LPS co-culture. Without LPS co-culture, there was a significant increase in lymphocyte apoptosis in the arginine

group on day 1 [H(2)=8.90, p=0.01]; and there was a significant reduction in lymphocyte apoptosis in the caerulein group on day 7 [H(2)=7.70, p=0.02].

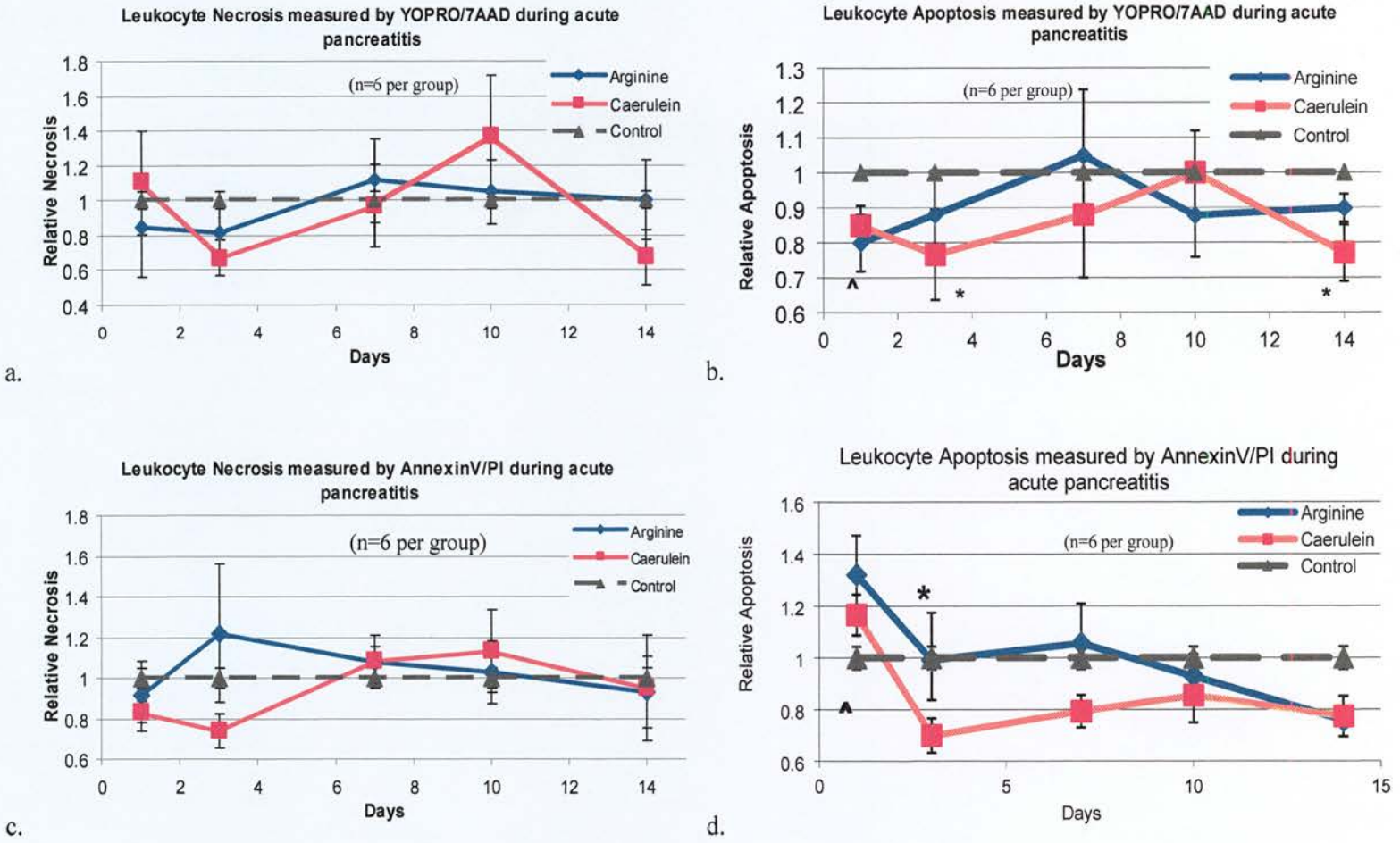

Figure 6-3. These graphs illustrate the relative overall leukocyte necrosis or apoptosis of all three treatment groups measured against various time-points using either YOPRO/7-AAd assay or Annexin V/ PI assay. (^ denotes statistically significant difference between the arginine and control groups at that particular time-point; whereas * represents statistical significance between the caerulein and control groups.)

Table 6-1 illustrates the relative values of total leukocyte apoptosis/ necrosis measured by either YOPRO/7AAD or AnnexinV/PI of the 3 treatment groups of acute pancreatitis at the studied time-points

Leukocyte necrosis of the 3 treatment groups measured by YOPRO/7AAD (n=6 per group)

	Arginine		Caerulein		Control		p-value
Day	Mean	S.E.	Mean	S.E.	Mean	S.E.	
1	0.85	0.28	1.11	0.30	1.00	0.05	0.46
3	0.81	0.16	0.67	0.10	1.00	0.05	0.05
7	1.11	0.24	0.97	0.23	1.00	0.05	0.78
10	1.05	0.19	1.37	0.35	1.00	0.05	0.73
14	1.00	0.23	0.68	0.16	1.00	0.05	0.11

Leukocyte apoptosis of the 3 treatment groups measured by YOPRO/7AAD (n=6 per group)

	Arginine		Caerulein		Control		p-value
Day	Mean	S.E.	Mean	S.E.	Mean	S.E.	
1	0.80	0.08	0.85	0.06	1.00	0.02	0.02
3	0.88	0.10	0.77	0.13	1.00	0.02	0.01
7	1.05	0.19	0.88	0.18	1.00	0.02	0.31
10	0.88	0.12	1.00	0.12	1.00	0.02	0.84
14	0.90	0.04	0.77	0.08	1.00	0.02	0.01

Leukocyte necrosis of the 3 treatment groups as measured by AnnexinV/PI (n=6 per group)

	Arginine		Caerulein		Control		p-value
Day	Mean	S.E.	Mean	S.E.	Mean	S.E.	
1	0.92	0.17	0.83	0.05	1.00	0.05	0.08
3	1.22	0.34	0.74	0.09	1.00	0.05	0.12
7	1.08	0.07	1.09	0.12	1.00	0.05	0.22
10	1.03	0.15	1.13	0.20	1.00	0.05	0.25
14	0.93	0.18	0.95	0.26	1.00	0.05	0.75

Leukocyte apoptosis of the 3 treatment groups as measured by AnnexinV/PI (n=6 per group)

	Arginine		Caerulein		Control		p-value
Day	Mean	S.E.	Mean	S.E.	Mean	S.E.	
1	1.32	0.15	1.17	0.08	1.00	0.04	<0.01
3	0.99	0.18	0.70	0.07	1.00	0.04	0.04
7	1.06	0.15	0.79	0.06	1.00	0.04	0.50
10	0.93	0.09	0.85	0.10	1.00	0.04	0.95
14	0.76	0.04	0.77	0.08	1.00	0.04	0.29

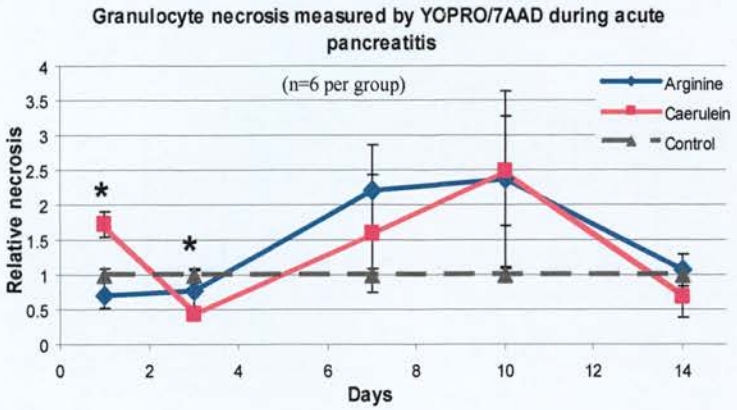

a.

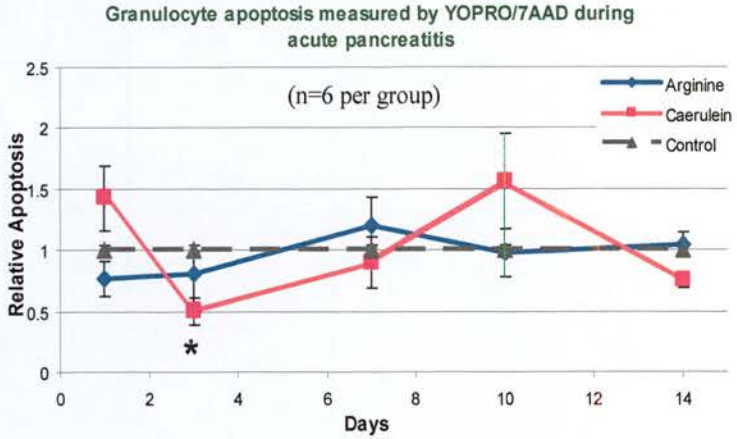

b.

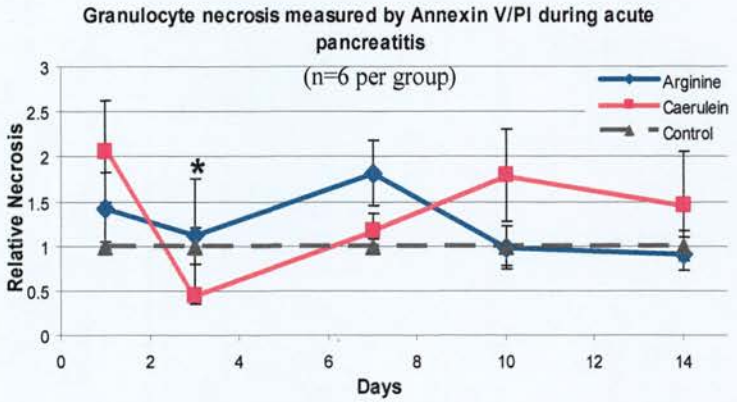

c.

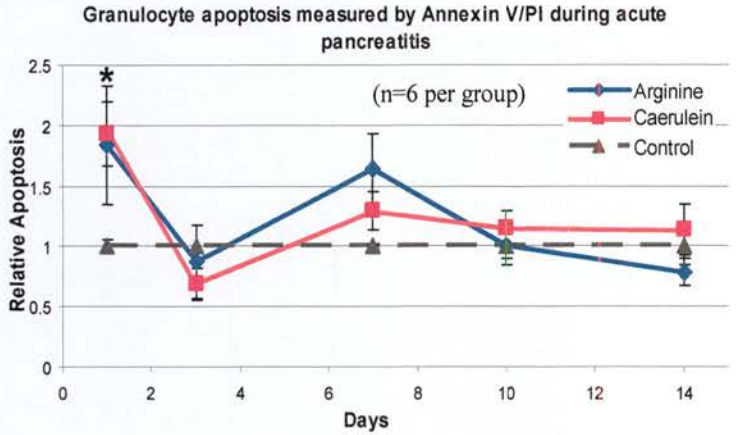

d.

Figure 6-4. These graphs illustrate the relative granulocyte necrosis or apoptosis of all three treatment groups at various time-points measured by either YOPRO/7-AAd assay or Annexin V/ PI assay. (^ denotes statistically significant difference between the arginine and control groups at that particular time-point; whereas * represents statistical significance between the caerulein and control groups.)

Table 6-2 illustrates the relative values of neutrophil apoptosis/ necrosis measured by either YOPRO/7AAD or AnnexinV/PI of the 3 treatment groups of acute pancreatitis at the studied time-points

Neutrophil Necrosis of the 3 treatment groups measured by YOPRO/7AAD (n=6 per group)							
	Arginine		Caerulein		Control		p-value
Day	Mean	S.E.	Mean	S.E.	Mean	S.E.	
1	0.71	0.19	1.72	0.19	1.00	0.08	<0.01
3	0.78	0.29	0.43	0.08	1.00	0.08	0.01
7	2.20	0.66	1.59	0.84	1.00	0.08	0.39
10	2.37	1.27	2.49	0.78	1.00	0.08	0.26
14	1.07	0.23	0.67	0.28	1.00	0.08	0.88

Neutrophils apoptosis of the 3 treatment groups measured by YOPRO/7AAD (n=6 per group)							
	Arginine		Caerulein		Control		p-value
Day	Mean	S.E.	Mean	S.E.	Mean	S.E.	
1	0.72	0.13	1.25	0.18	1.00	0.05	0.10
3	0.89	0.21	0.51	0.13	1.00	0.05	<0.01
7	1.44	0.34	1.36	0.52	1.00	0.05	0.48
10	0.97	0.19	1.47	0.36	1.00	0.05	0.71
14	1.02	0.11	0.69	0.07	1.00	0.05	0.05

Neutrophil Necrosis of the 3 treatment groups measured by AnnexinV/PI (n=6 per group)							
	Arginine		Caerulein		Control		p-value
Day	Mean	S.E.	Mean	S.E.	Mean	S.E.	
1	1.42	0.42	2.06	0.57	1.00	0.15	0.11
3	1.13	0.64	0.44	0.08	1.00	0.15	0.01
7	1.82	0.37	1.16	0.20	1.00	0.15	0.09
10	0.98	0.24	1.79	0.51	1.00	0.15	0.42
14	0.91	0.19	1.45	0.61	1.00	0.15	0.75

Neutrophil Apoptosis of the 3 treatment groups measured by AnnexinV/PI (n=6 per group)							
	Arginine		Caerulein		Control		p-value
Day	Mean	S.E.	Mean	S.E.	Mean	S.E.	
1	1.83	0.49	1.93	0.26	1.00	0.08	<0.01
3	0.87	0.30	0.69	0.13	1.00	0.08	0.11
7	1.64	0.29	1.29	0.16	1.00	0.08	<0.05
10	1.01	0.11	1.16	0.15	1.00	0.08	0.58
14	0.78	0.11	1.14	0.21	1.00	0.08	0.21

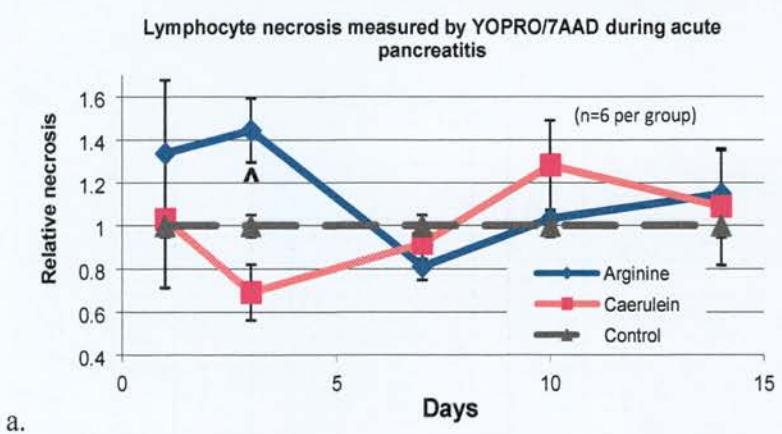

a.

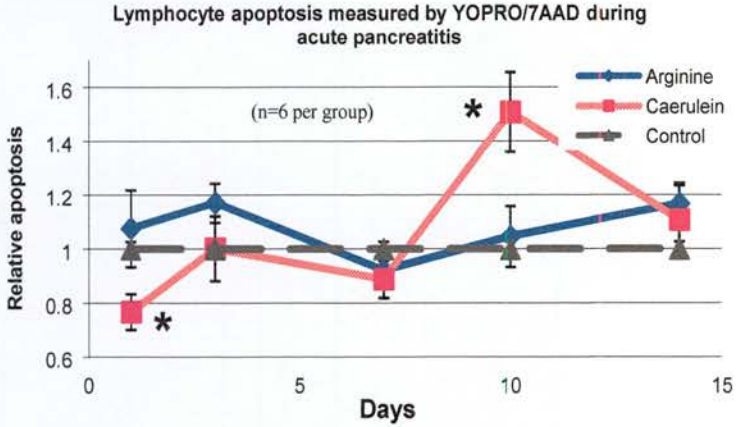

b.

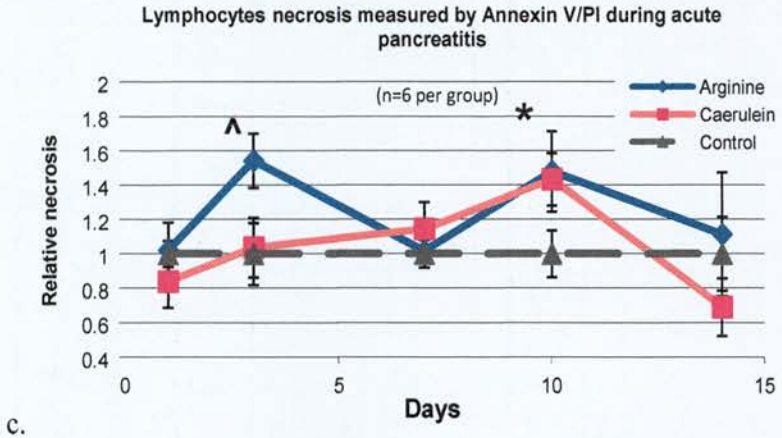

c.

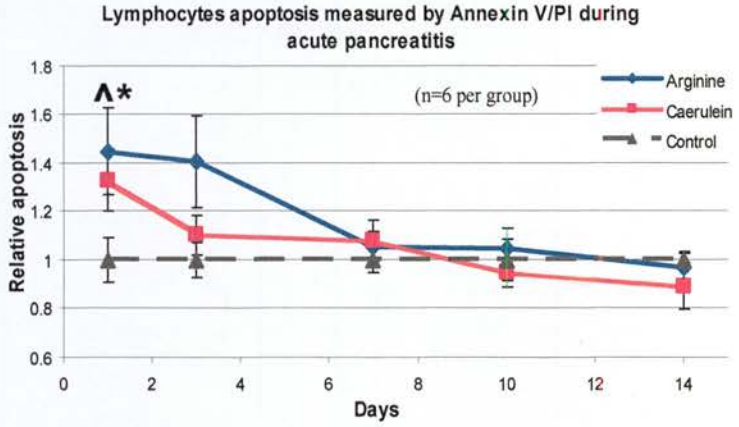

d.

Figure 6-5 illustrates the lymphocyte necrosis or apoptosis of all three treatment groups measured against various time-points using either YOPRO/7-AAd assay or Annexin V/ PI assay. (^ denotes statistically significant difference between the arginine and control groups at that particular time-point; whereas * represents statistical significance between the caerulein and control groups.)

Table 6-3 illustrates the relative values of lymphocyte apoptosis/ necrosis measured by either YOPRO/7AAD or AnnexinV/PI of the 3 treatment groups of acute pancreatitis at the studied time-points

Lymphocyte necrosis for the 3 treatment groups measured by YOPRO/7AAD (n=6 per group)							
	Arginine		Caerulein		Control		*p*-value
Day	Mean	S.E.	Mean	S.E.	Mean	S.E.	
1	1.34	0.34	1.03	0.32	1.00	0.05	0.33
3	1.44	0.15	0.69	0.13	1.00	0.05	<0.01
7	0.81	0.06	0.92	0.07	1.00	0.05	0.18
10	1.03	0.04	1.28	0.21	1.00	0.05	0.58
14	1.15	0.20	1.09	0.27	1.00	0.05	0.82

Lymphocyte apoptosis for the 3 treatment groups measured by YOPRO/7AAD (n=6 per group)							
	Arginine		Caerulein		Control		*p*-value
Day	Mean	S.E.	Mean	S.E.	Mean	S.E.	
1	1.06	0.15	0.77	0.06	1.00	0.03	0.02
3	1.16	0.07	1.05	0.12	1.00	0.03	0.15
7	0.92	0.06	0.89	0.07	1.00	0.03	0.17
10	1.00	0.10	1.45	0.13	1.00	0.03	<0.01
14	1.10	0.08	1.15	0.15	1.00	0.03	0.09

Lymphocytes necrosis for the 3 treatment groups measured by AnnexinV/PI (n=6 per group)							
	Arginine		Caerulein		Control		*p*-value
Day	Mean	S.E.	Mean	S.E.	Mean	S.E.	
1	1.02	0.16	0.84	0.15	1.00	0.09	0.48
3	1.54	0.16	1.04	0.17	1.00	0.09	0.02
7	1.02	0.07	1.14	0.16	1.00	0.09	0.65
10	1.48	0.23	1.43	0.15	1.00	0.09	0.02
14	1.11	0.36	0.69	0.17	1.00	0.09	0.31

Lymphocyte apoptosis for the 3 treatment groups measured by AnnexinV/PI (n=6 per group)							
	Arginine		Caerulein		Control		*p*-value
Day	Mean	S.E.	Mean	S.E.	Mean	S.E.	
1	1.45	0.18	1.33	0.13	1.00	0.04	0.01
3	1.41	0.19	1.10	0.08	1.00	0.04	0.08
7	1.05	0.07	1.08	0.08	1.00	0.04	0.56
10	1.05	0.09	0.95	0.06	1.00	0.04	0.68
14	0.97	0.07	0.89	0.10	1.00	0.04	0.52

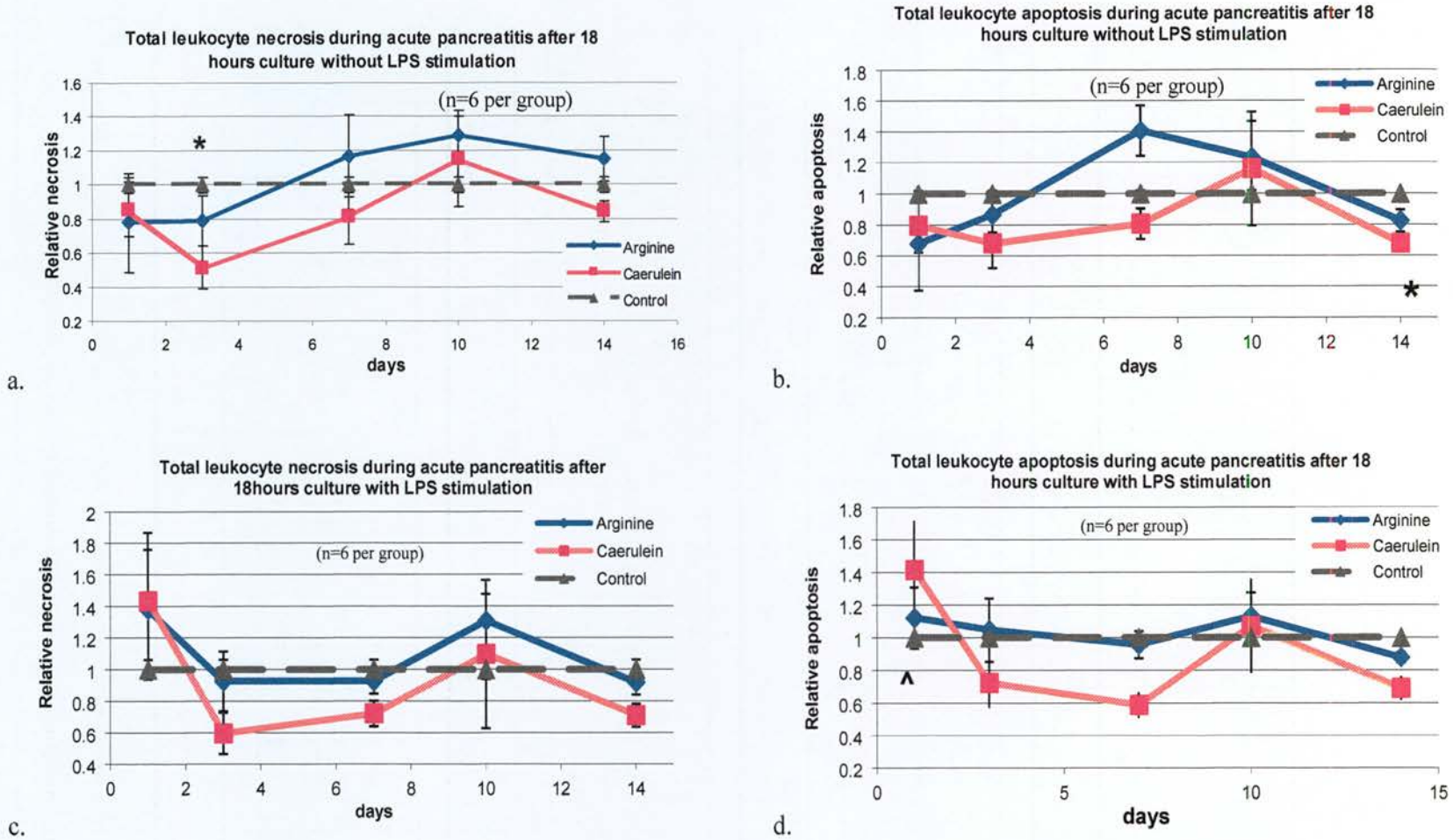

Figure 6-6 illustrates total leukocyte necrosis and apoptosis after 18 hours of in vitro whole blood culture at 370C with and without LPS stimulation at different time-points of severe acute pancreatitis. Annexin V/PI assay was used in both LPS culture conditions. (a) & (b) represent total leukocyte necrosis and apoptosis without the co-culture of LPS; whereas (c) & (d) represent leukocyte necrosis and apoptosis after 18 hours of co-culture with LPS. (^ denotes statistically significant difference in arginine group versus the control group at a particular time-point, where * represents that of the caerulein group versus the control group.)

Table 6-4 illustrates the relative values of total leukocyte apoptosis/ necrosis with or without LPS stimulation of the 3 treatment groups of acute pancreatitis at the studied time-points

Leukocyte necrosis for the 3 treatment groups with no LPS stimulation (n=6 per group)							
	Arginine		Caerulein		Control		*p*-value
Day	Mean	S.E.	Mean	S.E.	Mean	S.E.	
1	0.78	0.29	0.86	0.16	1.00	0.05	0.44
3	0.79	0.15	0.51	0.13	1.00	0.05	0.01
7	1.17	0.24	0.82	0.16	1.00	0.05	0.34
10	1.29	0.11	1.15	0.28	1.00	0.05	0.12
14	1.15	0.13	0.84	0.06	1.00	0.05	0.14

Leukocyte apoptosis for the 3 treatment groups with no LPS stimulation (n=6 per group)							
	Arginine		Caerulein		Control		*p*-value
Day	Mean	S.E.	Mean	S.E.	Mean	S.E.	
1	0.68	0.30	0.80	0.17	1.00	0.02	0.31
3	0.86	0.11	0.68	0.16	1.00	0.02	<0.05
7	1.41	0.16	0.81	0.10	1.00	0.02	0.01
10	1.23	0.24	1.16	0.37	1.00	0.02	0.50
14	0.82	0.07	0.68	0.05	1.00	0.02	<0.01

Leukocyte necrosis for the 3 treatment groups after 18 hrs LPS stimulation (n=6 per group)							
	Arginine		Caerulein		Control		*p*-value
Day	Mean	S.E.	Mean	S.E.	Mean	S.E.	
1	1.38	0.38	1.43	0.43	1.00	0.06	0.51
3	0.93	0.19	0.60	0.13	1.00	0.06	0.08
7	0.93	0.08	0.72	0.08	1.00	0.06	0.07
10	1.31	0.17	1.10	0.47	1.00	0.06	0.18
14	0.92	0.08	0.71	0.07	1.00	0.06	0.07

Leukocyte apoptosis for the 3 treatment groups after 18 hrs LPS stimulation (n=6 per group)							
	Arginine		Caerulein		Control		*p*-value
Day	Mean	S.E.	Mean	S.E.	Mean	S.E.	
1	1.12	0.19	1.42	0.30	1.00	0.05	0.04
3	1.05	0.19	0.72	0.15	1.00	0.05	0.28
7	0.96	0.08	0.59	0.08	1.00	0.05	0.06
10	1.13	0.14	1.07	0.29	1.00	0.05	0.55
14	0.88	0.03	0.69	0.07	1.00	0.05	0.15

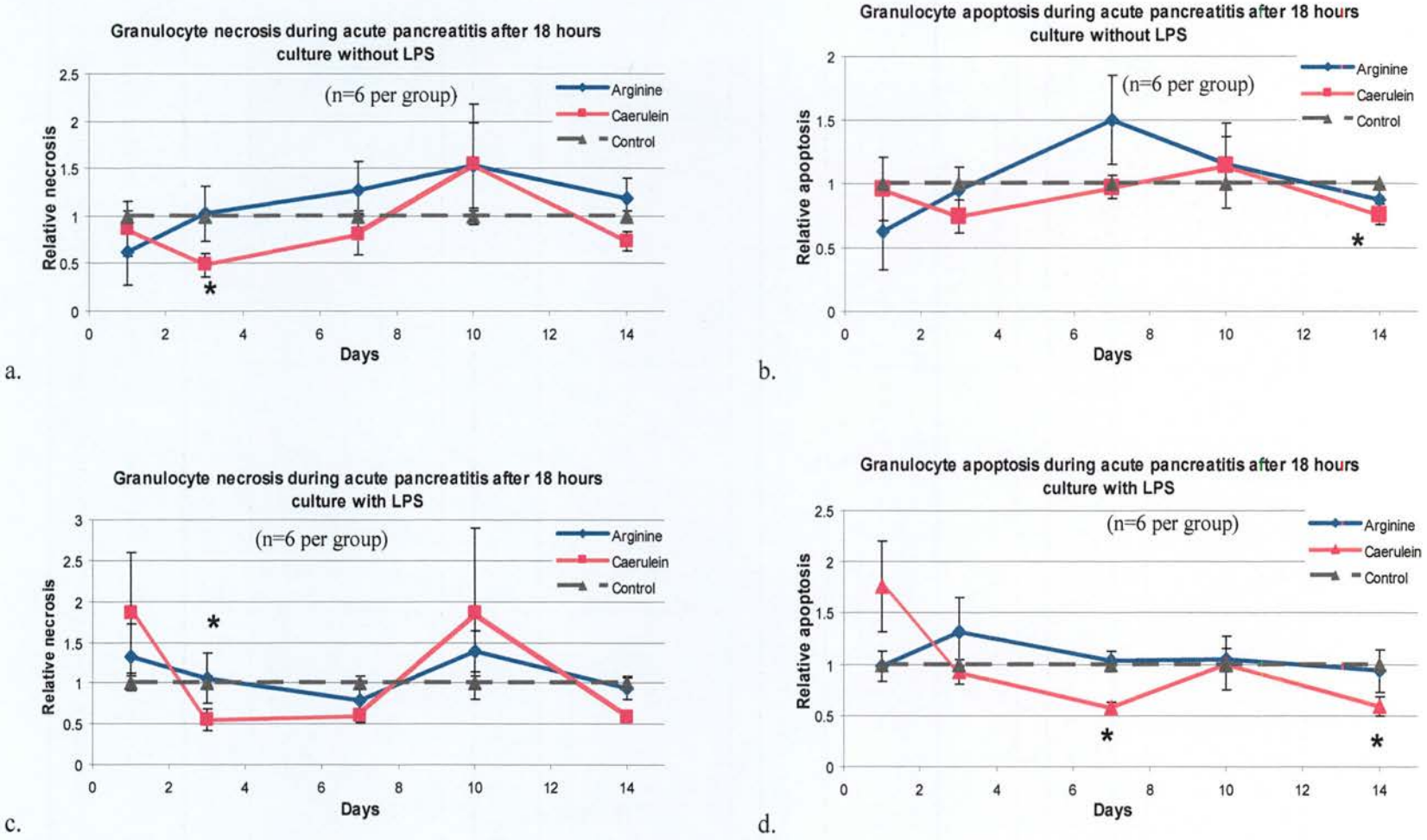

Figure 6-7 illustrates granulocyte necrosis and apoptosis after 18 hours of in vitro whole blood culture at 370C with and without LPS stimulation at different time-points of acute pancreatitis. Annexin V/PI assay was used in both with or without LPS culture conditions. (a) & (b) represent granulocyte necrosis and apoptosis without the co-culture of LPS; whereas (c) & (d) represent granulocyte necrosis and apoptosis after 18 hours of co-culture with LPS. (^ denotes statistically significant difference in arginine group versus the control group at a particular time-point, where * represents that of the caerulein group versus the control group.)

Table 6-5 illustrates the relative values of neutrophil apoptosis/ necrosis with or without LPS stimulation of the 3 treatment groups of acute pancreatitis at the studied time-points

Neutrophils necrosis for the 3 treatment groups with no LPS stimulation (n=6 per group)							
	Arginine		Caerulein		Control		p-value
Day	Mean	S.E.	Mean	S.E.	Mean	S.E.	
1	0.62	0.35	0.87	0.29	1.00	0.06	0.3
3	1.03	0.28	0.49	0.12	1.00	0.06	<0.05
7	1.27	0.31	0.81	0.21	1.00	0.06	0.42
10	1.53	0.45	1.54	0.64	1.00	0.06	0.46
14	1.19	0.22	0.73	0.10	1.00	0.06	0.1

Neutrophils apoptosis for the 3 treatment groups with no LPS stimulation (n=6 per group)							
	Arginine		Caerulein		Control		p-value
Day	Mean	S.E.	Mean	S.E.	Mean	S.E.	
1	0.62	0.30	0.96	0.25	1.00	0.03	0.30
3	0.94	0.18	0.74	0.13	1.00	0.03	0.12
7	1.50	0.35	0.97	0.09	1.00	0.03	0.48
10	1.15	0.21	1.14	0.33	1.00	0.03	0.58
14	0.88	0.10	0.76	0.08	1.00	0.03	0.04

Neutrophils necrosis for the 3 treatment groups after 18hrs LPS stimulation (n=6 per group)							
	Arginine		Caerulein		Control		p-value
Day	Mean	S.E.	Mean	S.E.	Mean	S.E.	
1	1.32	0.41	1.86	0.74	1.00	0.08	0.16
3	1.06	0.31	0.55	0.13	1.00	0.08	0.02
7	0.79	0.14	0.61	0.08	1.00	0.08	0.73
10	1.39	0.26	1.85	1.05	1.00	0.08	0.15
14	0.94	0.14	0.59	0.06	1.00	0.08	0.40

Neutrophils apoptosis for the 3 treatment groups after 18hrs LPS stimulation (n=6 per group)							
	Arginine		Caerulein		Control		p-value
Day	Mean	S.E.	Mean	S.E.	Mean	S.E.	
1	0.98	0.15	1.76	0.44	1.00	0.06	0.26
3	1.32	0.34	0.92	0.12	1.00	0.06	0.47
7	1.04	0.09	0.58	0.06	1.00	0.06	0.01
10	1.04	0.11	1.01	0.26	1.00	0.06	0.73
14	0.94	0.21	0.59	0.09	1.00	0.06	0.04

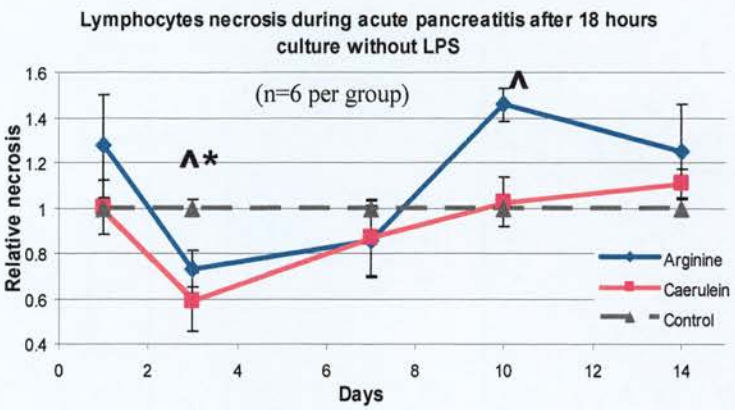

a.

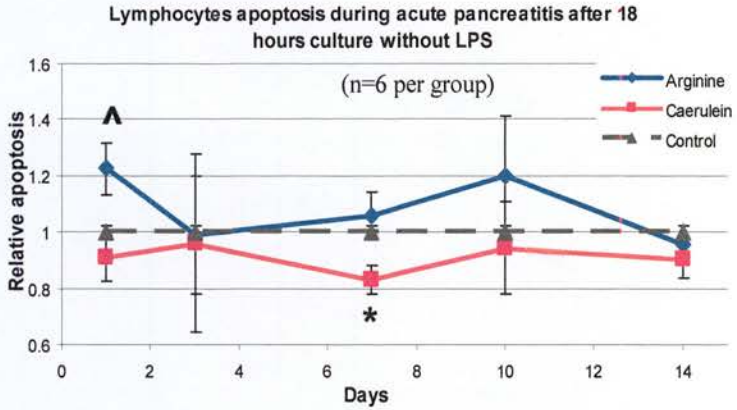

b.

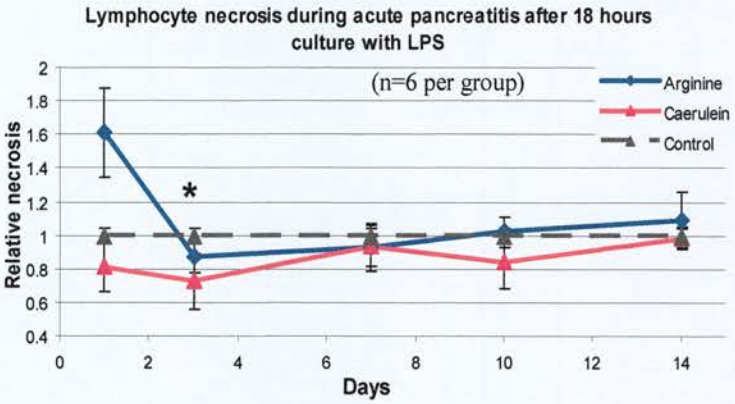

c.

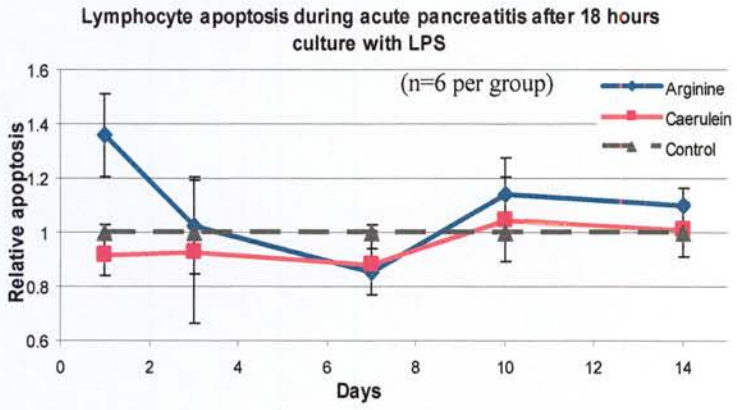

d.

Figure 6-8 illustrates lymphocyte necrosis and apoptosis after 18 hours of in vitro whole blood culture at 370Cwith and without LPS stimulation throughout an episode of acute pancreatitis. Annexin V/PI assay was used in both culture conditions. (a) & (b) represent lymphocyte necrosis and apoptosis without the co-culture of LPS; whereas (c) & (d) represent lymphocyte necrosis and apoptosis after 18 hours of co-culture with LPS. (^ denotes statistically significant difference in arginine group versus the control group at a particular time-point, where * represents that of the caerulein group versus the control group.)

Table 6-6 illustrates the relative values of lymphocyte apoptosis/ necrosis with or without LPS stimulation of the 3 treatment groups of acute pancreatitis at the studied time-points

Lymphocyte necrosis for the 3 treatment groups with no LPS stimulation (n=6 per group)							
	Arginine		Caerulein		Control		p-value
Day	Mean	S.E.	Mean	S.E.	Mean	S.E.	
1	1.27	0.23	1.01	0.12	1.00	0.04	0.44
3	0.73	0.08	0.59	0.13	1.00	0.04	<0.01
7	0.85	0.16	0.87	0.17	1.00	0.04	0.90
10	1.46	0.07	1.03	0.11	1.00	0.04	<0.01
14	1.25	0.21	1.11	0.06	1.00	0.04	0.13

Lymphocyte apoptosis for the 3 treatment groups with no LPS stimulation (n=6 per group)							
	Arginine		Caerulein		Control		p-value
Day	Mean	S.E.	Mean	S.E.	Mean	S.E.	
1	1.23	0.09	0.91	0.08	1.00	0.02	0.01
3	0.99	0.21	0.96	0.32	1.00	0.02	1.00
7	1.06	0.08	0.83	0.05	1.00	0.02	0.02
10	1.20	0.21	0.95	0.16	1.00	0.02	0.41
14	0.95	0.07	0.91	0.07	1.00	0.02	0.47

Lymphocyte necrosis for the 3 treatment groups after 18hrs LPS stimulation (n=6 per group)							
	Arginine		Caerulein		Control		p-value
Day	Mean	S.E.	Mean	S.E.	Mean	S.E.	
1	1.61	0.27	0.81	0.15	1.00	0.04	0.03
3	0.87	0.09	0.73	0.17	1.00	0.04	0.01
7	0.93	0.14	0.94	0.12	1.00	0.04	0.61
10	1.02	0.09	0.85	0.17	1.00	0.04	0.10
14	1.09	0.16	0.99	0.07	1.00	0.04	0.50

Lymphocyte apoptosis for the 3 treatment groups after 18hrs LPS stimulation (n=6 per group)							
	Arginine		Caerulein		Control		p-value
Day	Mean	S.E.	Mean	S.E.	Mean	S.E.	
1	1.36	0.15	0.92	0.07	1.00	0.03	<0.05
3	1.03	0.18	0.93	0.27	1.00	0.03	0.87
7	0.86	0.08	0.88	0.11	1.00	0.03	0.10
10	1.14	0.14	1.05	0.16	1.00	0.03	0.48
14	1.10	0.06	1.01	0.10	1.00	0.03	0.37

6.4 Discussion

6.4.1 The Choice of Apoptosis Assays

Each of the methods to detect and measure apoptosis has its advantages and limitations. Because the cellular mechanisms that result in apoptosis are complex, most published methods cannot by themselves detect apoptosis unambiguously. In measuring apoptosis, two or more methods of quantifying apoptosis have therefore been advocated by most studies. In general, apoptosis can be detected by using Caspase assays, TUNNEL and DNA fragmentation assays, cell permeability assays, Annexin V assays, protein cleavage assays, mitochondrial and ATP/ADP assays.

The applicability of any of these assays depends on the phase of apoptosis that is being studied, and the underlying scientific question to be addressed. For instance, TUNNEL and DNA fragmentation assays for apoptosis rely on the fact that DNA was cleaved into multiples of 180 – 200 base pairs, which is considered as the hallmark of programmed cell death, whereas necrotic cell death is accompanied by late and random DNA fragmentation (303). This technique can apply on both flow cytometry as well as immuohistochemistry. However, because it detects DNA fragmentation, it is not specific for apoptosis, and can overestimate apoptosis when quantitative measurement is important in an experiment.

Caspases are cysteine proteases located within the cytoplasm, and play essential roles in apoptosis, necrosis and inflammation. They are divided into initiator caspases (caspase 8, 10, 9& 2) and effector caspases (3, 7 & 6). To detect these caspases, permeabilisation of the interested cell type would be required prior to the addition of anti-caspase primary antibody. This technique is most suitable to fixated tissue section rather than flow cytometry (280). Its use is therefore limited for the purpose of our described experiments.

The Annexin V/ PI and YOPRO/ 7-AAD assays were selected to characterize apoptosis and necrosis of blood leukocytes in this study. The main reason was that both assays have been well characterized as valid tools for measuring apoptosis (279, 300, 304). The other advantage of using these assays as opposed to others mentioned above was the simplicity in their experimental procedures. This latter criterion is essential because of the number of live assays that were required to be conducted at each experimental time-point.

Despite some similarities between the Annexin V and YOPRO assays, there are differences in the final quantification of apoptosis and necrosis of blood leukocytes during acute pancreatitis. The exact reason accounting for this difference is unclear. One may speculate that the assays measure different stages of the apoptotic process. Although both apoptosis methods have been suggested to measure early apoptosis (305),

it has been suggested that YOPRO measures an earlier apoptotic stage, before the appearance of the blebbing and the subsequent externalization of phosphatidylserine (306). This could therefore account for the final net difference in the quantification of apoptosis by either method.

The other possible explanation is experimental error secondary to the small measured quantity in the percentage of apoptosis and necrosis. The gate setting in-between experiments was aimed to be as robust as possible. However, there is still chance of slight variation in gate settings between Annexin V and YOPRO assays. As seen in Figure 6-1 and Figure 6-2, the percentages of apoptosis and necrosis measured in all three groups (overall leukocytes, granulocytes and lymphocytes) were relatively small, viz. <10%. Any small alteration in the gate setting (or any drifting of the quadrant) would magnify the proportion of either apoptosis or necrosis, and therefore account for a measurable difference between the two assays. It is exactly because of this the relative values in reference to the corresponding control are used in order to minimize quantification errors.

Despite these slight variations of measurement between Annexin V and YOPRO assays, both methods provided a reasonable trend of apoptosis and necrosis in our pancreatitis models.

6.4.2 Responses from Arginine and Caerulein Pancreatitis Model

Although there are degrees of similarity in the trends of apoptosis or necrosis of arginine and caerulein pancreatitis models, our observations suggest a more consistent response in the caerulein model than the arginine model. This is reflected by the wider standard errors of apoptosis and necrosis at each time-point of the arginine model. The exact reason for this difference in the response of the inflammatory cells between the two models is again unknown. As discussed in section 3.10, the literature shows that the caerulein pancreatitis model has been extensively used to induce acute pancreatitis and has been well characterized over many years, whereas the L-arginine model has only become popular in acute pancreatitis research over the last 10-20 years since Tani et al first described the model (255). It has been reported that the morphological, biochemical and systemic changes of the L-arginine pancreatitis model are similar to those of acute pancreatitis induced by other methods (307). However, given that L-arginine is closely involved in the nitric oxide synthase pathway (308), which in turn is closely involved in the immunological response during acute pancreatitis (309), it is not unreasonable to believe that L-arginine itself might have a role in the immunomodulatory response to inflammatory cells. However, the exact role that L-arginine plays in terms of nitric oxide synthesis during acute pancreatitis is controversial. Some studies suggested a beneficial role in nitric oxide synthesis (310), whereas some reported a detrimental role in causing pancreatic injury (311). Some even suggested that the beneficial or harmful effect of nitric oxide is determined by its concentration (308). Nevertheless, it is feasible that L-arginine itself might have altered some of the immunological response of the leukocytes,

at least at the very beginning of the disease process. It is for this reason that the following discussion will focus mainly on the caerulein acute pancreatitis model.

6.4.3 Leukocyte Apoptosis/Necrosis During Caerulein-Induced Acute Pancreatitis

Despite an initial increase in granulocyte apoptosis in the caerulein pancreatitis model, the combined net effect was a reduction in overall leukocyte apoptosis. After the initial increase of granulocyte apoptosis, there was a net reduction in total leukocyte and granulocyte apoptosis for the first 3 days post caerulein induction. Our findings confirmed the findings of other studies that there is a delay of granulocyte apoptosis in the early phase of severe acute pancreatitis (218, 219) and sepsis (215, 216). This net effect of total leukocyte apoptosis was also witnessed after 18 hours of whole blood culture.

Given that apoptosis is associated with the resolution of inflammation (312-318), this should imply an increase in leukocyte apoptosis during the resolution of acute pancreatitis. Surprisingly, the above findings revealed a consistent overall reduction of the leukocyte and granulocyte apoptosis towards the end of the resolution of acute pancreatitis. *In vitro* whole blood culture after 18 hours of incubation at 37^0C also revealed similar results. Towards the recovery phase of severe acute pancreatitis, there was an increase in lymphocyte apoptosis at day 10. Since there was an abundant of

lymphocyte counts as compared to granulocytes and other leukocytes within the peripheral blood. The net effect could have been an increase in peripheral blood apoptosis during the resolution of the disease. However, this could only be a speculation. The exact reason could not be fully addressed in this thesis.

6.4.3.1 **Septic event during acute pancreatitis**

To further investigate how nosocomial infection would interfere with the inflammatory cells apoptosis during acute pancreatitis at different stages of the inflammatory process, *in vitro* whole blood culture without LPS co-culture was compared to culture with LPS stimulation. It has been shown that LPS delays neutrophil apoptosis (319), whereas some extrinsic (e.g. FAS-ligand, TNFα-ligand) and intrinsic (e.g. mitochondria) stimuli enhance neutrophil apoptosis. It is therefore the balance of all these stimuli that dictates the net effect of leukocyte survival. In comparing the *in vitro* culture condition with and without LPS stimulation, our results suggested that LPS stimulation did not alter the net effect of leukocyte apoptosis during the early stage (before day 3) and late stage (after day 10) of acute pancreatitis. Instead, LPS enhanced the leukocyte survival halfway (day 7) during the recovery process. This effect occurred in both arginine- and caerulein-induced acute pancreatitis models.

Our results therefore suggest that bacterial infection causing sepsis could potentially have an impact on leukocyte survival halfway through the recovery of acute pancreatitis,

whereas its impact was insignificant at the beginning and the end of the disease. As discussed in Chapter 5, this phenomenon could be partially explained by the malfunction of leukocyte phagocytosis halfway through the disease process.

7 PERIPHERAL BLOOD AND ALVEOLAR MACROPHAGE CYTOKINE ASSAY

7.1 INTRODUCTION

To understand the immunological and functional responses of leukocytes and alveolar macrophages described in previous chapters, it is important to understand how the pro- and anti-inflammatory mediators alter during acute pancreatitis. This could potentially provide an explanation to our findings of phagocytic capacity of phagocytes and their corresponding apoptotic/survival response during the disease process, which was described in previous chapters. This chapter aims to characterize cytokine concentration and secretion of both peripheral blood and alveolar macrophages during an episode of acute pancreatitis.

7.2 MATERIALS AND METHODS

7.2.1 DETERMINING EXPERIMENTAL CONDITIONS FOR CYTOKINE PRODUCTION

A series of experiments was carried out in order to determine the optimal duration of *in vitro* culture and the concentration of lipopolysaccharide (LPS) for cytokine secretion assays of both alveolar macrophages (AMs) and whole blood.

Three Sprague-Dawley rats were used for both AM and peripheral blood experiments. Sprague-Dawley rats were used because whole blood had been demonstrated to respond adequately in this cytokine secretion assay (320). AMs were harvested and prepared as described in Chapter 4. Concentrations of LPS at 0, 0.01, 0.1, 0.5, 1, 10μg/ml were tested. The samples were cultured for 3 and 18 hours at 37^0C with 5% CO_2. Figure 7-1 illustrates the results for tumour necrosis factor α (TNFα) secretion after culture of AMs in the presence of LPS at the two studied time-points.

After 3 hours of co-culture of AMs with LPS, there was an increase in the TNFα concentration, which peaked at 1μg/ml of LPS. There was significant elevation of TNFα concentration at 0.1, 1, 5 and 10μg/ml LPS concentrations when compared with no LPS stimulation, but this was not significant at 0.01μg/ml LPS [$H(5)=23.98$, $p<0.01$]. The TNFα concentration was markedly elevated after 18 hours of co-culture with LPS. The concentration of TNFα secretion peaked at 5μg/ml of LPS. There was significant elevations of TNFα concentration at 0.1, 1, 5 and 10μg/ml of LPS versus 0 and 0.01μg/ml [$H(5)= 30.05$, $p<0.01$].

Following the above experiments, 5μg/ml of LPS concentration and 18 hours of incubation period at 37^0C were chosen to be the culture conditions for the AM cytokine secretion assay. To accommodate with the experimental schedule of the AM cytokine

assay, an incubation period of 18 hours was selected for the whole blood culture cytokine secretion assay.

7.2.1.1 **Whole blood culture cytokine secretion assay**

Whole blood samples from the Sprague-Dawley rats were prepared as described above. The concentrations of LPS used in the AM cytokine secretion assay above were used to determine the optimal LPS concentration for whole blood culture. Figure 7-2 illustrates the whole blood TNFα secretion after 18 hours for various LPS concentrations. Similar to the AM TNFα secretion assay, there was a significant increase in TNFα secretion at all LPS concentrations [$H(5)=32.82$, $p<0.01$] when compared to zero LPS concentration.

Since there was no significant difference in whole blood TNFα secretion between 0.5, 1, 5 and 10μg/ml of LPS, a LPS concentration of 5μg/ml (the same dose as in the AM cytokine secretion assay) was chosen to be the optimal dose for all the subsequent whole blood cytokine secretion experiments.

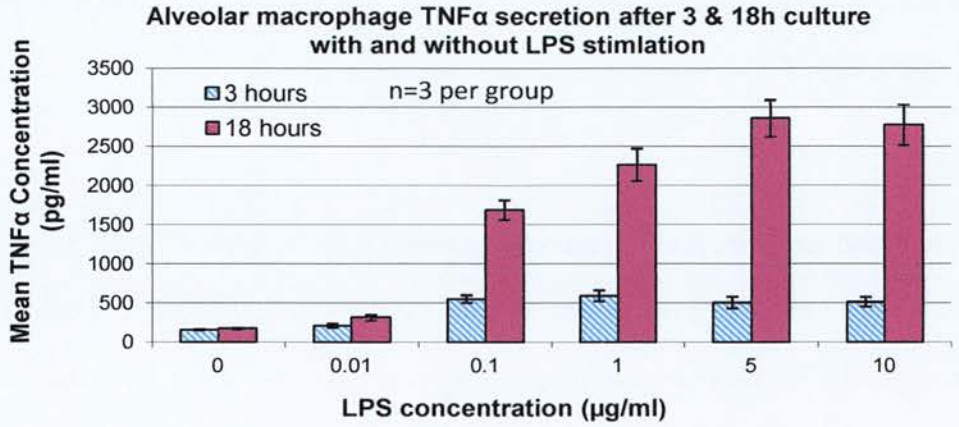

Figure 7-1 illustrates the mean and standard error of the secretion of TNFα by alveolar macrophages in correspondence to various concentrations of LPS after 3 and 18 hours of culture at 37^0C (n=3). After 3 and 18 hours of culture, there was significant elevation of TNFα at LPS concentrations above 0.1µg/ml, when compared to 0µg/ml of LPS.

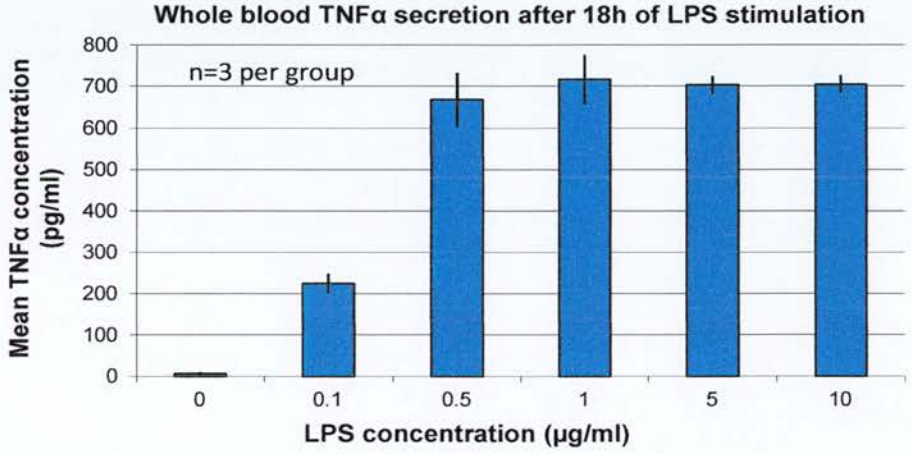

Figure 7-2 illustrates the mean and standard error of the secretion of TNFα by peripheral blood in correspondence to various concentrations of LPS after 18 hours of culture at 37^0C (n=3). After 18 hours of culture, there was significant elevation of TNFα at all LPS concentrations, when compared to 0µg/ml of LPS.

7.2.2 Peripheral Blood Cytokine Secretion Study

Cytokine production was determined using an *ex vivo* whole blood culture technique. The whole blood technique has previously been demonstrated to be reproducible and accurate in the production of monocytic cytokines (321, 322). This assay was performed in the same manner as previously described in section 6.2.3. The supernatants harvested from the experiment were used for the cytokine analysis after LPS co-culture.

7.2.3 Alveolar Macrophage Cytokine Secretion Study

Alveolar macrophages were prepared in the same manner as described in Chapter 4. At each studied time-point, 2.5 x 10^5/250µl of AMs [suspended in RPMI culture medium (Life Technologies, Paisley, UK) supplemented with penicillin 50units/mL, streptomycin 50µg/mL and glutamine 2mmol/L] of each subject was added into each well of a 48-well plate (Cat No. 3548, Corning Life sciences, UK). AMs were allowed to adhere to the bottom of the well for 2 hours. AMs were washed twice with PBS. Paired experiments were carried out for each assay with and without the addition of 5µg/ml LPS. Supernatant was harvested after 18 hours of incubation at 37^0C with 5% CO_2. Aliquots of supernatant were stored at -70^0C until analysis.

7.2.4 Cytokine Measurements

Alveolar macrophage and plasma TNFα cytokine measurements were determined with commercially available enzyme-linked immunosorbent assay (ELISA) kits (Cat. No.

RTA00, R&D Systems Inc., USA). The lower limit of detection was 5pg/ml, and the coefficients of variation were 2.1% to 5.1% (intra-assay precision) and 8.8% to 9.7% (inter-assay precision) for the kits used.

Interleukin (IL)-6 and IL-10 cytokines were determined with commercially available rat cytometric bead arrays (CBA; BD Biosciences, San Diego, CA, USA) and were analysed on a FACSarray Bioanalyzer. This multiplex bead array assay had been demonstrated to be a reliable quantitative method in comparison to ELISA (323, 324). Standard curves were determined for IL-6 and IL-10 from a range of 9.9–10,000pg/ml and 19.4–10,000pg/ml, respectively. The coefficient of variation for IL-6 was 4% to 9% (intra-assay precision) and 4% to 8% (inter-assay precision); whereas that of IL-10 was 6% to 7% (intra-assay precision) and 3% to 7% (inter-assay precision).

7.2.5 Statistical Analysis

Non-parametric Kruskal–Wallis One Way Analysis of Variance on Ranks was used as the statistical test of choice. $P<0.05$ was considered as statistically significance. Statistical analysis was carried out using the SigmaStat software package (Systat Software Inc., USA).

7.3 RESULTS

With reference to the "Declaration of major complications" on page 3 of this thesis regarding the contamination of the isogenic Fischer rats from the commercial source and the breakdown of the -70^0C freezer, only selective plasma samples of the cytokine secretion experiments were analysed. The samples of AM cytokine secretion experiments were not analysed in this thesis.

7.3.1 IL-6 CYTOKINE SECRETION ON DAYS 3 AND 7

Figure 7-3 illustrates the results of whole blood IL-6 and IL-10 cytokine secretion assay at days 3 and 7 after 18 hours of culture. There was significant elevation of cytokine secretion after 18 hours of LPS stimulation for all treatment groups compared to that without LPS co-culture. There were trends suggesting an increase in IL-6 and IL-10 secretion after LPS stimulation of the arginine-induced acute pancreatitis group at both studied time-points versus the control. However, no statistical differences were achieved between treatment groups and the control at those studied time-points.

Day 3:

IL-6 secretion without LPS stimulation: $H(2)=2.44$, $p=0.30$

IL-6 secretion with LPS stimulation: $H(2)=4.75$, $p=0.09$

IL-10 secretion without LPS stimulation: $H(2)=3.88$, $p=0.14$

IL-10 secretion with LPS stimulation: $H(2)=2.46$, $p=0.29$

Day 7:

IL-6 secretion without LPS stimulation: $H(2)=0.21$, $p=0.90$

IL-6 secretion with LPS stimulation: $H(2)=3.23$, $p=0.20$

IL-10 secretion without LPS stimulation: $H(2)=2.73$, $p=0.26$

IL-10 secretion with LPS stimulation: $H(2)=3.59$, $p=0.17$

Table 7-1 illustrates the IL- 6 concentration of whole blood culture with and without LPS stimulation at day 3 and day 7

Absolute concentration for IL-6 (pg/ml) without LPS stimulation							
Day	Arginine		Caerulein		Control		
	Mean	SE	Mean	SE	Mean	SE	*p*-value
3	29.25	6.24	42.18	6.24	30.48	4.98	0.30
7	30.00	4.18	28.22	1.44	30.48	4.98	0.90

Absolute concentration for IL-6 (pg/ml) with LPS stimulation							
Day	Arginine		Caerulein		Control		
	Mean	SE	Mean	SE	Mean	SE	*p*-value
3	572.08	133.76	372.26	94.13	278.10	17.25	0.09
7	454.36	82.75	315.93	85.42	278.10	17.25	0.20

Table 7-2 illustrates IL-10 concentration of whole blood culture with and without LPS stimulation at day 3 and day 7

Absolute concentration for IL-10 (pg/ml) without LPS stimulation							
Day	Arginine		Caerulein		Control		
	Mean	SE	Mean	SE	Mean	SE	*p*-value
3	104.91	12.45	128.77	21.42	82.97	11.39	0.14
7	117.83	21.65	76.26	16.14	82.97	11.39	0.26

Absolute concentration for IL-10 (pg/ml) with LPS stimulation							
Day	Arginine		Caerulein		Control		
	Mean	SE	Mean	SE	Mean	SE	*p*-value
3	446.57	88.57	315.55	56.43	379.27	39.47	0.29
7	531.88	61.55	348.66	67.58	379.27	39.47	0.14

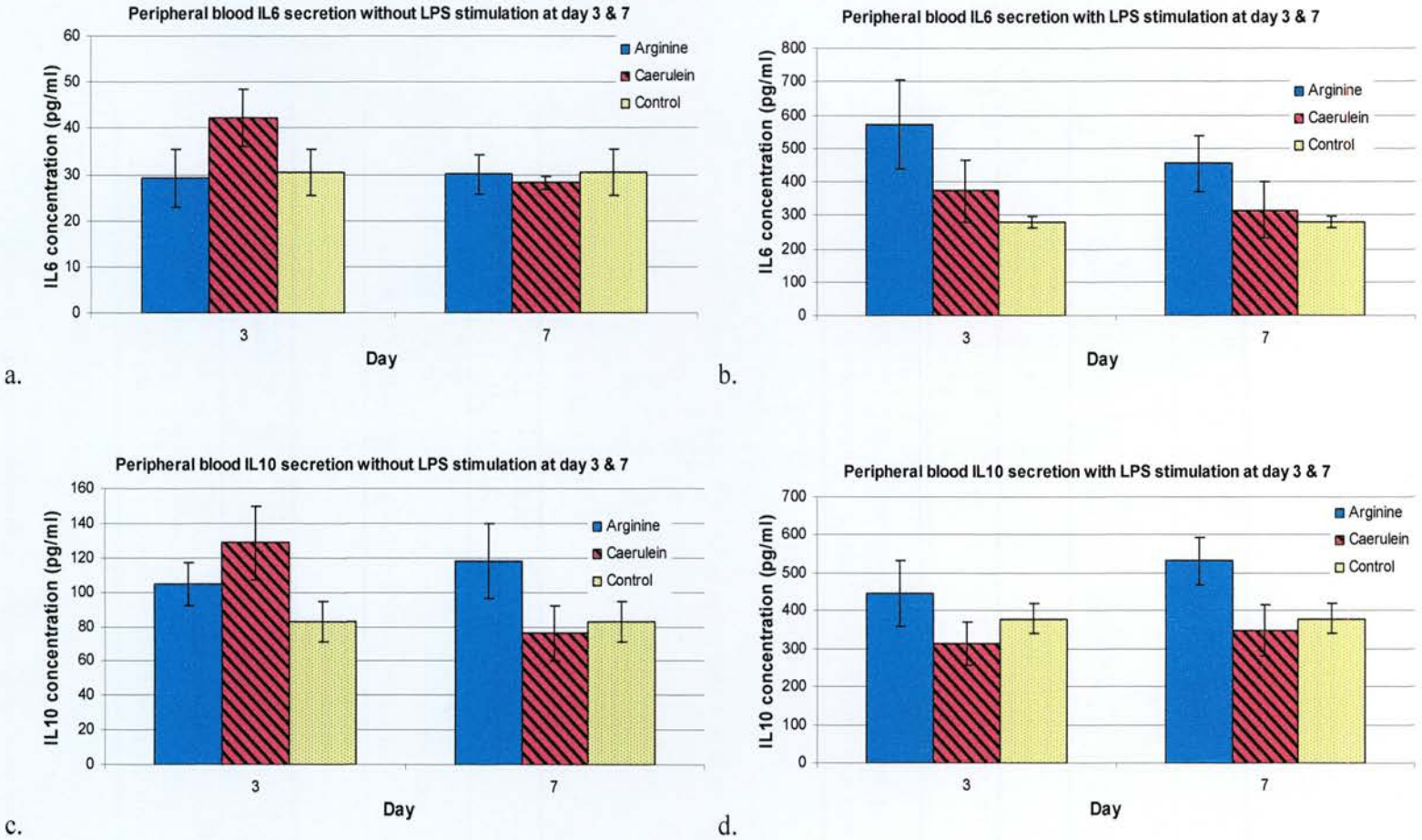

Figure 7-3 illustrates IL-6 (a) & (b) and IL-10 (c) & (d) cytokine secretion in peripheral blood of acute pancreatitis models (arginine & caerulein) and control at days 3 and 7. (a) & (c) represent whole blood culture without LPS stimulation, whereas (b) & (d) represent whole blood culture with LPS co-culture. N=6 per treatment group per time-point.

8 HEAT SHOCK PROTEIN AND OXIDATIVE RESPONSE IN THE LIVER DURING ACUTE PANCREATITIS

8.1 INTRODUCTION

As discussed in section1.5, there is evidence that oxidative stress occurs in severe acute pancreatitis, and the liver has been suggested to play a role in this during the disease process. The aim of this chapter is to investigate the association between reactive oxygen species (ROS) and haemoxygenase-1 (HO-1) in the liver during an episode of acute pancreatitis.

8.2 MATERIALS AND METHODS

8.2.1 EXTRACTION OF HAEMEOXYGENASE-1 FROM LIVER

Livers from each treatment group (arginine, caerulein and control) were harvested at each time-point as previously described. Approximately 40μg of liver tissue was homogenized in tissue homogenizing buffer (THB), which was made up of 50mM Tris–HCl at pH 7.4, 20mM NaCl, 10mM KCl, 1mM EDTA, 1% sodium dodecyl sulphate (SDS) (Sigma L3771), 0.1mM dithiothreitol (DTT) (Fluka Cat. No. 43816) and protease inhibitor (Roche, UK). After homogenization, the suspension was centrifuged at 13,000 x g for 10 minutes at 4^0C. The supernatant was stored at -70^0C till further analysis.

The concentration of total protein was measured by Lowry protein assay (BioRad protein assay kit, Cat. No. 500 - 0121). Reagent A' was prepared by adding 20μl of reagent S per ml of reagent A. 5μl of either protein standard or diluted liver homogenate (1:10 with homogenized solution) of each sample was added to each well. Triplicate measurement of each sample was performed. 25μl of reagent A' and 200μl of reagent B were added to each well. The suspension was shaken for 15 minutes at room temperature prior to microplate reading. The plate was analysed by a Biorad PR 2100 microplate reader with an absorbance wavelength of 750nm.

8.2.2 Western Blotting and Quantification for Haemoxygenase-1 in the Liver

Western blot analysis of liver haemoxygenase-1 (HO-1) was performed on the cytosolic fraction of the liver homogenate. Proteins were heated at 95^0C for 5 minutes before loading to the gel. 20μg of protein was loaded per lane. Samples underwent electrophoresis on an 10% SDS-polyacrylamide gel according to the method of Laemmli (325). The gels were transferred to a nitrocellulose membrane for 1 hour at 80mA. The membrane was blocked in 5% non-fat dried milk for 1 hour and incubated with rabbit anti-HO-1 (Stressgen Bioreagent Cat. No. SPA-895D, 1:5,000 dilution with 1% BSA/TBS Tween) polyclonal antibody for an additional 1 to 2 hours at room temperature. The membrane was washed three times of 5 minutes each with TBS/Tween. The immunoreactive protein was visualized by enhanced chemiluminescence, using horseradish peroxidase (HRP)-coupled anti-rabbit

immunoglobulin at 1:2,500 dilution (Dako, Glostrup, Denmark). The band was transferred onto film for 1–2 minutes. After probing the nitrocellulose with anti-HO-1 antibody, the antibody was washed away with TBS/Tween for 2 hours. The membrane was re-probed again with mouse anti-β-actin antibody (Abcam Cat. No. ab6276 – 100) to ensure equal loading of protein.

To allow semi-quantification, the intensities of the Western blot bands were quantified by using QuantityOne software ver 4 (Biorad). A relative value of the HO-1 quantity in the liver per subject was calculated in relation to the corresponding value of the β-actin.

8.2.3 Localization of HO-1 Protein in the Liver by Immunohistochemistry

Paraffin-embedded sections of liver 4μm thick were exposed to an anti-HO-1 rabbit polyclonal antibody (as above), after inhibiting endogenous peroxidase with 3% hydrogen peroxide. The endogenous liver biotin was blocked with the Avidin/Biotin kit (VectorLab, SP-2001). The sections were incubated with a biotinylated anti-rabbit mouse polyclonal antibody (Dako, UK), streptavidin–biotin–horseradish peroxidase complex (Dako, UK) and 3,3-diaminobenzidine (DAB) for visualization of staining. The sections were counterstained with haematoxylin. Normal mouse serum was substituted for primary antibody as a negative control.

8.2.4 Measurement of Lipid Peroxidation in the Liver

Liver tissue was homogenized with 1.55M potassium chloride/PBS. The homogenate was centrifuged at 1,500 x g for 10 minutes at 4^0C. The supernatant was removed. Butylated hydroxy toluene (BHT) (Sigma-Aldrich, UK Cat. No. W218405) was added to the supernatant to a final concentration of 5mM to stop the lipid from undergoing oxidation. Total protein concentration was measured by the Lowry method as described above.

Malondialdehyde (MDA) was diluted with 3 volumes of the reagent (10.3mM *N*-methyl-2-phenylindole, in acetonitrile) and 1 volume of 100% methanol (HPLC grade) prior to use. MDA standards (10mM 1,1,3,3-tetramethoxypropane, in 20mM Tris–HCl, pH 7.4) were prepared to final concentrations of 0 to 20mM. Liver total protein concentration was diluted to 5mg/ml with PBS. 50µl of total protein was mixed with 167.5µl of the above reagent. The solution was gently vortexed before adding 37.5µl of 12N (37%) HCl. The solution was mixed and incubated at 45°C for 60 minutes. Samples were centrifuged at 15,000 x g for 10 minutes and absorbance of the supernatant was read at 590nm using a 96-well plate reader.

8.2.5 MEASUREMENT OF GLUTATHIONE PEROXIDASE ACTIVITIES IN THE LIVER

Liver was homogenized as per the lipid peroxidation assay (section 8.2.4), but without the addition of BHT. 500μg of total protein was used for each assay. Glutathione peroxidase (GSH-Px) activity was determined at 22°C by using the Glutathione Peroxidase Assay kit (Calbiochem, Cat. No. 354104), which is based on the coupled-enzyme system described by Flohe et al (326). The final volume of the reaction mixture was 240 μl. Briefly, it consisted of 75μl assay buffer (50mM Tris–HCl, pH 7.6, 5mM EDTA), 75μl of NADPH reagent (containing 24μmol GSH, 4.8μmol NADPH and >12U glutathione reductase), and 15μl liver cytosol suspended in potassium phosphate buffer (as prepared above). 75μl of *tert*-butyl hydroperoxide (0.007% aqueous solution) was added prior to the measurement of the absorbance. The absorbance was read at 340nm and 22^0C for 4 minutes. The linearity of GSH-Px activity as a function of protein was examined using cellular Glutathione Peroxidase (c-GPx) control derived from bovine erythrocytes (supplied in 50mM Tris-HCl, pH 7.3, 5mM EDTA, 1mM ergothioneine, 1mM DTT, 1mg/ml bovine IgG) (data not shown). GSH-Px activity was expressed as mU/ml.

8.2.6 Measurement of Trolox Equivalent Antioxidant Capacity (TEAC) in the Liver

Liver homogenate was prepared as in the glutathione peroxidase assay above. TEAC was determined following an adapted method from a previously described assay, using a 96-well plate with the microplate assay filter at 750nm (327). Briefly, 2, 2'-azinobis 3-ethylbenzothiazoline-6-sulphonic acid (ABTS) radical cation (ABTS·+) was produced by reacting a 14-mM concentration of ABTS with an equal volume of 4.9mM of potassium persulphate (final concentration = 7mM ABTS in 2.45mM potassium persulphate).

The mixture was incubated in the dark at room temperature for 12–16 hours before use. The ABTS·+ solution was diluted with 5.5mM phosphate buffer saline (PBS; pH 7.4) to an absorbance of 0.70 (±0.02) at 734nm (using a spectrophotometer) and equilibrated at 30°C. Total volume per assay was 252.5µl. An aliquot of 2.5µl of liver homogenate (0.05mg of protein) or Trolox standard (6-hydroxy-2,5,7,8-tetramethychroman-2-carboxylic acid) was added to 250µl of diluted ABTS·+ solution and the absorbance was read at 30°C exactly 1 minute after the initial mix and measured every minute up to 6 minutes afterwards. The average readings from 1 to 6 minutes were taken from the final absorbance readings. As reference to the blank, the percentage of inhibition for each sample was calculated. A linear standard curve of TEAC against percentage of inhibition was plotted based on the Trolox standards. TEAC for each sample was therefore determined.

8.2.7 Statistical Analysis

Non-parametric Kruskall-Wallis ANOVA was used as the statistical analysis between arginine, caerulein and the control groups, with Dunn's method used as the post-hoc test when there was statistical significance. SigmaStat v3.1 (Systats Software, USA) was used as the statistical package for data analysis.

8.3 Results

8.3.1 Haemeoxygenase-1 Within the Liver During Acute Pancreatitis

Figure 8-1 illustrates the western blot using anti-HO1 antibody for arginine, caerulein and control groups of one of the three sets of experiment. HO-1 was significantly induced in the liver from both arginine and caerulein acute pancreatic rodents on day 1 [$H(2)=25.17$, $p<0.001$). The amount of induced HO-1 in the liver of the acute pancreatic rodents decreased rapidly after day 1. There was no statistical difference for HO-1 in the liver of the pancreatitis groups as compared to the control for the rest of the other studied time-points. (See Figure 8-2.)

Arginine Model:

Caerulein Model:

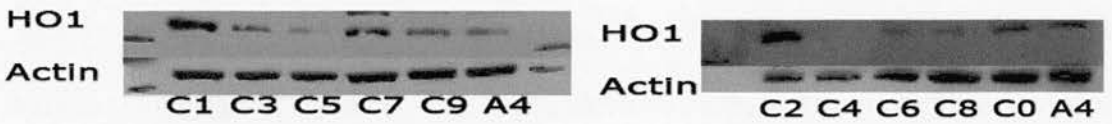

Control:

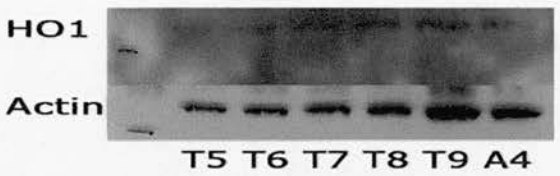

Figure 8-1 illustrates the western blotting using anti-HO1 antibody of arginine, caerulein and control groups. The top band is the band corresponding to HO1 immunoblotting, whereas the lower band is Actin immunoblotting. The relative value for the amount of HO1 for a corresponding time-point is derived from the division of the band density measured by QuantityOne analysis software between HO1 and Actin level. Specimen "A4" was used as the reference specimen for semi-quantitative purpose.

8.3.2 Localization of HO-1 Production in the Liver

As illustrated in Figure 8-6, HO-1 was mainly expressed along the same distribution as Kupffer cells of the liver in both control and arginine pancreatic groups. Positive staining was also demonstrated within hepatocytes. However, HO-1 appeared to be expressed less within the hepatocytes than the Kupffer cells.

It is difficult to quantify the difference of HO-1 expression between the control and two acute pancreatic groups using light microscopy. Semi-quantification by Western blotting as described in section 8.3.1 offers a more objective measurement of HO1 expression within the liver.

8.3.3 Oxidative Stress in the Liver During Acute Pancreatitis

In the arginine-induced acute pancreatitis, there was a significant increase in the MDA concentration within the liver of the arginine pancreatitis group versus the control on day 3 [$H(2)=9.07$, $p=0.01$] and day 10 [$H(2)=6.21$, $p<0.05$] . This pattern was not observed in the caerulein model. (See Figure 8-4.)

The increased MDA concentration in the liver on day 3 was accompanied by a significant reduction of GSH-Px activity [$H(2)=6.34$, $p=0.04$], suggesting a reduction of anti-oxidative ability. Although GSH-Px activity in the liver of the caerulein-induced

acute pancreatitis animals followed a similar trend to the arginine group, this did not achieve a statistical difference when compared to the control. (See Figure 8-5)

When measuring the total anti-oxidative capacity by the TEAC assay, neither of the two acute pancreatitis groups demonstrated significant differences in the total anti-oxidative capacity when compared to the control. (See Figure 8-3.)

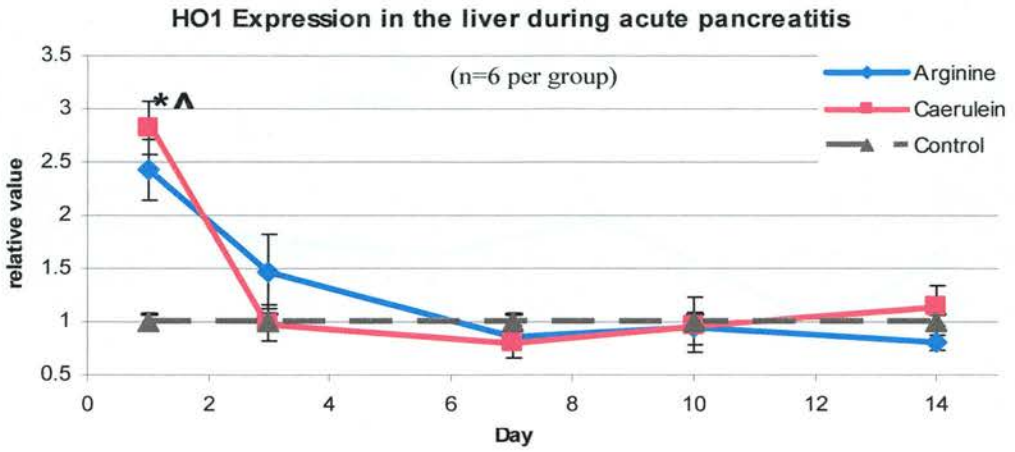

Figure 8-2 illustrates the relative value of HO-1 expression in the liver during an episode of acute pancreatitis. N=6 per group per time-point. (^ & * denote statistical significance of the relative expression of HO-1 in the liver of the arginine and caerulein groups respectively in reference to the control group.)

Table 8-1 illustrates the relative value of HO-1 in all three treatment groups of acute pancreatitis at various studied time-points

Relative value of HO-1 for all treatment groups of acute pancreatitis							
Day	Arginine		Caerulein		Control		P-value
	Mean	SE	Mean	SE	Mean	SE	
1	2.44	0.29	2.82	0.25	1.00	0.07	<0.01
3	1.47	0.35	0.99	0.17	1.00	0.07	0.52
7	0.86	0.10	0.80	0.15	1.00	0.07	0.37
10	0.94	0.15	0.97	0.26	1.00	0.07	0.76
14	0.81	0.07	1.15	0.18	1.00	0.07	0.25

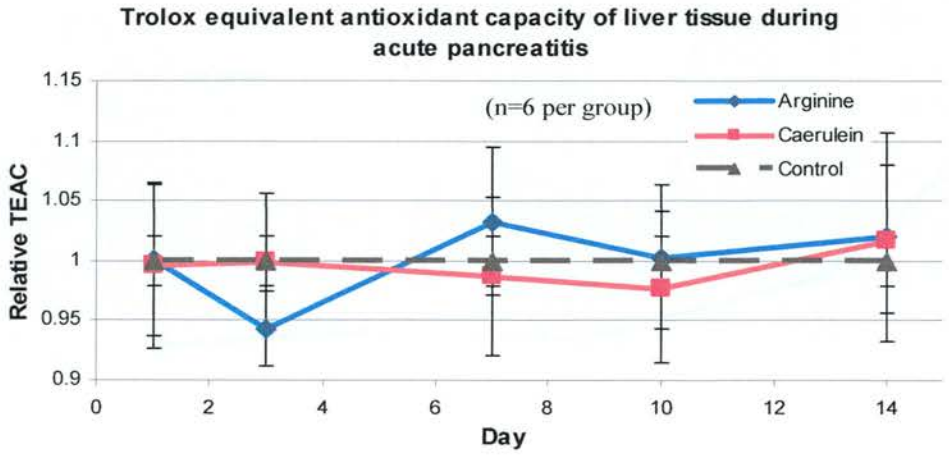

Figure 8-3 illustrates the relative value of Trolox equivalent antioxidant capacity of the liver during acute pancreatitis. N=6 per group per time-point. (No statistical significance was found between the two pancreatitis groups as compared to the control.)

Table 8-2 Relative values of TEAC of the liver of arginine, caerulein and control groups of acute pancreatitis.

Relative values of TEAC of the three treatment groups							
Day	Arginine		Caerulein		Control		P-value
	Mean	SE	Mean	SE	Mean	SE	
1	1.00	0.06	1.00	0.07	1.00	0.02	0.99
3	0.94	0.03	1.00	0.06	1.00	0.02	0.45
7	1.03	0.06	0.99	0.07	1.00	0.02	0.63
10	1.00	0.06	0.98	0.06	1.00	0.02	0.93
14	1.02	0.09	1.02	0.06	1.00	0.02	0.85

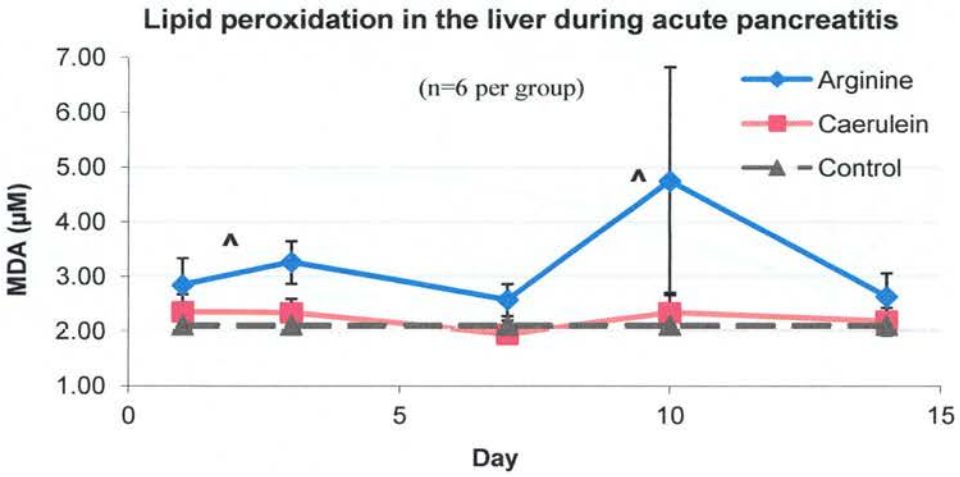

Figure 8-4 represents the lipid peroxidation in the liver during an episode of acute pancreatitis. N=6 per group per time-point. (^ denotes statistical significance ($p<0.05$) of the concentration of MDA measured in the liver of the arginine group as compared to the control group.)

Table 8-3. The absolute value of MDA (µM) in the liver of the three treatment groups of acute pancreatitis at all studied time-points

Absolute value MDA (µM) in the liver							
Day	Arginine		Caerulein		Control		p-value
	Mean	S.E.	Mean	S.E.	Mean	S.E.	
1	2.84	0.49	2.35	0.33	2.11	0.08	0.32
3	3.26	0.39	2.34	0.26	2.11	0.08	0.01
7	2.57	0.29	1.95	0.15	2.11	0.08	0.17
10	4.75	2.08	2.34	0.37	2.11	0.08	0.05
14	2.63	0.44	2.18	0.25	2.11	0.08	0.61

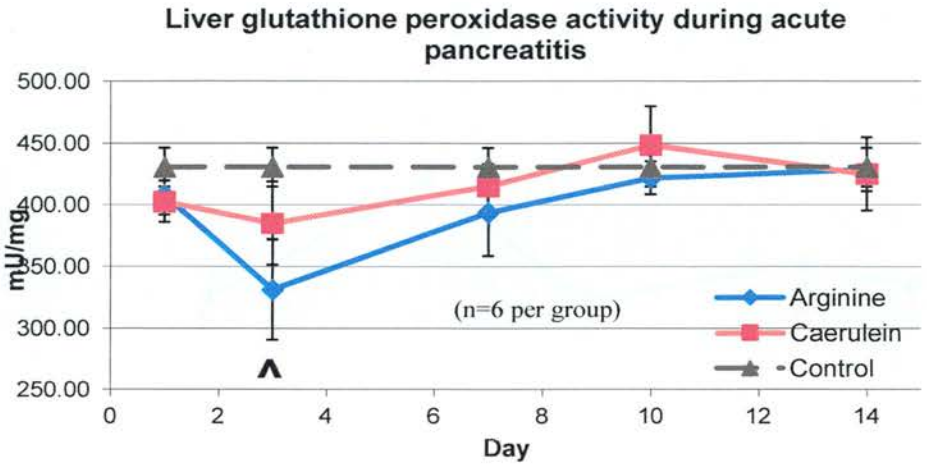

Figure 8-5 illustrates the glutathione peroxidase activity in the liver during an episode of acute pancreatitis. N=6 per group per time-point. (^ denotes statistical significance ($p<0.05$) of the glutathione peroxidase activity measured within the livers of the arginine group as compared to the control group.)

Table 8-4 The absolute value of GPx activity (mU/mg) in the liver of the three treatment groups of acute pancreatitis at all studied time-points

GPx activity (mU/mg) in the liver							
Day	Arginine		Caerulein		Control		p-value
	Mean	SE	Mean	SE	Mean	SE	
1	408.40	16.08	403.17	16.72	430.72	15.73	0.56
3	331.58	40.72	385.42	33.72	430.72	15.73	0.04
7	394.00	35.12	415.52	17.62	430.72	15.73	0.76
10	422.12	13.31	449.13	30.97	430.72	15.73	0.97
14	428.90	17.59	425.47	29.66	430.72	15.73	0.99

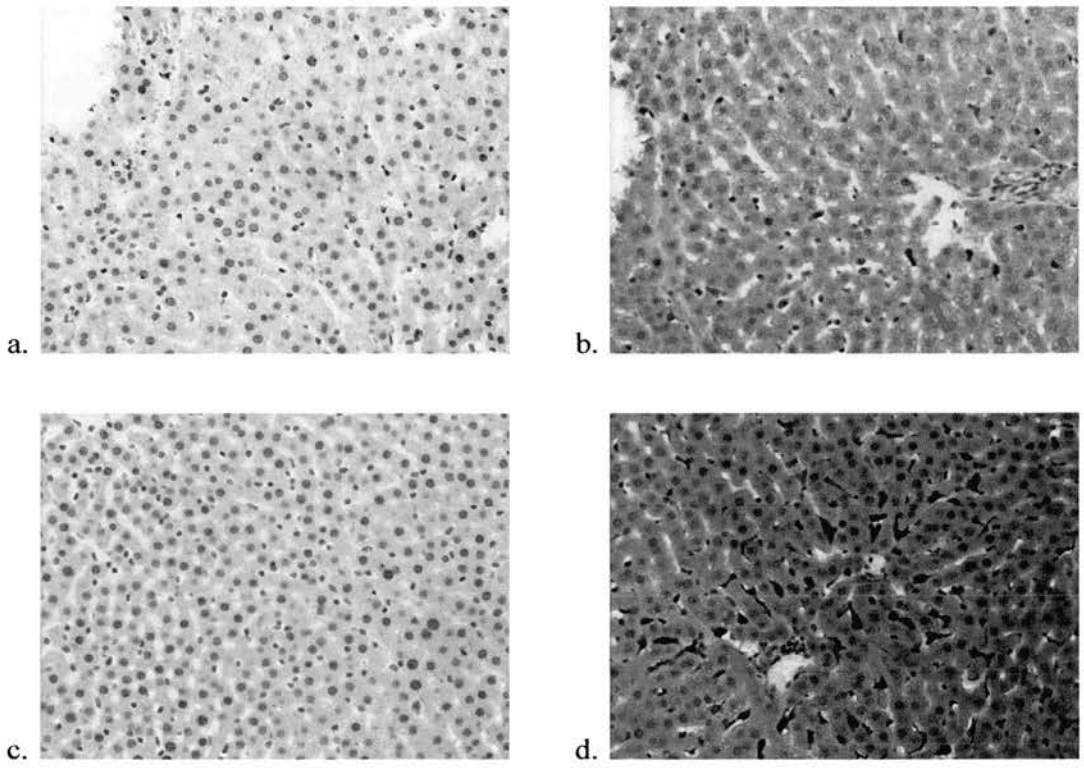

Figure 8-6 (a-d) illustrate the immunohistochemistry of the HO-1 expression in the liver of the control and arginine pancreatitis group at 1 day after induction of acute pancreatitis. (a) & (b) represent the negative control and HO-1 staining of the liver of the control group respectively (x20); whereas (c) & (d) represent the negative control and HO-1 staining of the liver of the arginine pancreatitis group respectively (x20). All pictures were taken at the same microscopic setting. There is more DAB staining in the liver of the arginine group as compared to the control. Most of this staining was highlighted along the distribution of the Kupffer cells (←). However, DAB staining was more markedly in the pancreatitis group (d) than the control group (b).

8.4 DISCUSSION

HO-1 induction has been demonstrated with various inducers, ranging from chemical to physical stimuli. Given that oxidative stress has been shown to occur during the early phase of acute pancreatitis, it is logical to predict an upregulation of HO-1 in the liver during acute pancreatitis in order to counteract the oxidative damage by ROS. However the sharp fall of HO-1 expression in the liver 1 day after the induction of acute pancreatitis was unexpected. This fall was demonstrated in both acute pancreatitis models.

During the investigation of the oxidative stress status using the biochemical markers within the liver of the arginine group, there was a significant increase in lipid peroxidation, as well as a reduction in GSH-Px activity at day 3. These results suggested an increase in oxidative stress within the liver during arginine-induced acute pancreatitis. This increase of oxidative stress coincided with the downregulation of HO-1 expression within the liver of arginine-induced acute pancreatitis. Allowing speculation, the reduction of HO-1 expression might contribute to a reduction of anti-oxidative power within the liver, which could therefore cause an upsurge of oxidative stress in the liver during the initial acute inflammatory process.

Although a similar trend of oxidative stress was witnessed in the liver of caerulein-induced acute pancreatitis, there was no significant difference between the caerulein and

the control group. There are potentially two explanations for these differences. One possibility is that arginine-induced and caerulein-induced models may produce a different oxidative stress response within the liver. The other explanation could be due to a different severity of acute pancreatitis being induced between the two models. Although there was no statistical significance found in the histological scoring between the two pancreatitis groups, Figure 3-15 demonstrated a milder trend of acute pancreatitis following caerulein-induction as compared to arginine induction. It could also be that a combination of the both explanations contributes to the differences in the oxidative responses in both acute pancreatitis models.

Our finding that HO-1 is expressed mainly within the Kupffer cells is similar to the results of studies from other research groups (328, 329). They have demonstrated that over-expression of HO-1 in c-Jun terminal kinase-2 gene-deleted mice protected the liver from sustaining ischaemic re-perfusion injuries. However, it is not clear whether this over-expression of HO-1 in the Kupffer cells is associated with a reduction in remote organ injury. Certainly, the protection of lung parenchyma injuries was not significant when Kupffer cells were inactivated by gadolinium; whereas significant reduction of lung parenchyma insult was observed when neutrophils were depleted during acute pancreatitis (193). To address the question of whether HO-1 upregulation within the liver during severe acute pancreatitis will influence the outcome of remote organ injuries will require either an induction of acute pancreatitis in transgenic rodents with deletion of the upstream regulatory proteins of HO-1 (e.g. c-Jun kinase deletion); or

it will require a specific blockade of HO-1 production in the liver during severe acute pancreatitis. Nevertheless, our preliminary results have demonstrated that there is an increase in oxidative stress response in the liver with a downregulation of HO-1 expression during early severe acute pancreatitis.

9 GENERAL DISCUSSION

9.1 CHOICE OF ACUTE PANCREATITIS MODELS:

There have been numerous descriptions regarding different types of induction techniques for severe acute pancreatitis of rodents in the literatures. In broad terms, they are divided into invasive and non-invasive modalities depending on the method of induction of acute pancreatitis. The invasive method includes closed duodenal loop ligation, antegrade pancreatic duct perfusion, bilopancreatic duct injection or combination of these techniques (330-333). These induction methods for acute pancreatitis are pathologically similar to the theory of the initiation of human acute pancreatitis, based on the Opie theory. Although they are reliable and reproducible, these methods require general anaesthesia or terminal anaesthesia to the animal with surgical intervention to the gastrointestinal tract or pancreas.

For instance, the antegrade pancreatic duct perfusion or bilopancreatic duct injection models will require the combination of cannulation of the pancreatic duct and continous perfusion of the inducing agent at a constant rate. This procedure is therefore complex and would not have been easily achievable technically and physically during the experimental time-points. If any of these invasive model had been used, more rodents would likely have had to have been euthanized. This is therefore against the three principles of refinement, reduction and replacement for animal research set out by the Home Office of the UK.

The other type of induction methodology is classified as non-invasive, including gene knockout, hormone-, alcohol-, diet-, and L-arginine- induced acute pancreatitis. Most non-invasive induction methods have the advantage of being simplier to induce acute pancreatitis, more cost effective, and larger scales of induction can be performed at the same setting. Hormone-, diet- and L-arginine- induced acute pancreatitis are the most commonly described methods in the literature (255, 334, 335).

The diet- induction method is the simplest of all. Severe acute pancreatitis is induced by feeding choline-deficient diet containing ethionine (CDE diet). However, it is species and gender specific, and has a variable onset of acute pancreatitis (336). Despite that, other research groups have successfully minimized the mortality associated with the model (337). This model produces high mortality, which occurs after 2 – 8 days. In addition to acute pancreatitis, there are changes in the liver and central nervous system, which could instigate multiple organ failure and therefore causes other than acute pancreatitis could contribute to the mortality. With these considerations, it would not have been the most suitable model to investigate the immuological responses outlined in this thesis. Caerulein and L-arginine induction models were the models of choice for this research project.

Caerulein- induced acute pancreatitis is one of the most characterised acute pancreatitis model (307). Its clinical properties after the induction of acute pancreatitis had been well documented in the literature. It is relatively simple and inexpensive to perform. Pulmonary injury in rats has also been reported with resemblance to the early stages of ARDS in human. Specific changes to intracellular membane systems of the acinar cells using the caerulein model has also been described as being similar to human acute pancreatitis. It is certainly the model of choice to investigate the healing and regeneration of injured pancreas during acute inflammation. However, its drawback is the induction of a milder form of acute pancreatitis (338).

On the contrary, L-arginine induction allows high reproducibility and the ability to achieve selective dose-dependent pancreatic acinar cell necrosis (339). By adjusting the arginine dose, it is suitable for investigating both early and late phases of acute pancreatitis. As stated in previous chapters, this model was relatively new and not as well characterised as compared to the caerulein model. L-arginine is also a substract within the NOS pathway and therefore could have immuno-modulatory properties. The L-arginine model was therefore not used as the sole model for the purpose of this project. This became more apparent in Chapter 6, when the immune response in relation to apoptosis/necrosis was examined more closely in peripheral blood leukocytes. To investigate whether L-arginine had a direct response on the immune function of leukocytes in L-arginine-induced acute pancreatitis model was beyond the scope of this thesis.

9.2 SYSTEMIC AND REMOTE ORGAN IMMUNE RESPONSE THROUGHOUT ACUTE PANCREATITIS

The immune response within whole blood was used to simulate the systemic immune response, whereas the lung immune response was used as the surrogate marker for the remote organ response. Phagocytosis, cytokine response and the quantification of cellular apopotosis/necrosis were chosen as the tools to characterize the immune response during the disease process. For the alveolar macrophage phagocytosis, there was close resemblance between the two acute pancreatitis models throughout the disease process. Although there was a tendency to increased alveolar macrophage phagocytosis halfway through the recovery of acute pancreatitis, there was no difference between the pancreatitis groups and the control groups until the disease had completely resolved. There was a sudden surge of increased alveolar macrophage phagocytosis ability towards the end of the disease. This finding contradicts our second hypothesis that AM phagocytosis is dampened at the later stage of the disease process. Instead there had been an enhancement of its phagocytosis capacity towards the complete resolution of acute pancreatitis. The exact mechanism is unclear. One of the possible explanations is that monocytes are activated via an alternative pathway as compared to the classical pathway, and therefore exert an anti-inflammatory influence, which contributed to the resolution of inflammation (340). At the same time, AMs could also be activated via this alternative activation pathway (341), which has been suggested to enhance phagocytosis. The other possibility is that the models themselves are not severe enough to replicate the clinical scenario of patients with severe acute pancreatitis in the intensive care setting.

This surge of alveolar macrophage phagocytic ability was also demonstrated in the peripheral blood leukocyte phagocytosis. The increase of peripheral phagocytosis at the end of acute pancreatitis was contributed mainly by the monocytes. These observations suggested that the peripheral blood monocytes and tissue macrophages are been activated towards the resolution of the acute inflammatory process.

As discussed in Chapter 1, there was an overall reduction in peripheral blood phagocytosis during the early phase of acute pancreatitis. Our findings were comparable with the findings in rodent models of sepsis (167, 168) and human severe acute pancreatitis (169). What is interesting is the finding that peripheral blood phagocytosis was significantly dampened halfway through the resolution of acute pancreatitis. Both granulocyte and monocyte phagocytosis were suppressed at day 7. This overall reduction was predominately contributed to by granulocytes. Not only was there reduction in granulocyte phagocytosis earlier on in the disease process, granulocytes were also shown to survive longer, with a reduction in their apoptosis and necrosis. This imply that there is a suppression of neutrophil bacterial clearance ability during acute pancreatitis, despite a lengthening of its survival. This again contradicts our initial hypothesis of *"lengthening leukocyte surivival and increase efficiency in bacterial engulfment at the early stage of the disease secondary to a pro-inflammatory state"*. This thesis could not pinpoint the exact mechanisms that might have contributed to the functional deficits in neutrophils. Other studies also demonstrated similar findings when

they investigated the activation of neutrophils and their corresponding phagocytosis capacity during acute pancreatitis (168, 169). Although there was a reduction of leukocyte apoptosis/necrosis towards the resolution of acute pancreatitis, there was an increase in the monocyte or granulocyte phagocytosis when the disease was resolved, as compared to reduction in leukocyte phagocytosis at the early stage of disease. Different cell signalling mechanisms are therefore likely to be involved at various stages of severe acute pancreatitis.

Lipopolysaccharide (LPS) suppresses apoptosis (319). Interestingly, when LPS was used to simulate a septic event during acute pancreatitis, the only time-point when LPS exerted its net effect in suppressing granulocyte apoptosis was again at day 7. This coincided with the reduction of granulocyte and monocyte phagocytic capacity. Given the close involvement of neutrophils in the pathophysiology of severe acute pancreatitis, it would not be unreasonable to speculate that a "second hit" infectious cause could trigger a second wave of SIRS response in addition to the response attributable to the initial insult. With the reduction in neutrophil bacterial phagocytosis during acute pancreatitis, this might induce a positive feedback cycle for an augmentation of this septic response, and lead to a detrimental outcome in patients.

One of the hypotheses of this thesis was that inflammatory cell apoptosis and phagocytosis were associated with the production of the pro- and anti-inflammatory

cytokines. Cytokine measurement in both peripheral blood and lung parenchyma at different time-points during the disease process could provide a plausible explanation regarding the corresponding phagocytic capacity and apoptotic rates. For instance, an upregulation of anti-inflammatory cytokines could be associated with the reduction of leukocyte phagocytic ability. Unfortunately, due to the technical complications as declared at the outset of the thesis, this part of the studies was not carried out. Only very limited samples at some time-points (described in chapter 7) were analysed. The accuracy of those results requires careful interpretation. There were therefore gaps in this research, which could not fully explain our observational findings in this thesis.

9.3 LIVER, HEMEOXYGENASE-1 AND ACUTE PANCREATITIS

Most researchers used lung injury as the surrogate marker for remote organ dysfunction in severe acute pancreatitis. Towards the end of this research project, it became apparent to me that the liver had been overlooked, despite the fact that the blood supply from the gastro-intestinal tract will always pass through the liver prior to entering the systemic circulation and the lung. With HO-1 being a potent antioxidant and playing a critical role in the anti-stress mechanism of inflammation, this thesis has confirmed its upregulation within the liver during the early phase of the disease process. Also, it was demonstrated that its upregulation was associated with an increase in antioxidative capacity using lipid peroxidation and glutathione peroxidase assays.

Although it was not immediate apparent regarding the direct association between HO-1 and the SIRS or systemic inflammatory changes discussed in previous chapters, this result can provide a platform of knowledge for further investigation in this area. One way for future research is to examine the systemic and lung inflammatory response after direct manipulation of HO-1 within the liver, which could be performed by either chemical inhibition or using over-expression of HO-1 in c-Jun knockout mice (328, 329).

9.4 SUMMARY AND FUTURE RESEARCH

This thesis has identified deficits in the ability of neutrophils as phagocytes during acute pancreatitis, despite the lengthening of their survival time. This deficit was most marked halfway through the recovery of the disease. This had no correlation with the phagocytic capacity of the AMs throughout acute pancreatitis. Since neutrophils are actively involved in the inflammatory process of acute pancreatitis, the increase in their survival could augment further SIRS, and the subsequent septic responses.

Regarding future research, there are three areas that would merit further investigation. First, the findings of this thesis in peripheral blood phagocytosis and leukocyte survival need to be demonstrated in a human clinical study, in order to affirm the extrapolation of these findings from rodent models to human. This is a difficult task by itself mainly because of the variation of timing when a patient presentsd to hospital with severe acute pancreatitis. Therefore, the exact time-point analysis could be difficult to achieve. Secondly, given the close association of neutrophil involvement during acute pancreatitis as well as its importance in the resolution of inflammation, it is undoubtly important to characterize the functional behaviour of neutrophils throughout severe acute pancreatitis locally and remotely. It is also vital to identify factors or signalling molecules causing the reduction of neutrophil phagocytosis but yet increased its survival during the recovery phase. Any of those factors affecting neutrophils can potentially be a target with therapeutic intent for future research. The final aspect that is worth

investigating is to further characterise the role of HO-1 in the liver during acute pancreatitis, as discussed in section 9.3.

List of References:

1. Bradley EL, III. A clinically based classification system for acute pancreatitis. Summary of the International Symposium on Acute Pancreatitis, Atlanta, Ga, September 11 through 13, 1992. ArchSurg. 1993 05;128(5):586-90.

2. Bang UC, Semb S, Nojgaard C, Bendtsen F. Pharmacological approach to acute pancreatitis. World J Gastroenterol. 2008 May 21;14(19):2968-76.

3. McKay CJ, Evans S, Sinclair M, Carter CR, Imrie CW. High early mortality rate from acute pancreatitis in Scotland, 1984-1995. Br J Surg. 1999 Oct;86(10):1302-5.

4. Gullo L, Migliori M, Olah A, Farkas G, Levy P, Arvanitakis C, et al. Acute pancreatitis in five European countries: etiology and mortality. Pancreas. 2002 Apr;24(3):223-7.

5. McKay CJ, Imrie CW. The continuing challenge of early mortality in acute pancreatitis. Br J Surg. 2004 Oct;91(10):1243-4.

6. Eland IA, Sturkenboom MJ, Wilson JH, Stricker BH. Incidence and mortality of acute pancreatitis between 1985 and 1995. Scand J Gastroenterol. 2000 Oct;35(10):1110-6.

7. Goldacre MJ, Roberts SE. Hospital admission for acute pancreatitis in an English population, 1963-98: database study of incidence and mortality. BMJ. 2004 Jun 19;328(7454):1466-9.

8. Tinto A, Lloyd DA, Kang JY, Majeed A, Ellis C, Williamson RC, et al. Acute and chronic pancreatitis--diseases on the rise: a study of hospital admissions in England 1989/90-1999/2000. Aliment Pharmacol Ther. 2002 Dec;16(12):2097-105.

9. Roberts SE, Williams JG, Meddings D, Goldacre MJ. Incidence and case fatality for acute pancreatitis in England: geographical variation, social deprivation, alcohol

consumption and aetiology--a record linkage study. Aliment Pharmacol Ther. 2008 Oct 1;28(7):931-41.

10. Lindkvist B, Appelros S, Manjer J, Borgstrom A. Trends in incidence of acute pancreatitis in a Swedish population: is there really an increase? Clin Gastroenterol Hepatol. 2004 Sep;2(9):831-7.

11. Floyd A, Pedersen L, Nielsen GL, Thorladcius-Ussing O, Sorensen HT. Secular trends in incidence and 30-day case fatality of acute pancreatitis in North Jutland County, Denmark: a register-based study from 1981-2000. Scand J Gastroenterol. 2002 Dec;37(12):1461-5.

12. Gislason H, Horn A, Hoem D, Andren-Sandberg A, Imsland AK, Soreide O, et al. Acute pancreatitis in Bergen, Norway. A study on incidence, etiology and severity. Scand J Surg. 2004;93(1):29-33.

13. Appelros S, Borgstrom A. Incidence, aetiology and mortality rate of acute pancreatitis over 10 years in a defined urban population in Sweden. Br J Surg. 1999 Apr;86(4):465-70.

14. Thomson HJ. Acute pancreatitis in north and north-east Scotland. J R Coll Surg Edinb. 1985 Apr;30(2):104-11.

15. Wilson C, Imrie CW. Changing patterns of incidence and mortality from acute pancreatitis in Scotland, 1961-1985. Br J Surg. 1990 Jul;77(7):731-4.

16. Corfield AP, Cooper MJ, Williamson RC. Acute pancreatitis: a lethal disease of increasing incidence. Gut. 1985 Jul;26(7):724-9.

17. Halangk W, Lerch MM. Early events in acute pancreatitis. Clin Lab Med. 2005 Mar;25(1):1-15.

18. Tsukamoto H, Towner SJ, Yu GS, French SW. Potentiation of ethanol-induced pancreatic injury by dietary fat. Induction of chronic pancreatitis by alcohol in rats. Am J Pathol. 1988 May;131(2):246-57.

19. Pandol SJ, Periskic S, Gukovsky I, Zaninovic V, Jung Y, Zong Y, et al. Ethanol diet increases the sensitivity of rats to pancreatitis induced by cholecystokinin octapeptide. Gastroenterology. 1999 Sep;117(3):706-16.

20. Schmidt DN, Pandol SJ. Differing effects of ethanol on in vitro stimulated pancreatic enzyme secretion in ethanol-fed and control rats. Pancreas. 1990;5(1):27-36.

21. Pandol SJ, Gukovsky I, Satoh A, Lugea A, Gukovskaya AS. Animal and in vitro models of alcoholic pancreatitis: role of cholecystokinin. Pancreas. 2003 Nov;27(4):297-300.

22. Pandol SJ, Gukovsky I, Satoh A, Lugea A, Gukovskaya AS. Emerging concepts for the mechanism of alcoholic pancreatitis from experimental models. J Gastroenterol. 2003;38(7):623-8.

23. Gukovskaya AS, Mouria M, Gukovsky I, Reyes CN, Kasho VN, Faller LD, et al. Ethanol metabolism and transcription factor activation in pancreatic acinar cells in rats. Gastroenterology. 2002 Jan;122(1):106-18.

24. Hamamoto T, Yamada S, Hirayama C. Nonoxidative metabolism of ethanol in the pancreas; implication in alcoholic pancreatic damage. Biochem Pharmacol. 1990 Jan 15;39(2):241-5.

25. Best CA, Laposata M. Fatty acid ethyl esters: toxic non-oxidative metabolites of ethanol and markers of ethanol intake. Front Biosci. 2003 Jan 1;8:e202-17.

26. Laposata EA, Lange LG. Presence of nonoxidative ethanol metabolism in human organs commonly damaged by ethanol abuse. Science. 1986 Jan 31;231(4737):497-9.

27. Laposata M. Fatty acid ethyl esters: nonoxidative ethanol metabolites with emerging biological and clinical significance. Lipids. 1999;34 Suppl:S281-5.

28. Haber PS, Apte MV, Applegate TL, Norton ID, Korsten MA, Pirola RC, et al. Metabolism of ethanol by rat pancreatic acinar cells. J Lab Clin Med. 1998 Oct;132(4):294-302.

29. Haber PS, Apte MV, Moran C, Applegate TL, Pirola RC, Korsten MA, et al. Non-oxidative metabolism of ethanol by rat pancreatic acini. Pancreatology. 2004;4(2):82-9.

30. Werner J, Saghir M, Warshaw AL, Lewandrowski KB, Laposata M, Iozzo RV, et al. Alcoholic pancreatitis in rats: injury from nonoxidative metabolites of ethanol. Am J Physiol Gastrointest Liver Physiol. 2002 Jul;283(1):G65-73.

31. Kubisch CH, Gukovsky I, Lugea A, Pandol SJ, Kuick R, Misek DE, et al. Long-term ethanol consumption alters pancreatic gene expression in rats: a possible connection to pancreatic injury. Pancreas. 2006 Jul;33(1):68-76.

32. Nathan JD, Romac J, Peng RY, Peyton M, Macdonald RJ, Liddle RA. Transgenic expression of pancreatic secretory trypsin inhibitor-I ameliorates secretagogue-induced pancreatitis in mice. Gastroenterology. 2005 Mar;128(3):717-27.

33. Howes N, Greenhalf W, Stocken DD, Neoptolemos JP. Cationic trypsinogen mutations and pancreatitis. Gastroenterol Clin North Am. 2004 Dec;33(4):767-87.

34. Gukovskaya AS, Hosseini S, Satoh A, Cheng JH, Nam KJ, Gukovsky I, et al. Ethanol differentially regulates NF-kappaB activation in pancreatic acinar cells through calcium and protein kinase C pathways. Am J Physiol Gastrointest Liver Physiol. 2004 Feb;286(2):G204-13.

35. Gukovsky I, Gukovskaya AS, Blinman TA, Zaninovic V, Pandol SJ. Early NF-kappaB activation is associated with hormone-induced pancreatitis. Am J Physiol. 1998 Dec;275(6 Pt 1):G1402-14.

36. Zaninovic V, Gukovskaya AS, Gukovsky I, Mouria M, Pandol SJ. Cerulein upregulates ICAM-1 in pancreatic acinar cells, which mediates neutrophil adhesion to these cells. Am J Physiol Gastrointest Liver Physiol. 2000 Oct;279(4):G666-76.

37. Gukovskaya AS, Gukovsky I, Zaninovic V, Song M, Sandoval D, Gukovsky S, et al. Pancreatic acinar cells produce, release, and respond to tumor necrosis factor-alpha. Role in regulating cell death and pancreatitis. J Clin Invest. 1997 Oct 1;100(7):1853-62.

38. Fortunato F, Berger I, Gross ML, Rieger P, Buechler MW, Werner J. Immune-compromised state in the rat pancreas after chronic alcohol exposure: the role of peroxisome proliferator-activated receptor gamma. J Pathol. 2007 Dec;213(4):441-52.

39. Opie EL. The etiology of acute hemorrhagic pancreatitis. Johns Hopks Hosp Bull. 1901 1901;12:182-8.

40. Vaquero E, Gukovsky I, Zaninovic V, Gukovskaya AS, Pandol SJ. Localized pancreatic NF-kappaB activation and inflammatory response in taurocholate-induced pancreatitis. Am J Physiol Gastrointest Liver Physiol. 2001 Jun;280(6):G1197-208.

41. Lerch MM, Saluja AK, Runzi M, Dawra R, Saluja M, Steer ML. Pancreatic duct obstruction triggers acute necrotizing pancreatitis in the opossum. Gastroenterology. 1993 Mar;104(3):853-61.

42. Samuel I, Zaheer S, Zaheer A. Bile-pancreatic juice exclusion increases p38MAPK activation and TNF-alpha production in ligation-induced acute pancreatitis in rats. Pancreatology. 2005;5(1):20-6.

43. Samuel I, Zaheer A, Zaheer S, Fisher RA. Bile-pancreatic juice exclusion increases cholinergic M3 and CCK-A receptor expression and interleukin-6 production in ligation-induced acute pancreatitis. Am J Surg. 2004 Nov;188(5):511-5.

44. Samuel I, Yorek MA, Zaheer A, Fisher RA. Bile-pancreatic juice exclusion promotes Akt/NF-kappaB activation and chemokine production in ligation-induced acute pancreatitis. J Gastrointest Surg. 2006 Jul-Aug;10(7):950-9.

45. Samuel I, Toriumi Y, Zaheer A, Joehl RJ. Mechanism of acute pancreatitis exacerbation by enteral bile-pancreatic juice exclusion. Pancreatology. 2004;4(6):527-32.

46. Samuel I, Toriumi Y, Wilcockson DP, Turkelson CM, Solomon TE, Joehl RJ. Bile and pancreatic juice replacement ameliorates early ligation-induced acute pancreatitis in rats. Am J Surg. 1995 Apr;169(4):391-9.

47. Samuel I, Tephly L, Williard DE, Carter AB. Enteral exclusion increases MAP kinase activation and cytokine production in a model of gallstone pancreatitis. Pancreatology. 2008;8(1):6-14.

48. Raraty MG, Murphy JA, McLoughlin E, Smith D, Criddle D, Sutton R. Mechanisms of acinar cell injury in acute pancreatitis. Scand J Surg. 2005;94(2):89-96.

49. Kribben A, Tyrakowski T, Schulz I. Characterization of Mg-ATP-dependent Ca2+ transport in cat pancreatic microsomes. Am J Physiol. 1983 May;244(5):G480-90.

50. Rosenzweig SA, Miller LJ, Jamieson JD. Identification and localization of cholecystokinin-binding sites on rat pancreatic plasma membranes and acinar cells: a biochemical and autoradiographic study. J Cell Biol. 1983 May;96(5):1288-97.

51. Voronina S, Longbottom R, Sutton R, Petersen OH, Tepikin A. Bile acids induce calcium signals in mouse pancreatic acinar cells: implications for bile-induced pancreatic pathology. J Physiol. 2002 Apr 1;540(Pt 1):49-55.

52. Fischer L, Gukovskaya AS, Penninger JM, Mareninova OA, Friess H, Gukovsky I, et al. Phosphatidylinositol 3-kinase facilitates bile acid-induced Ca(2+) responses in pancreatic acinar cells. Am J Physiol Gastrointest Liver Physiol. 2007 Mar;292(3):G875-86.

53. Lee MG, Xu X, Zeng W, Diaz J, Wojcikiewicz RJ, Kuo TH, et al. Polarized expression of Ca2+ channels in pancreatic and salivary gland cells. Correlation with initiation and propagation of [Ca2+]i waves. J Biol Chem. 1997 Jun 20;272(25):15765-70.

54. Maruyama Y, Petersen OH. Delay in granular fusion evoked by repetitive cytosolic Ca2+ spikes in mouse pancreatic acinar cells. Cell Calcium. 1994 Nov;16(5):419-30.

55. Raraty M, Ward J, Erdemli G, Vaillant C, Neoptolemos JP, Sutton R, et al. Calcium-dependent enzyme activation and vacuole formation in the apical granular region of pancreatic acinar cells. Proc Natl Acad Sci U S A. 2000 Nov 21;97(24):13126-31.

56. Nicotera P, Orrenius S. The role of calcium in apoptosis. Cell Calcium. 1998 Feb-Mar;23(2-3):173-80.

57. Nicotera P, Rossi AD. Nuclear Ca2+: physiological regulation and role in apoptosis. Mol Cell Biochem. 1994 Jun 15;135(1):89-98.

58. Mukherjee R, Criddle DN, Gukovskaya A, Pandol S, Petersen OH, Sutton R. Mitochondrial injury in pancreatitis. Cell Calcium. 2008 Jul;44(1):14-23.

59. Ward JB, Petersen OH, Jenkins SA, Sutton R. Is an elevated concentration of acinar cytosolic free ionised calcium the trigger for acute pancreatitis? Lancet. 1995 Oct 14;346(8981):1016-9.

60. Saluja AK, Bhagat L, Lee HS, Bhatia M, Frossard JL, Steer ML. Secretagogue-induced digestive enzyme activation and cell injury in rat pancreatic acini. Am J Physiol. 1999 Apr;276(4 Pt 1):G835-42.

61. Kruger B, Albrecht E, Lerch MM. The role of intracellular calcium signaling in premature protease activation and the onset of pancreatitis. Am J Pathol. 2000 Jul;157(1):43-50.

62. Bialek R, Willemer S, Arnold R, Adler G. Evidence of intracellular activation of serine proteases in acute cerulein-induced pancreatitis in rats. Scand J Gastroenterol. 1991 Feb;26(2):190-6.

63. Grady T, Saluja A, Kaiser A, Steer M. Edema and intrapancreatic trypsinogen activation precede glutathione depletion during caerulein pancreatitis. Am J Physiol. 1996 Jul;271(1 Pt 1):G20-6.

64. Luthen R, Owen RL, Sarbia M, Grendell JH, Niederau C. Premature trypsinogen activation during cerulein pancreatitis in rats occurs inside pancreatic acinar cells. Pancreas. 1998 Jul;17(1):38-43.

65. Luthen R, Niederau C, Grendell JH. Intrapancreatic zymogen activation and levels of ATP and glutathione during caerulein pancreatitis in rats. Am J Physiol. 1995 Apr;268(4 Pt 1):G592-604.

66. Mithofer K, Fernandez-del Castillo C, Rattner D, Warshaw AL. Subcellular kinetics of early trypsinogen activation in acute rodent pancreatitis. Am J Physiol. 1998 Jan;274(1 Pt 1):G71-9.

67. Saluja A, Hashimoto S, Saluja M, Powers RE, Meldolesi J, Steer ML. Subcellular redistribution of lysosomal enzymes during caerulein-induced pancreatitis. Am J Physiol. 1987 Oct;253(4 Pt 1):G508-16.

68. Saito I, Hashimoto S, Saluja A, Steer ML, Meldolesi J. Intracellular transport of pancreatic zymogens during caerulein supramaximal stimulation. Am J Physiol. 1987 Oct;253(4 Pt 1):G517-26.

69. Willemer S, Bialek R, Adler G. Localization of lysosomal and digestive enzymes in cytoplasmic vacuoles in caerulein-pancreatitis. Histochemistry. 1990;94(2):161-70.

70. Van Acker GJ, Saluja AK, Bhagat L, Singh VP, Song AM, Steer ML. Cathepsin B inhibition prevents trypsinogen activation and reduces pancreatitis severity. Am J Physiol Gastrointest Liver Physiol. 2002 Sep;283(3):G794-800.

71. Halangk W, Lerch MM, Brandt-Nedelev B, Roth W, Ruthenbuerger M, Reinheckel T, et al. Role of cathepsin B in intracellular trypsinogen activation and the onset of acute pancreatitis. JClinInvest. 2000 09;106(6):773-81.

72. Long J, Song N, Liu XP, Guo KJ, Guo RX. Nuclear factor-kappaB activation on the reactive oxygen species in acute necrotizing pancreatitic rats. World J Gastroenterol. 2005 Jul 21;11(27):4277-80.

73. Hietaranta AJ, Saluja AK, Bhagat L, Singh VP, Song AM, Steer ML. Relationship between NF-kappaB and trypsinogen activation in rat pancreas after supramaximal caerulein stimulation. Biochem Biophys Res Commun. 2001 Jan 12;280(1):388-95.

74. Altavilla D, Famulari C, Passaniti M, Galeano M, Macri A, Seminara P, et al. Attenuated cerulein-induced pancreatitis in nuclear factor-kappaB-deficient mice. Lab Invest. 2003 12;83(12):1723-32.

75. Rakonczay Z, Jr., Jarmay K, Kaszaki J, Mandi Y, Duda E, Hegyi P, et al. NF-kappaB activation is detrimental in arginine-induced acute pancreatitis. Free Radic Biol Med. 2003 Mar 15;34(6):696-709.

76. Shi C, Zhao X, Wang X, Andersson R. Role of nuclear factor-kappaB, reactive oxygen species and cellular signaling in the early phase of acute pancreatitis. Scand J Gastroenterol. 2005 Jan;40(1):103-8.

77. Virlos I, Mazzon E, Serraino I, Di Paola R, Genovese T, Britti D, et al. Pyrrolidine dithiocarbamate reduces the severity of cerulein-induced murine acute pancreatitis. Shock. 2003 Dec;20(6):544-50.

78. Steinle AU, Weidenbach H, Wagner M, Adler G, Schmid RM. NF-kappaB/Rel activation in cerulein pancreatitis. Gastroenterology. 1999 Feb;116(2):420-30.

79. McKay CJ, Buter A. Natural history of organ failure in acute pancreatitis. Pancreatology. 2003;3(2):111-4.

80. Bone RC, Balk RA, Cerra FB, Dellinger RP, Fein AM, Knaus WA, et al. Definitions for sepsis and organ failure and guidelines for the use of innovative therapies in sepsis. The ACCP/SCCM Consensus Conference Committee. American College of Chest Physicians/Society of Critical Care Medicine. Chest. 1992 Jun;101(6):1644-55.

81. Bone RC, Sibbald WJ, Sprung CL. The ACCP-SCCM consensus conference on sepsis and organ failure. Chest. 1992 Jun;101(6):1481-3.

82. Moore FA, Moore EE. Evolving concepts in the pathogenesis of postinjury multiple organ failure. Surg Clin North Am. 1995 Apr;75(2):257-77.

83. de Beaux AC, Palmer KR, Carter DC. Factors influencing morbidity and mortality in acute pancreatitis; an analysis of 279 cases. Gut. 1995 Jul;37(1):121-6.

84. Gloor B, Muller CA, Worni M, Martignoni ME, Uhl W, Buchler MW. Late mortality in patients with severe acute pancreatitis. Br J Surg. 2001 Jul;88(7):975-9.

85. Norman J. The role of cytokines in the pathogenesis of acute pancreatitis. Am J Surg. 1998 Jan;175(1):76-83.

86. Pezzilli R, Billi P, Miniero R, Barakat B. Serum interleukin-10 in human acute pancreatitis. Digestive diseases and sciences. 1997 Jul;42(7):1469-72.

87. Chen CC, Wang SS, Lu RH, Chang FY, Lee SD. Serum interleukin 10 and interleukin 11 in patients with acute pancreatitis. Gut. 1999 Dec;45(6):895-9.

88. Berney T, Gasche Y, Robert J, Jenny A, Mensi N, Grau G, et al. Serum profiles of interleukin-6, interleukin-8, and interleukin-10 in patients with severe and mild acute pancreatitis. Pancreas. 1999 May;18(4):371-7.

89. Wereszczynska-Siemiatkowska U, Dabrowski A, Siemiatkowski A, Mroczko B, Laszewicz W, Gabryelewicz A. Serum profiles of E-selectin, interleukin-10, and interleukin-6 and oxidative stress parameters in patients with acute pancreatitis and nonpancreatic acute abdominal pain. Pancreas. 2003 03;26(2):144-52.

90. Bone RC. Toward a theory regarding the pathogenesis of the systemic inflammatory response syndrome: what we do and do not know about cytokine regulation. Critical care medicine. 1996 Jan;24(1):163-72.

91. Collins T, Read MA, Neish AS, Whitley MZ, Thanos D, Maniatis T. Transcriptional regulation of endothelial cell adhesion molecules: NF-kappa B and cytokine-inducible enhancers. FASEB J. 1995 Jul;9(10):899-909.

92. van de Stolpe A, van der Saag PT. Intercellular adhesion molecule-1. J Mol Med. 1996 Jan;74(1):13-33.

93. Springer TA. Traffic signals on endothelium for lymphocyte recirculation and leukocyte emigration. Annu Rev Physiol. 1995;57:827-72.

94. Frossard JL, Saluja A, Bhagat L, Lee HS, Bhatia M, Hofbauer B, et al. The role of intercellular adhesion molecule 1 and neutrophils in acute pancreatitis and pancreatitis-associated lung injury. Gastroenterology. 1999 Mar;116(3):694-701.

95. Kaufmann P, Tilz GP, Smolle KH, Demel U, Krejs GJ. Increased plasma concentrations of circulating intercellular adhesion molecule-1 (cICAM-1) in patients with necrotizing pancreatitis. Immunobiology. 1996 Jul;195(2):209-19.

96. Ramudo L, Manso MA, Vicente S, De DI. Pro- and anti-inflammatory response of acinar cells during acute pancreatitis. Effect of N-acetyl cysteine. Cytokine. 2005 11/03/;32(3-4):125-31.

97. de la Mano AM, Sevillano S, Manso MA, Perez M, de Dios I. Cholecystokinin blockade alters the systemic immune response in rats with acute pancreatitis. Int J Exp Pathol. 2004 Apr;85(2):75-84.

98. Hotter G, Closa D, Gelpi E, Prats N, Rosello-Catafau J. Role of xanthine oxidase and eicosanoids in development of pancreatic ischemia-reperfusion injury. Inflammation. 1995 08;19(4):469-78.

99. Gukovskaya AS, Vaquero E, Zaninovic V, Gorelick FS, Lusis AJ, Brennan ML, et al. Neutrophils and NADPH oxidase mediate intrapancreatic trypsin activation in murine experimental acute pancreatitis. Gastroenterology. 2002 04;122(4):974-84.

100. Pastor CM, Vonlaufen A, Georgi F, Hadengue A, Morel P, Frossard JL. Neutrophil depletion--but not prevention of Kupffer cell activation--decreases the severity of cerulein-induced acute pancreatitis. World JGastroenterol. 2006 02/28/;12(8):1219-24.

101. Poch B, Gansauge F, Rau B, Wittel U, Gansauge S, Nussler AK, et al. The role of polymorphonuclear leukocytes and oxygen-derived free radicals in experimental acute pancreatitis: mediators of local destruction and activators of inflammation. FEBS Lett. 1999 Nov 19;461(3):268-72.

102. Hardman J, Shields C, Schofield D, McMahon R, Redmond HP, Siriwardena AK. Intravenous antioxidant modulation of end-organ damage in L-arginine-induced experimental acute pancreatitis. Pancreatology. 2005;5(4-5):380-6.

103. Adler G, Hupp T, Kern HF. Course and spontaneous regression of acute pancreatitis in the rat. Virchows Arch A Pathol Anat Histol. 1979 May 14;382(1):31-47.

104. Norman JG, Fink GW, Franz MG. Acute pancreatitis induces intrapancreatic tumor necrosis factor gene expression. Arch Surg. 1995 Sep;130(9):966-70.

105. Titheradge MA. Nitric oxide in septic shock. Biochim Biophys Acta. 1999 May 5;1411(2-3):437-55.

106. Biffl WL, Moore EE, Moore FA, Peterson VM. Interleukin-6 in the injured patient. Marker of injury or mediator of inflammation? Annals of surgery. 1996 Nov;224(5):647-64.

107. Ishibashi T, Zhao H, Kawabe K, Oono T, Egashira K, Suzuki K, et al. Blocking of monocyte chemoattractant protein-1 (MCP-1) activity attenuates the severity of acute pancreatitis in rats. J Gastroenterol. 2008;43(1):79-85.

108. Jambrik Z, Gyongyosi M, Hegyi P, Czako L, Takacs T, Farkas A, et al. Plasma levels of IL-6 correlate with hemodynamic abnormalities in acute pancreatitis in rabbits. Intensive Care Med. 2002 Dec;28(12):1810-8.

109. Leser HG, Gross V, Scheibenbogen C, Heinisch A, Salm R, Lausen M, et al. Elevation of serum interleukin-6 concentration precedes acute-phase response and reflects severity in acute pancreatitis. Gastroenterology. 1991 Sep;101(3):782-5.

110. Pezzilli R, Miniero R, Cappelletti O, Barakat B. Serum interleukin 6 in the prognosis of acute biliary pancreatitis. Ital J Gastroenterol Hepatol. 1998 Jun;30(3):291-4.

111. Papachristou GI, Whitcomb DC. Inflammatory markers of disease severity in acute pancreatitis. ClinLab Med. 2005 03;25(1):17-37.

112. Suzuki S, Miyasaka K, Jimi A, Funakoshi A. Induction of acute pancreatitis by cerulein in human IL-6 gene transgenic mice. Pancreas. 2000 Jul;21(1):86-92.

113. Chao KC, Chao KF, Chuang CC, Liu SH. Blockade of interleukin 6 accelerates acinar cell apoptosis and attenuates experimental acute pancreatitis in vivo. Br J Surg. 2006 Mar;93(3):332-8.

114. Murphy PM. The molecular biology of leukocyte chemoattractant receptors. Annu Rev Immunol. 1994;12:593-633.

115. Baggiolini M. Chemokines in pathology and medicine. J Intern Med. 2001 Aug;250(2):91-104.

116. Gross V, Andreesen R, Leser HG, Ceska M, Liehl E, Lausen M, et al. Interleukin-8 and neutrophil activation in acute pancreatitis. European journal of clinical investigation. 1992 Mar;22(3):200-3.

117. Osman MO, Kristensen JU, Jacobsen NO, Lausten SB, Deleuran B, Deleuran M, et al. A monoclonal anti-interleukin 8 antibody (WS-4) inhibits cytokine response and

acute lung injury in experimental severe acute necrotising pancreatitis in rabbits. Gut. 1998 Aug;43(2):232-9.

118. Gerard C, Frossard JL, Bhatia M, Saluja A, Gerard NP, Lu B, et al. Targeted disruption of the beta-chemokine receptor CCR1 protects against pancreatitis-associated lung injury. JClinInvest. 1997 10/15/;100(8):2022-7.

119. Pezzilli R, Billi P, Miniero R, Fiocchi M, Cappelletti O, Morselli-Labate AM, et al. Serum interleukin-6, interleukin-8, and beta 2-microglobulin in early assessment of severity of acute pancreatitis. Comparison with serum C-reactive protein. Digestive diseases and sciences. 1995 Nov;40(11):2341-8.

120. Benveniste J, Henson PM, Cochrane CG. Leukocyte-dependent histamine release from rabbit platelets. The role of IgE, basophils, and a platelet-activating factor. J Exp Med. 1972 Dec 1;136(6):1356-77.

121. Kald B, Kald A, Ihse I, Tagesson C. Release of platelet-activating factor in acute experimental pancreatitis. Pancreas. 1993 Jul;8(4):440-2.

122. Emanuelli G, Montrucchio G, Dughera L, Gaia E, Lupia E, Battaglia E, et al. Role of platelet activating factor in acute pancreatitis induced by lipopolysaccharides in rabbits. European journal of pharmacology. 1994 Aug 22;261(3):265-72.

123. Yotsumoto F, Manabe T, Kyogoku T, Hirano T, Ohshio G, Yamamoto M, et al. Platelet-activating factor involvement in the aggravation of acute pancreatitis in rabbits. Digestion. 1994;55(4):260-7.

124. Jancar S, De Giaccobi G, Mariano M, Mencia-Huerta JM, Sirois P, Braquet P. Immune complex induced pancreatitis: effect of BN 52021, a selective antagonist of platelet-activating factor. Prostaglandins. 1988 May;35(5):757-70.

125. Dabrowski A, Gabryelewicz A, Chyczewski L. The effect of platelet activating factor antagonist (BN 52021) on cerulein-induced acute pancreatitis with reference to oxygen radicals. Int J Pancreatol. 1991 Jan;8(1):1-11.

126. Tomaszewska R, Dembinski A, Warzecha Z, Banas M, Konturek SJ, Stachura J. Platelet activating factor (PAF) inhibitor (TCV-309) reduces caerulein- and PAF-induced pancreatitis. A morphologic and functional study in the rat. J Physiol Pharmacol. 1992 Dec;43(4):345-52.

127. Kingsnorth AN, Galloway SW, Formela LJ. Randomized, double-blind phase II trial of Lexipafant, a platelet-activating factor antagonist, in human acute pancreatitis. Br J Surg. 1995 Oct;82(10):1414-20.

128. McKay CJ, Curran F, Sharples C, Baxter JN, Imrie CW. Prospective placebo-controlled randomized trial of lexipafant in predicted severe acute pancreatitis. Br J Surg. 1997 Sep;84(9):1239-43.

129. Johnson CD, Kingsnorth AN, Imrie CW, McMahon MJ, Neoptolemos JP, McKay C, et al. Double blind, randomised, placebo controlled study of a platelet activating factor antagonist, lexipafant, in the treatment and prevention of organ failure in predicted severe acute pancreatitis. Gut. 2001 Jan;48(1):62-9.

130. Greenman RL, Schein RM, Martin MA, Wenzel RP, MacIntyre NR, Emmanuel G, et al. A controlled clinical trial of E5 murine monoclonal IgM antibody to endotoxin in the treatment of gram-negative sepsis. The XOMA Sepsis Study Group. JAMA. 1991 Aug 28;266(8):1097-102.

131. Ziegler EJ, Fisher CJ, Jr., Sprung CL, Straube RC, Sadoff JC, Foulke GE, et al. Treatment of gram-negative bacteremia and septic shock with HA-1A human monoclonal antibody against endotoxin. A randomized, double-blind, placebo-controlled trial. The HA-1A Sepsis Study Group. N Engl J Med. 1991 Feb 14;324(7):429-36.

132. Bone RC. Sir Isaac Newton, sepsis, SIRS, and CARS. Critical care medicine. 1996 Jul;24(7):1125-8.

133. Kasama T, Strieter RM, Lukacs NW, Burdick MD, Kunkel SL. Regulation of neutrophil-derived chemokine expression by IL-10. J Immunol. 1994 Apr 1;152(7):3559-69.

134. Seitz M, Loetscher P, Dewald B, Towbin H, Gallati H, Baggiolini M. Interleukin-10 differentially regulates cytokine inhibitor and chemokine release from blood mononuclear cells and fibroblasts. Eur J Immunol. 1995 Apr;25(4):1129-32.

135. Lo CJ, Fu M, Cryer HG. Interleukin 10 inhibits alveolar macrophage production of inflammatory mediators involved in adult respiratory distress syndrome. The Journal of surgical research. 1998 Oct;79(2):179-84.

136. Armstrong L, Millar AB. Relative production of tumour necrosis factor alpha and interleukin 10 in adult respiratory distress syndrome. Thorax. 1997 May;52(5):442-6.

137. Czermak BJ, Sarma V, Pierson CL, Warner RL, Huber-Lang M, Bless NM, et al. Protective effects of C5a blockade in sepsis. Nat Med. 1999 Jul;5(7):788-92.

138. Huber-Lang MS, Sarma JV, McGuire SR, Lu KT, Guo RF, Padgaonkar VA, et al. Protective effects of anti-C5a peptide antibodies in experimental sepsis. FASEB J. 2001 Mar;15(3):568-70.

139. Bhatia M, Saluja AK, Singh VP, Frossard JL, Lee HS, Bhagat L, et al. Complement factor C5a exerts an anti-inflammatory effect in acute pancreatitis and associated lung injury. Am J Physiol Gastrointest Liver Physiol. 2001 May;280(5):G974-8.

140. Monsinjon T, Gasque P, Chan P, Ischenko A, Brady JJ, Fontaine MC. Regulation by complement C3a and C5a anaphylatoxins of cytokine production in human umbilical vein endothelial cells. FASEB J. 2003 Jun;17(9):1003-14.

141. Riedemann NC, Guo RF, Sarma VJ, Laudes IJ, Huber-Lang M, Warner RL, et al. Expression and function of the C5a receptor in rat alveolar epithelial cells. J Immunol. 2002 Feb 15;168(4):1919-25.

142. Riedemann NC, Guo RF, Bernacki KD, Reuben JS, Laudes IJ, Neff TA, et al. Regulation by C5a of neutrophil activation during sepsis. Immunity. 2003 Aug;19(2):193-202.

143. Steinberg W, Tenner S. Acute pancreatitis. NEnglJMed. 1994 04/28/;330(17):1198-210.

144. Muhs BE, Patel S, Yee H, Marcus S, Shamamian P. Inhibition of matrix metalloproteinases reduces local and distant organ injury following experimental acute pancreatitis. The Journal of surgical research. 2003 Feb;109(2):110-7.

145. McFadden DW. Organ failure and multiple organ system failure in pancreatitis. Pancreas. 1991;6 Suppl 1:S37-43.

146. Interiano B, Stuard ID, Hyde RW. Acute respiratory distress syndrome in pancreatitis. Ann Intern Med. 1972 Dec;77(6):923-6.

147. Talamini G, Uomo G, Pezzilli R, Rabitti PG, Billi P, Bassi C, et al. Serum creatinine and chest radiographs in the early assessment of acute pancreatitis. Am J Surg. 1999 Jan;177(1):7-14.

148. De Troyer A, Naeije R, Yernault JC, Englert M. Impairment of pulmonary function in acute pancreatitis. Chest. 1978 Mar;73(3):360-3.

149. Robertson CS, Basran GS, Hardy JG. Lung vascular permeability in patients with acute pancreatitis. Pancreas. 1988;3(2):162-5.

150. Milani Junior R, Pereira PM, Dolhnikoff M, Saldiva PH, Martins MA. Respiratory mechanics and lung morphometry in severe pancreatitis-associated acute lung injury in rats. Critical care medicine. 1995 Nov;23(11):1882-9.

151. Closa D, Sabater L, Fernandez-Cruz L, Prats N, Gelpi E, Rosello-Catafau J. Activation of alveolar macrophages in lung injury associated with experimental acute pancreatitis is mediated by the liver. Annals of surgery. 1999 Feb;229(2):230-6.

152. Oppenheim JJ, Zachariae CO, Mukaida N, Matsushima K. Properties of the novel proinflammatory supergene "intercrine" cytokine family. Annu Rev Immunol. 1991;9:617-48.

153. Miller EJ, Cohen AB, Nagao S, Griffith D, Maunder RJ, Martin TR, et al. Elevated levels of NAP-1/interleukin-8 are present in the airspaces of patients with the adult respiratory distress syndrome and are associated with increased mortality. The American review of respiratory disease. 1992 Aug;146(2):427-32.

154. Lundberg AH, Granger N, Russell J, Callicutt S, Gaber LW, Kotb M, et al. Temporal correlation of tumor necrosis factor-alpha release, upregulation of pulmonary ICAM-1 and VCAM-1, neutrophil sequestration, and lung injury in diet-induced pancreatitis. J Gastrointest Surg. 2000 May-Jun;4(3):248-57.

155. Skoutelis AT, Kaleridis V, Athanassiou GM, Kokkinis KI, Missirlis YF, Bassaris HP. Neutrophil deformability in patients with sepsis, septic shock, and adult respiratory distress syndrome. Critical care medicine. 2000 Jul;28(7):2355-9.

156. Yang J, Murphy C, Denham W, Botchkina G, Tracey KJ, Norman J. Evidence of a central role for p38 map kinase induction of tumor necrosis factor alpha in pancreatitis-associated pulmonary injury. Surgery. 1999 Aug;126(2):216-22.

157. Gao HK, Zhou ZG, Chen YQ, Han FH, Wang C. Expression of platelet endothelial cell adhesion molecule-1 between pancreatic microcirculation and peripheral circulation in rats with acute edematous pancreatitis. Hepatobiliary Pancreat Dis Int. 2003 Aug;2(3):463-6.

158. Liu XM, Liu QG, Xu J, Pan CE. Microcirculation disturbance affects rats with acute severe pancreatitis following lung injury. World J Gastroenterol. 2005 Oct 21;11(39):6208-11.

159. Sibille Y, Reynolds HY. Macrophages and polymorphonuclear neutrophils in lung defense and injury. The American review of respiratory disease. 1990 Feb;141(2):471-501.

160. Broug-Holub E, Toews GB, van Iwaarden JF, Strieter RM, Kunkel SL, Paine R, 3rd, et al. Alveolar macrophages are required for protective pulmonary defenses in murine Klebsiella pneumonia: elimination of alveolar macrophages increases neutrophil recruitment but decreases bacterial clearance and survival. Infection and immunity. 1997 Apr;65(4):1139-46.

161. Steinhauser ML, Hogaboam CM, Kunkel SL, Lukacs NW, Strieter RM, Standiford TJ. IL-10 is a major mediator of sepsis-induced impairment in lung antibacterial host defense. J Immunol. 1999 Jan 1;162(1):392-9.

162. Traeger T, Kessler W, Hilpert A, Mikulcak M, Entleutner M, Koerner P, et al. Selective depletion of alveolar macrophages in polymicrobial sepsis increases lung injury, bacterial load and mortality but does not affect cytokine release. Respiration. 2009;77(2):203-13.

163. Reddy RC, Chen GH, Newstead MW, Moore T, Zeng X, Tateda K, et al. Alveolar macrophage deactivation in murine septic peritonitis: role of interleukin 10. Infection and immunity. 2001 Mar;69(3):1394-401.

164. Abraham E. Neutrophils and acute lung injury. Crit Care Med. 2003 Apr;31(4 Suppl):S195-9.

165. Lomas-Neira J, Chung CS, Perl M, Gregory S, Biffl W, Ayala A. Role of alveolar macrophage and migrating neutrophils in hemorrhage-induced priming for ALI subsequent to septic challenge. Am J Physiol Lung Cell Mol Physiol. 2006 Jan;290(1):L51-8.

166. Lu MC, Liu TA, Lee MR, Lin L, Chang WC. Apoptosis contributes to the decrement in numbers of alveolar macrophages from rats with polymicrobial sepsis. Journal of microbiology, immunology, and infection = Wei mian yu gan ran za zhi. 2002 Jun;35(2):71-7.

167. Simms HH, D'Amico R, Burchard KW. Intraabdominal sepsis: effects on polymorphonuclear leukocyte Fc receptor-mediated phagocytosis. The Journal of surgical research. 1990 Jul;49(1):49-54.

168. Holzer K, Konietzny P, Wilhelm K, Encke A, Henrich D. Phagocytosis by emigrated, intra-abdominal neutrophils is depressed during human secondary peritonitis. Eur Surg Res. 2002 Jul-Aug;34(4):275-84.

169. Liras G, Carballo F. An impaired phagocytic function is associated with leucocyte activation in the early stages of severe acute pancreatitis. Gut. 1996 Jul;39(1):39-42.

170. Rinderknecht H. Fatal pancreatitis, a consequence of excessive leukocyte stimulation? Int J Pancreatol. 1988 Mar;3(2-3):105-12.

171. Albelda SM, Smith CW, Ward PA. Adhesion molecules and inflammatory injury. FASEB J. 1994 May;8(8):504-12.

172. Zemans RL, Colgan SP, Downey GP. Transepithelial migration of neutrophils: mechanisms and implications for acute lung injury. Am J Respir Cell Mol Biol. 2009 May;40(5):519-35.

173. Yamauchi J, Sunamura M, Shibuya K, Takeda K, Kobari M, Matsuno S. **A novel diamino-pyridine derivative prevents excessive leukocyte infiltration in aggravation of acute necrotizing pancreatitis**. Digestion. 1999;60 Suppl 1:40-6.

174. Yamanaka K, Saluja AK, Brown GE, Yamaguchi Y, Hofbauer B, Steer ML. Protective effects of prostaglandin E1 on acute lung injury of caerulein-induced acute pancreatitis in rats. Am J Physiol. 1997 Jan;272(1 Pt 1):G23-30.

175. de Dios I, Perez M, de La Mano A, Sevillano S, Orfao A, Ramudo L, et al. **Contribution of circulating leukocytes to cytokine production in pancreatic duct obstruction-induced acute pancreatitis in rats**. Cytokine. 2002 Dec 21;20(6):295-303.

176. Zhao X, Dib M, Andersson E, Shi C, Widegren B, Wang X, et al. Alterations of adhesion molecule expression and inflammatory mediators in acute lung injury induced by septic and non-septic challenges. Lung. 2005 Mar-Apr;183(2):87-100.

177. Shi C, Zhao X, Lagergren A, Sigvardsson M, Wang X, Andersson R. Immune status and inflammatory response differ locally and systemically in severe acute pancreatitis. Scand J Gastroenterol. 2006 Apr;41(4):472-80.

178. Hac S, Dobosz M, Kaczor J, Rzepko R. Influence of molecule CD 11b blockade on the course of acute ceruleine pancreatitis in rats. ExpMolPathol. 2004 08;77(1):57-65.

179. Hac S, Dobosz M, Kaczor JJ, Rzepko R, eksandrowicz-Wrona E, Wajda Z, et al. Neutrophil engagement and septic challenge in acute experimental pancreatitis in rats. World JGastroenterol. 2005 11/07/;11(41):6459-65.

180. Hatano N, Sugiyama M, Watanabe T, Atomi Y. Opsonin receptor expression on peritoneal exudative and circulatory neutrophils in murine acute pancreatitis. Pancreas. 2001 Jul;23(1):55-61.

181. Huizinga TW, van Kemenade F, Koenderman L, Dolman KM, von dem Borne AE, Tetteroo PA, et al. The 40-kDa Fc gamma receptor (FcRII) on human neutrophils is essential for the IgG-induced respiratory burst and IgG-induced phagocytosis. J Immunol. 1989 Apr 1;142(7):2365-9.

182. Huizinga TW, Dolman KM, van der Linden NJ, Kleijer M, Nuijens JH, von dem Borne AE, et al. Phosphatidylinositol-linked FcRIII mediates exocytosis of neutrophil granule proteins, but does not mediate initiation of the respiratory burst. J Immunol. 1990 Feb 15;144(4):1432-7.

183. Strasser A, Harris AW, Huang DC, Krammer PH, Cory S. Bcl-2 and Fas/APO-1 regulate distinct pathways to lymphocyte apoptosis. EMBO J. 1995 Dec 15;14(24):6136-47.

184. Krueger A, Fas SC, Baumann S, Krammer PH. The role of CD95 in the regulation of peripheral T-cell apoptosis. Immunol Rev. 2003 Jun;193:58-69.

185. Roy S, Nicholson DW. Cross-talk in cell death signaling. J Exp Med. 2000 Oct 16;192(8):F21-5.

186. Hotchkiss RS, Swanson PE, Freeman BD, Tinsley KW, Cobb JP, Matuschak GM, et al. Apoptotic cell death in patients with sepsis, shock, and multiple organ dysfunction. Critical care medicine. 1999 Jul;27(7):1230-51.

187. Nishikawa J, Takeyama Y, Ueda T, Hori Y, Ueno N, Yamamoto M, et al. Induction of apoptotic cell death by pancreatitis-associated ascitic fluid in Madin-Darby canine kidney cells. FEBS Lett. 1995 Oct 2;373(1):19-22.

188. Criddle DN, Gerasimenko JV, Baumgartner HK, Jaffar M, Voronina S, Sutton R, et al. Calcium signalling and pancreatic cell death: apoptosis or necrosis? Cell Death Differ. 2007 Jul;14(7):1285-94.

189. Bhatia M. Apoptosis versus necrosis in acute pancreatitis. AmJPhysiol GastrointestLiver Physiol. 2004 02;286(2):G189-G96.

190. bu-Zidan FM, Bonham MJ, Windsor JA. Severity of acute pancreatitis: a multivariate analysis of oxidative stress markers and modified Glasgow criteria. BrJSurg. 2000 08;87(8):1019-23.

191. Formela LJ, Galloway SW, Kingsnorth AN. Inflammatory mediators in acute pancreatitis. BrJSurg. 1995 01;82(1):6-13.

192. Fujimoto K, Hosotani R, Doi R, Wada M, Lee JU, Koshiba T, et al. Role of neutrophils in cerulein-induced pancreatitis in rats: possible involvement of apoptosis. Digestion. 1997;58(5):421-30.

193. Pastor CM, Vonlaufen A, Georgi F, Hadengue A, Morel P, Frossard JL. Neutrophil depletion--but not prevention of Kupffer cell activation--decreases the

severity of cerulein-induced acute pancreatitis. World J Gastroenterol. 2006 Feb 28;12(8):1219-24.

194. Wittel UA, Rau B, Gansauge F, Gansauge S, Nussler AK, Beger HG, et al. Influence of PMN leukocyte-mediated pancreatic damage on the systemic immune response in severe acute pancreatitis in rats. DigDisSci. 2004 08;49(7-8):1348-57.

195. Antal L, Szabo G, Sonkoly S, Paloczi K, Szegedi G. Abnormalities in humoral and cellular immunoactivity in pancreatitis. II. Study of the cellular immune system. Acta Med Acad Sci Hung. 1978;35(2):81-7.

196. Christophi C, McDermott F, Hughes ES. Prognostic significance of the absolute lymphocyte count in acute pancreatitis. Am J Surg. 1985 Sep;150(3):295-6.

197. Hotchkiss RS, Tinsley KW, Swanson PE, Chang KC, Cobb JP, Buchman TG, et al. Prevention of lymphocyte cell death in sepsis improves survival in mice. Proc Natl Acad Sci U S A. 1999 Dec 7;96(25):14541-6.

198. Hotchkiss RS, Swanson PE, Knudson CM, Chang KC, Cobb JP, Osborne DF, et al. Overexpression of Bcl-2 in transgenic mice decreases apoptosis and improves survival in sepsis. J Immunol. 1999 Apr 1;162(7):4148-56.

199. Takeyama Y, Takas K, Ueda T, Hori Y, Goshima M, Kuroda Y. Peripheral lymphocyte reduction in severe acute pancreatitis is caused by apoptotic cell death. J Gastrointest Surg. 2000 Jul-Aug;4(4):379-87.

200. Salomone T, Tosi P, Raiti C, Guariento A, Tomassetti P, Migliori M, et al. Apoptosis in the peripheral blood mononuclear cells as a self-limitation process in human acute pancreatitis. Pancreatology. 2002;2(3):204-10.

201. Hiramatsu M, Hotchkiss RS, Karl IE, Buchman TG. Cecal ligation and puncture (CLP) induces apoptosis in thymus, spleen, lung, and gut by an endotoxin and TNF-independent pathway. Shock. 1997 Apr;7(4):247-53.

202. Hotchkiss RS, Swanson PE, Cobb JP, Jacobson A, Buchman TG, Karl IE. Apoptosis in lymphoid and parenchymal cells during sepsis: findings in normal and T- and B-cell-deficient mice. Critical care medicine. 1997 Aug;25(8):1298-307.

203. Yasuda T, Takeyama Y, Ueda T, Takase K, Nishikawa J, Kuroda Y. Splenic atrophy in experimental severe acute pancreatitis. Pancreas. 2002 May;24(4):365-72.

204. Ueda T, Takeyama Y, Yasuda T, Takase K, Nishikawa J, Kuroda Y. Functional alterations of splenocytes in severe acute pancreatitis. The Journal of surgical research. 2002 Feb;102(2):161-8.

205. Hotchkiss RS, Chang KC, Grayson MH, Tinsley KW, Dunne BS, Davis CG, et al. Adoptive transfer of apoptotic splenocytes worsens survival, whereas adoptive transfer of necrotic splenocytes improves survival in sepsis. Proc Natl Acad Sci U S A. 2003 May 27;100(11):6724-9.

206. Jimenez MF, Watson RW, Parodo J, Evans D, Foster D, Steinberg M, et al. Dysregulated expression of neutrophil apoptosis in the systemic inflammatory response syndrome. Arch Surg. 1997 Dec;132(12):1263-9; discussion 9-70.

207. Keel M, Ungethum U, Steckholzer U, Niederer E, Hartung T, Trentz O, et al. Interleukin-10 counterregulates proinflammatory cytokine-induced inhibition of neutrophil apoptosis during severe sepsis. Blood. 1997 Nov 1;90(9):3356-63.

208. Fialkow L, Fochesatto Filho L, Bozzetti MC, Milani AR, Rodrigues Filho EM, Ladniuk RM, et al. Neutrophil apoptosis: a marker of disease severity in sepsis and sepsis-induced acute respiratory distress syndrome. Critical care (London, England). 2006;10(6):R155.

209. Colotta F, Re F, Polentarutti N, Sozzani S, Mantovani A. Modulation of granulocyte survival and programmed cell death by cytokines and bacterial products. Blood. 1992 Oct 15;80(8):2012-20.

210. Brach MA, deVos S, Gruss HJ, Herrmann F. Prolongation of survival of human polymorphonuclear neutrophils by granulocyte-macrophage colony-stimulating factor is caused by inhibition of programmed cell death. Blood. 1992 Dec 1;80(11):2920-4.

211. Cox G, Gauldie J, Jordana M. Bronchial epithelial cell-derived cytokines (G-CSF and GM-CSF) promote the survival of peripheral blood neutrophils in vitro. Am J Respir Cell Mol Biol. 1992 Nov;7(5):507-13.

212. Pericle F, Liu JH, Diaz JI, Blanchard DK, Wei S, Forni G, et al. Interleukin-2 prevention of apoptosis in human neutrophils. Eur J Immunol. 1994 Feb;24(2):440-4.

213. Lee A, Whyte MK, Haslett C. Inhibition of apoptosis and prolongation of neutrophil functional longevity by inflammatory mediators. Journal of leukocyte biology. 1993 Oct;54(4):283-8.

214. Kennedy AD, DeLeo FR. Neutrophil apoptosis and the resolution of infection. Immunol Res. 2009;43(1-3):25-61.

215. Fanning NF, Porter J, Shorten GD, Kirwan WO, Bouchier-Hayes D, Cotter TG, et al. Inhibition of neutrophil apoptosis after elective surgery. Surgery. 1999 Sep;126(3):527-34.

216. Fanning NF, Kell MR, Shorten GD, Kirwan WO, Bouchier-Hayes D, Cotter TG, et al. Circulating granulocyte macrophage colony-stimulating factor in plasma of patients with the systemic inflammatory response syndrome delays neutrophil apoptosis through inhibition of spontaneous reactive oxygen species generation. Shock. 1999 Mar;11(3):167-74.

217. van den Berg JM, Weyer S, Weening JJ, Roos D, Kuijpers TW. Divergent effects of tumor necrosis factor alpha on apoptosis of human neutrophils. Journal of leukocyte biology. 2001 Mar;69(3):467-73.

218. O'Neill S, O'Neill AJ, Conroy E, Brady HR, Fitzpatrick JM, Watson RW. Altered caspase expression results in delayed neutrophil apoptosis in acute pancreatitis. JLeukocBiol. 2000 07;68(1):15-20.

219. Chen HM, Hsu JT, Chen JC, Ng CJ, Chiu DF, Chen MF. Delayed neutrophil apoptosis attenuated by melatonin in human acute pancreatitis. Pancreas. 2005 Nov;31(4):360-4.

220. Kaiser AM, Saluja AK, Sengupta A, Saluja M, Steer ML. Relationship between severity, necrosis, and apoptosis in five models of experimental acute pancreatitis. Am J Physiol. 1995 Nov;269(5 Pt 1):C1295-304.

221. Gukovskaya AS, Perkins P, Zaninovic V, Sandoval D, Rutherford R, Fitzsimmons T, et al. Mechanisms of cell death after pancreatic duct obstruction in the opossum and the rat. Gastroenterology. 1996 Mar;110(3):875-84.

222. Fadok VA, Bratton DL, Frasch SC, Warner ML, Henson PM. The role of phosphatidylserine in recognition of apoptotic cells by phagocytes. Cell Death Differ. 1998 Jul;5(7):551-62.

223. Fadok VA, Bratton DL, Konowal A, Freed PW, Westcott JY, Henson PM. Macrophages that have ingested apoptotic cells in vitro inhibit proinflammatory cytokine production through autocrine/paracrine mechanisms involving TGF-beta, PGE2, and PAF. J Clin Invest. 1998 Feb 15;101(4):890-8.

224. Bellingan GJ, Caldwell H, Howie SE, Dransfield I, Haslett C. In vivo fate of the inflammatory macrophage during the resolution of inflammation: inflammatory macrophages do not die locally, but emigrate to the draining lymph nodes. J Immunol. 1996 Sep 15;157(6):2577-85.

225. Medeiros AI, Serezani CH, Lee SP, Peters-Golden M. Efferocytosis impairs pulmonary macrophage and lung antibacterial function via PGE2/EP2 signaling. J Exp Med. 2009 Jan 16;206(1):61-8.

226. Saad B, Frei K, Scholl FA, Fontana A, Maier P. Hepatocyte-derived interleukin-6 and tumor-necrosis factor alpha mediate the lipopolysaccharide-induced acute-phase response and nitric oxide release by cultured rat hepatocytes. Eur J Biochem. 1995 Apr 15;229(2):349-55.

227. Callery MP, Kamei T, Flye MW. Endotoxin stimulates interleukin-6 production by human Kupffer cells. Circ Shock. 1992 Jul;37(3):185-8.

228. Gray KD, Simovic MO, Blackwell TS, Christman JW, May AK, Parman KS, et al. Activation of nuclear factor kappa B and severe hepatic necrosis may mediate systemic inflammation in choline-deficient/ethionine-supplemented diet-induced pancreatitis. Pancreas. 2006 Oct;33(3):260-7.

229. Mole DJ, Taylor MA, McFerran NV, Diamond T. The isolated perfused liver response to a 'second hit' of portal endotoxin during severe acute pancreatitis. Pancreatology. 2005;5(4-5):475-85.

230. Gloor B, Blinman TA, Rigberg DA, Todd KE, Lane JS, Hines OJ, et al. Kupffer cell blockade reduces hepatic and systemic cytokine levels and lung injury in hemorrhagic pancreatitis in rats. Pancreas. 2000 Nov;21(4):414-20.

231. Gloor B, Todd KE, Lane JS, Lewis MP, Reber HA. Hepatic Kupffer cell blockade reduces mortality of acute hemorrhagic pancreatitis in mice. J Gastrointest Surg. 1998 Sep-Oct;2(5):430-5.

232. Gilgenast O, Brandt-Nedelev B, Wiswedel I, Lippert H, Halangk W, Reinheckel T. Differential oxidative injury in extrapancreatic tissues during experimental pancreatitis: modification of lung proteins by 4-hydroxynonenal. DigDisSci. 2001 04;46(4):932-7.

233. Ponka P. Cell biology of heme. Am J Med Sci. 1999 Oct;318(4):241-56.

234. Balla G, Jacob HS, Eaton JW, Belcher JD, Vercellotti GM. Hemin: a possible physiological mediator of low density lipoprotein oxidation and endothelial injury. Arterioscler Thromb. 1991 Nov-Dec;11(6):1700-11.

235. Balla G, Vercellotti GM, Muller-Eberhard U, Eaton J, Jacob HS. Exposure of endothelial cells to free heme potentiates damage mediated by granulocytes and toxic oxygen species. Lab Invest. 1991 May;64(5):648-55.

236. Jeney V, Balla J, Yachie A, Varga Z, Vercellotti GM, Eaton JW, et al. Pro-oxidant and cytotoxic effects of circulating heme. Blood. 2002 Aug 1;100(3):879-87.

237. Maines MD. The heme oxygenase system: a regulator of second messenger gases. Annu Rev Pharmacol Toxicol. 1997;37:517-54.

238. Katori M, Buelow R, Ke B, Ma J, Coito AJ, Iyer S, et al. Heme oxygenase-1 overexpression protects rat hearts from cold ischemia/reperfusion injury via an antiapoptotic pathway. Transplantation. 2002 Jan 27;73(2):287-92.

239. Kato H, Amersi F, Buelow R, Melinek J, Coito AJ, Ke B, et al. Heme oxygenase-1 overexpression protects rat livers from ischemia/reperfusion injury with extended cold preservation. Am J Transplant. 2001 Jul;1(2):121-8.

240. Amersi F, Buelow R, Kato H, Ke B, Coito AJ, Shen XD, et al. Upregulation of heme oxygenase-1 protects genetically fat Zucker rat livers from ischemia/reperfusion injury. J Clin Invest. 1999 Dec;104(11):1631-9.

241. Amersi F, Shen XD, Anselmo D, Melinek J, Iyer S, Southard DJ, et al. Ex vivo exposure to carbon monoxide prevents hepatic ischemia/reperfusion injury through p38 MAP kinase pathway. Hepatology. 2002 Apr;35(4):815-23.

242. Guo Y, Stein AB, Wu WJ, Tan W, Zhu X, Li QH, et al. Administration of a CO-releasing molecule at the time of reperfusion reduces infarct size in vivo. Am J Physiol Heart Circ Physiol. 2004 May;286(5):H1649-53.

243. von Dobschuetz E, Schmidt R, Scholtes M, Thomusch O, Schwer CI, Geiger KK, et al. Protective role of heme oxygenase-1 in pancreatic microcirculatory dysfunction after ischemia/reperfusion in rats. Pancreas. 2008 May;36(4):377-84.

244. Lee PJ, Alam J, Sylvester SL, Inamdar N, Otterbein L, Choi AM. Regulation of heme oxygenase-1 expression in vivo and in vitro in hyperoxic lung injury. Am J Respir Cell Mol Biol. 1996 Jun;14(6):556-68.

245. Inoue S, Suzuki M, Nagashima Y, Suzuki S, Hashiba T, Tsuburai T, et al. Transfer of heme oxygenase 1 cDNA by a replication-deficient adenovirus enhances interleukin 10 production from alveolar macrophages that attenuates lipopolysaccharide-induced acute lung injury in mice. Hum Gene Ther. 2001 May 20;12(8):967-79.

246. Siow RC, Sato H, Mann GE. Heme oxygenase-carbon monoxide signalling pathway in atherosclerosis: anti-atherogenic actions of bilirubin and carbon monoxide? Cardiovasc Res. 1999 Feb;41(2):385-94.

247. Dabrowski A, Konturek SJ, Konturek JW, Gabryelewicz A. Role of oxidative stress in the pathogenesis of caerulein-induced acute pancreatitis. EurJPharmacol. 1999 07/14/;377(1):1-11.

248. Hirano T, Manabe T, Printz H, Saluja A, Steer M. Secretion of lysosomal and digestive enzymes into pancreatic juice under physiological and pathological conditions in rabbits. Nippon Geka Hokan. 1992 Mar 1;61(2):103-24.

249. Willemer S, Elsasser HP, Adler G. Hormone-induced pancreatitis. Eur Surg Res. 1992;24 Suppl 1:29-39.

250. Guice KS, Oldham KT, Wolfe RR, Simon RH. Lung injury in acute pancreatitis: primary inhibition of pulmonary phospholipid synthesis. Am J Surg. 1987 Jan;153(1):54-61.

251. Guice KS, Oldham KT, Johnson KJ, Kunkel RG, Morganroth ML, Ward PA. Pancreatitis-induced acute lung injury. An ARDS model. Annals of surgery. 1988 Jul;208(1):71-7.

252. Feddersen CO, Willemer S, Karges W, Puchner A, Adler G, Wichert PV. Lung injury in acute experimental pancreatitis in rats. II. Functional studies. Int J Pancreatol. 1991 May;8(4):323-31.

253. Willemer S, Feddersen CO, Karges W, Adler G. Lung injury in acute experimental pancreatitis in rats. I. Morphological studies. Int J Pancreatol. 1991 May;8(4):305-21.

254. Bhatia M, Saluja AK, Hofbauer B, Frossard JL, Lee HS, Castagliuolo I, et al. Role of substance P and the neurokinin 1 receptor in acute pancreatitis and pancreatitis-associated lung injury. Proc Natl Acad Sci U S A. 1998 Apr 14;95(8):4760-5.

255. Tani S, Itoh H, Okabayashi Y, Nakamura T, Fujii M, Fujisawa T, et al. New model of acute necrotizing pancreatitis induced by excessive doses of arginine in rats. Digestive diseases and sciences. 1990 Mar;35(3):367-74.

256. Dabrowski A, Gabryelewicz A. Nitric oxide contributes to multiorgan oxidative stress in acute experimental pancreatitis. ScandJGastroenterol. 1994 10;29(10):943-8.

257. Weidenbach H, Lerch MM, Gress TM, Pfaff D, Turi S, Adler G. Vasoactive mediators and the progression from oedematous to necrotising experimental acute pancreatitis. Gut. 1995 Sep;37(3):434-40.

258. Liu X, Nakano I, Yamaguchi H, Ito T, Goto M, Koyanagi S, et al. Protective effect of nitric oxide on development of acute pancreatitis in rats. Digestive diseases and sciences. 1995 Oct;40(10):2162-9.

259. Tsukahara Y, Horita Y, Anan K, Morisaki T, Tanaka M, Torisu M. Role of nitric oxide derived from alveolar macrophages in the early phase of acute pancreatitis. The Journal of surgical research. 1996 Nov;66(1):43-50.

260. Varga IS, Matkovics B, Czako L, Hai DQ, Kotorman M, Takacs T, et al. Oxidative stress changes in L-arginine-induced pancreatitis in rats. Pancreas. 1997 05;14(4):355-9.

261. Varga IS, Matkovics B, Hai DQ, Kotorman M, Takacs T, Sasvari M. Lipid peroxidation and antioxidant system changes in acute L-arginine pancreatitis in rats. Acta Physiol Hung. 1997;85(2):129-38.

262. Frick TW, Fernandez-del Castillo C, Bimmler D, Warshaw AL. Elevated calcium and activation of trypsinogen in rat pancreatic acini. Gut. 1997 Sep;41(3):339-43.

263. Bulbuller N, Dogru O, Umac H, Gursu F, Akpolat N. [The effects of melatonin and pentoxiphylline on L-arginine induced acute pancreatitis]. Ulus Travma Acil Cerrahi Derg. 2005 Apr;11(2):108-14.

264. Dawra R, Sharif R, Phillips P, Dudeja V, Dhaulakhandi D, Saluja AK. Development of a new mouse model of acute pancreatitis induced by administration of L-arginine. Am J Physiol Gastrointest Liver Physiol. 2007 Apr;292(4):G1009-18.

265. Kishino Y, Takama S, Kitajima S. Ultracytochemistry of pancreatic damage induced by excess lysine. Virchows Arch B Cell Pathol Incl Mol Pathol. 1986;52(2):153-67.

266. Hardman J, Jamdar S, Shields C, McMahon R, Redmond HP, Siriwardena AK. Intravenous selenium modulates L-arginine-induced experimental acute pancreatitis. JOP. 2005 09;6(5):431-7.

267. Tashiro M, Schafer C, Yao H, Ernst SA, Williams JA. Arginine induced acute pancreatitis alters the actin cytoskeleton and increases heat shock protein expression in rat pancreatic acinar cells. Gut. 2001 Aug;49(2):241-50.

268. Shields CJ, Winter DC, Sookhai S, Ryan L, Kirwan WO, Redmond HP. Hypertonic saline attenuates end-organ damage in an experimental model of acute pancreatitis. Br J Surg. 2000 Oct;87(10):1336-40.

269. Schmidt J, Rattner DW, Lewandrowski K, Compton CC, Mandavilli U, Knoefel WT, et al. A better model of acute pancreatitis for evaluating therapy. Annals of surgery. 1992 Jan;215(1):44-56.

270. Zhou W, Levine BA, Olson MS. Platelet-activating factor: a mediator of pancreatic inflammation during cerulein hyperstimulation. Am J Pathol. 1993 May;142(5):1504-12.

271. Furukawa M, Kimura T, Yamaguchi H, Kinjoh M, Nawata H. Role of oxygen-derived free radicals in hemorrhagic pancreatitis induced by stress and cerulein in rats. Pancreas. 1994 Jan;9(1):67-72.

272. Liu XH, Kimura T, Ishikawa H, Yamaguchi H, Furukawa M, Nakano I, et al. Effect of endothelin-1 on the development of hemorrhagic pancreatitis in rats. Scand J Gastroenterol. 1995 Mar;30(3):276-82.

273. Maeda S, Suzuki S, Suzuki T, Endo M, Moriya T, Chida M, et al. Analysis of intrapulmonary vessels and epithelial-endothelial interactions in the human developing lung. Lab Invest. 2002 Mar;82(3):293-301.

274. Mead R. The design of experiments : statistical principles for practical applications. Cambridge [England] ; New York: Cambridge University Press; 1988.

275. Meyerholz DK, Samuel I. Morphologic characterization of early ligation-induced acute pancreatitis in rats. Am J Surg. 2007 Nov;194(5):652-8.

276. Saluja A, Hofbauer B, Yamaguchi Y, Yamanaka K, Steer M. Induction of apoptosis reduces the severity of caerulein-induced pancreatitis in mice. Biochem Biophys Res Commun. 1996 Mar 27;220(3):875-8.

277. Cao Y, Adhikari S, Clement MV, Wallig M, Bhatia M. Induction of apoptosis by crambene protects mice against acute pancreatitis via anti-inflammatory pathways. Am J Pathol. 2007 May;170(5):1521-34.

278. Frossard JL, Rubbia-Brandt L, Wallig MA, Benathan M, Ott T, Morel P, et al. Severe acute pancreatitis and reduced acinar cell apoptosis in the exocrine pancreas of mice deficient for the Cx32 gene. Gastroenterology. 2003 Feb;124(2):481-93.

279. Overbeeke R, Steffens-Nakken H, Vermes I, Reutelingsperger C, Haanen C. Early features of apoptosis detected by four different flow cytometry assays. Apoptosis. 1998 Mar;3(2):115-21.

280. Stadelmann C, Lassmann H. Detection of apoptosis in tissue sections. Cell Tissue Res. 2000 Jul;301(1):19-31.

281. Schmidt J, Lewandrowski K, Fernandez-del Castillo C, Mandavilli U, Compton CC, Warshaw AL, et al. Histopathologic correlates of serum amylase activity in acute experimental pancreatitis. Digestive diseases and sciences. 1992 Sep;37(9):1426-33.

282. Schmidt J, Lewandrowsi K, Warshaw AL, Compton CC, Rattner DW. Morphometric characteristics and homogeneity of a new model of acute pancreatitis in the rat. Int J Pancreatol. 1992 Aug;12(1):41-51.

283. Hegyi P, Rakonczay Z, Jr., Sari R, Gog C, Lonovics J, Takacs T, et al. L-arginine-induced experimental pancreatitis. World JGastroenterol. 2004 07/15/;10(14):2003-9.

284. Thiele L, Rothen-Rutishauser B, Jilek S, Wunderli-Allenspach H, Merkle HP, Walter E. Evaluation of particle uptake in human blood monocyte-derived cells in vitro. Does phagocytosis activity of dendritic cells measure up with macrophages? JControl Release. 2001;76(1-2):59-71.

285. Drevets DA, Campbell PA. Macrophage phagocytosis: use of fluorescence microscopy to distinguish between extracellular and intracellular bacteria. JImmunolMethods. 1991;142(1):31-8.

286. Nuutila J, Lilius EM. Flow cytometric quantitative determination of ingestion by phagocytes needs the distinguishing of overlapping populations of binding and ingesting cells. Cytometry A. 2005;65(2):93-102.

287. Busetto S, Trevisan E, Patriarca P, Menegazzi R. A single-step, sensitive flow cytofluorometric assay for the simultaneous assessment of membrane-bound and ingested Candida albicans in phagocytosing neutrophils. Cytometry A. 2004;58(2):201-6.

288. Alhan E, Turkyilmaz S, Ercin C, Kaklikkaya N, Kural BV. Effects of omega-3 fatty acids on acute necrotizing pancreatitis in rats. EurSurgRes. 2006;38(3):314-21.

289. Flaishon R, Szold O, Weinbroum AA. Acute lung injury following pancreas ischaemia-reperfusion: role of xanthine oxidase. EurJClinInvest. 2006 11;36(11):831-7.

290. Maygarden SJ, Iacocca MV, Funkhouser WK, Novotny DB. Pulmonary alveolar proteinosis: a spectrum of cytologic, histochemical, and ultrastructural findings in bronchoalveolar lavage fluid. Diagn Cytopathol. 2001 Jun;24(6):389-95.

291. Van Amersfoort ES, van Strijp JA. Evaluation of a flow cytometric fluorescence quenching assay of phagocytosis of sensitized sheep erythrocytes by polymorphonuclear leukocytes. Cytometry. 1994;17(4):294-301.

292. Bjerknes R, Bassoe CF. Phagocyte C3-mediated attachment and internalization: flow cytometric studies using a fluorescence quenching technique. Blut. 1984;49(4):315-23.

293. Heinzelmann M, Gardner SA, Mercer-Jones M, Roll AJ, Polk HC, Jr. Quantification of phagocytosis in human neutrophils by flow cytometry. MicrobiolImmunol. 1999;43(6):505-12.

294. Gross NT, Camner P, Chinchilla M, Jarstrand C. In vitro effect of lung surfactant on alveolar macrophage defence mechanisms against Cryptococcus neoformans. Mycopathologia. 1998;144(1):21-7.

295. Overton WR. Modified histogram subtraction technique for analysis of flow cytometry data. Cytometry. 1988 Nov;9(6):619-26.

296. Moffat FL, Jr., Han T, Li ZM, Peck MD, Jy W, Ahn YS, et al. Supplemental L-arginine HCl augments bacterial phagocytosis in human polymorphonuclear leukocytes. J Cell Physiol. 1996 Jul;168(1):26-33.

297. Larvin M, Alexander DJ, Switala SF, McMahon MJ. Impaired mononuclear phagocyte function in patients with severe acute pancreatitis: evidence from studies of plasma clearance of trypsin and monocyte phagocytosis. Digestive diseases and sciences. 1993 Jan;38(1):18-27.

298. Martins PS, Kallas EG, Neto MC, Dalboni MA, Blecher S, Salomao R. Upregulation of reactive oxygen species generation and phagocytosis, and increased apoptosis in human neutrophils during severe sepsis and septic shock. Shock. 2003 Sep;20(3):208-12.

299. Savill J. Apoptosis in resolution of inflammation. Journal of leukocyte biology. 1997 Apr;61(4):375-80.

300. Idziorek T, Estaquier J, De Bels F, Ameisen JC. YOPRO-1 permits cytofluorometric analysis of programmed cell death (apoptosis) without interfering with cell viability. Journal of immunological methods. 1995 Sep 25;185(2):249-58.

301. Philpott NJ, Turner AJ, Scopes J, Westby M, Marsh JC, Gordon-Smith EC, et al. The use of 7-amino actinomycin D in identifying apoptosis: simplicity of use and broad spectrum of application compared with other techniques. Blood. 1996 Mar 15;87(6):2244-51.

302. Victor VM, Rocha M, Esplugues JV, De la Fuente M. Role of free radicals in sepsis: antioxidant therapy. Current pharmaceutical design. 2005;11(24):3141-58.

303. Wyllie AH. Apoptosis: an overview. Br Med Bull. 1997;53(3):451-65.

304. Watanabe M, Hitomi M, van der Wee K, Rothenberg F, Fisher SA, Zucker R, et al. The pros and cons of apoptosis assays for use in the study of cells, tissues, and organs. Microsc Microanal. 2002 Oct;8(5):375-91.

305. van Engeland M, Nieland LJ, Ramaekers FC, Schutte B, Reutelingsperger CP. Annexin V-affinity assay: a review on an apoptosis detection system based on phosphatidylserine exposure. Cytometry. 1998 Jan 1;31(1):1-9.

306. Choucroun P, Gillet D, Dorange G, Sawicki B, Dewitte JD. Comet assay and early apoptosis. Mutat Res. 2001 Jul 1;478(1-2):89-96.

307. Hue Su K, Cuthbertson C, Christophi C. Review of experimental animal models of acute pancreatitis. HPB (Oxford). 2006;8(4):264-86.

308. Werner J, Rivera J, Fernandez-del Castillo C, Lewandrowski K, Adrie C, Rattner DW, et al. Differing roles of nitric oxide in the pathogenesis of acute edematous versus necrotizing pancreatitis. Surgery. 1997 Jan;121(1):23-30.

309. Dobosz M, Hac S, Mionskowska L, Dymecki D, Dobrowolski S, Wajda Z. Organ microcirculatory disturbances in experimental acute pancreatitis. A role of nitric oxide. Physiol Res. 2005;54(4):363-8.

310. Sanchez-Bernal C, Garcia-Morales OH, Dominguez C, Martin-Gallan P, Calvo JJ, Ferreira L, et al. Nitric oxide protects against pancreatic subcellular damage in acute pancreatitis. Pancreas. 2004 01;28(1):e9-15.

311. Sandstrom P, Brooke-Smith ME, Thomas AC, Grivell MB, Saccone GT, Toouli J, et al. Highly selective inhibition of inducible nitric oxide synthase ameliorates experimental acute pancreatitis. Pancreas. 2005 Jan;30(1):e10-5.

312. Haslett C. Resolution of acute inflammation and the role of apoptosis in the tissue fate of granulocytes. Clin Sci (Lond). 1992 Dec;83(6):639-48.

313. Haslett C. Granulocyte apoptosis and its role in the resolution and control of lung inflammation. Am J Respir Crit Care Med. 1999 Nov;160(5 Pt 2):S5-11.

314. Leitch AE, Duffin R, Haslett C, Rossi AG. Relevance of granulocyte apoptosis to resolution of inflammation at the respiratory mucosa. Mucosal Immunol. 2008 Sep;1(5):350-63.

315. Rossi AG, Hallett JM, Sawatzky DA, Teixeira MM, Haslett C. Modulation of granulocyte apoptosis can influence the resolution of inflammation. Biochem Soc Trans. 2007 Apr;35(Pt 2):288-91.

316. Savill J, Haslett C. Granulocyte clearance by apoptosis in the resolution of inflammation. Semin Cell Biol. 1995 Dec;6(6):385-93.

317. Serhan CN, Brain SD, Buckley CD, Gilroy DW, Haslett C, O'Neill LA, et al. Resolution of inflammation: state of the art, definitions and terms. FASEB J. 2007 Feb;21(2):325-32.

318. Hallett JM, Leitch AE, Riley NA, Duffin R, Haslett C, Rossi AG. Novel pharmacological strategies for driving inflammatory cell apoptosis and enhancing the resolution of inflammation. Trends Pharmacol Sci. 2008 May;29(5):250-7.

319. Yamamoto C, Yoshida S, Taniguchi H, Qin MH, Miyamoto H, Mizuguchi Y. Lipopolysaccharide and granulocyte colony-stimulating factor delay neutrophil apoptosis and ingestion by guinea pig macrophages. Infect Immun. 1993 May;61(5):1972-9.

320. Connor TJ, Kelly JP, Leonard BE. An assessment of the acute effects of the serotonin releasers methylenedioxymethamphetamine, methylenedioxyamphetamine and fenfluramine on immunity in rats. Immunopharmacology. 2000 Mar;46(3):223-35.

321. Damsgaard CT, Lauritzen L, Calder PC, Kjaer TM, Frokiaer H. Whole-blood culture is a valid low-cost method to measure monocytic cytokines - A comparison of cytokine production in cultures of human whole-blood, mononuclear cells and monocytes. Journal of immunological methods. 2009 Jan 30;340(2):95-101.

322. Elsasser-Beile U, von Kleist S, Gallati H. Evaluation of a test system for measuring cytokine production in human whole blood cell cultures. Journal of immunological methods. 1991 Jun 3;139(2):191-5.

323. Elshal MF, McCoy JP. Multiplex bead array assays: performance evaluation and comparison of sensitivity to ELISA. Methods. 2006 Apr;38(4):317-23.

324. Young SH, Antonini JM, Roberts JR, Erdely AD, Zeidler-Erdely PC. Performance evaluation of cytometric bead assays for the measurement of lung cytokines in two rodent models. Journal of immunological methods. 2008 Feb 29;331(1-2):59-68.

325. Laemmli UK. Cleavage of structural proteins during the assembly of the head of bacteriophage T4. Nature. 1970 08/15/;227(5259):680-5.

326. Flohe L, Gunzler WA. Assays of glutathione peroxidase. Methods Enzymol. 1984;105:114-21.

327. Shea TB, Rogers E, Ashline D, Ortiz D, Sheu MS. Quantification of antioxidant activity in brain tissue homogenates using the 'total equivalent antioxidant capacity'. JNeurosciMethods. 2003 05/30/;125(1-2):55-8.

328. Devey L, Ferenbach D, Mohr E, Sangster K, Bellamy CO, Hughes J, et al. Tissue-resident macrophages protect the liver from ischemia reperfusion injury via a heme oxygenase-1-dependent mechanism. Mol Ther. 2009 Jan;17(1):65-72.

329. Devey L, Mohr E, Bellamy C, Simpson K, Henderson N, Harrison EM, et al. c-Jun terminal kinase-2 gene deleted mice overexpress hemeoxygenase-1 and are

protected from hepatic ischemia reperfusion injury. Transplantation. 2009 Aug 15;88(3):308-16.

330. Chetty U, Gilmour HM, Taylor TV. Experimental acute pancreatitis in the rat--a new model. Gut. 1980 Feb;21(2):115-7.

331. Johnson RH, Doppman J. Duodenal reflux and the etiology of pancreatitis. Surgery. 1967 Sep;62(3):462-7.

332. Nance FC, Cain JL. Studies of hemorrhagic pancreatitis in germ-free dogs. Gastroenterology. 1968 Sep;55(3):368-74.

333. Orda R, Hadas N, Orda S, Wiznitzer T. Experimental acute pancreatitis. Inducement by taurocholate sodium-trypsin injection into a temporarily closed duodenal loop in the rat. Arch Surg. 1980 Mar;115(3):327-9.

334. Mizuma K, Schroder T, Kaarne M, Korpela H, Lempinen M. Serum phospholipase A2 in diet-induced pancreatitis. Eur Surg Res. 1984;16(3):156-61.

335. Fu K, Tomita T, Sarras MP, Jr., De Lisle RC, Andrews GK. Metallothionein protects against cerulein-induced acute pancreatitis: analysis using transgenic mice. Pancreas. 1998 10;17(3):238-46.

336. Niederau C, Luthen R, Niederau MC, Grendell JH, Ferrell LD. Acute experimental hemorrhagic-necrotizing pancreatitis induced by feeding a choline-deficient, ethionine-supplemented diet. Methodology and standards. Eur Surg Res. 1992;24 Suppl 1:40-54.

337. Gilliland L, Steer ML. Effects of ethionine on digestive enzyme synthesis and discharge by mouse pancreas. Am J Physiol. 1980 Nov;239(5):G418-26.

338. Watanabe O, Baccino FM, Steer ML, Meldolesi J. Supramaximal caerulein stimulation and ultrastructure of rat pancreatic acinar cell: early morphological changes

during development of experimental pancreatitis. Am J Physiol. 1984 Apr;246(4 Pt 1):G457-67.

339. Weaver C, Bishop AE, Polak JM. Pancreatic changes elicited by chronic administration of excess L-arginine. Exp Mol Pathol. 1994 Apr;60(2):71-87.

340. Stein M, Keshav S, Harris N, Gordon S. Interleukin 4 potently enhances murine macrophage mannose receptor activity: a marker of alternative immunologic macrophage activation. J Exp Med. 1992 Jul 1;176(1):287-92.

341. Stahl PD. The macrophage mannose receptor: current status. Am J Respir Cell Mol Biol. 1990 Apr;2(4):317-8.